Vol. 119 No. 2, October 1, 1980
Completing Vol. 119

ISSN 0003-2670

ANALYTICA CHIMICA ACTA

International journal devoted to all branches of analytical chemistry

ELSEVIER SCIENTIFIC PUBLISHING COMPANY

ANALYTICA CHIMICA ACTA

International journal devoted to all branches of analytical chemistry
Revue internationale consacrée à tous les domaines de la chimie analytique
Internationale Zeitschrift für alle Gebiete der analytischen Chemie

PUBLICATION SCHEDULE FOR 1980 (incorporating the section on Computer Techniques and Optimization).

	J	F	M	A	M	J	J	A	S	O	N	D
Analytica Chimica Acta	113/1 113/2	114	115	116/1	116/2	117	118/1	118/2	119/1	119/2	120	121
Section on Computer Techniques and Optimization			122/1			122/2			122/3			122/4

Scope. *Analytica Chimica Acta* publishes original papers, short communications, and reviews dealing with every aspect of modern chemical analysis, both fundamental and applied. The section on *Computer Techniques and Optimization* is devoted to new developments in chemical analysis by the application of computer techniques and by interdisciplinary approaches, including statistics, systems theory and operation research. The section deals with the following topics: Computerized acquisition, processing and evaluation of data. Computerized methods for the interpretation of analytical data including chemometrics, cluster analysis, and pattern recognition. Storage and retrieval systems. Optimization procedures and their application. Automated analysis for industrial processes and quality control. Organizational problems.

Submission of Papers. Manuscripts (three copies) should be submitted as designated below for rapid and efficient handling:

Papers from the Americas to: Professor Harry L. Pardue, Department of Chemistry, Purdue University, West Lafayette, IN 47090, U.S.A.

Papers from all other countries to: Dr. A. M. G. Macdonald, Department of Chemistry, The University, P.O. Box 363, Birmingham B15 2TT, England.

For the section on *Computer Techniques and Optimization:* Dr. J. T. Clerc, Universität Bern, Pharmazeutisches Institut, Sahlistrasse 10, CH-3012 Bern, Switzerland.

American authors are recommended to send manuscripts and proofs by INTERNATIONAL AIRMAIL.

Information for Authors. Papers in English, French and German are published. There are no page charges. Manuscripts should conform in layout and style to the papers published in this Volume. Authors should consult Vol. 111, p. 343 for detailed information. Reprints of this information are available from the Editors or from: Elsevier Editorial Services Ltd., Mayfield House, 256 Banbury Road, Oxford OX2 7DE (Great Britain).

Reprints. Fifty reprints will be supplied free of charge. Additional reprints (minimum 100) can be ordered. An order form containing price quotations will be sent to the authors together with the proofs of their article.

Advertisements. Advertisement rates are available from the publisher.

Subscriptions. Subscriptions should be sent to: Elsevier Scientific Publishing Company, P.O. Box 211, 1000 AE Amsterdam, The Netherlands. The section on *Computer Techniques and Optimization* can be subscribed to separately.

Publication. *Analytica Chimica Acta* (including the section on *Computer Techniques and Optimization*) appears in 10 volumes in 1980. The subscription for 1980 (Vols. 113–122) is Dfl. 1390.00 plus Dfl. 160.00 (postage) (total approx. U.S. $795.00). The subscription for the *Computer Techniques and Optimization* section only (Vol. 122) is Dfl. 139.00 plus Dfl. 16.00 (postage) (total approx. U.S. $79.50). Journals are sent automatically by airmail to the U.S.A. and Canada at no extra cost and to Japan, Australia and New Zealand for a small additional postal charge. All earlier volumes (Vols. 1–103) except Vols. 23 and 28 are available at Dfl. 153.00 (U.S. $78.50), plus Dfl. 11.00 (U.S. $5.50) postage and handling, per volume.

Claims for issues not received should be made within three months of publication of the issue, otherwise they cannot be honoured free of charge.

Customers in the U.S.A. and Canada who wish to obtain additional bibliographic information on this and other Elsevier journals should contact Elsevier/North Holland Inc., Journal Information Center, 52 Vanderbilt Avenue, New York, NY 10017. Tel: (212) 867-9040.

PARIS
8~13 DECEMBER 1980
PORTE DE VERSAILLES

INTERNATIONAL LABORATORY SHOW 1980

in 1980, the most important international event in Europe concerning the Laboratory

On 25.000 M², 825 firms from 21 countries will make a presentation of techniques, methods and equipment relating to the laboratory

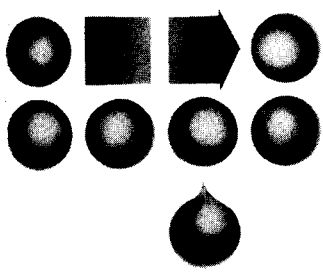

For details and entry-cards, please apply to:

SEPIC S.A.
40, Rue du Colisée
75381 PARIS CEDEX 08, France
Tel.: (1) 225.3776
Telex: 640450

STICHTING BEVORDERING FRANSE VAKBEURZEN
Prins Hendrikkade 20-21
1012 TL AMSTERDAM, The Netherlands
Tel. (020) 24 86 70 / 23 92 04
Telex: 12644 PROSA

THREE VOLUMES IN THE ANALYTICAL CHEMISTRY SYMPOSIA SERIES

Volume 4: NEW

Recent Developments in Mass Spectrometry in Biochemistry and Medicine, 6

Proceedings of the 6th International Symposium on Mass Spectrometry in Biochemistry and Medicine, Venice, 21 and 22 June, 1979

A FRIGERIO, *Mario Negri Institute for Pharmacological Research, Milan, Italy, and* M. McCAMISH, *University of Queensland, Brisbane, Australia (Editors)*

This book, comprising 52 papers, presents the latest research and developments in biochemistry, medicine, forensic science, drug research, clinical chemistry and pollution, as reported at the meeting.

Sections: Endogenous compounds : qualitative studies *(6 papers).* Endogenous compounds: quantitative studies *(14 papers).* Exogenous compounds: qualitative studies *(10 papers).* Exogenous compounds: quantitative studies *(5 papers).* Instrumentation and methodology *(12 papers).* Environmental studies *(5 papers).*

1980 about 550 pages
US $ 83.00/Dfl. 170.00
ISBN 0-444-41870-9

Volume 3: NEW

Recent Developments in Chromatography and Electrophoresis, 10

Proceedings of the 10th International Symposium on Chromatography and Electrophoresis, Venice, 19 and 20 June, 1979

A. FRIGERIO and M. McCAMISH *(Editors)*

Comprising a total of 34 papers, this volume is devoted to potential applications of chromatography and electrophoresis with special emphasis on newer developments.

Sections: Drug analysis *(9 papers).* Electrophoresis *(5 papers).* Analysis of endogenous compounds *(7 papers).* Environmental studies *(3 papers).* Fluorometry *(5 papers).* Instrumental *(5 papers).*

1980 350 pages
US $ 68.25/Dfl. 140.00
ISBN 0-444-41871-7

Volume 1:

Recent Developments in Chromatography and Electrophoresis

Proceedings of the 9th International Symposium on Chromatography and Electrophoresis, Riva del Garda, 15-17 May, 1978

A. FRIGERIO, *Mario Negri Institute for Pharmacological Research, Milan, Italy, and* L. RÉNOZ, *Belgian Society for Pharmaceutical Sciences, Belgium (Editors)*

These proceedings, providing 34 general reviews on chromatography and electrophoresis, cover a wide range of potential applications of these techniques.
Of interest to: research workers in chemistry, biochemistry, medicine, toxicology, drug metabolism, forensic science, clinical chemistry and pollution studies

1979 368 pages
US $ 58.50/Dfl. 120.00
ISBN 0-444-41785-0

ELSEVIER

P.O. Box 211,
1000 AE Amsterdam,
The Netherlands
52 Vanderbilt Avenue
New York, N.Y. 10017

The Dutch guilder price is definitive. US $ prices are subject to exchange rate fluctuations.

Analytica Chimica Acta, 119 (1980) 189—205

Review

THE DEVELOPMENT OF ROOM TEMPERATURE PHOSPHORESCENCE INTO A NEW TECHNIQUE FOR CHEMICAL DETERMINATIONS
Part 1. Physical Aspects of Room Temperature Phosphorescence

R. T. PARKER,[a] RICHARD S. FREEDLANDER[b] and R. BRUCE DUNLAP*
Department of Chemistry, University of South Carolina, Columbia, SC 29208 (U.S.A.)
(Received 29th February 1980)

SUMMARY

The development and physical aspects of room temperature phosphorescence are reviewed in this first part of a two-part series. Certain fundamental aspects of phosphorescence are presented. The novel phenomenon of room temperature phosphorescence (strong phosphorescence for organic compounds adsorbed on appropriate substrates) is then treated in detail. Specific attention is given to the nature of the support-phosphor interaction and the quenching effects of moisture and oxygen on room temperature phosphorescence. Thorough coverage is also given to the heavy-atom effect. The effects of the sample matrix on certain phosphorescent properties, such as lifetime, intensity and spectral characteristics, are mentioned.

Although fluorescence spectrometry has found widespread use in numerous areas of chemical analysis [1—3], phosphorimetric techniques have generally lagged far behind fluorimetry in practical applications. The number of experimental difficulties and limitations associated with traditional methods in phosphorimetry has been the primary factor in preventing broader application of this valuable technique. One particularly troublesome aspect of phosphorimetry has been the fact that most determinations were conducted at very low temperatures (typically 77 K) [4—7]. Since the phosphorescent state of organic molecules is quite susceptible to radiationless decay by molecular collision processes, supercooling of analyte solutions was found to be one of the few ways of observing strong phosphorescence from a broad spectrum of organic compounds [4—7]. However, recent developments have shown that a wide variety of organic compounds exhibit strong phosphorescence at room temperature when adsorbed on a suitable support such as cellulose, silica gel or sodium acetate [8—42]. These developments are opening up many new frontiers in the application of phosphorimetry to chemical problems and are providing additional insight into the phenomenon of phosphorescence of organic compounds.

[a]Present address: Monsanto Industrial Chemicals Company, Nitro, WV 25143, U.S.A.
[b]Present address: ICI Americas, Inc., Biological Research Center, P.O. Box 208, Goldsboro, NC 27530, U.S.A.

The development of room temperature phosphorescence will be presented in a two part series. This first part deals predominantly with the physical nature of the phenomenon. The second part concentrates on the practical analytical aspects of room temperature phosphorimetry. Although Part 1 is written largely from a physical standpoint, the information is invaluable in understanding and applying room temperature phosphorescence for analytical purposes.

ELECTRON TRANSITIONS AND THE PHOSPHORESCENT STATE OF ORGANIC MOLECULES

Phosphorescence has been observed in a wide variety of conjugated organic compounds and is generally distinguished from fluorescence by its long-lived afterglow upon extinguishing the exciting light source. The lifetime of fluorescence is usually between 10^{-9} and 10^{-7} s, while that of phosphorescence lies between 10^{-6} and 10 s [43]. A classic report by Lewis and Kasha in 1944 first identified the phosphorescent state as the triplet state [44]. This report also verified the pathways of triplet excitation and decay which were proposed somewhat earlier by Jablonski [45]. An updated version of the electron transitions associated with luminescence as proposed by Jablonski is shown in Fig. 1. For clarity, the various vibrational manifolds of the energy levels in the Jablonski diagram are not shown. These manifolds are responsible for the broad absorption and emission bands associated with electronic transitions of molecules having vibrational modes of freedom [46–48].

The ground state of most organic molecules is the singlet state (S_0). Absorption of electromagnetic radiation by a molecule in the S_0 state may promote the molecule to any one of several excited singlet states (S_n), depending on the frequency of the radiation (Fig. 1). Absorptions directly promoting molecules from the S_0 state to an excited triplet state are spin-forbidden and occur with very low probability [4, 49]. In the absence of photochemical reactions, a molecule having been excited to an S_n state may return to the ground state by radiative transitions and/or radiationless transitions. Radiationless transitions usually result in the production of heat energy. An excited molecule in an upper level S_n state will relax very rapidly (10^{-13}–10^{-10} s) by non-radiative means (internal conversion) to the lowest-excited singlet state (S_1) [4]. The molecule may now proceed back to the ground state by several of the basic pathways illustrated in Fig. 1. The radiative S_1 and S_0 transition gives rise to fluorescence. Internal conversion from the S_1 to S_0 state is also a possible course of relaxation to the ground state. Another pathway of deactivation requires that the molecule enter the triplet state in a process called intersystem crossing. This occurs in compounds where the S_1—T_1 energy levels are favorably spaced and involves the unpairing of the spins of two electrons. The lowest-excited triplet state (T_1) lies slightly lower in energy than the S_1 state due to the energy required in

spin pairing two electrons [43]. Once in the T_1 state, the molecule may return to the ground state by emission of radiation and/or by radiationless intersystem crossing (i.e. collisional deactivation). Emission by a T_1 to S_0 transition is termed phosphorescence, and the spin-forbidden nature of the process is responsible for the relatively long lifetime of phosphorescence. The term "spin forbidden" arises from the fact that transitions involving changes in spin multiplicity are not allowed by quantum mechanical selection rules, and such transitions occur slowly relative to spin allowed processes.

Other modes of excited state decay, not shown in Fig. 1, can sometimes play significant roles in the return of excited molecules to the ground state [4, 48, 50–52]. Electronic energy transfer from the excited molecule to impurities or the solvent (thus placing the impurity or the solvent in an excited state) has been characterized as a mode of deactivation of both singlet and triplet states. Energy transfer of this nature depends on close spacing of the energy levels of the donor and acceptor molecules [4, 50]. An appropriate acceptor molecule may also show luminescence upon relaxation to the ground state. This type of luminescence is sometimes referred to as sensitized luminescence [47]. Triplet state oxygen and other paramagnetic species are highly effective in deactivating excited triplet states [4, 50]. Such species must often be excluded in order to observe phosphorescence [4, 50, 52].

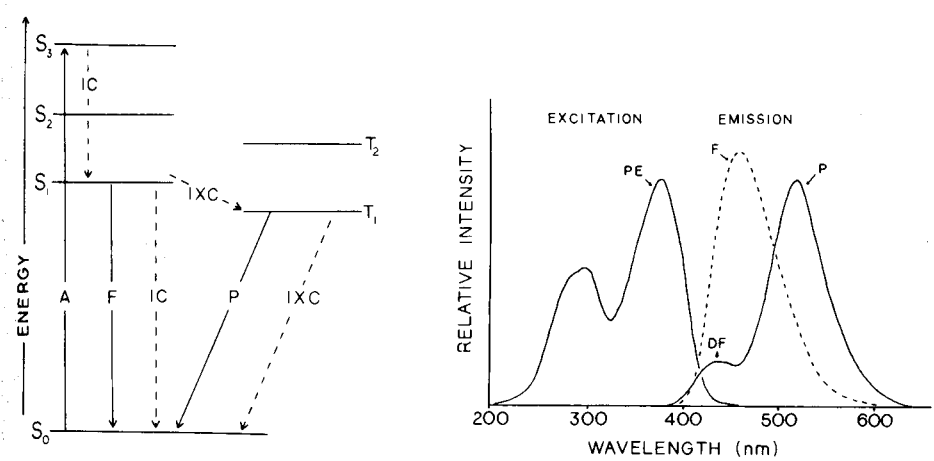

Fig. 1. Jablonski diagram of the electron transitions associated with luminescence in organic molecules. (A) Absorption; (F) fluorescence; (IC) internal conversion; (P) phosphorescence; (IXC) intersystem crossing.

Fig. 2. Fluorescence (------, emission from fluid solution) and room temperature phosphorescence (——, excitation and emission from compound adsorbed on paper) spectra of pterin-6-aldehyde. Intensities were arbitrarily adjusted and samples were prepared as described earlier [36]. (F) Normal fluorescence from fluid solution; (P) room temperature phosphorescence; (DF) delayed fluorescence; (PE) phosphorescence excitation spectrum.

Another deactivation pathway, which gives rise to a "slow fluorescence," is sometimes encountered [47, 50, 51]. In molecules having closely spaced S_1—T_1 energy levels, thermal energy can be sufficient to reactivate a molecule in the T_1 state back to the slightly higher energy S_1 state (Fig. 1). Upon return to the S_1 state, the molecule may relax to the ground state by fluorescence. However, in this case, the fluorescence will be delayed because of the time the molecule spends in the triplet state. This type of emission has been named E-type delayed fluorescence after eosin [51]. Delayed fluorescence due to triplet—triplet energy transfer has also been observed [47, 50, 51]. Fluorescence of this nature has been named P-type delayed fluorescence after pyrene [51].

Many luminescent compounds can relax by a combination of the pathways shown in Fig. 1 depending on the conditions. The rate constants of the various relaxation processes determine the most favorable deactivation pathways [4]. Pterin-6-aldehyde is representative of a class of compounds which is capable of phosphorescence, fluorescence and E-type delayed fluorescence. The compound shows all three luminescence processes simultaneously when adsorbed on filter paper at room temperature as shown in Fig. 2 [53]. Since this compound displays only fluorescence in fluid solution at room temperature, rapid collisional deactivation of the triplet state probably prevents the observation of phosphorescence, and delayed fluorescence, from pterin-6-aldehyde under these conditions. Figure 2 also illustrates the relative positions of fluorescence and phosphorescence emission bands. Phosphorescence emission occurs at longer wavelengths than fluorescence due to the lower energy of the triplet state [45—48]. Delayed fluorescence occurs at the same wavelengths as normal fluorescence.

CONDITIONS FOR THE OBSERVATION OF PHOSPHORESCENCE

Strong phosphorescence of organic compounds is not commonly observed in fluid solution at room temperature [48, 52, 54]. Because of the long lifetime of the triplet state, collisional deactivation is highly effective in bringing about radiationless decay of triplet states in fluid media. Quenching of the triplet state by small amounts of dissolved oxygen is also very efficient in preventing phosphorescence in fluid solution. As such, only a limited number of cases of phosphorescence from fluid solution have been observed, and usually thorough degassing of the solution is necessary in order to prevent quenching by oxygen [52, 55—60]. Phosphorescence from fluid solution is also too weak in many cases to be useful analytically [3].

Several methods have been employed to restrict collisional deactivation and thus allow the observation of strong phosphorescence from organic compounds. One of the most common techniques is supercooling solutions to a rigid glass state [4—7, 61—66]. Liquid nitrogen (77 K) is usually employed as the coolant. Molecular collisions are greatly restricted at such low temperatures, and strong phosphorescence can be observed even in the presence

of oxygen. In the past, most analytical applications of phosphorimetry have relied on low temperature procedures.

Several techniques have been utilized to observe phosphorescence at room temperature. For example, some compounds show phosphorescence in the gas phase [49, 50, 54, 67]. At low pressures, the frequency of molecular collisions is reduced and the triplet state has a greater chance of radiative decay. A number of compounds show strong phosphorescence when embedded in media which are rigid at room temperature [68]. For example, many classic studies on phosphorescence were conducted with phosphors embedded in boric acid glasses [44, 49, 69, 70]. Rigid glasses have also been prepared from a variety of other materials such as glucose, citric acid and tartaric acid [69, 71]. A number of studies have used various plastics such as poly(methylmethacrylate) and poly(vinyl alcohol) as rigid media for embedded phosphors [72—78]. Phosphorescence has even been observed from the tryptophan residues in wool keratin at room temperature [79—81]. Although the room temperature techniques thus far discussed have provided fruitful physical studies of the phosphorescent state, these methods have been of very limited analytical value because of considerable problems with uniform sample preparation and various time consuming procedures [4].

ROOM TEMPERATURE PHOSPHORESCENCE

Recent reports by Roth [8] and by Schulman and Walling [9, 10] have revealed that a number of polar or ionic organic compounds exhibit phosphorescence at room temperature when adsorbed on a suitable material such as silica, alumina or cellulose. Thorough drying of the sample was found necessary in order to observe the emission. Since the appearance of these reports, the phenomenon has attracted considerable attention, resulting in a number of physical and analytical studies [11—36]. The phenomenon is now generally referred to as room temperature phosphorescence (r.t.p.) and is rapidly finding its place as a new analytical technique. In order not to confuse this phenomenon with other techniques of observing phosphorescence at room temperature, r.t.p. should be strictly defined as phosphorescence of organic compounds adsorbed on a solid support material.

Although the studies by Roth [8] and by Schulman and Walling [9, 10] first illustrated that r.t.p. is a general property of a large number of polar or ionic organic compounds, isolated cases of r.t.p. had been observed prior to these reports. Several of these cases were pointed out in a recent communication by Lloyd and Miller [42]. Our literature search has revealed that as early as 1896, phosphorescence was observed from dye stuffs adsorbed on solid gels, such as gelatine [82]. In 1943, Franck and Pringsheim reported r.t.p. from trypaflavine adsorbed on silica gel, paper and gelatine [83]. Other early accounts of r.t.p. have also been noted from adsorbed compounds [68, 69]; however, these studies failed to recognize the large number of compounds capable of r.t.p. and the usefulness of this phenomenon in

analytical applications. The scope of the phenomenon was not fully revealed until the report by Schulman and Walling in 1973 [10].

INTERACTIONS BETWEEN THE PHOSPHOR AND SUPPORT MATERIAL

R.t.p. has been viewed as a unique phenomenon because of the simplicity involved in observing strong phosphorescence at room temperature [8—11]. For example, numerous organic compounds show strong phosphorescence when adsorbed on filter paper and thoroughly dried [10—12]. Other methods of observing strong phosphorescence require much more stringent conditions to prevent the radiationless decay of the triplet state as discussed previously. Schulman and Walling [10] suggested that surface adsorption of the phosphor molecules held them rigid enough to restrict collisional deactivation of the triplet state. Their studies showed that many ionic organic compounds (such as salts of carboxylic acids) displayed very intense r.t.p. when adsorbed on paper. Nonionic forms of the compounds showed little or no phosphorescence under the same conditions [10]. Since adsorption of an ionic compound should be considerably stronger than with the nonionic counterpart, adsorption interactions appeared to be a primary factor in the observation of r.t.p. Subsequent studies have shown that molecules capable of strong adsorption interactions with the support material generally prove to be the most intense phosphors at room temperature [12, 17, 20, 24, 31, 32].

In a study by Winefordner et al. [12] a trend was noted between compounds with the most ionic sites and the efficiency of r.t.p. emission from the compounds adsorbed on paper. The emission intensity ratio of r.t.p. to l.t.p. (low temperature phosphorescence) serves as an index for this effect. Higher ratios infer tighter binding of the phosphor to the support, and compounds with the most ionic sites generally have the highest r.t.p./l.t.p. ratios. In a similar fashion, Schulman and Parker have shown that reducing the polarity of the adsorbent can drastically decrease the intensity of r.t.p. from ionic compounds. This was demonstrated by comparing the r.t.p. intensities of compounds adsorbed on filter paper with those of the same compound adsorbed on similar filter paper which had been silanized to reduce polarity. A 90% reduction in phosphorescence intensity was reported for sodium 1-naphthoate upon switching from a regular paper support to a silanized paper support.

Schulman and Parker extended the adsorption hypothesis of r.t.p. and suggested that hydrogen bonding of the phosphor to the support material might serve as an important means of restricting collisional deactivation of the phosphor in some cases [17]. The experiments by these workers using silanized paper supports indicated that reducing the number of hydroxyl groups on the adsorbent, thereby reducing the hydrogen bonding interactions between the support and the phosphor, produced a concomitant decrease in r.t.p. intensity from the samples. Also, these studies showed a progressive increase in the level of r.t.p. quenching for samples exposed to atmospheres

of increasing humidity [17]. These results indicate that moisture might be competing with the phosphor molecule for hydrogen bonding sites on the adsorbent thus increasing the mobility of the phosphor and the chances of collisional deactivation. Von Wandruszka and Hurtubise, employing i.r. spectrometry, added evidence supporting the involvement of hydrogen bonding in a study on the r.t.p. of *p*-aminobenzoic acid and other compounds adsorbed on sodium acetate [24]. In the case of *p*-aminobenzoic acid, which is hydrogen-bonded to the adsorbent according to i.r. data, strong r.t.p. was observed. *o*-Aminobenzoic acid did not show r.t.p.; however, i.r. measurements revealed no strong hydrogen bonding interactions with the adsorbent. These findings are probably due to intramolecular hydrogen bonding between the amino and carboxyl groups in *o*-aminobenzoic acid. Additional evidence for the role of hydrogen bonding in r.t.p. was provided in a study of phthalic acid isomers and several related compounds adsorbed on silica gel [31]. Compounds with the potential of strong hydrogen bonding to the support provided more intense r.t.p. than similar compounds with less polar functional groups and presumably weaker hydrogen bonding capability. For example, the r.t.p. of terephthalic acid was 9 times greater than that of terephthalamide, and terephthaldehyde displayed no r.t.p. emission. Low temperature phosphorescence measurements indicated that these results were not simply artifacts of drastically different quantum yields at 77 K. When dried terephthalic acid samples were submerged in n-hexane, virtually no loss in r.t.p. intensity was noted [31]. This result would be expected if hydrogen bonding was responsible for immobilizing the phosphor molecules. Dipping samples in water resulted in the total quenching of r.t.p. This agrees with the assumption of Schulman and Parker that moisture quenches r.t.p. by disrupting the hydrogen bonding between the support material and the phosphor [17].

R.t.p. has also been observed from several nonpolar polynuclear aromatic hydrocarbons adsorbed on paper [18, 19, 29, 30, 33] or sodium acetate [29]. These findings are somewhat unexpected since strong adsorption interactions are difficult to envisage between a nonpolar compound and a polar adsorbent. In order to observe r.t.p. from the polynuclear aromatic compounds, however, it is necessary to add a heavy atom perturber such as silver nitrate to the sample. Also, the r.t.p. emission from the nonpolar compounds is generally weaker than the emission from polar or ionic organic compounds. Enhancement of the phosphorescence quantum efficiency by the heavy-atom effect might be one reason for the observation of r.t.p. from these compounds. Even in the presence of a heavy atom, the compounds should still be quite susceptible to collisional deactivation. Another possible explanation of this phenomenon might lie in the formation of polar π-complexes between the aromatic compound and the heavy atom perturber [29]. In this case, adsorption of the polar π-complex could provide protection against collisional deactivation. Recent reports by Boutilier and Winefordner involving the effects of thallium and silver ions on phosphorescence at 77 K have indicated that the r.t.p. of phenanthrene and other aromatic hydrocarbons in the

presence of those ions may not be strictly due to the heavy-atom effect [84]. Based on results from their studies [84] and earlier work [29], these researchers suggested that other factors "such as the way the molecule is held on the paper are also of major importance."

Although the nature of the support-phosphor interaction is not yet fully understood, compounds capable of strong adsorption interactions with the support material appear to be the most likely candidates for r.t.p. Molecules with the ability to hydrogen bond to the adsorbent generally offer excellent potential of showing r.t.p. Still, a number of anomalies exist, and the picture could be much more complex than immobilization of the phosphor purely because of ionic and/or hydrogen-bonding interactions between the phosphor and the support. Investigations in our laboratories currently suggest the involvement of additional factors.

THE EFFECTS OF MOISTURE ON ROOM TEMPERATURE PHOSPHORESCENCE

Schulman and Walling [9, 10] noted the necessity of thorough drying in order to observe r.t.p. from compounds adsorbed on paper and other supports. This point cannot be over-emphasized since r.t.p. cannot be observed (except in few special cases [16, 24]) unless the sample is adequately dried. In many cases, drying under a hot-air blow dryer or in an oven for a few minutes is sufficient [10, 11]; however, in other instances, drying in a desiccator for an extended period of time may be necessary [36]. In any case, once a sample is exposed to the natural humidity in air, quenching of the r.t.p. emission occurs [10, 11, 14, 17, 36]. Depending on the particular compound involved, visible phosphorescence may cease in a matter of several seconds or may persist as long as several minutes upon exposure of the sample to naturally humid air.

The effects of moisture on the r.t.p. of sodium 4-biphenylcarboxylate adsorbed on paper have been investigated in detail [17]. The r.t.p. intensity from this compound was measured as a function of humidity in atmospheres ranging in relative humidity from 3—100%. The emission intensity was found to decrease quite dramatically in atmospheres of increasing relative humidity. For example, a 90% reduction of the r.t.p. intensity was noted for samples in argon at 40% relative humidity as opposed to the intensity obtained in dry argon. Only an 8.4% reduction in emission intensity was noted in an atmosphere of 8.5% relative humidity. Since hydrogen bonding of sodium 4-biphenylcarboxylate to the paper support was proposed to be the primary adsorption process, the reduction in the r.t.p. emission was ascribed to the displacement of the hydrogen-bound phosphor from the paper by water. Radiationless collisional deactivation should then predominate over r.t.p.

Von Wandruszka and Hurtubise [16, 24] noted that the r.t.p. of *p*-aminobenzoic acid (PABA) adsorbed on sodium acetate was quite insensitive to quenching by moisture in humid air. When samples were prepared by adding anhydrous ethanolic solutions of PABA to anhydrous sodium acetate, r.t.p.

could be observed from these samples even without the evaporation of the solvent [16]. Samples prepared from aqueous media, however, required thorough drying in order to observe r.t.p. Also, the addition of water to the ethanolic samples destroyed the r.t.p. [53]. Prolonged exposure of PABA samples on sodium acetate to humid air ultimately leads to the quenching of r.t.p. emission; however, this rate is much slower than those found with similar samples adsorbed on paper. The sodium acetate matrix appears to afford some protection from the quenching effects of humid air for several other compounds [24]. Exactly why this is the case is not yet clear, and no quantitative data on the quenching effects of humidity for the sodium acetate support are available for comparison with the data of Schulman and Parker on the cellulose support [17].

R.t.p. has been noted from several compounds in the adsorbed state while the adsorbent was "wet" with a nonaqueous solvent [16, 26]. The case of r.t.p. from PABA adsorbed on sodium acetate in the presence of anhydrous ethanol was discussed earlier [16]. A communication by Lloyd has revealed that a number of compounds show r.t.p. when samples are "wet" with anhydrous diethyl ether [26]. Lloyd used an adsorbent which was prepared by mixing the lint scraped from Whatman 544 paper with crushed quartz. The adsorbent mixture was packed in a flow-through cell and the sample was applied by injecting the analyte solution into the cell. In order to observe r.t.p., the applied sample had to be rinsed with dry diethyl ether. This was necessary in order to remove traces of moisture from the sample. Rinsing the sample with diethyl ether that contained very little water (95 μg ml^{-1}) reduced the r.t.p. intensity by 47% as compared to sodium-dried diethyl ether [26]. In most cases, r.t.p. is so sensitive to the presence of moisture that this phenomenon might find practical use in the determination of trace amounts of moisture.

THE EFFECTS OF OXYGEN ON ROOM TEMPERATURE PHOSPHORESCENCE

Oxygen is a potent quenching agent of the excited triplet state [2–4]. Interaction of triplet state oxygen (the natural ground state of oxygen) with a molecule in an excited triplet state results in the radiationless return of the excited triplet to the ground singlet state and the production of excited singlet-state oxygen. In view of this, it is somewhat surprising that strong r.t.p. occurs in free contact with air or even in pure oxygen [9, 10]. Early reports suggested that r.t.p. is "completely" insensitive to oxygen quenching in dry atmospheres and that the sample matrix somehow inhibits oxygen quenching [10]. Subsequent studies with paper as the sample matrix have shown that r.t.p. is quenched to some degree by oxygen, although this is not serious in dry atmospheres [17, 18]. The r.t.p. emission of sodium 4-biphenylcarboxylate was reduced 30% when the sample was dried under argon and then exposed to dry oxygen [17]. The same sample shows a 55% reduction in r.t.p. emission when dried from the beginning under oxygen as

compared to argon [17]. These differences in oxygen quenching based on drying techniques seem to indicate some oxygen is trapped in the sample matrix when it is dried in the presence of oxygen. Winefordner and co-workers [18] have also noted that r.t.p. signals are generally 50% lower when samples are dried in pure oxygen as opposed to nitrogen. Other workers using samples adsorbed on silica gel have noted that r.t.p. signals are slightly lower in air than in other gases such as nitrogen or helium [32].

Bower and Winefordner [29] have indicated that certain polynuclear aromatic compounds adsorbed on paper are quite sensitive to oxygen quenching in air. The r.t.p. emission of pyrene adsorbed on paper was found to be approximately 75% lower in air than in nitrogen or argon. These results seem to be peculiar to polynuclear aromatic samples. Such strong quenching effects in air have not been reported for highly polar compounds, whose r.t.p. intensities generally are reduced less than 25% in air as compared to inert atmospheres such as nitrogen, helium or argon [18, 32]. Since polynuclear aromatics should not be as strongly adsorbed to the support material as polar compounds, it appears likely that the lack of strong interaction of the phosphor with the support material has reduced the ability of the sample matrix to inhibit oxygen quenching.

Using paper as the sample matrix, Schulman and Parker have demonstrated that oxygen quenching occurs much more freely in humid atmospheres [17]. It was shown that the efficiency of oxygen quenching increases dramatically as the relative humidity of the atmosphere increases. These workers proposed that moisture weakens the support-phosphor interaction and integrity of the sample matrix thus allowing increased penetration of oxygen to the phosphor. Results from this study confirmed that a dry cellulose matrix affords protection against oxygen quenching. As long as the sample is protected from moisture, r.t.p. can be carried out quite successfully in air or even pure oxygen. However, for maximum r.t.p. intensity, inert atmospheres are recommended. Also, the presence of oxygen has been implicated in reducing the precision of r.t.p. measurements [17].

THE HEAVY-ATOM EFFECT

The external heavy-atom effect was first reported by Kasha in the case of the effects of ethyl iodide on the singlet—triplet transitions of 1-chloronaphthalene [85]. Since that report, it has been noted generally that the presence of heavy atoms such as iodide can significantly affect luminescence quantum yields [48]. Most commonly, the addition of heavy atoms results in a decrease in the fluorescence yield and a corresponding increase in the phosphorescence yield. An internal heavy-atom effect, which comes about when the heavy atom is chemically bound to the compound, is also known and was discovered somewhat earlier [86].

The heavy-atom effect has been ascribed to increased spin-orbit coupling induced by the heavy-atom perturber [85—90]. Under these conditions,

spin-forbidden transitions are more likely to occur. One major aspect of the heavy-atom effect is that the singlet—triplet intersystem crossing rate is enhanced (Fig. 1) [48, 90]. This results in a lowering of the fluorescence yield and an increased triplet yield. The presence of the heavy atom can also increase both the radiative and radiationless rates of triplet state decay to the ground singlet state (Fig. 1) [48]. Although the radiative decay is generally more strongly enhanced, the opposite effect has also been noted [21, 48, 91].

Seybold and White [13] first demonstrated the external heavy-atom effect on r.t.p. These workers found a 20-fold enhancement in the r.t.p. of sodium 2-naphthalenesulfonate when sodium iodide was added to the sample. Several similar compounds also showed strong r.t.p. enhancement in the presence of sodium iodide. Sample solutions were made up in 1 M sodium iodide, and filter paper was used as the adsorbent in this study. Since the report of Seybold and White, a number of workers have employed the heavy-atom effect to enhance r.t.p. intensities [15, 18, 19, 21, 22, 29, 40]. Sodium iodide has been used to increase the intensity and lower the detection limit of a selection of biologically important compounds adsorbed on paper [15]. Jakovljevic [22] has reported the effects of a variety of heavy atoms (such as thallium, lead, thorium and many others) on the r.t.p. intensity of cinoxicin adsorbed on paper. As mentioned earlier, r.t.p. has been observed from several polynuclear aromatic compounds with the aid of heavy atom perturbers such as silver, lead, and thallium [18, 19, 29, 40]. Bower and Winefordner [29] investigated the effects of several heavy metal ions on the r.t.p. of polynuclear aromatics adsorbed on paper and found the following enhancement trend: $Tl^+ > Ag^+ > Pb^{2+} > Hg^{2+}$. It has been suggested that π-complex formation between the heavy metal ion and the polynuclear aromatic might be providing an internal heavy-atom effect in some of these cases [20, 29]. Although it appears that the heavy-atom effect plays a significant role in the r.t.p. of polynuclear aromatics, caution should be exercised in explaining these emissions totally in terms of the heavy-atom effect [29, 84].

The addition of heavy atom perturbers to r.t.p. samples generally results in shorter phosphorescence lifetimes and a considerable reduction in fluorescence emission intensity as would be expected. White and Seybold [21] have investigated in detail the effects of the addition of various sodium halide salts on the r.t.p. of sodium 2-naphthalenesulfonate adsorbed on paper. The enhancement in r.t.p. follows the expected trend of $I^- > Br^- > Cl^- > F^-$. Virtually no enhancement in r.t.p. was noted with fluoride or chloride ions; however, appreciable enhancement was displayed with bromide and an even greater enhancement was observed with iodide. The r.t.p. intensity was also found to be highly dependent on the concentration of the heavy atom perturber. The phosphorescence intensity progressively increased as the halide concentration was increased; however, the enhancement effect appeared to level off as halide concentrations in the sample solutions surpassed the 1 M level.

The enhancement of phosphorescence by heavy atom perturbers is not

totally due to an increase in the intersystem crossing rate [21, 48, 84]. The increase in r.t.p. from sodium 2-naphthalenesulfonate upon the addition of sodium iodide has been reported to be much too large to be accounted for strictly in terms of an increased intersystem crossing rate [21]. It appears that the radiative rate of triplet state deactivation has also been enhanced with respect to the radiationless pathway. Similar observations have been made at low temperature [84]. The opposite case has also been observed by Parker et al. [36]. A decline in the r.t.p. of pterin-6-carboxylate (sodium salt) was noted upon the addition of iodide. Although an enhancement in the intersystem crossing rate seemed likely as evidenced by a decline in both normal fluorescence [53] and the delayed fluorescence to phosphorescence ratios [36], the expected enhancement in phosphorescence was not realized. These workers speculated that the radiationless decay of the triplet state had been increased with respect to the radiative mode of decay. In support of this contention, it was noted that the presence of iodide seemed to disrupt the sample matrix as evidenced by increased susceptibility of the sample to the quenching effects of moisture (Fig. 3) [53].

SPECTRAL CHARACTERISTICS AND THE SAMPLE MATRIX

In phosphorescence as well as fluorescence, two spectra can be obtained from the compound [2, 3]. The excitation spectrum (sometimes called the activation spectrum) corresponds qualitatively to the absorption spectrum

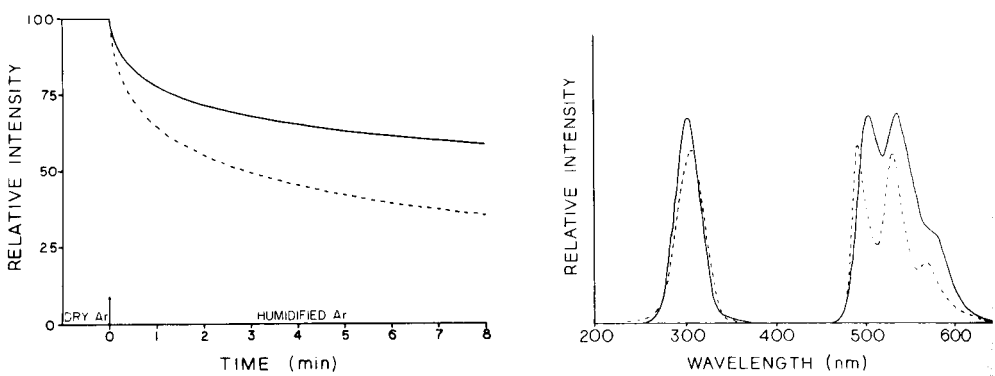

Fig. 3. The quenching effects of moisture on the r.t.p. intensity of pterin-6-carboxylic acid adsorbed on sodium acetate-treated paper containing KI (------) and without KI (——). The r.t.p. intensity of both samples was arbitrarily adjusted to 100% in dry argon. The samples were exposed to humid argon (19% relative humidity) at time = 0 min, and the decline in relative intensity as a function of time was monitored. Samples were prepared in a manner similar to that previously reported [36].

Fig. 4. Phosphorescence spectra of sodium 1-naphthoate at 77 K (------) and 300 K (——). The r.t.p. spectrum was made from the analyte adsorbed on paper. The low temperature spectrum was obtained from a supercooled solution of the analyte. Intensities were arbitrarily adjusted, and samples were prepared as described earlier [17].

and represents the transition from the ground state to the excited singlet state. The emission spectrum is that of the actual luminescence process (Fig. 2). As mentioned previously, phosphorescence occurs at longer wavelengths than fluorescence. Quite commonly, both excitation and emission spectra are displayed together, and caution should be exercised to distinguish the two individual spectra.

R.t.p. spectral features are very similar to those observed at low temperature as illustrated in Fig. 4 [10, 11]. Spectra at room temperature generally provide less resolution than at low temperature due to increased vibrational freedom of the molecule at the higher temperature. Emission peaks are also shifted to slightly longer wavelengths at room temperature, although shifts are typically less than 10 nm. R.t.p. spectra may sometimes possess a band where fluorescence normally occurs that is not present in the low temperature spectrum (Fig. 5) [36]. This is the result of E-type delayed fluorescence and is not observed at low temperature owing to insufficient thermal energy to promote this emission. R.t.p. offers a very convenient means of observing delayed fluorescence in compounds with close enough spacing between the S_1 and T_1 levels since adequate thermal energy is available to promote reverse intersystem crossing in this situation.

The nature of the adsorbent employed in r.t.p. usually has only a minor effect on spectral features. When comparing r.t.p. spectra of the same compound adsorbed on different support materials, virtually no differences can be discerned in many cases (Fig. 6) [53]. Sometimes minor wavelength shifts (usually less than 10 nm) may be noted. The addition of heavy atom perturbers to r.t.p. samples usually results in some loss of spectral detail

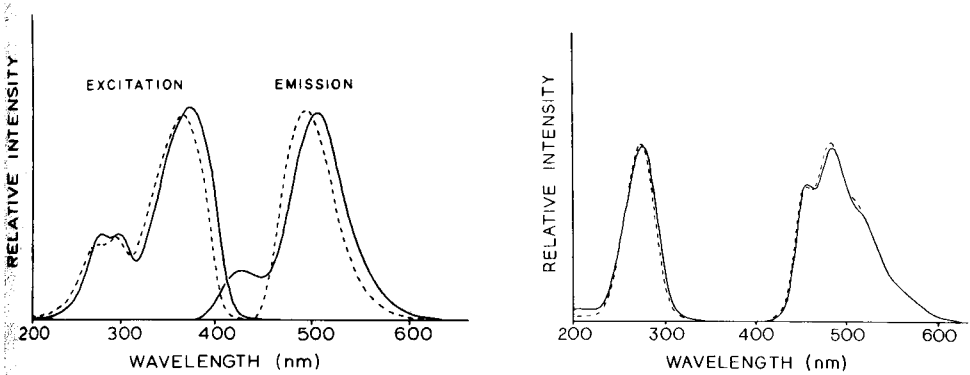

Fig. 5. R.t.p. excitation and emission spectra of pterin-6-carboxylic acid at 77 K (------) and 300 K (——). Both 77 K and 300 K spectra were made from samples adsorbed on sodium acetate treated paper. Intensities were arbitrarily adjusted. (Reprinted with permission from Anal. Chem., 51 (1979) 1921. Copyright 1979, the American Chemical Society.)

Fig. 6. Comparison of the r.t.p. spectra of 4-biphenylcarboxylate adsorbed on paper (——) and potassium trifluoroacetate (------). Intensities were arbitrarily adjusted, and samples were prepared in a manner similar to that reported earlier [36].

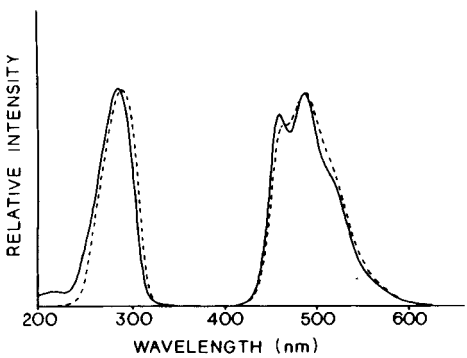

Fig. 7. Comparison of the r.t.p. spectra of sodium 4-biphenylcarboxylate adsorbed on paper (——) and on potassium iodide-treated paper (------). Intensities were arbitrarily adjusted, and samples were prepared as described earlier [36].

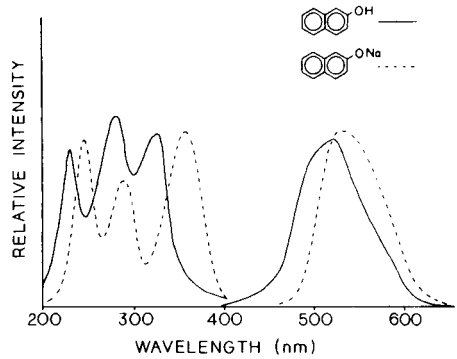

Fig. 8. Comparison of the r.t.p. spectra of 2-naphthol (——) and the sodium salt of 2-naphthol (------) adsorbed on a paper support. Intensities were arbitrarily adjusted, and 0.1 mM solutions of analyte were used to prepare the samples in a manner similar to that described earlier [36].

(Fig. 7) [53]. As would be expected, different ionic forms of a compound can show considerable spectral shifts in some instances; therefore, the pH of sample solutions can have a significant effect on the r.t.p. spectrum [10, 14]. This is illustrated in the case of 2-naphthol and its sodium salt (Fig. 8) [53]. Although no cases have been reported, it seems likely that changing from a basic support such as sodium acetate to an acidic support such as boric acid could produce similar pH effects.

While the sample matrix may only have minor effects on spectral features, r.t.p. intensities and lifetimes can be significantly affected by the sample matrix. The considerable enhancements in intensity and reductions in lifetime that occur when heavy atoms are added to the sample matrix were noted earlier. Niday and Seybold [25] have studied the lifetime of sodium 2-naphthalenesulfonate adsorbed on paper in the presence of a number of other added substances. Compounds such as ammonium chloride, potassium hydroxide, boric acid and others were found to increase the r.t.p. lifetime when added to the paper sample matrix. Although the effects on r.t.p. intensity were reported to be somewhat unpredictable, notable enhancement in the r.t.p. intensity and lifetime was observed when sucrose was added to the paper matrix. Other workers have also reported phosphorescence intensity enhancements when agents like sodium acetate or sodium citrate were added to samples adsorbed on paper [29, 36]. Finally, r.t.p. lifetimes tend to be somewhat shorter than those measured at low temperature [20, 25]; however, r.t.p. lifetimes typically fall in the respectable range of 0.1 to 1 s [10, 25].

CONCLUSION

The novel phenomenon of room temperature phosphorescence is providing many fruitful studies on the physical aspects of phosphorescence. New insights into the heavy-atom effect, delayed fluorescence, triplet quenching by oxygen and collisional deactivation processes have been gained by the study of this phenomenon. In this laboratory novel r.t.p. investigations are currently being concluded, involving cases of intramolecular energy transfer in certain bichromophoric molecules. R.t.p. is rapidly finding its place as a valuable analytical technique because of the extreme selectivity and sensitivity of the method. Part 2 of this article [92] presents an in-depth look at the practical analytical side of room temperature phosphorimetry.

These investigations were supported by NIH grant CA12842 from the National Cancer Institute. R. Bruce Dunlap is the recipient of a Faculty Research Award (FRA-144) from the American Cancer Society.

REFERENCES

1 S. Udenfriend, Fluorescence Assay in Biology and Medicine, Vol. I, Academic Press, New York, 1962.
2 S. Udenfriend, Fluorescence Assay in Biology and Medicine, Vol. II, Academic Press, New York, 1969.
3 G. G. Guilbault, Practical Fluorescence, M. Dekker, New York, 1973.
4 S. K. Lower and M. A. El-Sayed, Chem. Rev., 66 (1966) 199.
5 C. A. Parker and C. G. Hatchard, Analyst, 87 (1963) 664.
6 J. J. Aaron and J. D. Winefordner, Talanta, 22 (1975) 707.
7 C. M. O'Donnell and J. D. Winefordner, Clin. Chem., (Winston-Salem, NC), 21 (1975) 285.
8 M. Roth, J. Chromatogr., 30 (1967) 276.
9 E. M. Schulman and C. Walling, Science, 178 (1972) 53.
10 E. M. Schulman and C. Walling, J. Phys. Chem., 77 (1973) 902.
11 R. A. Paynther, S. L. Wellons and J. D. Winefordner, Anal. Chem., 46 (1974) 736.
12 S. L. Wellons, R. A. Paynther and J. D. Winefordner, Spectrochim. Acta, Part A, 30 (1974) 2133.
13 P. G. Seybold and W. White, Anal. Chem., 47 (1975) 1199.
14 E. M. Schulman, J. Chem. Educ., 53 (1976) 522.
15 T. Vo-Dinh, E. Lue Yen and J. D. Winefordner, Anal. Chem., 48 (1976) 1186.
16 R. M. A. von Wandruszka and R. J. Hurtubise, Anal. Chem., 48 (1976) 1784.
17 E. M. Schulman and R. T. Parker, J. Phys. Chem., 81 (1977) 1932.
18 T. Vo-Dinh, G. L. Walden and J. D. Winefordner, Anal. Chem., 49 (1977) 1126.
19 T. Vo-Dinh, E. Lue Yen and J. D. Winefordner, Talanta, 24 (1977) 146.
20 T. Vo-Dinh and J. D. Winefordner, Appl. Spectrosc. Rev., 13 (1977) 261.
21 W. White and P. G. Seybold, J. Phys. Chem., 81 (1977) 2035.
22 I. M. Jakovljevic, Anal. Chem., 49 (1977) 2048.
23 R. M. A. von Wandruszka and R. J. Hurtubise, Anal. Chim. Acta, 93 (1977) 331.
24 R. M. A. von Wandruszka and R. J. Hurtubise, Anal. Chem., 49 (1977) 2164.
25 G. J. Niday and P. G. Seybold, Anal. Chem., 50 (1978) 1577.
26 J. B. F. Lloyd, Analyst, 103 (1978) 775.
27 C. G. de Lima and E. M. de M. Nicola, Anal. Chem., 50 (1978) 1658.
28 E. L. Y. Bower and J. D. Winefordner, Anal. Chim. Acta, 101 (1978) 319.

29 E. L. Y. Bower and J. D. Winefordner, Anal. Chim. Acta, 102 (1978) 1.
30 T. Vo-Dinh and R. B. Gammage, Anal. Chem., 50 (1978) 2054.
31 C. D. Ford and R. J. Hurtubise, Anal. Chem., 50 (1978) 610.
32 C. D. Ford and R. J. Hurtubise, Anal. Chem., 51 (1979) 659.
33 E. L. Y. Bower and J. D. Winefordner, Appl. Spectrosc., 33 (1979) 9.
34 T. Vo-Dinh and R. B. Gammage, Anal. Chim. Acta, 107 (1979) 261.
35 R. T. Parker, R. S. Freedlander, E. M. Schulman and R. B. Dunlap, in R. L. Kisliuk and G. M. Brown (Eds.), Chemistry and Biology of Pteridines, Elsevier-North Holland, New York, 1979, p. 61.
36 R. T. Parker, R. S. Freedlander, E. M. Schulman and R. B. Dunlap, Anal. Chem., 51 (1979) 1921.
37 T. Vo-Dinh, R. B. Gammage, A. R. Hawthorne and J. H. Thorngate, Environ. Sci. Technol., 12 (1978) 1297.
38 G. L. Walden and J. D. Winefordner, Appl. Spectrosc., 33 (1979) 166.
39 M. L. Meyers and P. G. Seybold, Anal. Chem., 51 (1979) 1609.
40 T. Vo-Dinh and J. R. Hooyman, Anal. Chem., 51 (1979) 1915.
41 J. J. Aaron, E. M. Kaleel and J. D. Winefordner, J. Agric. Food Chem., 27 (1979) 1233.
42 J. B. F. Lloyd and J. N. Miller, Talanta, 26 (1979) 180.
43 D. G. Peters, J. M. Hayes and G. M. Hieftje, Chemical Separations and Measurements, W. B. Saunders, Philadelphia, 1974.
44 G. N. Lewis and M. Kasha, J. Am. Chem. Soc., 66 (1944) 2100.
45 A. Jablonski, Z. Phys., 94 (1935) 38.
46 R. S. Becker, Theory and Interpretation of Fluorescence and Phosphorescence, J. Wiley, New York, 1969.
47 J. D. Winefordner, S. G. Schulman and T. C. O'Haver, Luminescence Spectrometry in Analytical Chemistry, J. Wiley, New York, 1972.
48 S. G. Schulman, Fluorescence and Phosphorescence Spectroscopy: Physiochemical Principles and Practice, Pergamon Press, Elmsford, NY, 1977.
49 G. N. Lewis and M. Kasha, J. Am. Chem. Soc., 67 (1945) 994.
50 P. Seybold and M. Gouterman, Chem. Rev., 65 (1965) 413.
51 C. A. Parker and C. G. Hatchard, Trans. Faraday Soc., 57 (1961) 1894.
52 C. A. Parker, Photoluminescence of Solutions, Elsevier, New York, 1968, pp. 45—46.
53 R. T. Parker, R. S. Freedlander and R. B. Dunlap, 1978, unpublished results.
54 M. Zander, Phosphorimetry, Academic Press, New York, 1968, p. 117.
55 R. B. Bonner, M. K. DeArmond and G. H. Wahl, Jr., J. Am. Chem. Soc., 94 (1972) 988.
56 E. Vander Donckt, M. Matagne and M. Sapir, Chem. Phys. Lett., 20 (1973) 81.
57 L. Giering, M. Berger and C. Steel, J. Am. Chem. Soc., 96 (1974) 953.
58 K. Kalyanasundaram, F. Grieser and J. K. Thomas, Chem. Phys. Lett., 51 (1977) 501.
59 Y. J. Lee, W. A. Summer and J. B. Burr, Tetrahedron, 34 (1978) 2861.
60 K. Yamamoto, T. Takemura and H. Baba, Bull. Chem. Soc. Jpn., 51 (1978) 729.
61 H. C. Hollifield and J. D. Winefordner, Anal. Chem., 40 (1978) 1759.
62 R. J. Lukasiewiez, P. A. Rozynes, L. B. Sanders and J. D. Winefordner, Anal. Chem., 44 (1972) 237.
63 R. J. Lukasiewiez, J. J. Mousa and J. D. Winefordner, Anal. Chem., 44 (1972) 1339.
64 E. L. Wehry, Fluoresc. News, 8 (1974) 21.
65 J. D. Winefordner and P. A. St. John, Anal. Chem., 35 (1963) 2211.
66 R. A. Zweidinger and J. D. Winefordner, Anal. Chem., 42 (1970) 639.
67 N. A. Borisevich and A. A. Kotov, Spectrosc. Lett., 11 (1978) 465.
68 P. Pringsheim, Fluorescence and Phosphorescence, J. Wiley, New York, 1965.
69 G. N. Lewis, D. Lipkin and T. M. Magel, J. Am. Chem. Soc., 63 (1941) 3005.
70 M. Kasha, Chem. Rev., 41 (1947) 401.
71 G. Oster, J. Joussot-Dubien and B. Boyde, J. Am. Chem. Soc., 81 (1959) 1896.
72 P. F. Jones and S. Siegel, J. Chem. Phys., 50 (1969) 1134.
73 P. F. Jones, Polym. Lett., 6 (1968) 487.

74 B. A. Baldwin and H. W. Offen, J. Chem. Phys., 49 (1968) 2933.
75 M. Hilbert and B. Nemet, Acta Phys. Chem., 24 (1978) 365.
76 P. F. Jones and S. Siegel, in: E. C. Lim (Ed.), Molecular Luminescence, W. A. Benjamin, New York, 1969, pp. 15–19.
77 J. L. Kropp and W. R. Dawson, in Molecular Luminescence, E. C. Lim (Ed.), W. A. Benjamin, New York, 1969, pp. 39–52.
78 E. Kuntz, R. Canada, R. Wagner and L. Augenstein, in: E. C. Lim (Ed.), Molecular Luminescence, W. A. Benjamin, New York, 1969, pp. 551–567.
79 A. C. Giese and P. A. Leighton, Science, 85 (1937) 428.
80 K. P. Ghiggino, C. H. Nichols and M. T. Pailthorpe, Photochem. Photobiol., 22 (1975) 169.
81 I. H. Leaver, Photochem. Photobiol., 27 (1978) 439.
82 E. Wiedemann and G. C. Schmidt, Ann. Phys. (Leipzig), 58 (1896) 103.
83 J. Franck and P. Pringsheim, J. Chem. Phys., 11 (1943) 21.
84 G. D. Boutilier and J. D. Winefordner, Anal. Chem., 51 (1979) 1391.
85 M. Kasha, J. Chem. Phys., 20 (1952) 71.
86 D. S. McClure, J. Chem. Phys., 17 (1949) 905.
87 E. H. Gilmore, G. E. Gibson and D. S. McClure, J. Chem. Phys., 20 (1952) 829.
88 S. P. McGlynn, R. Sunseri and N. J. Christodouleas, J. Chem. Phys., 37 (1962) 1818.
89 M. A. El-Sayed, Acc. Chem. Res., 1 (1968) 8.
90 S. P. McGlynn, T. Asumi and M. Kinoshita, Molecular Spectroscopy of the Triplet State, Prentice-Hall, Englewood Cliff, NJ, 1969.
91 S. P. McGlynn, J. Daigre and F. J. Smith, J. Chem. Phys. 39 (1963) 675.
92 R. T. Parker, R. S. Freedlander and R. B. Dunlap, Anal. Chim. Acta, 120 (1980) 1.

Analytica Chimica Acta, 119 (1980) 207—216

COLOURED LIQUID ANION-EXCHANGERS

H.M.N.H. IRVING and J. HAPGOOD

Department of Analytical Science, University of Cape Town, Rondebosch 7700 C.P. (South Africa)

(Received 15th May 1980)

SUMMARY

Of the several stable and coloured uninegative ions examined, *trans*-bis(dimethylglyoximato)dinitritocobaltate(III) ($[Co(C_4H_7O_2)_2(NO_2)_2]^-$, termed goldenate ion, G^-) can advantageously replace the erdmannate ion in the formation of a more photochemically stable coloured anion-exchanger derived from Aliquat-336 chloride. Quantitative spectrophotometric measurements of its displacement by chloride, bromide and perchlorate ions were made and are discussed together with literature data to examine the effect of parameters such as the nature of the cation and of the anion and change in the organic solvent on the relative and absolute values of extraction constants.

The use of long-chain alkylamines as liquid anion-exchangers is now very well established in analytical practice and these reagents are well suited to preconcentration and separation procedures on both the laboratory and the industrial scale [1, 2]. If attention is restricted to the use of unipositive quaternary ammonium ions ($R_1R_2R_3R_4N^+ = Q^+$) the equation

$$n(Q^+A^-) + B^{n-} \rightleftarrows (Q_n^+B^{n-})_o + nA^- \quad (1)$$

expresses a generalised extraction reaction in which the n-valent anion B^{n-} displaces the anion A^- to a greater or less extent. The equilibrium constant will be defined by $K_{ex}^{(A,B)} = [Q_n^+B^{n-}]_o[A^-]^n/[Q^+A^-]_o^n[B^{n-}]$; the subscript o distinguishes species in the water-immiscible phase.

As long ago as 1964, Clifford and Irving [3] pointed out the advantages of using a liquid anion-exchanger with a coloured anion in order to facilitate spectrophotometric studies of anion-exchange [3] and showed how typical quaternary ammonium salts such as tetra-n-hexylammonium iodide (Q^+I^-) could be converted into the deeply coloured quaternary ammonium erdmannate (Q^+E^-), where E^- represents the anion of Erdmann's salt, $K^+[Co(NH_3)_2(NO_2)_4]^-$. The displacement reaction

$$(Q^+E^-)_o(\text{coloured}) + B^- \rightleftarrows (Q^+B^-)_o + E^-(\text{coloured}) \quad (2)$$

which ensues on equilibrium of an aqueous solution of B^- with one of (Q^+E^-) dissolved in an immiscible organic solvent could be used in procedures for the determination of perchlorate ($B^- = ClO_4^-$) [3, 4], for determining orders of relative extractability and selectivity coefficients [3—5], and for

studying the extraction and composition of complexes of mercury(II) with cyanide ions [6].

Used in the reverse way, small amounts of long-chain quaternary ammonium salts or long chain tertiary amines in effluents can be determined spectrophotometrically after equilibration with an excess of Erdmann's salt [7] in a procedure some eight times as sensitive as an earlier extractive method [8] in which the presence of iron caused difficulties. The more readily available sulphonphthalein indicator, bromocresol green, can be used in place of Erdmann's salt, but since it behaves as a diprotic acid, H_2BCG, both the total concentration of indicator and the pH must be controlled although there is some gain in sensitivity since the linear molar absorptivity (ϵ_{615} = 4080 m^2 mol^{-1}) is about three times greater than that of the erdmannate ion (ϵ_{353} = 1400 m^2 mol^{-1}).

Commercial tricetylmethylammonium chloride in the form of Aliquat-336 chloride (TOMA-Cl) has recently been used in extensive studies on factors governing selectivity in anion extractions, in which 4-(2-pyridylazo)-resorcinol (PAR;H_2R) is employed at pH 10 to provide a coloured anion [9]. The molar absorptivity of $TOMA^+HR^-$ in chlorobenzene is reported as ϵ_{395} = 30000 l mol^{-1} cm^{-1}.

If we consider the two extraction equilibria

$$(Q^+Col^-)_o + X^- \rightleftarrows (Q^+X^-)_o + Col^- \quad (3a)$$

$$(Q^+Col^-)_o + Y^- \rightleftarrows (Q^+Y^-)_o + Col^- \quad (3b)$$

where Col^- denotes any uninegative coloured anion and the respective equilibrium constants are $K_{ex}^{(Col,X)}$ and $K_{ex}^{(Col,Y)}$, it is obvious that the equilibrium constant of the exchange reaction

$$(Q^+X^-)_o + Y^- \rightleftarrows (Q^+Y^-)_o + X^- \quad (4)$$

which could well be difficult to measure directly if X^- and Y^- are chemically and physically similar (e.g. two colourless halide ions), follows directly from $K_{ex}^{(X,Y)} = K_{ex}^{(Col,Y)}/K_{ex}^{(Col,X)}$, thus giving a constant which is a measure of the relative tendencies of the two ions to be extracted and hence the selectivity of the anion-exchanger. The numerical value of $K_{ex}^{(X,Y)}$ should clearly be independent of the nature of the coloured anion, Col^-, though this has not previously been tested experimentally. However, the precision with which $K_{ex}^{(X,Y)}$ can be determined must clearly depend on the magnitudes of the component constants. This raises a number of questions concerning the choice of the coloured anion, Col^-. Clearly a high molar absorptivity is advantageous as will be a structure that does not demand a rigid control of pH in the aqueous phase. Large size and low hydrophilicity are factors which will favour its movement into the organic phase; but if the resulting ion-pair, Q^+Col^-, is too strongly associated the extent of displacement of Col^- by another anion may be extremely small ($K_{ex} \ll 1$) and such a coloured anion exchanger would have no practical value. It is not yet certain whether the relative order of extraction of different anions will

remain the same when (a) the cation Q^+ and (b) the organic solvent are changed [10]. In particular, it would be very useful to be able to predict the effects of these parameters on the absolute and the relative values of the extraction constants, K_{ex}, and hence on the degree of anion separation that can be achieved.

As part of a larger programme, some preliminary studies on the effect of changing the nature of the coloured anion, Col^-, are reported here. If the coloured anion were to be made more hydrophobic a decrease in the value of K_{ex} would be expected. Our attempts to prepare an analogue of Erdmann's salt with the two amino groups replaced by a bulkier and less hydrophilic chelated ethylenediamine (en), viz. Co $en(NO_2)_4^-$, gave inseparable mixtures. The ammonium salt of diaminodinitritoxalatocobaltate(III), $[Co(NH_3)_2(NO_2)_2(C_2O_4)]^-$, was prepared and purified, but like the anion of ammonium aquoethylenediaminetetraacetatochromium(III), $[CrY(H_2O)]^-$ (where H_4Y = EDTA), it proved too hydrophilic to yield a coloured anion-exchanger.

When a solution of Aliquat-336 chloride in chloroform was shaken with one of dithizone (3-mercapto-1,5-diphenylformazan; H_2Dz) in the same solvent, the unchanged spectrum (λ_{max}440 and 605) showed that no reaction had taken place. However, on shaking up with concentrated ammonia, a pink-orange organic phase and an orange aqueous phase containing the anion HDz^- resulted. Since all the excess of dithizone had been stripped out by the ammonia, the coloured organic phase must contain the ion-pair Q^+HDz^- (λ_{max} 494) formed by the reaction

$$(Q^+Cl^-)_o + H_2Dz \rightarrow (Q^+HDz^-)_o + Cl^- + H^+ \qquad (5)$$

However, shaking the chloroform phase with a large excess of perchlorate ions (well known to have the greatest displacing power of any common anion [3, 7]) failed to displace any dithizonate ions into the aqueous phase and one must conclude that the ion-pair Q^+HDz^- is too stable for use as an anion-exchanger.

When sodium hexanitritocobaltate(III) was treated with dimethylglyoxime, the sodium salt of *trans*-bis(dimethylglyoximato)dinitritocobalt(III), was formed [11] and purified as the less soluble ammonium salt which formed golden-yellow crystals of $(NH_4)[Co(NO_2)_2(C_4H_7O_2)_2]$. In the anion (called a goldenate ion, G^-, for short), the two glyoxime residues are coplanar and attached to one another by strong intramolecular hydrogen bonds as in bis(dimethylglyoximato)nickel(II) and the anion is sufficiently hydrophobic to form an extractable ion-pair with Aliquat-336 in chloroform. The resulting coloured liquid anion-exchanger has a single sharp absorption band at 350 nm (ϵ_{max} = 773 m^2 mol^{-1}) in the organic phase and at 340 nm (ϵ_{max} = 724 m^2 mol^{-1}) in the aqueous phase. Although the molar absorptivity is less than that of the erdmannate ions, goldenate ions are appreciably more stable: the extent of decomposition in organic solutions is negligible and photochemical decomposition in aqueous solution is far less than that of the erdmannate both in bright sunlight and in artificial light up to periods of

TABLE 1

Decomposition of 10^{-4} M solutions of erdmannate (E^-) salts in an organic or aqueous phase on exposure to bright sunlight or when kept in the dark

Time elapsed (h)	Percentage decomposition in Organic phase		Aqueous phase	
	Dark	Light	Dark	Light
0.33	0	3.6	0.1	3.2
1.0	0	13.8	0.8	11.1
2.0	0	24.6	2.3	27.3
5.5	0	48.6	6.9	67.3

TABLE 2

Decomposition of 10^{-4} M aqueous solutions of erdmannate and goldenate ions in artificial light or in the dark

Time elapsed (h)	Percentage decomposition[a]			
	Erdmannate ions		Goldenate ions	
	Dark	Light	Dark	Light
0.5	0	0	0	0
1.0	0	0.2	0	0
1.5	0	1.2	0	0
2.0	0 (0)	2.0(0.4)	0(0)	0 (0)
40.0	10.4(0)	25.0(5.2)	0(0)	3.7(0)

[a]The figures in parentheses refer to solutions in chlorobenzene.

40 h (Tables 1 and 2). All solutions were however stored in the dark, and equilibrations and phase separations were carried out in a darkened room.

When Aliquat-336 goldenate in chloroform was used, it was readily established that the order of increasing extractability was $SO_4^{2-} \ll Cl^- < Br^- < I^- < ClO_4^-$ in agreement with the order reported for the erdmannate salt [3], viz. $PO_4^{3-} < CO_3^{2-} < SO_4^{2-} \ll Cl^- < NO_3^- < ClO_3^- \ll ClO_4^-$ and the more extended $OH^- < F^- < AcO^- < HCO_3^- < HSO_4^- < Cl^- < Br^- < BzO^- < NO_3^- < I^- < ClO_4^-$ reported by Ivanov et al. [12] for the extraction of 0.1 M KX by a 0.1 M solution of tetraoctylammonium chloride in toluene.

For extractions by a solution of Aliquat-336 in chlorobenzene, Itoh et al. [9] report $SO_4^{2-} \ll Cl^- < Br^- < NO_3^- < I^- < ClO_4^-$ which agrees with the above. Similar orders (except for the position of the nitration) have been reported for ion-pair extraction by tris-(1,10-phenanthroline)iron(II) cations into nitrobenzene [13], and by tris-(8-quinolinol)zinc(II) ions into chloroform, viz. $SO_4^{2-} \ll Cl^- < Br^- < SCN^- < I^- < ClO^-$ [14]. When studying the extraction of anions into chloroform by surfactant cations, Biswas and Mandal [15] reported the order SO_4^{2-}, $F^- \ll Cl^- < NO^- < Br^- < I^- < ClO_4^-$ for dodecyl-, di-*n*-heptyl- and cetyltrimethylammonium ions. In studies of erdmannate

extractions, the orders $ClO_4^- < IO_4^-$; $BF_4 < PF_6^-$; $BeF_4^{2-} < BF_4^-$; $SiF_6^{2-} < PF_6^-$ [16] and $Ag(CN)_2^- \ll Au(CN)_2^-$ (linear ions, $Zn(CN)_4^{2-} \ll Cd(CN)_4^{2-} < Hg(CN)_4^{2-}$ (tetrahedral ions), and $Ni(CN)_4^{2-} \ll Pd(CN)_4^{2-} < Pt(CN)_4^{2-}$ (square planar ions) were determined for solutions of tetrahexylammonium erdmannate in hexone (MIBK), and it was noted that $Cu(CN)_4^{3-}$, $Fe(CN)_6^{3-}$ and $Fe(CN)_6^{4-}$ could not be extracted under comparable conditions [5]. In contrast, Itoh et al. [9] found the extractability of $Fe(CN)_6^{3-}$ by a solution of Aliquat-336 chloride in chlorobenzene to exceed that of the perchlorate ion. Further, since large and highly-charged anionic complexes of EDTA (such as FeY^-, $FeY(OH)^{2-}$, $FeY(OH)_2^{3-}$, VO_2HY^{2-} and VO_2Y^{3-}) can be extracted by solutions of this amine in dichloroethane whereas $CrY(H_2O)^-$ does not extract into chloroform, it must be concluded that no invariant order of extractabilities has yet been rigorously established for different quaternary ammonium ions, Q^+, and that change of the organic solvent may increase the range of anions that can be extracted (by inducing larger values of K_{ex}) without greatly altering the above orders. The effect of solvent on values of $K_{ex}^{E,X}$ is illustrated by the data given in Table 3, which also demonstrates the fact that the relative extractability for ClO_3^- and ClO_4^- (or NO_3^- and ClO_4^-) is also solvent-dependent, although the order chloroform < hexane < xylene for an increasing preference for perchlorate over chlorate (or nitrate) ions is evinced by values of log $K_{ex}^{(E,X)}$. Table 4 shows that the order of increasing extractability $Cl^- < NO_3^- < Br^- < I^- < ClO_3^- < ClO_4^-$ does not depend on the nature of the three cations illustrated and that the tendency to extract a particular ion generally increases in the cation order cetyltrimethylammonium < tetrahexylammonium < trioctylmethyl (or tricetylmethyl) ammonium. Restricting attention to the latter two quaternary ions which have been studied under comparable conditions, it is noteworthy that the Aliquat-336 gives uniformly larger values of $K_{ex}^{(E,X)}$ but lower discrimination between the pairs Cl^- and ClO_4^-, NO_3^- and ClO_4^-, Br^- and ClO_4^- or ClO_3^- and ClO_4^- than tetrahexylammonium salts [Table 4]. The same effect is observed in many liquid—liquid extraction systems where solvents which favour increasing percentage extraction under arbitrarily fixed conditions cause a concomitant decrease in separation factors for pairs of solutes [17, 18].

TABLE 3

The effect of solvent on the value of extraction constants with solutions of tetrahexylammonium erdmannate

Solvent						
Xylene (%)	100	90	75	50	0	Chloroform
Hexone (%)	0	10	25	50	100	(100%)
Values of log $K_{ex}^{(E,X)}$						
$X^- = NO_3^-$	−3.17	—	—	−3.52	−3.70	−2.46
$= ClO_3^-$	−2.53	−2.59	−2.59	−3.12	−3.44	−2.11
$= ClO_4^-$	0.12	0.08	0.09	−0.28	−0.80	−0.31
log $K_{ex}^{(ClO_3, ClO_4)}$	2.65	2.67	2.68	2.84	2.64	1.81
log $K_{ex}^{(NO_3, ClO_4)}$	3.29	—	—	3.24	2.90	2.15

TABLE 4

The effect of changing the nature of the quaternary ammonium ion on extractions into chloroform

	$10^3 K_{ex}^{(Br, Cl)}$[a]	$10^3 K_{ex}^{(E,X)}$[b]	
	CTA^+Br^-	THA^+E^-	$TOMA^+E^-$
$X^- = Cl^-$	0.16	0.113	0.465
$= NO_3^-$	2.0	3.46	7.05
$= Br^-$	3.0	—	7.38
$= I^-$	54	—	—
$= ClO_3^-$	—	7.73	16.6
$= ClO_4^-$	107	492	752
$\log K_{ex}^{Cl, ClO_4}$	2.78	3.64	3.12
$\log K_{ex}^{NO_3, ClO_4}$	1.73	2.15	2.03
$\log K_{ex}^{Br, ClO_4}$	1.55	—	2.01
$\log K_{ex}^{ClO_3, ClO_4}$	—	1.80	1.66

[a]Cetyltrimethylammonium bromide [15].
[b]Tetrahexylammonium erdmannate [3] and Aliquat-336 erdmannate [3]. The aqueous phase comprised ca. 0.1 M NaX and 0.9 M Na_2SO_4.

Finally, some values are reported (Table 5) for the displacement of erdmannate (or goldenate) ions from solutions of the Aliquat-336 salts in chloroform by Cl^- and Br^- measured under the same conditions (see Experimental). The values obtained for $\log K_{ex}^{(Cl,Br)}$ should, theoretically, be identical but the discrepancy (ca. 15%) may well lie within the cumulative experimental error. Itoh et al. [9] obtained the value of $\log K_{ex}^{(Cl,Br)} = 1.34$ in their measurements with the salt derived from Aliquat-336 and PAR. Since the solvent they used was chlorobenzene, and the considerable effect of changes in the organic solvent have now been established, the agreement with our values is probably fortuitous and more work needs to be done. In some measurements using chlorobenzene here, satisfactory mass-balances were not obtained and direct comparison with the earlier extensive measurements [9] was impossible.

EXPERIMENTAL

Reagents and syntheses

All reagents used were of analytical-reagent quality wherever possible. Ammonium hydroxide and hydrochloric acid were obtained pure by isopiestic distillation [19].

Preparation of Erdmann's salt. Jørgensen's method [20] was modified as follows. Ammonium hydroxide (25 ml of 20%) was added to a solution of ammonium chloride (100 g) and sodium nitrite (135 g) in water (750 ml) followed by cobalt chloride (90 g of $CoCl_2 \cdot 6H_2O$) dissolved in water (250 ml), and the mixture was oxidised by drawing in a rapid current of

TABLE 5

A comparison of displacement reactions involving erdmannate and goldenate ions under the same conditions[a]

Col^-	X^-	$10^3 K_{ex}^{(E \text{ or } G,X)}$	$\log K_{ex}^{(Cl,Br)}$
Erdmannate ion, E^-	Cl^-	0.465(0.356)	1.20(1.26)
	Br^-	7.38 (6.50)	
Goldenate ion, G^-	Cl^-	0.134(0.087)	1.35(1.47)
	Br^-	3.02 (2.61)	

[a]The figures in parentheses are corrected for blanks (see Experimental).

air (1.5 h). The filtered solution was left to stand in an open evaporating basin (5 days) when large reddish-brown rhombic needles were formed together with fine yellow crystals. The solids were collected and washed twice with ice water, and finally crushed to a fine yellow powder. Sufficient water at 40°C was added to dissolve about half the product; after filtration the filtrate was allowed to crystallise in an open dish whereupon Erdmann's salt separated free from the less soluble triaminotrinitrocobalt(III) which accompanies the crude product [20]. (Found 3.5% H, 32.6% N, 20.05% Co; calc. for $(NH_4)[Co(NH_3)_2(NO_2)_4]$, 3.4% H, 33.2% N, 20.09% Co.)

Preparation of ammonium diaminodinitritooxalatocobaltate(III). Erdmann's salt (5 g) dissolved in water (25 ml) was added to crystalline oxalic acid (2.5 g) in water (15 ml). After 3 days the double salt $Co(NH_4)[Co(NH_3)_2(NO_2)_2(C_2O_4)]$ which separated first had changed to the desired single ammonium salt which was collected and washed with small amounts of ice water which dissolved the single, but not the double salt [21]. Excess of ammonium chloride was added to the combined filtrates to precipitate the oxalato-salt as fine shining orange-red crystals which were recrystallized from water at 80°C and dried to constant weight in vacuo over silica gel for analysis. (Found 7.65% C, 3.9% H, 22.25% N; calc. for $(NH_4)[Co(NH_3)_2(NO_2)_2(C_2O_4)]\cdot H_2O$, 7.8% C, 3.9% H, 22.7% N.)

The two isomeric forms of this salt (*trans—cis* and *cis—cis*) which are formed simultaneously [22], were not separated.

Preparation of sodium-bis(dimethylglyoximato)dinitritocobaltate(III). This salt appears to have been prepared by Tschugaeff but no analysis was given [11]. Dimethylglyoxime (20 g; 0.17 mol) was added to a solution of sodium cobaltinitrite (25 g; 0.062 mol) in water (250 ml) and the mixture digested on a steambath (5 h). The large red crystals which separated were collected and washed with successive small amounts of cold water which dissolved the desired salt but not the oxime. All the filtrates were combined and concentrated under reduced pressure (Buchi evaporator) until crystallization occurred. On crystallization from hot 95% ethanol, the product gave fine

yellow-orange crystals which were dried to constant weight in vacuo over silica gel. Cobalt was determined complexiметrically after fuming down first with a mixture of hydrochloric and nitric acids (1:1) and then with concentrated sulphuric acid [23]. (Found: 14.5, 13.6% Co; calc. for $Na[Co(NO_2)_2(dmg)_2]$, 14.58% Co.)

Preparation of ammonium trans-bis(dimethylglyoximato)dinitritocobalt(III)monohydrate. To purify the above sodium salt, 5 g (0.012 mol) was dissolved in water (50 ml) and treated with excess of ammonium chloride (6.6 g; 0.12 mol) dissolved in water (40 ml). The less soluble ammonium salt which separated immediately as an orange-yellow precipitate was collected and recrystallized from glass-distilled water at about 60°C. After drying to constant weight in vacuo over silica gel, the salt was analysed. (Found, 23.0% C, 4.8% H, 23.35% N; calc. for $(NH_4)[Co(NO_2)_2(dmg)_2]\cdot H_2O$, 23.0% C, 4.8% H, 23.5% N.) As reported previously one molecule of water is lost at 100°C [11].

Preparation of a solution of aquoethylenediaminotetraacetatochromium(III), $CrY(H_2O)$. A violet solution of this anionic complex was prepared by boiling an aqueous solution of $Cr(NO_3)_3\cdot 9H_2O$ (0.024 M) with an aqueous solution of the disodium salt of EDTA (0.26 M) whereafter the pH was adjusted to 5 where the concentration of $CrY(H_2O)^-$ is maximal [24].

Preparation of stock solutions of coloured anion exchangers. Aliquat-336 chloride (2.5 ml) in chloroform (500 ml) was first equilibrated with 0.1 M HCl (500 ml) and then washed 5 times with distilled water (500-ml portions). Replacement of Cl^- by E^- (or G^-) was effected by shaking this solution with 100 ml of 0.01 M ammonium erdmannate (or goldenate) and rejecting the aqueous phase. The process was repeated 5 times although the absorbance of the organic phase at 350 nm (after 100-fold dilution) had become constant after the fourth equilibration. The separated organic phase was then washed once with water.

Determination of the concentrations of stock solutions. The stock solution of $(Q^+Col^-)_o$ was diluted 100-fold to give an approximately 10^{-4} M solution. Sodium perchlorate (2.5 M, 5 ml) was vigorously shaken (5 min) with an equal volume of the diluted anion exchanger to strip out the coloured anion. After centrifugation, the absorbance was measured at 350 nm in a 1-cm quartz cell using a Varian Superscan 3 spectrophotometer. Before equilibration, A_{350} (organic) was 1.228 and afterwards 0.005, 0.007 and 0.005 in triplicate measurements. The absorbance of the aqueous phase increased from zero to 1.073, 1.011 and 1.073, respectively. Since $\epsilon_{350} = 1180\ m^2\ mol^{-1}$ for E^- in the aqueous phase, $[Q^+E^-]_o = 8.57 \times 10^{-5}$ M and $\epsilon_{350} = 1430\ m^2\ mol^{-1}$ in the organic phase. The corresponding results for the goldenate salt were $A_{350} = 0.700$ before equilibration and 0.000 after equilibration in the organic phase, and $A_{340} = 0.655$, 0.659, 0.654 in the aqueous phase. Since $\epsilon_{340} = 724\ m^2\ mol^{-1}$, $[Q^+G^-]_o = 9.06 \times 10^{-5}$ M and $\epsilon_{350} = 773\ m^2\ mol^{-1}$ for the goldenate salt in the organic phase.

TABLE 6

Typical measurements for determination of equilibrium constants

Col^-	Concentrations X^-	$[Q^+Col^-]$ ($\times 10^{-4}$ mol l^{-1})	$[X^-]$ (mol l^{-1})	$[Q^+Col^-]$ ($\times 10^{-4}$ mol l^{-1})	$[Col^-]$ ($\times 10^{-4}$ mol l^{-1})	K_{ex}(Col,X) ($\times 10^{-4}$)
Erdmannate ion, E^-	Cl^-	10.16	0.101	8.20	1.96	4.65(3.56)
	Br^-	9.65	0.099	4.15	5.50	73.8(65.0)
Goldenate ion, G^-	Cl^-	10.56	0.101	9.44	1.13	1.34(0.891)
	Br^-	10.28	0.099	6.05	4.24	30.2(26.1)

Measurements of extraction constants

These were performed at room temperature (21 ± 1°C) as described previously [4]; vigorous shaking for 10 min was allotted for equilibration followed by centrifugation for 5 min before phase separation. To minimise effects from changes in ionic strength, the aqueous phase always contained 0.9 M sodium sulphate. To avoid volume changes, the aqueous phase was presaturated with chloroform: the organic solution of (Q^+Col^-) had become presaturated with water during its preparation. Some typical measurements are shown in Table 6 for the determination of equilibrium constants, according to eqn. (4), of salts of Aliquat-336 in chloroform at 21 ± 1°C. Values of $K_{ex}^{(Col,\,X)}$ were calculated as described previously [3, 4].

In each case the aqueous phase contained 0.9 M Na_2SO_4 and ca. 0.1 M NaX. The figures in parentheses in Table 6 were calculated after making corrections for blanks (i.e. for the partition of Q^+Col^- in the absence of added NaX). For example, on shaking a ca. 10^{-3} M solution of Q^+Col^- in chloroform with 0.9 M Na_2SO_4 a slight colour appeared in the aqueous phase because of the normal distribution $Q^+ + Col^- \rightleftarrows [Q^+Col^-]_o$. Spectrophotometric measurements gave the value $K \approx 10^{6.3}$ for the equilibrium constant for both the erdmannate and goldenate. Itoh et al. obtained the value $K = 10^4$ for the partition of Aliquat-336 chloride between chlorobenzene and water and the value $K = 10^{5.11}$ has been reported for benzyl tetradecyldimethylammonium chloride between chloroform and water [25].

1 R. Kunin and A. G. Winger, Angew. Chem. Int. Ed. Engl., (1962) 149.
2 H. Green, Talanta, 20 (1973) 139.
3 W. E. Clifford, and H. M. N. H. Irving, Anal. Chim. Acta, 31 (1964) 1.
4 H. M. N. H. Irving and A. D. Damodaran, Analyst, 90 (1965) 443.
5 H. M. N. H. Irving and A. D. Damodaran, Anal. Chim. Acta, 53 (1971) 267.
6 H. M. N. H. Irving and A. D. Damodaran, Anal. Chim. Acta, 53 (1971) 277.
7 H. M. N. H. Irving and J. J. Markham, Anal. Chim. Acta, 39 (1967) 7.
8 A. W. Ashbrook, Analyst, 84 (1959) 177.
9 J. Itoh, H. Kobayashi and K. Ueno, Anal. Chim. Acta, 105 (1979) 383.
10 H. M. N. H. Irving and R. H. Al-Jarrah, Anal. Chim. Acta, 65 (1973) 77.
11 L. Tschugaeff, Chem. Ber., 41 (1908) 2230.
12 I. M. Ivanov, L. M. Gindin and G. N. Chichagova, Khim. Protsessov Ekstr., Mater. Conf. Khim. Ekstr., 3rd, 1969 (1972) 207.

13 Y. Yamamoto, Bunseki Kagaku, 21 (1972) 418.
14 E. Sekido, Y. Yoshimura and Y. Masuda, J. Inorg. Nucl. Chem., 38 (1976) 1183.
15 H. K. Biswas and B. M. Mandal, Anal. Chem., 44 (1972) 1636.
16 A. D. Damodaran, Ph. D. Thesis, Leeds, 1965.
17 H. M. N. H. Irving, F. J. C. Rossotti and R. J. P. Williams, J. Chem. Soc., (1955) 1906.
18 H. Irving and J. F. C. Rossotti, J. Chem. Soc., (1955) 1946.
19 H. Irving and J. J. Cox, Analyst, 83 (1958) 526.
20 I. R. Jørgensen, Z. Anorg. Allg. Chem., 17 (1898) 476.
21 E. Riesenfeld and R. Klement, Z. Anorg. Allg. Chem., 124 (1922) 14.
22 W. Thomas, J. Chem. Soc., 123 (1923) 618.
23 G. Schwarzenbach and H. Flaschka, Complexiметric Titration, 2nd English edn., revised and translated, H. Irving, Methuen, London, 1969.
24 H. M. N. H. Irving and R. H.Al-Jarrah, Anal. Chim. Acta, 55 (1971) 135.
25 H. Hoshino, T. Yotsuyanagi and K. Ueno, Bunseki Kakagu, 27 (1978) 602.

Analytica Chimica Acta, 119 (1980) 217—223

COMPARISON OF LINEAR SCAN AND DIFFERENTIAL PULSE ANODIC STRIPPING VOLTAMMETRY AT A THIN MERCURY FILM GLASSY CARBON ELECTRODE

T. M. FLORENCE

Analytical Chemistry Section, Australian Atomic Energy Commission Research Establishment, Lucas Heights, N.S.W. 2234 (Australia)

(Received 30th April 1980)

SUMMARY

The use of the differential pulse mode in anodic stripping voltammetry with an electrode consisting of a thin mercury film deposited in situ on a glassy carbon support leads to detection limits which are 3—5 times lower than if a simple linear scan is used at the same electrode. If the glassy carbon electrode has a high base current, the improvement in detection limit with differential pulse will be even greater. Differential pulse peak currents, however, are more susceptible to interference by surface-active substances, and undetected adsorption/desorption effects can cause serious errors. Precautions which are necessary to maintain a glassy carbon electrode in good condition are described.

A thin mercury film deposited in situ on a glassy carbon substrate has been shown [1—9] to be the most sensitive and convenient electrode configuration for the determination of trace heavy metals by anodic stripping voltammetry. It has been stated [4, 6, 7] that the use of a differential pulse waveform with this electrode leads to much higher stripping currents and lower limits of detection than if a simple linear scan is applied, although this advantage has not been demonstrated conclusively. The situation has been confused by the use of glassy carbon electrodes with inferior base current characteristics [4], by some authors equating sensitivity to limit of detection, and by the fact that the most commonly used differential pulse voltammeter, the Princeton Applied Research Polarographic Analyzer Model 174 (PAR 174), employs an amplifier in the differential pulse circuit so that the displayed current is ten times the actual cell current [10].

In this paper, the peak current sensitivities and limits of detection are compared for differential pulse and linear scan anodic stripping voltammetry (d.p.a.s.v. and l.s.a.s.v.) at a thin mercury film glassy carbon electrode (MFE). The problem of the effects of surface-active substances on the differential pulse current is discussed, and methods for maintaining the glassy carbon electrode in good working condition are given.

EXPERIMENTAL

Apparatus

Differential pulse voltammograms were recorded at 25°C with an unmodified Princeton Applied Research Polarographic Analyzer Model 174. Linear scan results were obtained by using an ORNL model Q-2792 voltammeter [2]. The perspex voltammetric cell and Beckman rotating electrode (25 rev s^{-1}) used in this work have been described previously [11]. The glassy carbon tips of the Beckman electrode assembly had a diameter of 0.6 cm and were initially polished metallographically with diamond dust. After each analysis, the mercury film was removed from the glassy carbon electrode by wiping with a moistened piece of Whatman No. 542 filter paper, and then polished with a dry piece of the same paper. Between analyses, the electrode was stored in the empty cell.

Reagents

A 2×10^{-2} M mercury(II) nitrate solution was prepared from Merck 'Suprapur' nitric acid and mercury, ensuring that the solution was first taken to fumes of nitric acid to oxidize any mercury(I), which precipitates in chloride media. A concentration of 5×10^{-5} M mercury(II) was added to all test solutions for the in situ mercury film deposition. All other reagents were Merck 'Suprapur'.

Test procedure

Differential pulse and linear scan voltammograms were recorded successively on the same solution after a 15-min deaeration and after two deposition-stripping sequences to condition the electrode. The potential scan rates used for d.p.a.s.v. and l.s.a.s.v. were 5 mV s^{-1} and 83 mV s^{-1}, respectively.

RESULTS AND DISCUSSION

The equation for the d.p.a.s.v. peak current (i_{pd}) at a thin mercury film electrode (MFE) is given [12], for reversible systems and large (>50—100 mV) pulse amplitudes, by $i_{pd} = -0.138\, q/t$, where q is the total charge passed during deposition, and t is the pulse duration (s). The equivalent equation for l.s.a.s.v. [12] is, $i_{pl} = -11.6\, nvq$, where i_{pl} is the linear scan stripping peak current, n is the number of electrons involved in the electrode reaction, and v is the potential scan rate (V s^{-1}). The ratio of the d.p.a.s.v. and l.s.a.s.v. peak currents at the MFE is therefore,

$$i_{pd}/i_{pl} = 0.0119/nvt$$

With a linear scan rate of 0.083 V s^{-1} (5 V min^{-1}), and a pulse duration of 0.040 s (the preset value in the PAR 174), $i_{pd}/i_{pl} = 1.79$, for a 2-electron reaction and large pulse amplitudes (ΔE). With pulse amplitudes below 50

mV, the differential peak current is approximately proportional to ΔE [4], so that for ΔE = 25 mV, a value commonly used in practical d.p.a.s.v., the ratio i_{pd}/i_{pl} should be about 0.9.

Anodic stripping voltammetry of copper, lead and cadmium

Table 1 lists some experimental results for i_{pd}/i_{pl} for copper, lead and cadmium in various electrolytes. For the anodic stripping of cadmium and lead, which are highly reversible in chloride media, the experimental peak ratios are close to the value predicted for ΔE = 25 mV. Note that the measured d.p.a.s.v. currents have been divided by 10 to allow for the gain in the PAR 174 differential pulse circuit. In the case of copper, however, which has a lower reversibility, the differential pulse mode is relatively less sensitive.

The ability of the differential pulse waveform to discriminate against base current was determined by comparing the slopes of the base currents of the d.p.a.s. and l.s.a.s. voltammograms measured on a sample of Pacific Ocean water (Table 2). Similar results were obtained for standard metal solutions in chloride media. Two Beckman glassy carbon electrode tips were used to produce the three sets of results shown in Table 2; the first electrode had been metallographically polished two years before and correctly maintained since, while the second had been polarized anodically (+ 2.5 V vs. SCE for 15 s) in 0.5 M chloride to degrade the polished surface. This damaged electrode was used to record one set of results, and was then cleaned by polishing successively with Whatman No. 542 filter paper soaked in 1 M mercury(II) nitrate acidified with 1 M nitric acid, 1 M nitric acid, ethanol, water, and dry paper, in that order. The partially restored electrode was then used for the third set of results (Fig. 1).

TABLE 1

Comparative sensitivities of differential pulse and linear scan anodic stripping voltammetry

Sample[a]	Pulse amplitude (mV)	Peak current ratio for d.p.a.s.v./l.s.a.s.v.[b,c]		
		Cd	Pb	Cu
1×10^{-7} M metals in 0.1 M NaCl	25	0.94	1.17	0.64
	10	0.45	0.49	0.21
1×10^{-8} M metals in 0.02 M acetate buffer pH 4.7 + 0.05 M chloride	25	0.90	0.99	0.58
	10	0.40	0.46	0.20
Pacific Ocean water + 0.02 M acetate buffer pH 4.7[d]	25	0.88	0.93	0.53

[a]All samples plus 5×10^{-5} M Hg(II). [b]Measured d.p.a.s.v. peak currents were divided by 10 to allow for gain in PAR 174 differential pulse circuit. [c]Linear scan voltammograms were recorded with a scan rate of 0.083 V s^{-1}. [d]The sea water contained 0.040 μg Cd l^{-1}, 0.029 μg Pb l^{-1}, and 0.19 μg Cu l^{-1}.

TABLE 2

Base current slopes for differential pulse and linear scan anodic stripping voltammetry[a]

Condition of glassy carbon electrode	Technique[b]	Base current slope (μA V^{-1})	
		Cd—Pb	Cu
Polished, well maintained	L.s.a.s.v.	1.25	2.5
	D.p.a.s.v.	0.24	0.84
Polarized at +2.5 V vs. SCE in chloride media	L.s.a.s.v.	7.5	21.3
	D.p.a.s.v.	0.64	3.2
Damaged electrode chemically cleaned and polished with filter paper	L.s.a.s.v.	3.3	9.4
	D.p.a.s.v.	0.48	2.3

[a]Sample was Pacific Ocean water. [b]D.p.a.s.v. with 25 mV pulse amplitude; l.s.a.s.v. with 0.083 V s^{-1} scan rate. A pulse amplitude of 10 mV gave similar results.

Table 2 shows that appreciable base current discrimination is achieved with the differential pulse waveform, and that the greatest advantage is with glassy carbon electrodes in poor condition, and with reversible electrode reactions. With a well maintained electrode, d.p.a.s.v. base current slopes are lower by a factor of five for cadmium and lead, and by a factor of three for copper. The glassy carbon electrode used by Lund and Onshus [4] had a base current slope of 11 μA V^{-1} for cadmium and lead in sea water, which explains why these workers found d.p.a.s.v. to be so advantageous. Since the current sensitivities (ΔE = 25 mV) and the noise levels on the voltammograms are similar for d.p.a.s.v. and l.s.a.s.v., it can be concluded that, for the solutions studied, d.p.a.s.v. at a glassy carbon MFE has a limit of detection which is about a factor of five lower for a reversible reaction (Cd, Pb) and a factor of three lower for a quasi-reversible reaction (Cu). Higher pulse amplitudes provide greater current sensitivity with d.p.a.s.v., but peak resolution is degraded progressively with amplitudes above 10 mV; to obtain resolution equivalent to that of l.s.a.s.v., a 10-mV pulse amplitude must be used, although 25 mV provides a reasonable compromise between sensitivity and resolution.

Effect of surface-active agents

There is a serious problem associated with the use of the differential pulse mode in practical a.s.v. analysis. Surface-active agents have a greater effect on d.p.a.s.v. than on l.s.a.s.v. because the differential peak currents are more sensitive to small changes in the rate of the electrode reaction. This situation is illustrated in Table 3, where a typical surfactant, n-octanol (4.2 ppm), causes much larger depressions of the differential pulse peak currents for copper, lead and cadmium. It is important to realise that labile metal and

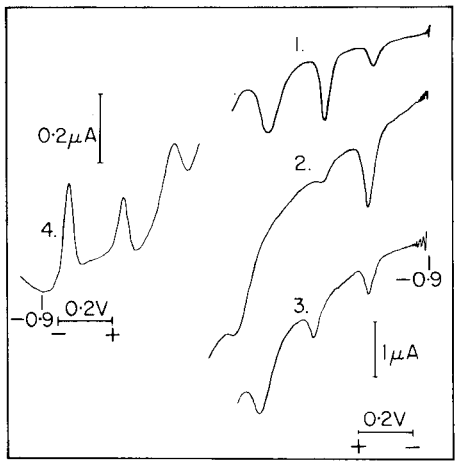

Fig. 1. Differential pulse and linear scan anodic stripping voltammetry (d.p.a.s.v. and l.s.a.s.v.) of cadmium, lead and copper at thin mercury film glassy carbon electrodes. Curve (1): l.s.a.s.v. at a correctly maintained glassy carbon electrode; Pacific Ocean water (Cd — 0.035, Pb — 0.11, Cu — 0.22 $\mu g\ l^{-1}$); deposition time 20 min; scan rate 83 mV s^{-1}. Curve (2): l.s.a.s.v. at a glassy carbon electrode damaged by polarization at +2.5 V vs. SCE in chloride media: test solution, 0.05 M chloride in acetate buffer pH 4.7; deposition time 15 min; scan rate 83 mV s^{-1}. Curve (3): l.s.a.s.v. at the damaged electrode (No. 2) which had been partially restored by chemical cleaning and filter paper polishing; Pacific Ocean water (Cd — 0.040, Pb — 0.029, Cu — 0.19 $\mu g\ l^{-1}$); deposition time 25 min; scan rate 83 mV s^{-1}. Curve (4): d.p.a.s.v. at the glassy carbon electrode used for Curve 3 with the same sea-water sample; deposition time 15 min; pulse amplitude 25 mV; scan rate 2 mV s^{-1}.

speciation measurements may lead to different results for d.p.a.s.v. and l.s.a.s.v. because of these adsorption effects [13]. An insidious but perhaps more important effect associated with d.p.a.s.v. and surfactants is that the differential pulse mode may give rise to organic adsorption/desorption peaks [13–16] similar to the well known tensammetric waves of a.c. polarography [17]. As shown by Batley and Florence [14], these differential pulse tensammetric waves can be hidden under the faradaic waves of cadmium, lead or copper, and so be undetected and give erroneously high results for the metals. This problem will not arise if organic matter is destroyed and only total metal is measured.

Anodic polarization in chloride media

The performance of a glassy carbon electrode will be seriously degraded if it is polarized anodically in chloride media, because a film of mercury(I) chloride (calomel, Hg_2Cl_2) will form on the electrode at a potential, E, given [18] by $E = +0.026 - 0.0296 \log_{10} [Cl^-]^2$ (in V vs. SCE). To prevent any significant formation of calomel, the electrode should not be polarized at potentials more positive than 0 V, +0.03 V, or +0.14 V vs. SCE in 0.5 M, 0.1 M, and 10^{-3} M chloride, respectively. Even if the test solution originally

TABLE 3

Effect of n-octanol on a.s.v. peak heights (4.2 ppm n-octanol added to 2×10^{-7} M Cu, Pb, Cd in 0.1 M NaCl)

Technique	Peak height depression (%)		
	Cu	Pb	Cd
Differential pulse[a]	30.6	12.5	74
Linear scan[b]	0	3.4	49

[a]25 mV pulse amplitude. [b]0.083 V s^{-1} scan rate.

contained no chloride, a concentration of 10^{-3} M chloride can easily be added by leakage from the salt bridge of a saturated calomel or Ag/AgCl reference electrode. A film of calomel on the glassy carbon leads to high base currents and erratic performance, and the film is particularly difficult to remove completely without repolishing the electrode. The procedure used by Clem and co-workers [19, 20] of continuing the anodic scan to +0.35 or +0.50 V vs. SCE when carrying out l.s.a.s.v. with glassy carbon and other carbon electrodes, may have resulted in the formation of calomel films and led to their conclusion that glassy carbon was unsatisfactory for a.s.v. because of poor hydrogen overvoltage characteristics.

If a glassy carbon electrode is polarized at potentials more positive than +1.5 V vs. SCE in chloride media, chlorine may be evolved. Although glassy carbon is highly inert chemically, it is, like all forms of carbon, rapidly attacked by free chlorine [21]. The polished surface of the electrode is destroyed, and very high base currents result. Some powerful oxidants such as cobalt(III) produce the same effect. It was found that potentials sufficiently positive to produce chlorine are developed at the working electrode if the reference circuit of the PAR 174 is interrupted during operation by, for example, the level of the salt bridge solution falling below the tip of the reference electrode. If the reference electrode is disconnected while the PAR 174 is scanning anodically in the differential pulse mode, the potential of the working electrode instantly swings to +3.6 V vs. SCE. If the disconnection is made while the instrument is set at "initial potential", the potential of the working electrode oscillates between +2.5 and −2.5 vs. SCE. When scanning in the d.c. mode with the PAR 174, the working electrode potential changes to a value between +1.6 and +2.0 V vs. SCE when the reference circuit is interrupted. By contrast, when the same test was carried out with the ORNL voltammeter, the working electrode changed to only +0.08 to +0.15 V vs. SCE when the reference electrode was disconnected during scanning.

CONCLUSIONS

The choice of d.p.a.s.v. or l.s.a.s.v. with a MFE glassy carbon electrode will be dictated by the nature of the test solution. The 3—5-fold decrease in

limit of detection available with d.p.a.s.v. (unmodified PAR 174, 25 mV pulse amplitude) is useful in the analysis of natural waters with very low metal concentrations, because correspondingly shorter deposition times can be used. The gain is even greater if poorly prepared glassy carbon electrodes are used. This advantage must be balanced against the need to ensure that surface-active materials are not distorting the d.p.a.s.v. results or affecting speciation calculations. When the concentration of the metal to be determined is above 5×10^{-9} M, a 10-min deposition followed by l.s.a.s.v. provides stripping peaks sufficiently large for accurate measurement, and they are obtained with the simpler and less expensive linear scan instrument. Whichever technique is used, the maintenance of the glassy carbon electrode is critical; the electrode must never be polarized at potentials sufficiently positive to cause calomel formation or chlorine generation. With correct electrode maintenance, the original metallographic polishing of the electrode should only rarely have to be repeated; we have used electrodes which have retained their original calibrations and base current slopes for over five years with only routine filter paper cleaning.

REFERENCES

1 T. M. Florence, J. Electroanal. Chem., 26 (1970) 293.
2 T. M. Florence, J. Electroanal. Chem., 27 (1970) 273.
3 W. Lund and M. Salberg, Anal. Chim. Acta, 76 (1975) 131.
4 W. Lund and D. Onshus, Anal. Chim. Acta, 86 (1976) 109.
5 J. Dieker and W. E. van der Linden, Fresenius Z. Anal. Chem., 274 (1975) 97.
6 P. Valenta, L. Mart and H. Rützel, J. Electroanal. Chem., 82 (1977) 327.
7 J. Gomilowski, P. Valenta, M. Stoeppler and H. W. Nürnberg, Talanta, 26 (1979) 649.
8 H. W. Nürnberg, Sci. Total Environ., 12 (1979) 35.
9 V. D. Nguyen, P. Valenta and H. W. Nürnberg, Sci. Total Environ., 12 (1979) 151.
10 T. R. Copeland, J. H. Christie, R. A. Osteryoung and R. K. Skogerboe, Anal. Chem., 45 (1973) 2171.
11 G. E. Batley and T. M. Florence, Electroanal. Chem., 55 (1974) 23.
12 R. A. Osteryoung and J. H. Christie, Anal. Chem., 46 (1974) 351.
13 H. P. van Leeuwen, Anal. Chem., 51 (1979) 1322.
14 G. E. Batley and T. M. Florence, J. Electroanal. Chem., 72 (1976) 121.
15 E. Jacobsen and H. Lindseth, Anal. Chim. Acta, 86 (1976) 123.
16 J. B. Flanagan, K. Takahashi and F. C. Anson, J. Electroanal. Chem., 81 (1977) 261.
17 B. Breyer and H. H. Bauer, Alternating Current Polarography and Tensammetry, Interscience, New York, 1963.
18 W. M. Latimer, Oxidation Potentials, Prentice Hall, New Jersey, 2nd edn., 1952.
19 R. G. Clem, G. Litton and L. D. Ornelas, Anal. Chem., 45 (1973) 1306.
20 R. G. Clem, Anal. Chem., 47 (1975) 1778.
21 F. C. Cowlard and J. C. Lewis, J. Mater. Sci., 2 (1967) 507.

Analytica Chimica Acta, 119 (1980) 225—233

DETERMINATION OF ARSENIC AND ANTIMONY IN ELECTROLYTIC COPPER BY ANODIC STRIPPING VOLTAMMETRY AT A GOLD FILM ELECTRODE

T. W. HAMILTON and J. ELLIS*

Chemistry Department, University of Wollongong, P.O. Box 1144, Wollongong, N.S.W. 2500 (Australia)

T. M. FLORENCE

Analytical Chemistry Section, Australian Atomic Energy Commission Research Establishment, Lucas Heights, N.S.W., 2234 (Australia)

(Received 20th May 1980)

SUMMARY

A simple procedure is described for the determination of arsenic and antimony in electrolytic copper. The copper is digested with nitric acid and copper is separated from arsenic and antimony by passing an ammoniacal solution of the sample through a column of Chelex-100 resin. After digestion with sulphuric acid and reduction to arsenic(III) and antimony(III) with sodium sulphite in 7 M sulphuric acid at 80°C, both arsenic and antimony are deposited at —0.30V and their total is determined by anodic stripping; antimony is then selectively deposited at —0.05 V for anodic stripping. The lower limits of determination are 56 ng As and 28 ng Sb per gram of copper; relative standard deviations (n = 5) are in the ranges 6.1—15.0% for 5.5—0.5 ppm arsenic in copper and 4.1—6.8% for 2.6—0.6 ppm antimony.

The routine determination of arsenic and antimony in electrolytic copper is important to the copper refining industry because of the effect of these impurities on the conductivity and other properties of copper. Emission spectroscopy is used widely to provide rapid determination of a range of impurities in copper, but it exhibits poor sensitivity for arsenic and antimony. Alternative analytical methods for these elements invariably involve initial dissolution of the copper in nitric acid followed by separation of the bulk of the copper from the elements to be determined.

Although distillation with hydrogen bromide [1] and solvent extraction [2—5] have been used for the separation of arsenic and antimony from large concentrations of copper, the approaches most often reported are coprecipitation of arsenic and antimony with iron(III) hydroxide [6, 7], lanthanum hydroxide [8, 9], hydrated manganese dioxide [10] or zirconium hydroxide [11]. Each of these approaches has its drawbacks. The distillation technique is time-consuming and not suited to routine usage, and the extraction and coprecipitation approaches fail to achieve complete separation of copper from the elements of interest. In addition, many of the co-

precipitation methods require very accurate pH control. Because of its simplicity and speed, an ion-exchange technique developed in this laboratory for the determination of selenium and tellurium in copper [12] was adapted and used in the proposed arsenic and antimony determination.

Arsenic and antimony have been determined by a wide variety of analytical techniques. These include flame and electrothermal atomic absorption spectrometry [13—16], microwave-induced [17] and inductively-coupled plasma [18, 19], emission spectrometry, d.c. and differential pulse polarography, anodic stripping voltammetry (a.s.v.) with graphite [20, 21], mercury [22], gold [23] and gold film [24] electrodes, spectrophotometry [5, 9, 19, 25]; neutron activation analysis [26, 27] and chromatography [28, 29]. A cathodic stripping voltammetry method has also been reported for antimony [30] and an atomic fluorescence technique for arsenic [31, 32]. Of these methods, only neutron activation analysis and plasma source atomic emission spectrometry were considered to have the required sensitivity and the potential to determine arsenic and antimony simultaneously. The method chosen in this work was a.s.v. at a gold film electrode. This electrode has been used for the determination of selenium and tellurium [12] and arsenic [24] and is used here for the simultaneous determination of arsenic(III) and antimony(III).

EXPERIMENTAL

Apparatus

Voltage ramps were generated by a PAR-175 Universal Programmer linked to a PAR-174 potentiostat and current-to-voltage converter. Output voltage was recorded on a Houston 2000 x-y recorder. A PAR-173 potentiostat/galvanostat and PAR-179 digital coulometer were used for coulometric measurements. A PAR cell and glassy carbon electrode (GCE) were used, in conjunction with a saturated calomel electrode (SCE) and a platinum auxiliary electrode. The SCE was isolated from the sample solution by a salt bridge containing 0.5 M sodium nitrate. Flow of moist high-purity nitrogen into the cell was directed through one of two valves: the first allowed the gas to bubble through the solution for purging while the second directed the gas over the top of the solution during a determination. These valves were operated by an automatic controller as were all stages of the a.s.v. procedure. Details of this controller have been described elsewhere [33].

Reagents

Aristar (B.D.H.) nitric, sulphuric and hydrochloric acids and ammonia solutions were used without further purification. Standard solutions of arsenic or antimony (5×10^{-2} M) were made by dissolving sodium arsenite (B.D.H., >99%) in water or antimony trioxide (B.D.H., >99%) in a nitric—hydrochloric acid mixture and diluting each day to give the working solutions (1.0—7.5 ppm). The gold(III) stock solution was made by dissolving gold

sponge (Fluka, 99.9995%) in a minimum of aqua regia and diluting with 1 M nitric acid. Sodium perchlorate was Merck Suprapur. Sodium sulphite was B.D.H. Analar. Water was distilled and redistilled twice from quartz. Chelex-100 resin (Bio-Rad Laboratories) was 100—200 mesh and was regenerated by washing with 2 M nitric acid (analytical reagent), water, 0.5 M ammonia solution (analytical reagent) and finally with 0.1 M ammonia solution (Aristar grade).

Electrode preparation

Before each deposition of a gold film, polish the electrode with alumina powder (0.5-μm diameter) and wash it successively with methanol, nitric acid and distilled water. Submerge the electrode in 15 ml of 0.1 M sodium perchlorate and leave in open circuit during a 20-min purge with nitrogen. Add an aliquot of gold(III) solution (to give a gold concentration of 50 ppm) and purge the solution for a further 5 min. After ensuring that gas bubbles are not lodged on the surface of the GCE, apply —0.2 V to the electrode and deposit the equivalent of 2×10^{-2} coulomb of gold on the surface (28 mm^2). For optimum performance, keep the electrode in purged 0.1 M sulphuric acid for 24 h before use and store under these conditions between analyses.

Procedure

Dissolve 0.5 g of the copper sample in 2 ml of 15 M nitric acid. After dissolution, heat the sample solution briefly to expel most of the nitrous fumes and dilute with an equal quantity of water. Add 3 ml of 15 M ammonia solution, stir the solution to dissolve any hydroxide, and elute through a 30-ml column (1.5 × 15 cm) of Chelex-100 resin with 0.1 M ammonia solution. Collect 50 ml of eluate, acidify with 3 ml of concentrated sulphuric acid, and evaporate to sulphur trioxide fumes to expel the bulk of the nitrate as nitrogen dioxide. Cool the solution to 80°C and add 3 ml of sodium sulphite solution (50% w/v; heated to 70—80°C) in a single addition. Stir the solution, and keep for 30 min at about 80°C; then boil the solution for a few minutes to remove the last of the sodium sulphite. Transfer the warm solution to a 25-ml volumetric flask, allow to cool and dilute to volume. Analysis of this solution, as described below, is performed in two parts: firstly, arsenic and antimony are determined together and secondly antimony is determined alone, in the same solution. The arsenic concentration is calculated by difference.

Pipette 5 or 10 ml of sample solution into the cell and purge with nitrogen for 15 min before immersing the gold film electrode. Then, with the auxiliary electrode in open circuit and the working electrode earthed, purge for a further 5 min. Commence stirring, condition the working electrode for 30 s at +0.9 V, and then deposit arsenic and antimony on the working electrode at —0.3 V for 10—500 s, depending on their concentration. Cease stirring and after 20s, scan the working electrode voltage from —0.3 to +0.9 V at 40 mV s^{-1}, recording the resulting voltammogram. Repeat the procedure

from the conditioning step to ensure a constant peak height. Add a spike of standard arsenic(III) solution (sufficient to cause a 50—80% increase in peak height) and repeat the a.s.v. determination. At a deposition potential of —0.3 V, the electrode response to arsenic(III) and antimony(III) is the same, thus making it unnecessary to make a standard addition of antimony.

To determine the concentration of antimony(III), adjust the deposition potential to —0.05 V and repeat the procedure used for the arsenic—antimony determination, but adding a standard amount of antimony(III) in place of arsenic.

When the concentration of antimony has been calculated, the concentration of arsenic(III) can be obtained from $[As] = (C_{As} \times P_1/P_2) - [Sb]$, where C_{As} is the increase in arsenic(III) concentration after the standard addition, P_1 is the height of the initial As—Sb peak, and P_2 is the increase in peak height from the standard arsenic(III) addition.

RESULTS AND DISCUSSION

Sample preparation

The initial step of dissolving the copper in nitric acid caused two problems: partial oxidation of arsenic and antimony to the pentavalent state, and the generation of nitrite which interfered with the electrode response in the final voltammetric determination.

Because arsenic(V) and antimony(V) are electro-inactive in the range of potentials available with a gold electrode, preliminary reduction to the trivalent state was necessary. Reduction to arsenic(III) with sodium sulphite in solutions of high acidity has been reported [34, 35] and was found to work well for antimony(V) and arsenic(V) in high concentrations of sulphuric acid. A trial reduction of arsenic(V) with sulphite in 4 M sulphuric acid in the presence of copper(II) ions (0.1 M) caused partial reduction to copper(I) and gave incomplete reduction of arsenic(V). The reduction must therefore be carried out after ion-exchange separation of copper(II) ions from the sample.

Both problems were overcome by adding a few ml of sulphuric acid to the eluate from the ion-exchange column and boiling down to sulphur trioxide fumes before adding the sodium sulphite. This procedure removed nitrite, and also nitrate which would otherwise be reduced by the sulphite. The extent of reduction to arsenic(III) and antimony(III) was better than 97%. Addition of sodium sulphite solution to the sample required some care; it resulted in rapid evolution of sulphur dioxide and some violent sputtering could occur if the sample solution was too hot. However, when the sample solution or the sulphite solution was not hot enough, crystallisation of sodium sulphate occurred, which could occlude some arsenic(V) or antimony(V). Traces of sulphur dioxide remaining in the solution after the sample preparation were quickly driven off during the initial purge in the determination step.

Arsenic(V) and antimony(V) in the presence of tetraammine copper(II) ions were quantitatively eluted from a Chelex-100 column under the conditions described.

Electrochemical analysis

The potentials of the stripping peaks for both arsenic and antimony occur at +0.18 V (Fig. 1), are independent of the deposition potential and vary with pH (Table 1). All attempts to achieve separation between the oxidation potentials of arsenic and antimony by altering the solution conditions and electrolyte composition were unsuccessful, as were attempts to reduce one of the elements selectively to the hydride with various reducing agents. In particular, the Fleitmann test (selective reduction of arsenite to arsine by aluminium in aqueous sodium hydroxide solution) was not effective at the concentration levels of arsenic and antimony encountered in this study; antimony(III) was also reduced, probably to the elemental state, and could not be easily oxidised to antimony(III). Reduction with tetrahydroborate under nitrogen showed the most promise (the presence of traces of oxygen raised the efficiency of the reduction) but the separation was no better than 80%, with antimony(III) being preferentially reduced. Selective reduction to the trivalent state did not look promising and attempts to oxidise one of the elements selectively from the trivalent to the pentavalent state were unsuccessful.

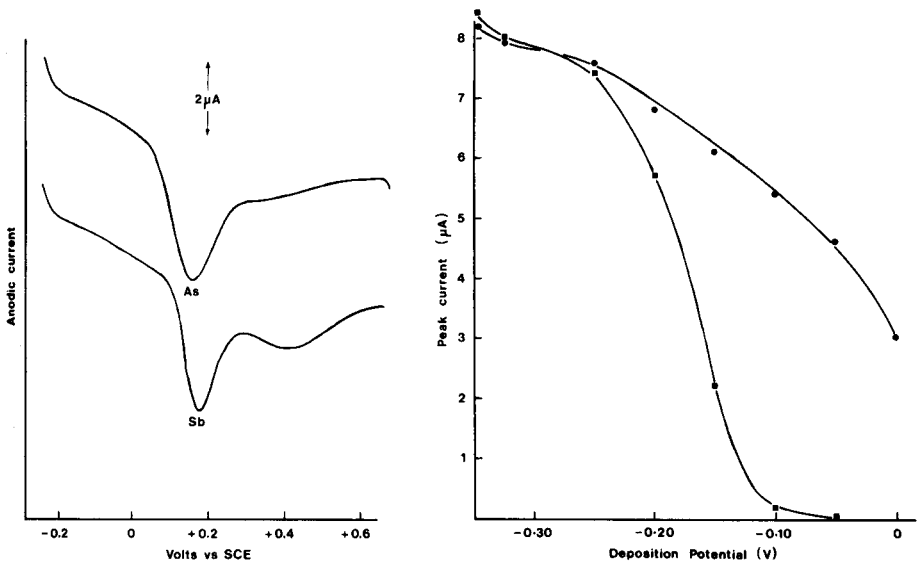

Fig. 1. Anodic stripping current–voltage curve for 15 ppb As(III) and 13 ppb Sb(III); 200 s deposition at −0.35 V in 1 M H_2SO_4; prior deposition of 2 × 10^{-2} coulombs of gold on the GCE.

Fig. 2. Anodic stripping peak height versus deposition potential for As (▪) and Sb (•); As, Sb = 33 ppb; deposition time 200 s.

TABLE 1

The potential (E_p in V) of stripping peaks for arsenic and antimony at a gold film electrode with a scan rate of +40 mV s^{-1}

pH[a]	0	1	2	4.5	6.5[b]
E_p (As)	+0.18	+0.18	+0.175	+0.04	—
E_p (Sb)	+0.20	+0.185	+0.175	+0.03	—

[a] H_2SO_4 for pH 0 and 1; phosphate buffer for pH ≥2.
[b] No peaks obtained at a deposition potential of —0.25 V.

A solution to the problem lay in selective electrodeposition. Figure 2 shows the effect of deposition potential on stripping peak height. It shows that by applying —0.05 V to the gold film electrode during the deposition step, antimony is deposited whereas arsenic is not. The resultant stripping peak height is therefore determined only by the antimony concentration. By adjusting the deposition potential to —0.30 V, antimony and arsenic are both deposited and the resulting stripping peak enables the arsenic concentration to be calculated by difference. The deposition potential of —0.30 V was chosen because the electrode response to arsenic and to antimony was the same for both elements at that potential, thus simplifying the standard addition procedures and the final calculations.

In addition to the deposition potential, the sensitivity of the determination is affected by conditioning potential, conditioning time, scan rate, solution stirring efficiency and the condition of the gold film. The effect of gold-plating conditions on deposition efficiency has been reported previously in relation to the determination of selenium and tellurium [12], and the same considerations apply equally to this work. Peak heights increase with deposition time (Fig. 3) until the surface of the gold film nears saturation, beyond which the proportionality of peak height to concentration is no longer obeyed.

A positive conditioning potential is applied to the electrode prior to the deposition step to ensure an electrochemically reproducible surface for deposition. A conditioning potential of +0.9 V gave the most reproducible arsenic and antimony stripping peaks, and the optimum conditioning time was 20—30 s. A scan rate of 40 mV s^{-1} represented a suitable compromise between peak height and baseline slope. With these parameters, the absolute responses (peak height versus concentration) for arsenic and antimony were as shown in Fig. 4. These results were calculated from both peak height and peak area and although peak area gave slightly more accurate results, the differences were not great and so peak height was used for convenience.

Application to electrolytic copper

Two certified samples of electrolytic copper (certified by the Spectroscopic Society of Canada) and designated SSC-1 and SSC-3) were analysed

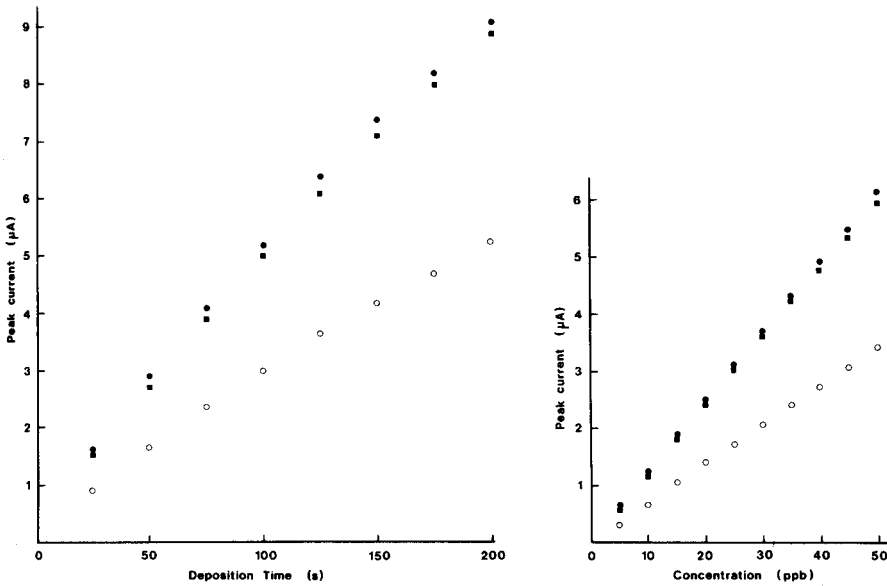

Fig. 3. Variation of As and Sb peak heights with deposition time. (■) 45 ppb As; (●), (○) 45 ppb Sb; deposition potential −0.30 V (■), (●) and −0.05 V (○).

Fig. 4. Calibration graphs for As and Sb; deposition at −0.30 V for As (■) and −0.30 V (●) and −0.05 V (○) for Sb in 1 M H_2SO_4; deposition time 100 s.

TABLE 2

Determination of arsenic and antimony in copper

Element	Sample	As or Sb present ($\mu g\ g^{-1}$)	Conc. added ($\mu g\ g^{-1}$)	Conc. found ($\mu g\ g^{-1}$)	Recovery (%)	R.s.d.[b] (%)
As	SSC-3	5.45[a]	—	5.44	100	6.1
	SSC-1	1.16[a]	—	1.29	111	15.0
	Copper	0.05	1.0	1.12	107	11.9
	Copper	0.05	0.5	0.52	95	12.1
	Blank	—	—	0.12	—	17.8
Sb	SSC-3	1.63[a]	—	1.61	98.5	6.8
	SSC-1	2.64[a]	—	2.75	104	4.1
	Copper	<0.03	1.0	0.97	97	5.5
	Copper	<0.03	0.5	0.48	95	6.9
	Blank	—	—	0.06	—	15.2

[a]Certified values. [b]Single analyses of five 0.5-g samples.

for arsenic and antimony. The determination of lower concentrations of arsenic and antimony was examined by spiking solutions of duplicate samples of high-purity copper. The results are given in Table 2. The relatively high blanks were due principally to impurities in the sodium sulphite used. The method of determining the arsenic concentration by difference resulted in the relative standard deviations being significantly higher for arsenic than for antimony when the two elements were present in similar concentrations.

The limits of detection were calculated as $2^{1.5} \times$ the standard deviation of the blank. This gives a limit of detection in solution of 0.56 $\mu g\ l^{-1}$ (4.6×10^{-9} M) for antimony and 1.12 $\mu g\ l^{-1}$ (1.5×10^{-8} M) for arsenic. These limits correspond respectively to 0.028 and 0.056 ppm in copper. The relative standard deviation was improved by about 35% by duplicating the final measurement and averaging the results.

The time required for the dissolution and separation was 30 min. The electrochemical analysis required 20 min excluding the preliminary purge and allowing a deposition time of 3 min. A single gold film could be used for more than 200 determinations before declining sensitivity required repolishing of the GCE and deposition of a new gold film.

No interference was caused by 10 ppm of the following elements in copper: Ag, Cd, Ni, Pb, Sn, Zn, S, Fe, Bi and Mn. These concentrations exceed those normally found in electrolytic copper.

The procedure for arsenic and antimony determination may be combined with the previously reported procedure for selenium and tellurium [12] by proceeding as for the selenium and tellurium method as far as eluting through the column of Chelex-100 resin. After elution, the 50-ml solution should be split into two 25-ml portions to be used for the Se + Te determination and As + Sb determinations, respectively.

REFERENCES

1 G. Van Dyke and F. Verbeek, Anal. Chim. Acta, 66 (1973) 251.
2 A. P. Grimanis and A. G. Souliotis, Analyst, 92 (1967) 549.
3 P. Pakalns, Anal. Chim. Acta, 47 (1969) 225.
4 A.S.T.M., Chemical Analysis of Metals. Sampling and Analysis of Metal Bearing Ores, Philadelphia, PA, American Society for Testing and Materials, 1969.
5 B. W. Budesinsky, Microchem. J., 24 (1979) 80.
6 E. M. Donaldson, Talanta, 24 (1977) 105.
7 J. D. Mullen, Talanta, 24 (1977) 657.
8 M. Bedard and J. D. Kerbyson, Can. J. Spectrosc., 21 (1976) 64.
9 E. M. Donaldson, Talanta, 26 (1979) 999.
10 E. Ya. Neiman and M. F. Sumenkova, Zavod. Lab., 43 (1977) 405.
11 I. Adamiec and Z. Marczenko, Chem. Anal. (Warsaw), 20 (1975) 985.
12 T. W. Hamilton, J. Ellis and T. M. Florence, Anal. Chim. Acta, 110 (1979) 87.
13 D. D. Siemer and P. Koteel, Anal. Chem., 49 (1977) 1096.
14 D. L. Collett, D. E. Fleming and G. A. Taylor, Analyst, 103 (1978) 1074.
15 B. A. Milner, P. J. Whiteside and W. J. Price, Analyst, 104 (1979) 474.
16 S. Nakashima, Analyst, 104 (1979) 172.

17 W. B. Robins and J. A. Caruso, Analyst, 104 (1979) 35.
18 A. Montaser and J. Mortazavi, Anal. Chem., 52 (1980) 255.
19 M. Thompson, B. Phalavanpour, S. J. Walton and G. F. Kirkbright, Analyst, 103 (1978) 568.
20 T. A. Krapivkina, E. M. Roizenblat, V. V. Nosacheva, L. S. Zaretskii and V. S. Utenko, Zh. Anal. Khim., 29 (1974) 1818.
21 E. Ya. Neiman and M. F. Sumenkova, Zh. Anal. Khim., 31 (1976) 912.
22 V. F. Toropova, Yu. N. Polyakov and L. N. Soboleva, Zh. Anal. Khim., 32 (1977) 985.
23 G. Forsberg, J. W. O'Laughlin and R. G. Megargle, Anal. Chem., 47 (1975) 1586.
24 P. H. Davis, G. R. Dulude, R. M. Griffin, W. R. Matson and E. W. Zink, Anal. Chem., 50 (1978) 137.
25 A. A. Yadav and S. M. Khopkar, Bull. Chem. Soc. Jpn., 44 (1971) 693.
26 K. Rengan, J. P. Haushalter and J. D. Jones, J. Radioanal. Chem., 54 (1979) 347.
27 D. Hoede and H. A. v.d. Sloot, Anal. Chim. Acta, 111 (1979) 321.
28 L. D. Hansen, B. E. Richter, D. K. Rollins, J. D. Lamb and D. J. Eatough, Anal. Chem., 51 (1979) 633.
29 R. K. Skogerboe and A. P. Bejmuk, Anal. Chim. Acta, 94 (1977) 297.
30 Kh. Z. Brainina and A. B. Tchernyshova, Talanta, 21 (1974) 287.
31 T. Nakahara, S. Kobayashi and S. Musha, Anal. Chim. Acta, 104 (1979) 173.
32 J. Azad, G. F. Kirkbright and R. D. Snook, Analyst, 105 (1980) 79.
33 T. W. Hamilton, J. Ellis and T. J. Hunt, Chem. Biomed. Environ. Instrum., 9 (1979) 353.
34 P. L. Buldini, Anal. Chim. Acta, 106 (1979) 137.
35 F. T. Henry, T. O. Kirch and T. M. Thorpe, Anal. Chem., 51 (1979) 215.

Analytica Chimica Acta, 119 (1980) 235—241

THE DETERMINATION OF ZINC, CADMIUM, LEAD AND COPPER IN HUMAN HAIR BY DIFFERENTIAL PULSE ANODIC STRIPPING VOLTAMMETRY AT A HANGING MERCURY DROP ELECTRODE AFTER NITRATE FUSION

GLEN CHITTLEBOROUGH*[a] and BARRY J. STEEL

Department of Physical and Inorganic Chemistry and Centre for Environmental Studies, University of Adelaide, South Australia (Australia)

(Received 19th April 1980)

SUMMARY

Samples of hair are digested with nitric acid and fused with alkali metal nitrates, prior to the determination of Zn, Cd, Pb and Cu by differential pulse anodic stripping voltammetry at a hanging mercury drop electrode. Recoveries from spiked samples range from 91 to 101%. Relative standard deviations vary from 2.6 to 13%, depending on the metal and sample source. Some causes of poor reproducibility are discussed.

Hair analysis for trace elements is an area of increasing interest in the fields of medical, biological, forensic and environmental science [1, 2]. Most of the recently developed techniques for trace element determinations have been applied to hair, each technique having its characteristic strengths and weaknesses. Differential pulse anodic stripping voltammetry (d.p.a.s.v.), which has frequently been reviewed [3—6], is relatively inexpensive and suitable for simultaneous determinations of a number of metals at levels of about 10^{-8}—10^{-10} mol dm^{-3}. This sensitivity is ample for the analysis of hair for Zn, Cd, Pb and Cu, where the levels generally lie in the range from one to several hundred micrograms per gram in the hair. However, although d.p.a.s.v. has been applied to environmental samples [3, 7—9], food [10], urine [11], blood [3, 12] and teeth [13, 13a], its use in hair analysis has been reported only briefly [14]. The present paper makes a further contribution in this area and a suitable preliminary digestion procedure is discussed.

Before trace metals can be determined in a hair sample by d.p.a.s.v., organic material must be completely destroyed because residual organic species may have metal-binding effects [14] and may interfere at the electrode. Digestion with concentrated acids has disadvantages [13, 15]. Bowen [16] found that fusion of samples with an excess of an equimolar mixture of molten potassium and sodium nitrates avoided most of these disadvantages.

[a]Present address: Department of Physical Science, Adelaide College of the Arts and Education, 46 Kintore Avenue, Adelaide, South Australia 5000, Australia.

Holak [10] adapted Bowen's procedure to the digestion of foodstuffs, using a concentrated aqueous solution of Bowen's mixture (2.15 mol dm^{-3} in each salt) which was added after a preliminary treatment with warm concentrated nitric acid. This procedure was suited to subsequent trace metal determinations by d.p.a.s.v. because, after fusion at 400°C, the remaining salts could serve as a supporting electrolyte for the analyte solution.

In this paper, a modification of Holak's procedure is presented as a convenient, safe digestion technique for the decomposition of hair.

EXPERIMENTAL

Apparatus

A Princeton Applied Research Corporation polarographic analyser Model 174 was used with the PAR hanging mercury drop electrode (Model 9323) and cell (Model K64). Voltammograms were recorded on a Houston Omnigraphic 2200-3-3 X-Y recorder. The reference electrode was isolated from the analyte solution by a bridge tube fitted with teflon heat-shrink tubing enclosed by an unfired Vycor plug. When a saturated calomel electrode was used, the bridge tube contained equi-molar nitrate solution. For an Ag/AgCl reference electrode, the bridge electrolyte was 0.1 mol dm^{-3} potassium chloride. The platinum wire counter electrode was placed directly in the analyte solution.

A stirring rate of 371 ± 3 rpm was achieved by means of a laboratory-made stepper motor/magnet/stirrer bar assembly actuated by a pulse generator.

Standard additions of zinc sulphate were made from a Micro/pettor syringe (Scientific Manufacturing Industries, Emeryville, California). Other standard additions were made from 10 or 20 mm^3 constriction pipettes. Concentrations and volumes are indicated in Table 1.

Glassware. Except for the digestion beakers, all glassware was treated with siliconizing solution prior to use.

The 50-cm^3 digestion beakers were specially cleaned by soaking in 6 mol dm^{-3} nitric acid, rinsing copiously with water, rinsing several times with boiling 6 mol dm^{-3} nitric acid (Aristar) and then rinsing copiously with water; the beakers were oven-dried and stored in a dust-proof container.

TABLE 1

Volumes and concentrations of solutions commonly used for standard additions

	Zn	Cd	Pb	Cu
Concentration (mol dm^{-3})	0.1	3×10^{-4}	3×10^{-4}	1.5×10^{-3}
Volume added (mm^3)	4	10	10	20

This cleaning procedure was necessary to ensure that blank levels remained sufficiently low.

The electrochemical cell, purge tube, bridge tube and HMDE capillary were cleaned with nitric acid (Aristar), washed copiously with water, and siliconized. The interior of the HMDE capillary was given special attention as recommended by the manufacturers.

Reagents

Water from ion-exchange columns was distilled and stored in polythene containers previously used for "conductance water". This water was used for all solution preparation and rinsing.

Some of the nitric acid used was BDH Aristar grade. Acid of similar quality was prepared by distillation of analytical reagent-grade acid as described by Mattinson [17].

Aqueous nitrate solution (2.15 mol dm^{-3} in each of KNO_3 and $NaNO_3$) was purified by potentiostatic deposition of heavy metals at a mercury pool in a cell constructed for the purpose. A simple potentiostat, capable of delivering 20 mA, applied a cathode potential of —1.20 V vs. SCE, the anode being separated from the bulk solution by a glass frit. During the purification (5—7 days), the pH of the bulk solution rose despite occasional mixing of the contents of the anode and cathode compartments. Since effective removal of heavy metals depends on maintaining a slightly acidic solution, a calculated quantity (0.75 cm^3 dm^{-3}) of Aristar acetic acid was added to the bulk solution; this stopped or reduced the rate of increase of pH.

Aristar-grade sodium acetate and acetic acid were used, each at concentrations of 0.1 mol dm^{-3}, to prepare a buffer solution with a pH of 4.65. This solution was also purified in the electrolytic purification cell before use.

Mercury for the HMDE was prepared by oxidising the metallic impurities in "triple-distilled" mercury with oxygen [7]. Commercial high-purity nitrogen was scrubbed with vanadium(II) solution in the usual way. Potassium chloride solutions for the reference electrodes were prepared from Aristar-grade salt.

Standard solutions used for calibration were all 0.1000 mol dm^{-3} prepared from $ZnSO_4 \cdot 7H_2O$, $3CdSO_4 \cdot 8H_2O$, $Pb(NO_3)_2$ and $CuSO_4 \cdot 5H_2O$ (dried analytical-reagent grade). Appropriate dilutions were made as needed.

Collection and storage of hair samples

At no stage were hair samples subjected to any washing or cleaning procedures [2]. Lengths of scalp hair were chopped into smaller pieces with stainless steel scissors. Facial hair was removed with an electric razor. Hair samples were kept in loosely stoppered phials placed in a desiccator used as a constant humidity vessel; the relative humidity was kept at 45% by a slush of potassium nitrite crystals and saturated solution placed in the bottom of

the vessel [18]. This was necessary because hair is hygroscopic. It was shown that 1 g of hair equilibrated with air at a relative humidity of 45% at 21°C lost 4.5% in weight when completely dried. Dried hair when exposed to air of 100% humidity gained 20.7% in weight. Although it is possible to dry the hair completely and store it in this condition, such a procedure could lead to major inconsistencies through water absorption during weighing. Storage at 45% relative humidity reduced the chances of such inconsistency.

Recommended procedures

Digestion. Predigest each 50-mg sample of hair in a 50-cm^3 beaker with 5 cm^3 of warm concentrated nitric acid for 10 min. Add 5 cm^3 of the aqueous equimolar mixture of potassium and sodium nitrates. Evaporate to dryness overnight under an infrared lamp. Place the beakers in an oven at 400°C for 3 h. Inspect hourly during this period to ensure that the char is covered by the melt.

Preparation of analyte solution. Dissolve each cooled solidified melt in 5 cm^3 of warm 0.15 mol dm^{-3} nitric acid. Transfer the solution quantitatively to the electrochemical cell, rinsing the beaker with 5 cm^3 of acetic acid/acetate buffer and then about 3 cm^3 water. (The eventual concentration calculation makes it unnecessary to have a known volume.) The analyte solution now has a pH of about 4.7.

Voltammetric procedure. Remove dissolved oxygen from the solution by passing pure nitrogen for 15 min. Set the polarograph as follows: initial potential −1.2 V vs. SCE (or −1.25 V vs. Ag/AgCl/0.1 mol dm^{-3} KCl), range 1.5 V, pulse amplitude 25 mV, pulse repetition time 0.5 s, and scan rate 5 mV s^{-1}. Use a mercury drop-size equivalent to three micrometer divisions. Remove the first drop extruded and use a second drop for analysis.

Redirect the nitrogen stream over the surface of the analyte solution and electrolyse for 180 s; maintain a steady stirring rate for the first 165 s and then switch the stirrer off. Begin the stripping scan and use the hold facility reproducibly to change the instrumental sensitivity at about −0.8 V and about −0.25 V. Repeat the above procedure after each set of standard additions (see Table 1). Measure the peak currents for each scan to check on the linearity of the current response of each species to changes in concentration.

RESULTS AND DISCUSSION

Blanks for Zn, Cd and Cu generally contributed less than 6% to the current peaks of the sample while the blank for lead provided less than about 17%.

The concentrations of metals in the hair were calculated directly from peak currents by the method of standard additions [10].

Precision was evaluated by analysing batches of 6 samples of a larger uniform sample of hair. Means and standard deviations were calculated. Two

such batches were so treated, a different individual providing the hair on each occasion. Table 2 summarizes the results obtained. (Comparison in this Table of the respective means for a given element gives, incidentally, an indication of the possible differences between individuals.) While the results for Zn, Pb and Cu are acceptable, those for cadmium are somewhat disappointing. The lower precision for cadmium originates from difficulties in choosing a satisfactory baseline for this peak.

Recovery studies

In each recovery study, half of a batch of six samples from a uniform stock of hair was spiked with aliquots of each analyte prior to analysis. The whole batch was then subjected to the digestion/analysis procedure. Comparison of results for the spiked samples with those of the unspiked samples indicated the losses of analytes during the digestion and other stages of the analysis. Recovery data for a batch of six 50-mg samples of a composite hair mixture are shown in Table 3. These recoveries may be regarded as satisfactory, comparing favourably with those of Holak [10].

Reproducibility and the hanging mercury drop electrode

Sagberg and Lund [19] have commented on the design of some HMDE's. They found optimal reproducibility in electrodes operating with capillaries which have reservoirs with inner diameters between 2.7 mm and about 2.3 mm. The internal diameter of our capillary reservoir was 3.3 mm. Here, too, problems of reproducibility with the PAR model 9323 electrode were encountered. The cause was traced to faults in the seal between the reservoir and the micrometer-syringe head. In the HMDE 9323 initially used, the capillary was supported internally at the bottom of the assembly by a thick rubber gasket which gripped the capillary tube and fitted tightly inside the bottom of the assembly. However, the gasket failed to keep the capillary rigidly coaxial with the micrometer-syringe head, thus spoiling the seal. This design weakness, which caused considerable nuisance, was remedied by placing a similarly sized rubber gasket below the reservoir flange to hold the

TABLE 2

Precision of analyses of two samples of human hair[a]
(Means and standard deviations given as $\mu g\ g^{-1}$)

Sample source	Zn			Cd			Pb			Cu		
	Mean	S.d.	R.s.d (%)	Mean	S.d.	R.s.d (%)	Mean	S.d.	R.s.d. (%)	Mean	S.d.	R.s.d (%)
MML (scalp) (100-mg samples)	521	31	6.0	4.91	0.57	11.6	8.10	0.39	4.8	192	5.8	3.0
GC (beard) (50-mg samples)	172	10.5	6.1	1.91	0.25	13.0	4.56	0.12	2.6	11.8	0.87	7.4

[a]From each large sample of hair obtained from the given individual, six smaller uniform samples were taken as a "batch".

TABLE 3

Recovery for six 50-mg samples of a beard hair mixture
(Concentrations are given as $\mu g\ g^{-1}$)

	Mean hair	Spike added	Total	Found	Recovery (%)
Zn	173	497	670	611	91
Cd	1.84	6.41	8.25	8.36	101
Pb	4.20	11.8_2	16.0_2	15.9_3	99
Cu	11.0_9	18.1_3	29.2_2	27.6_9	95

capillary tube firm. More recent kits contain a rigid polymer gasket to support the reservoir flange.

Reversed current peak

Almost without exception voltammograms produced for hair samples exhibited a curious phenomenon between about −0.8 and −0.7 V (vs. SCE). In this region the trace went below the calibrated current zero to reach a minimum in the vicinity of −0.75 V. Thereafter the trace rose sharply crossing the zero line at an atypical slope to merge into a characteristic peak for cadmium. A typical trace is shown in Fig. 1. These minima were not observed for blank runs.

When the concentration of cadmium was changed by standard addition, the minimum decreased and in some cases became positive but the peak retained the general shape shown. The peak could also be reduced or removed by dilution with water but the volume required (about 10 cm^3) then significantly reduced all peak currents. Clearly the presence of this minimum posed a problem in choosing a baseline for cadmium and lead. The upper line on Fig. 1 was a typical choice. As indicated earlier, the uncertainty in the baseline undoubtedly causes the larger relative standard deviations in the determination of cadmium.

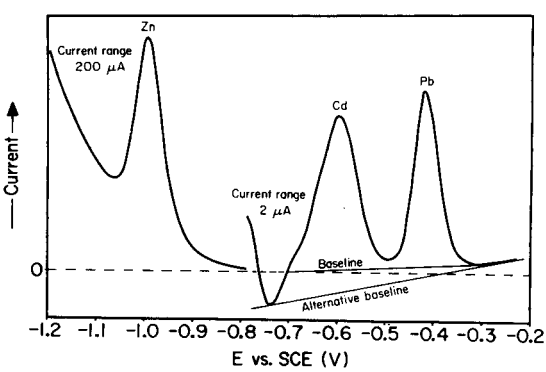

Fig. 1. "Reversed current" near −0.75 V (vs. SCE). Facsimile of an actual differential pulse anodic stripping voltammogram.

Despite this problem, linearity of peak current with concentration was observed for all four elements throughout and beyond the range of analyte concentrations pertaining during the analyses. Highest working concentrations of analyte tested were about 5 $\mu g\ cm^{-3}$ for Zn and about 0.5 $\mu g\ cm^{-3}$ for Cd, Pb and Cu.

Since the "reversed current" phenomenon occurred only in the presence of a hair digest matrix, the cause may lie in the presence of inorganic species in the concentrated nitrates mix. In their analyses of teeth, Attramadal and Jonsen [13a] ascribed poor reproducibility to inorganic phosphates derived from the tooth matrix; these difficulties were solved by dilution. Oehme et al. [13], also working with teeth, used hydroxyapatite as a reference material; the values of Zn, Pb and Cu in this reference, as determined by a.s.v. and by atomic absorption, agreed reasonably well, whereas the cadmium levels were significantly different. Kinard's study of trace metals in hair [14] by d.p.a.s.v. has no evidence of the phenomenon. The minima found in the present work appear to be peculiar to the hair/nitrate system.

In conclusion, the successful outcome of the above trials of the digestion and d.p.a.s.v. procedures permitted the authors to proceed with a study of beard hair levels of the metals Zn, Cu, Cd and Pb during substantial dosing of one of them (GC) with zinc sulphate. The procedures outlined above were successfully used in that study [20]. A short trial also indicated that the digestion—d.p.a.s.v. procedure is also suitable for the analysis of finger nails.

REFERENCES

1 See, e.g., V. Valkovic, Trace Elements in Human Hair, Garland STPM Press, New York, 1978.
2 G. Chittleborough, Sci. Total Environ., 14 (1980) 53.
3 H. W. Nurnberg, Sci. Total Environ., 12 (1979) 35.
4 H. Siegerman and G. O'Dom, Am. Lab., 4 (1972) 59.
5 T. R. Copeland and R. K. Skogerboe, Anal. Chem., 46 (1974) 1257A.
6 G. E. Batley and T. M. Florence, J. Electroanal. Chem., 55 (1974) 23.
7 G. C. Whitnack and R. Sasseli, Anal. Chim. Acta, 47 (1969) 267.
8 T. M. Florence, J. Electroanal. Chem., 35 (1972) 237.
9 G. Gillain, G. Duyckaerts and A. Distecke, Anal. Chim. Acta, 106 (1979) 23.
10 W. Holak, J. Assoc. Off. Anal. Chem., 58 (1975) 777.
11 W. Lund and R. Eriksen, Anal. Chim. Acta, 107 (1979) 37.
12 M. J. Pinchin and J. Newham, Anal. Chim. Acta, 90 (1977) 91.
13 M. Oehme, W. Lund and J. Jonsen, Anal. Chim. Acta, 100 (1978) 389.
13a A. Attramadal and J. Jonsen, Acta Odontol. Scand., 34 (1976) 127.
14 J. T. Kinard, Anal. Lett., 10 (1977) 1147.
15 T. T. Gorsuch, The Destruction of Organic Matter, Pergamon, New York, 1970.
16 H. J. M. Bowen, Anal. Chem., 40 (1968) 969.
17 J. M. Mattinson, Anal. Chem., 44 (1972) 1715.
18 R. C. Weast (Ed.), Handbook of Chemistry and Physics, 52nd edn., The Chemical Rubber Company, Cleveland, Ohio, 1971—72, p. E40.
19 P. Sagberg and W. Lund, Anal. Chim. Acta, 94 (1977) 457.
20 G. Chittleborough and B. J. Steel, Sci. Total Environ., 15 (1980) 25.

Analytica Chimica Acta, 119 (1980) 243—249

DETERMINATIONS OF TRACE AMOUNTS OF 9,10-ANTHRAQUINONE IN AQUEOUS SYSTEMS BY DIFFERENTIAL PULSE POLAROGRAPHY

J. O. BRØNSTAD and K. H. SCHRØDER*

University of Trondheim, Department of Chemistry, NLHT, N-7000 Trondheim (Norway)

H. O. FRIESTAD

Agricultural University of Norway, Chemical Research Laboratory, N-1432 Ås-NLH (Norway)

(Received 10th April 1980)

SUMMARY

A differential pulse polarographic method for the determination of 9,10-anthraquinone is presented. Methanolic solutions with 0.1 mol l^{-1} tetrabutylammonium tetrafluoroborate as supporting electrolyte give the most satisfactory results. For the determination of 9,10-anthraquinone in relatively pure substances, e.g. natural waters, a direct extraction procedure with chloroform is recommended. The detection limit is about 2 μg ml^{-1}, and the standard deviation is 2.4%. In more complex materials e.g. pulping products from the paper industry (black liquor), the interfering compounds require a modified procedure involving steam distillation/extraction.

Anthraquinones, and particularly the 9,10 compound, are of great importance in chemistry mainly in connection with production of dyestuffs and pharmaceuticals. Recently, anthraquinones have become of considerable interest in pulp and paper production [1, 2] because of the promising results obtained when they are used as pulping additives during delignification in the soda pulping process or in the Kraft sulphate pulping method. Although only small quantities of anthraquinone, in fact less than mg kg^{-1} of the total pulping wood, are added, this involves very large total quantities of the compound used in the production.

This new utilization of anthraquinones necessitates improvements in the analytical methods available for their determination Analytical methods are required not only in production control, but also for determining residual contents of anthraquinones in the paper produced, and in control of environmental pollution. The early titrimetric [3] or gravimetric [4] chemical methods for anthraquinone are time-consuming and labour-intensive, and are not suitable for trace quantities. Very recently, gas chromatography combined with mass spectrometry has been used for anthraquinone determinations in pulp- and paper- type materials [5].

Because of the pronounced oxidation—reduction properties of anthraquinones, electrochemical methods of analysis are convenient. Several polarographic studies of the compounds have been reported, and quantitative methods, with dimethylformamide [6] or chloroform—methanol—hydro-

chloric acid as solvents [7], have been reported. However, these methods could not be used in the mg l^{-1} concentration range of 9,10-anthraquinone because of insufficiently developed polarographic waves, and poor reproducibility, at such concentrations. Recently, soda-anthraquinone pulping liquor has been investigated polarographically [8] as an anodic wave in very alkaline aqueous solutions after reduction with sodium dithionite. However, that method, which seems useful in order to follow the process of pulping, lacks adequate precision for determinations of trace quantities of the compound. The renewed interest in analytical methods for anthraquinones, and the need for trace methods based on equipment of moderate cost to allow extensive analytical control of production and deposit in the environment, led to the polarographic investigations reported in this paper.

EXPERIMENTAL

Reagents and standard solutions

All reagents were of reagent-grade quality. Methanol, iso-octane, chloroform and 9,10-anthraquinone (Merck, Darmstadt, Germany) were used without further purification. Tetrabutylammonium tetrafluoroborate (Bu_4NBF_4; m.p. 164—165°C) was prepared [9] by mixing equivalent amounts of tetrabutylammonium hydrogensulphate (Bu_4NHSO_4) and sodium tetrafluoroborate in water. The precipitate was dissolved in dichloromethane and dried over a molecular sieve. Finally, the solvent was evaporated and the residue was washed with ether and dried at 70°C.

Standard solutions (4.802×10^{-4} mol l^{-1}) of 9,10-anthraquinone were prepared by dissolving 10.0 mg of the compound and diluting to 100.0 ml in methanol. The solutions were allowed to stand at room temperature for 24 h before being used.

Distilled water from quartz equipment was used in all experiments. Highly purified nitrogen gas was used for de-aerating purposes (Norsk Hydro, Norway). Standard glass equipment was used.

Apparatus

The Princeton Applied Research polarograph, model 174 (Princeton, NJ), used, was connected to a PAR M174/70 drop-timer head with a three-electrode system. The working electrode was a dropping mercury electrode (DME), and the drop time was 1 s in all the experiments. The saturated calomel reference electrode (PAR 9331) was connected to the test solution with a PAR 9332 salt bridge filled with saturated potassium chloride. The auxiliary electrode was a platinum wire. The polarographic cell (PAR 9300 and PAR 9301) was kept at 25.0°C. The polarograms were recorded with an Omnigraph 2000 recorder (Houston Instruments, TX, U.S.A.). Evaporations were carried out with Rotavapor-R equipment (Büchi, Switzerland). The continuous steam distillation/extractions were done in a modified Bleidner device [10] as shown in Fig. 1. By using this method, the anthraquinone was continuously steam-distilled and extracted into iso-octane.

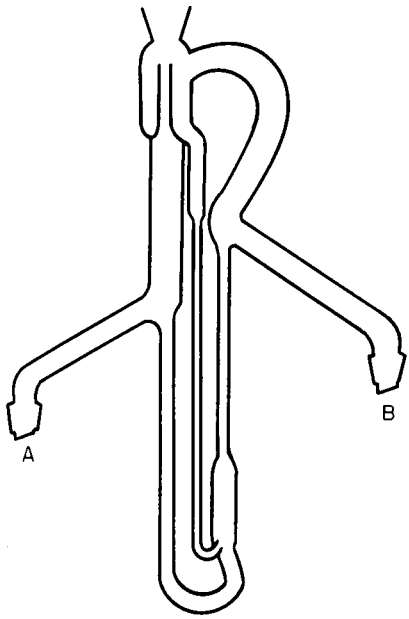

Fig. 1. The continuous steam distillation/extraction device used in Method B. The relative proportions of the device are critical. The total height is 50 cm. (A) The water side (1-l round-bottom flask); (B) the iso-octane side (250-ml round-bottom flask).

Procedures

Method A. Determination of anthraquinone in water. Shake 50 ml of the aqueous sample with 50 ml of chloroform in a separatory funnel, and allow to stand for 30 min. Withdraw the chloroform phase and evaporate to dryness with the Rotavapor. Add 50 ml of methanol to the residue, shake the mixture and allow it to stand for 1 h. Add the supporting electrolyte Bu_4NBF_4 to give a concentration of 0.1 mol l^{-1}. Bubble nitrogen gas through the solution for 5 min. Then record the differential pulse polarogram with a scan rate of 5 mV s^{-1} and a pulse amplitude of 50 mV. Pass nitrogen gas over the solution while the polarograms are recorded.

Method B. Determination of anthraquinone in paper, pulping materials (e.g. black liquor) and other industrial samples. Add 500 ml of water to 100 ml of the sample (e.g. black liquor) and transfer this to the steam distillation/extraction device (Fig. 1), using a 1-l round-bottom flask. This is connected to a 250-ml round-bottom flask with 100 ml of iso-octane on the other side of the device. Add some anti-foam (2—3 drops) and anti-bumping granules to the aqueous side, and keep boiling for 4 h. Evaporate the iso-octane phase to dryness by using the Rotavapor, and dissolve the residue in 50 ml of methanol. Shake the mixture and allow to stand for 1 h. Then add the supporting electrolyte, and follow procedure A, starting from "Bubble nitrogen gas . . .".

RESULTS

As discussed below, the polarographic behaviour of 9,10-anthraquinone is very sensitive to, and dependent on, the nature of the solution and the supporting electrolyte. Thus great efforts were made to find a proper electrolyte in order to optimize the analytical method. The most satisfactory results were obtained with 0.1 mol l^{-1} tetrabutylammonium tetrafluoroborate dissolved in methanol.

Figure 2 shows differential pulse polarograms of a 0.1 mol l^{-1} solution of tetrabutylammonium tetrafluoroborate in methanol, with increasing amounts of a standard solution of anthraquinone added. A calibration graph prepared for methanolic solutions with anthraquinone standards was linear for the range 125—3000 μg (= 2.5—60 μg ml^{-1}) of anthraquinone (peak heights 0.2—5.6 μA) and then curved gradually up to 5000 μg (= 100 μg ml^{-1}). When aqueous standard samples containing 400—2000 μg of anthraquinone were subjected to chloroform extraction as in Method A, the calibration graph was again linear (range of peak heights, 0.72—3.7 μA). It is clear from these results that acceptably low detection limits can be obtained.

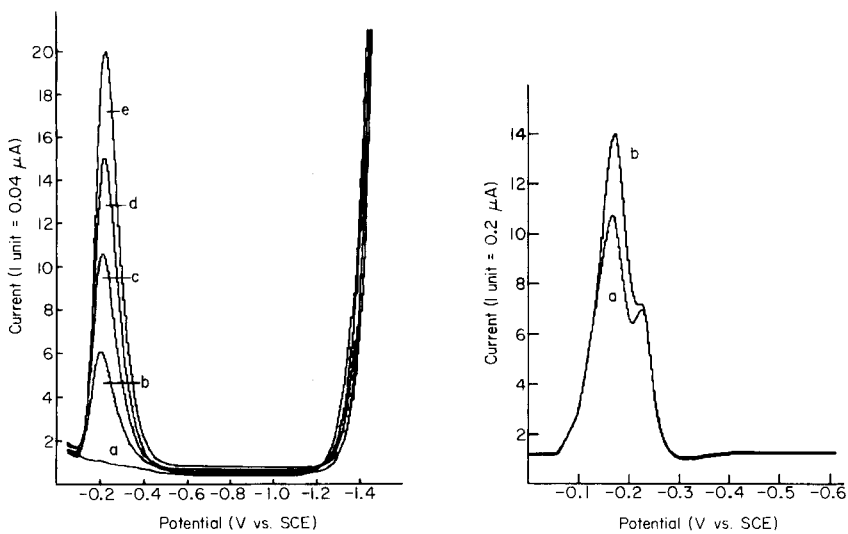

Fig. 2. Differential pulse polarograms of 9,10-anthraquinone in 50.0 ml of 0.1 mol l^{-1} Bu_4NBF_4 in methanol with added amounts of methanolic anthraquinone standard solution (100 μg ml^{-1}; 4.802 × 10^{-4} mol l^{-1}). Volumes added: (a) 0; (b) 1; (c) 2; (d) 3; (e) 4 ml.

Fig. 3. A typical differential pulse polarogram of anthraquinone in presence of interfering substances by Method B. (a) 100 ml of black liquor with anthraquinone added (25 μg ml^{-1}); steam distillation/extraction for 5 h; (b) repeat polarogram of (a) after introduction of 5 ml of a methanolic 100 μg ml^{-1} anthraquinone standard into the 50 ml of methanolic solution already in the cell.

When strongly contaminated samples are analyzed, Method B is required in order to avoid interferences. Its efficiency was tested by analyzing the most complex material of analytical interest available, i.e., the black liquor from the pulping industry. Figure 3 shows the different pulse polarogram obtained for a sample of that liquor, containing 25 μg of anthraquinone per ml, treated according to Method B. The black liquor sample standard was prepared by adding an appropriate quantity of the methanolic anthraquinone standard to a round-bottom flask; all the methanol was then evaporated and the black liquor sample containing no anthraquinone was added. The extraction procedure was then applied. Curve (b) in Fig. 3 is the polarogram recorded after further addition of 5 ml of the methanolic anthraquinone standard directly into the polarographic cell.

As can be seen from Fig. 2, 9,10-anthraquinone is reduced at a somewhat concentration-dependent peak potential in the range 0.20—0.25 V. Increasing concentration of the compound shifts the potential about 0.05 V towards more negative values when the concentration is increased from 1 to 100 μg ml^{-1}.

In order to examine the reproducibility of Method A, twelve identical samples in natural water were analyzed individually. The samples contained 24.0 μg ml^{-1} of anthraquinone, added from the standard after evaporation of the methanol. A relative standard deviation of 2.3% was calculated from the results obtained.

The degree of recovery of the extraction in Method A was checked by comparing with anthraquinone samples added directly to the polarographic cell. Recoveries were found to be higher than 98%, and thus within probable experimental error, in all experiments.

DISCUSSION

The polarographic studies of 9,10-anthraquinone were initially done in aqueous solutions in order to evaluate a quantitative analytical method suitable for concentrations below 100 μg ml^{-1}. This did not succeed, because of the very low solubility of the compound in water. Efforts to increase the solubility by addition of detergents as described by Proske [11] were unsuccessful in the actual concentration range.

Two polarographic waves appeared in some solutions, e.g. when an aqueous 0.1 mol l^{-1} acetate buffer (pH 4.7) was used and a methanolic anthraquinone standard was added. The wave which appeared at the more positive potential was small and too badly defined to be of analytical value. The other wave, however, was well defined with a high peak current and seems to have potential for analytical purposes. It was found that the wave appeared as a result of exposure of the solution to light, and an effort was made to establish the mechanism and to evaluate an analytical method based on the effect. A fully satisfactory explanation has not yet been found. However, the polarographic curves obtained for a methanolic 9,10-anthraquinone standard

in aqueous 0.1 mol l^{-1} acetate buffer (pH 4.7) exposed to light in the absence of oxygen were found to be very similar to the curves obtained when hydrogen peroxide was added to the same system. Thus there is some evidence to believe that the curves are due to some peroxide formation. At present, it is not possible to utilize the wave analytically because of its poor reproducibility. The wave height was found to increase with increase in radiation time, but to decrease with time when the radiation was stopped. The wave height increased to a maximum value with increasing radiation intensity, but further radiation caused a decrease in the peak height. Efforts to stabilize the waves have not yet proved successful.

Systematic testing of different methanol/water systems with various supporting electrolytes (potassium chloride, lithium chloride, potassium bromide, tetramethylammonium chloride and tetramethylammonium bromide) did not give satisfactory reproducibility for analytical purposes. A large number of non-aqueous systems with different supporting electrolytes was therefore tested. It was found that methanol as solvent with tetrabutylammonium tetrafluoroborate as supporting electrolyte gave a system greatly superior to all other systems tested. The waves were well developed even at low concentrations of the anthraquinone, and the results were very reproducible. Only one polarographic peak wave appeared, and it was not affected by light. In this system, the small shift of the peak potential with increasing quantities of anthraquinone can be ascribed to the low buffering capacity of the solution. However, such a shift is of minor interest in quantitative analyses and thus was not further studied.

In the analytical procedure, chloroform extraction of aqueous samples gives the most satisfactory results. However, very crude samples, e.g. black liquor from the pulping industry, cannot be analyzed by a direct extraction procedure because of the presence of interfering species. When the steam distillation/extraction procedure (B) is used, it becomes possible to determine 9,10-anthraquinone at levels below 5 μg ml^{-1} in the black liquor matrix, as indicated in Fig. 3. The analysis of such samples, however, provides a lower accuracy than that available with Method A for natural waters, because of the low (about 60%) recovery of the anthraquinone in the extraction procedure. However, the recovery increases with increasing extraction times. Experiments to improve the present method further, especially for application to paper, pulp and pulping materials (black liquor) and industrial sewage samples, are now in progress.

Gravimetric analyses showed that the solubility of anthraquinone is 110 μg ml^{-1}, 8570 μg ml^{-1} and 33 μg ml^{-1} in methanol, chloroform and isooctane, respectively, at 23°C. The curvature of the calibration curve near 100 μg ml^{-1} can therefore be explained from the low solubility of anthraquinone in methanol.

The authors thank Kristin Finserås for skilful technical assistance. Financial support from the Norwegian Research Council for Science and Humanities is greatly appreciated.

REFERENCES

1 H. H. Holton, Pulp Pap. Can., 78, 10 (1977) 19.
2 G. Gellerstedt, Sven. Träforskningsinst. Stockholm, Report B529, 1979.
3 O. A. Nilson and C. E. Senseman, J. Ind. Eng. Chem., 14 (1922) 956.
4 H. Pirak, Angew. Chem., 41 (1928) 231.
5 J. E. Currah, Tappi, 62 (1979) 73.
6 R. L. Edsberg, D. Eichlin and J. J. Garis, Anal. Chem., 25 (1953) 798.
7 P. D. Garn and M. C. Bott, Anal. Chem., 33 (1961) 84.
8 B. I. Fleming, G. J. Kubes, J. M. Macleod and H. I. Bolker, Tappi, 62 (1979) 55.
9 K. Nyberg, Acta Chem. Scand., 24 (1970) 1609.
10 Pesticide Analytical Manual U.S. Dept. of Health, Education and Welfare, Pesticide Reg. Sec. 120.250.
11 G. E. O. Proske, Anal. Chem., 24 (1952) 1834.

Analytica Chimica Acta, 119 (1980) 251—261

THIN-LAYER HYDRODYNAMIC BIAMPEROMETRIC END-POINT DETECTION: APPLICATION TO THE COULOMETRIC TITRATION OF ARSENIC(III) WITH BROMINE

M. A. de SOTO PERERA** and D. J. CURRAN*

Department of Chemistry, GRC Tower I, University of Massachusetts, Amherst, MA 01003 (U.S.A.)

(Received 26th March 1980)

SUMMARY

A sandwich-type thin-layer cell has been applied to hydrodynamic biamperometric end-point detection in coulometric titrations. The detector cell, constructed from two pieces of teflon, has platinum indicator electrodes and is placed in a flow loop attached to the coulometric titration cell. The thin-layer cavity has a volume of 6.5 μl and a thickness of 51 μm, which are obtained using teflon tape as a spacer. A peristaltic pump maintains a continual flow through the loop. The titration cell is a closed vessel completely filled with the solution to be titrated. Operational amplifier circuits control the potential difference applied across the two thin-layer electrodes, and to measure the current developed in the thin-layer cell. Noise arising from the pulsed nature of the flow is reduced by a factor of 25 by using an electronic filter. The titration of arsenic(III) with electrogenerated bromine was used to study the performance of the system. Concentrations from 24 ppb to 1.6 ppm can be determined with relative inaccuracies of +4 and +0.1%, respectively.

The high sensitivity of biamperometric end-point detection is well known, and the technique has been described by Lingane [1] and Bishop [2]. Typically, a pair of identical electrodes, usually wire, are inserted into a titration vessel which incorporates magnetic stirring. The method is particularly compatible with coulometric titrations and there are many examples in the literature. Thus far, there appear to be no reports on the use of flow-through thin-layer cells for biamperometric end-point detection. In this work, a thin-layer cell with twin platinum electrodes is placed in a flow loop attached to a coulometric titration vessel. Such a detector is expected to have very high sensitivity, making it compatible with the end-point detection requirements of coulometric titrations of solutions in the sub-ppm concentration range. The coulometric titration of arsenic(III) with bromine was chosen to investigate this. Meyers and Swift [3] were the first to study this reaction using biamperometric end-point detection. They were able to determine down to 34.9 μg of arsenic(III) in 50 ml of solution (698 ppb) with an absolute error of about 0.4 μg. Lee and Adams [4] determined as

**Present address: Dow Chemical U.S.A., P.O. Box 68511, Indianapolis, IN 46268, U.S.A.

little as 48.67 μg in 35 ml of solution (1.39 ppm), with errors ranging from +0.06 to +0.72% relative, using a potentiometric end-point. These authors pregenerated bromine in an effort to eliminate reducing agents in the titration medium before adding the sample, and thus conditioned the indicator electrodes according to the procedure of Meyers and Swift [3]. In the method of Christian [5] an excess of bromine is generated coulometrically and a sample is added which will not consume all of the bromine. The change in current produced by the addition of sample is measured amperometrically, which together with the slope of the current—time curve obtained upon generating the excess of bromine, is used to calculate the time of electrolysis required to generate the bromine consumed. The kinetics of the chemical reaction are used to best advantage in this fashion and as little as 2.54×10^{-4} μeq of arsenic(III) in 35 ml of solution (0.272 ppb) were determined with a relative error of 3.7%. The point was made that the end-point could not be obtained graphically because of the extreme curvature of the titration curve.

Jennings et al. [6] first reported the use of vitreous carbon as an electrode to generate bromine. The current efficiency was estimated to be better than 99.9%. A potentiometric end-point was employed in the titration of arsenic(III) with bromine and about 100 μeq in 150 ml of solution (25.0 ppm) were titrated with an accuracy and precision of 0.1 μeq. It was observed that the titration error became more positive as the amount of arsenic(III) titrated decreased, a trend also found with platinum generator electrodes. In a later paper, Jennings et al. [7] titrated from 3 to 15 μg of arsenic(III) in 2 ml of solution (1.5—7.5 ppm) with an imprecision of 2%, using a vitreous carbon anode and a form of differential electrolytic potentiometry for end-point detection. In the present work, platinum electrodes were used in both the titration and detector cells. Successive samples of arsenic(III) were titrated in the same titration cell solution and concentrations from 24 ppb to 1.6 ppm were determined.

EXPERIMENTAL

Apparatus and instrumentation

The coulometric titrator was constructed previously in this laboratory. It is discussed in detail elsewhere [8] and has been used in several applications [8—10]. The other major parts of the titration system were as follows: micro-submersible magnetic stirrer (model MS-7, Tri-R Instruments, Long Island, NY), constant temperature bath (model T-9, P.M. Tamson, Holland), 3-roller peristaltic pump (Cole-Palmer Masterflex with head No. 7013 equipped with Viton tubing), DVM (Fluke model 8300A), recorder (Honeywell model Electronik 194), compound regulated supply (Philbrick Researches PR-300), and URS (Heath Model EU-POA).

The complete titration system is shown in block diagram in Fig. 1. The solution in the coulometric titration cell (b) was continuously pumped

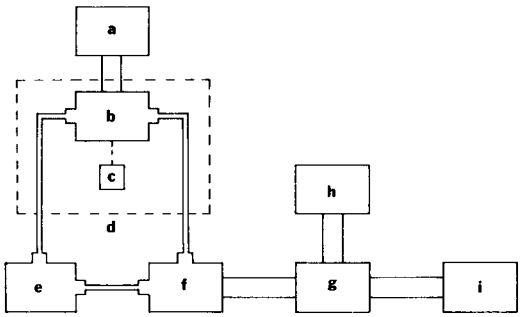

Fig. 1. The titration system: (a) coulometric titrator; (b) titration cell; (c) submersible magnetic stirrer; (d) constant temperature bath; (e) peristaltic pump; (f) thin-layer biamperometric detector cell; (g) unit for thin-layer electrode voltage control and current-to-voltage conversion; (h) digital voltmeter; (i) recorder.

through the thin-layer detector (f) and back to the titration cell. The detector cell current was converted to a voltage by an operational amplifier circuit and the output measured by the DVM and recorder. The circuit for control of the potential across the thin-layer cell was a conventional OA voltage control circuit. The input voltage set on the VRS appeared across the detector cell with a sign inversion. Analog Devices 52K FET electrometer amplifiers were selected because of their low current and voltage noise characteristics, excellent long-term stability (5 μV/month) and fast thermal response. They were mounted on modified Heath EU-900NC dual OA cards. All resistors used were precision (±1%) metal film and were hand-selected to give desired ratios. Pump noise on the output of the current-to-voltage converter was reduced by an RC filter (time constant, 0.8 s). The d.c. output across the capacitor was buffered with an OA voltage follower before measurement with the recorder or DVM.

The coulometric titration cell. The cell, shown in Fig. 2, was designed to have no gas space above the solution and to connect to the flow loop containing the end-point detector cell. The two halves were held together by a pinch clamp (not shown) and sealed by a rubber O-ring (f) wrapped with teflon tape. The bottom half had an outlet (i) with a teflon stopcock through which the solution flowed to the pump and then to the thin-layer cell. The outlet contained a plug of glass wool (h) used as a filter to prevent particulate matter from reaching the thin-layer cavity and clogging it. A magnetic stirring bar (g) was used to mix the solution during the titration. The top half incorporated the cathode compartment, tube (a): the upper section was a female 14/20 joint and the lower end was terminated in a fine frit. A threaded glass port (d) (Ace-Thred-5027-20) was used to introduce a micrometer-driven microburet for delivering the sample. Alternatively, a thermometer could be inserted in this port. The anode (e) was blown onto the main body of the top. A platinum flag electrode of 2 cm^2 area was used and a spiral of platinum wire served as the cathode. An inlet glass tube (b) was used as a

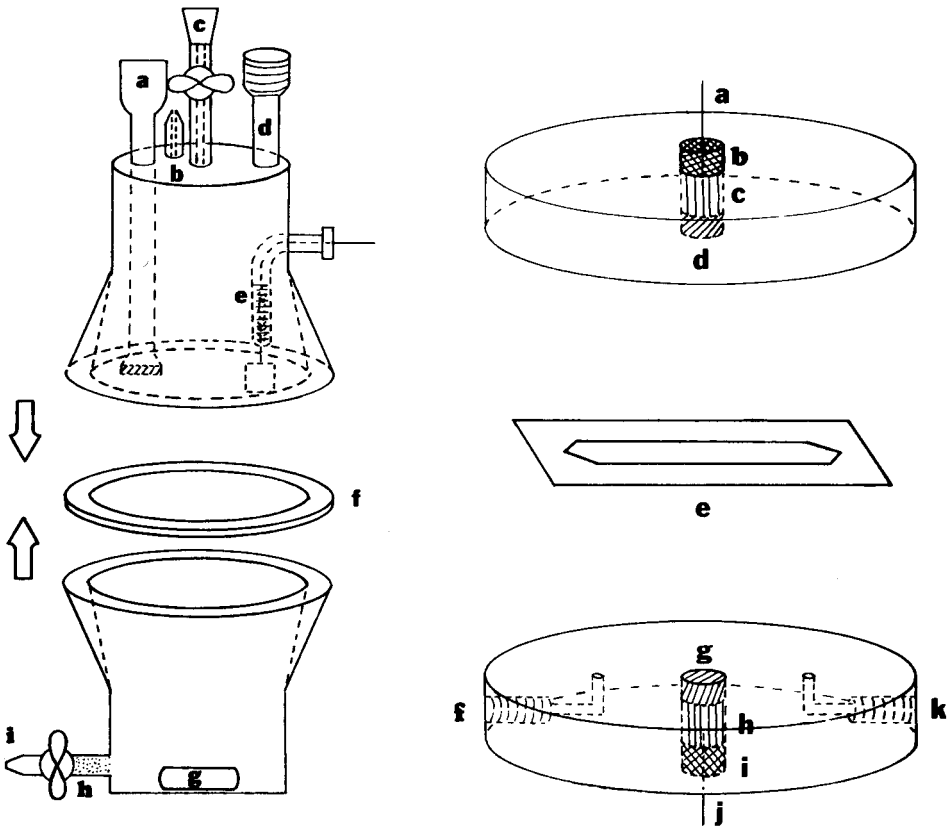

Fig. 2. The titration cell: (a) cathode compartment; (b) inlet from the thin-layer detector cell; (c) capillary stopcock and reservoir for excess solution; (d) microburet port; (e) anode; (f) O-ring; (g) magnetic stirring bar; (h) glass wool plug; (i) outlet to pump.

Fig. 3. The thin-layer detector cell: (a) and (j) platinum wires; (b) and (i) teflon plugs; (c) and (h) mercury pools; (d) and (g) platinum rod electrodes; (e) teflon spacer; (f) and (k) inlet and outlet.

return line for the solution pumped from the thin-layer cell. A teflon capillary stopcock (c) was placed in the center of the top as shown in Fig. 2. This feature was used to fill the cell entirely with solution. Excess of solution overflowed up the capillary to the small reservoir when the cell was assembled and filled. The stopcock was closed after the cell was filled and the buret put in place, and it remained closed during a titration. The whole assembly stood 19 cm high and held 242 ml of solution, not including the flow loop.

The thin-layer cell. The design of the thin-layer cell is shown in Fig. 3. The two halves, made of teflon, were 5.08 cm in diameter and 1.27 cm thick. A hole slightly smaller than the platinum rod electrodes (0.635-cm diameter) was drilled exactly in the center of each of the pieces. The inlet

and outlet (f and k) were 0.17 cm in diameter and terminated in ports threaded to accept teflon Cheminert Altex fittings (No. 200-00 for 1.5 mm o.d. tubing). Four additional 0.4-cm diameter holes (not shown), equidistant from each other, were drilled near the edges of the teflon pieces for the nylon bolts used to fasten together the two halves of the cell. After machining, the pieces were immersed in a solution of water, hydrochloric acid and EDTA to remove any metal particles left from the drilling process. The pieces were further cleaned by placing them in an ultrasonic bath. After rinsing they were dried with a stream of prepurified nitrogen and placed for about 15 min in a muffle furnace (Lindberg, Sola Basic Industries) set at 220°C. They were taken out and the platinum rods (d and g) were immediately forced into the holes from the back side until the polished, flat face was parallel to the face of the pieces. They were allowed to cool so that the teflon could contract and form a good seal around the rods. The pieces were polished on Beuhler equipment using standard metallurgical techniques. The finest grit paper used was 600. To avoid leaking, care was taken to end the polishing procedure with the polishing lines aligned in the direction of solution flow. Electrical contact to the electrodes was made by placing a small amount of mercury in the space above the platinum rods. Teflon plugs (b and i) were machined to fit tightly in the cavity. Two small holes were drilled through the plugs: in one a platinum wire (a and j) was inserted to make contact with the mercury. The other hole served to let air escape from the cavity when the plug was forced into place. Afterwards, this second hole was sealed with a small platinum wire.

Before the two cell halves were fastened together, a teflon spacer (e) [1.27 cm wide and 51 μm (2 mil) thick; Dilectrix Corp., 69 Allen Blvd., Farmingdale, NY 11735], with a channel cut out to define the path travelled by the solution from inlet to outlet, was placed between them. Care was taken that no dust particles were trapped between the two cell halves, since this would either clog the thin-layer cavity or prevent them from sealing properly upon tightening the nuts. The resistance of the assembled cell was checked in air to ensure that the electrodes were not contacting each other. The volume of the cavity was estimated as 6.5 μl, based on the dimensions of the channel. After repeated use, it was necessary to disassemble the cell and clean it. If the electrode surfaces were not shiny, they were repolished.

The flow loop. Viton tubing (0.413 cm o.d., 0.080 cm i.d.) was used in the pump head. One end of a 33-cm length was attached to the titration cell outlet and the tubing then passed through the pump head. The other end was joined to 13.5 cm of teflon tubing (0.15 cm o.d., 0.080 cm i.d.) which was terminated with an Altex fitting for connection to the thin-layer cell. The same teflon tubing (16 cm) was used for the return line from the detector to the titration cell. The entire loop volume was estimated to be 1.4 ml.

Chemicals and solutions

For most of the work, deionized, distilled water (resistance, 8—9 megohm) was obtained from the Natural Water Chemistry Laboratory, Univ. of Mass., Amherst. In other cases, deionized water was distilled from alkaline permanganate. All chemicals were reagent grade unless otherwise stated. For studies involving the electronic filter, the electrolyte was 0.1 M sulfuric acid, 0.2 M in sodium bromide. Primary standard (99.98%) arsenic trioxide was dried in an oven for 1 h at 110°C. Solutions were prepared by dissolving 0.5 g of the compound in 10 ml of water containing 1 g of sodium hydroxide, acidifying with 21 ml of 1.2 M sulfuric acid, and diluting to 500 ml. These solutions were usually not kept for more than five days.

Procedures

Flow rates were determined by measuring the time taken to fill a 10-ml graduated cylinder with the test solution and correlating the result with the dial settings on the pump control unit. Typically, flow rates of about 16 ml min^{-1} were used for the titrations. Higher flow rates produced too much back-pressure from the thin-layer cell.

Titrations were carried out with generating currents of 5 or 0.5 mA. The potential difference applied across the thin-layer cell was 170 mV. The temperature was held constant in the range 18—24.5°C. All data points were read from the digital voltmeter, and the time display of the titrator. When not in use, the electrodes were stored in water. Approximately 5 g of sodium bromide was weighed, transferred to the titration cell and dissolved with water; 1 ml of the 1.2 M sulfuric acid solution was then added. The titration cell was placed in the constant temperature bath and the magnetic stirrer was started. The pump was turned on as more water was added to the titration cell, being careful that no air bubbles were trapped inside and the entire volume was finally occupied with solution. The cathode compartment was filled with 1.2 M sulfuric acid and the platinum spiral electrode was secured in place. A Gilmont S-3200, 2.5-ml microburet was filled with the standard arsenic(III) solution and placed in the titration cell. Excess of solution from the titration cell overflowed into the reservoir and the stopcock was closed. Electrical connections from the coulometric titrator to the generator electrodes were made and the titration was started by generating bromine in small increments of time and measuring the current after each increment by disconnecting the generator anode, connecting the thin-layer electrodes, and waiting for a few seconds until a stable signal was obtained on the DVM. A known volume of arsenic(III) solution was added from the microburet. The titration was continued incrementally as before, until well after the end-point, as signaled by an increase in the current due to the presence of excess bromine. Making sure from prior knowledge of the sample that the amount of bromine now in solution is less than that needed to react with the next sample of arsenic(III), another sample is added, after the stopcock to the reservoir has been opened. As many as 15 samples can

be titrated in the same solution. After all the determinations are done, the titration cell is dismantled and rinsed with water. The thin-layer cell is also rinsed by pumping water through it. End-points were determined by computer calculation and statistical treatment of the results was done in the same fashion.

RESULTS AND DISCUSSION

The titration cell, pump and flow loop

The literature on the titration of arsenic(III) with electrogenerated bromine revealed that the titration error was usually positive. Preliminary experiments in a titration vessel with a gas space above the solution produced similar results. Positive errors could arise from loss of bromine to the gas phase so the cell shown in Fig. 2 was designed to eliminate the gas phase. A peristaltic pump was chosen, for its convenience, relatively low cost, and the fact that no moving parts of the pump come in direct contact with the solution. This latter point is important for two reasons: many materials are attacked by bromine, and the problems of losses or contamination become more acute when dealing quantitatively with very dilute solutions. These problems reduce to selecting the tubing for the pump head when a peristaltic pump is used. Several types of tubing were tried but Viton was the most satisfactory. It was observed that, while a solution of electrogenerated bromine could be kept in a closed vessel for about one day with very little loss, the rate of disappearance of bromine increased significantly with the solution flowing. To ascertain if the tubing were the problem, its length was doubled, which was expected to double the rate of loss of bromine. The rate changed very little. Possibly the pump action on the tubing is responsible. Photodecomposition was considered but titrations performed in the presence and absence of light showed no significant difference. The loss of bromine was not significant over the time span of a series of titrations and the tubing was replaced periodically. The disadvantage of the peristaltic pump is that the flow is pulsed and this generates noise which appears on the output signal. Mechanical damping devices would increase the volume of the flow loop so electronic filtering was used to remove the noise. Figure 4 shows recorder tracings of the output signal from the current-to-voltage converter at two different flow rates both before and after filtering. The noise is reduced by a factor of at least 25, and the filtering is slightly better at the higher flow rate. The waveforms shown in Fig. 4 include noise contributions from the electronics. The reason for the appearance of nodes at the lower flow rate is not clear but they might result from an interaction of the flow due to the pump and a contribution from the magnetic stirring action.

A time delay in the output signal of 4 s is introduced by the RC time constant of the filter circuit. An additional delay in the detector response is produced by the flow loop volume that was 0.6% of the volume of the

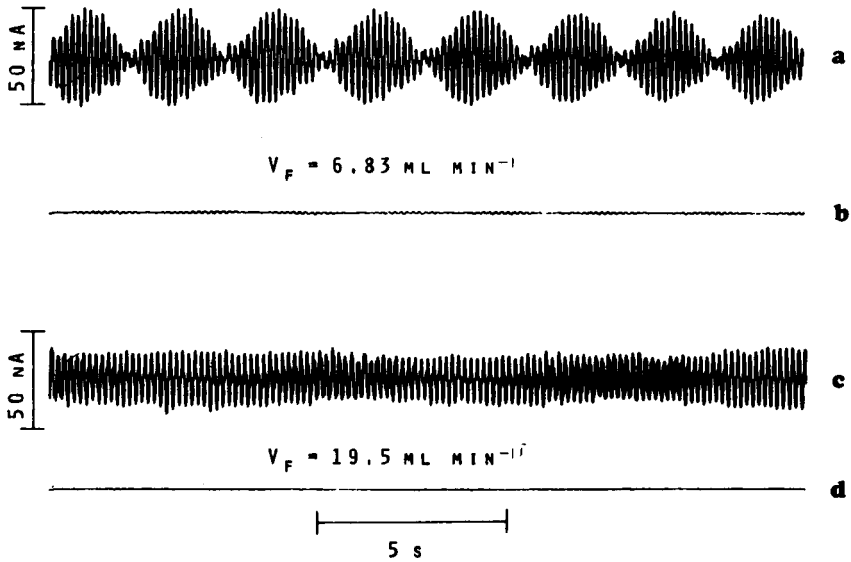

Fig. 4. Recorder tracings of current-to-voltage converter output signal: (a) and (c) unfiltered; (b) and (d) filtered.

titration cell. Most titrations were carried out at a flow rate of 16 ml min^{-1} and the residence time in the loop was therefore 5.3 s. Since the current measured is steady-state and the titrations were performed by incremental generation of titrant, neither of the above time delays is significant. However, in the interest of producing a homogeneous solution as rapidly as possible, the volume of the flow loop should be small compared to the volume of the titration cell.

Arsenic titrations

Most published procedures for the coulometric titration of arsenic(III) with bromine use a supporting electrolyte with a pH in the range 0—1. However, no discussion of the pH dependence of the titration reaction was found in the literature. Examination of the potential—pH diagram presented by Laitinen [11] for the arsenic couple shows that arsenic(III) is a stronger reducing agent at higher pH. Thermodynamically, less acidic supporting electrolytes would favor the titration reaction. However, titrations of 413 ppb solutions of As(III) at pH 3 and 4 yielded results with relative inaccuracies of 2.3 and 1.3%, respectively. Titration of 321 ppb solutions at pH 2 produced a relative error of 0.1%. On this basis, a pH of 2 was chosen, where it seems that the kinetics of the reaction are more favorable. At this pH, arsenic(III) is present entirely as H_3AsO_3 and arsenic(V) as a mixture of H_3AsO_4 and $H_2AsO_4^-$.

Titrations were performed by adding samples of arsenic(III) successively to the titration cell. The first run was always a blank to remove any im-

purities which might react with bromine. The sample was added to the solution containing an excess of bromine which was present in an amount less than that equivalent to the amount of arsenic(III) added. The titration was then carried out and thus an excess of bromine generated again. The procedure was then repeated for the next sample. It was not necessary to generate the same excess of bromine each time. A feature of the coulometric titrator is that the length of time for an increment of titrant to be generated can be selected by six thumbwheel switches. The current is automatically shut off when this time interval elapses. The time interval is automatically added to the previous total electrolysis time and the new total is displayed on a 6-digit readout. In addition to summing the electrolysis time for a single titration, the instrument can continue the process for a whole series of titrations.

The arsenic couple is irreversible so that the hydrodynamic biamperometric titration curve shows little current prior to the end-point and a linear rise afterwards because of the presence of excess bromine. It was observed that the titration curves before the end-point were essentially flat, very reproducible and parallel to the time axis. An end-point taken as the intersection of the rising portion with the time axis would be in error but the difference between two such intersections for two successive titrations will yield the correct titration time for the second titration, if the slopes of the lines beyond the end-points are the same. This will be the case if dilution is negligible, the flow rate is the same, and the temperature is constant. All of these conditions were met in these titrations, and a series is shown in Fig. 5. Curve a is the blank. The volume of sample used for titration k was twice that of the others. The computer program was used to calculate the least-squares best line for each titration, the intercept on the time axis, and the difference in intercepts between each titration and the preceding one. The average slope of the lines after the end-point in Fig. 5 is 0.1408 μA s^{-1} with a relative standard deviation (RSD) of ±1.8%. The reproducibility of the slope is satisfactory. In fact, nine of the slopes had an average of 0.1400 μA s^{-1} with a RSD of ±0.1%. An electrolysis time of 1 s at a current of 4.994×10^{-3} A will generate 5.8×10^{-8} eq of bromine, which corresponds to 2.05 μM in this cell. The slope can therefore be expressed as 1.32 mA mM^{-1}, which illustrates the high sensitivity of the detector.

Titrations were done with amounts of arsenic(III) which corresponded to concentrations in the titration cell ranging from 24.2 ppb to 1.598 ppm. The data and results are summarized in Table 1. Excellent precision and accuracy were achieved. A significant contribution to the errors shown in the last three columns comes from the microburet used to deliver the samples. Although the buret is precise to 1 part in 25,000, it is accurate only to 5—10 parts in 25,000. Another source of positive error involves the solution displaced during addition of a new sample. Roughly 85% of the bromine required for a titration is present when the sample is added so that some bromine is lost with the solution displaced up the capillary tube. For a 0.5-ml

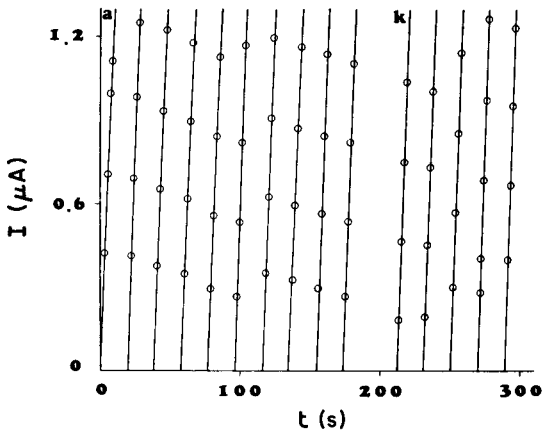

Fig. 5. Titration curves for 154 ppb arsenic(III) solution: (a) blank; (k) twice the volume of sample added.

sample this would result in an error of 0.17%, but would be negligible for smaller samples. The precision shown in the penultimate column of the Table for the 35.6 ppb solution seemed somewhat poor. The experiments were repeated, lowering the current by an order of magnitude. The result in the last column shows a definite improvement in precision. The coulometric titrator is quite capable of measuring time to the nearest millisecond so the improvement is attributed to the slower rate of generation of bromine.

The results clearly demonstrate the practicality of the thin-layer detector cell for the titration of solutions in the ppb concentration range. Expressed as molarity, the 24.2 ppb solution of arsenic(III) is 3.22×10^{-7} M. The results also show that the use of titration cells which contain no gas phase is advantageous for titrants like bromine which are volatile in aqueous solution. The use of the method in a continuously recorded mode for the determination of certain steroids is described in a subsequent paper [12].

TABLE 1

Results of the determination of arsenic(III) with electrogenerated bromine

Conc. of stock soln. (mM)	10.38	10.38	10.38	9.94_3	11.57	11.57
Replicates	4	9	13	12	12	6
Vol. of stock soln. (μl)	500.0	250.0	100.0	50.0	25.0	10.0
Equiv. of As taken (μeq)	10.38	5.19	2.076	0.994	0.578	0.231
Conc. of soln. (ppb)	1597	798.7	320.0	153.0	89.0	35.6
Generating current (mA)	4.995	4.997	4.998	4.994	5.003	4.990
Av. end-point (s)	200.6	100.3	40.14	19.22	11.36	4.621
Av. equiv. of As found (μeq)	10.38	5.19	2.079	0.995	0.589	0.239
Rel. std. deviation (%)	0.1	0.01	0.4	0.5	2.3	7.8
Rel. inaccuracy (%)	±0.0	+0.1	+0.1	+0.1	+1.8	+3.3

This paper is taken in part from the Ph.D. thesis of M.A. de Soto Perera and was presented at the 1980 Pittsburgh Conference, Atlantic City, NJ.

REFERENCES

1 J. J. Lingane, Electroanalytical Chemistry, Interscience, New York, 1958, pp. 290—295.
2 E. Bishop, Coulometric Analysis, in C. L. Wilson and D. W. Wilson (Eds.), Comprehensive Analytical Chemistry, Elsevier, Amsterdam, 1975, Vol. II-D, pp. 148—151.
3 R. J. Meyers and E. H. Swift, J. Am. Chem. Soc., 70 (1948) 1047.
4 J. K. Lee and R. N. Adams, Anal. Chem., 30 (1958) 240.
5 G. D. Christian, Microchem. J., 9 (1965) 484.
6 V. J. Jennings, A. Dodson and A. M. Atkinson, Analyst, 97 (1972) 923.
7 V. J. Jennings, A. Dodson and A. Harrison, Analyst, 99 (1974) 145.
8 L. B. Jaycox and D. J. Curran, Anal. Chem., 48 (1976) 1061.
9 L. B. Jaycox, G. E. Cadwgan and D. J. Curran, Anal. Lett., 6 (1973) 1061.
10 G. E. Cadwgan and D. J. Curran, Mikrochim. Acta, (1977) 461.
11 H. A. Laitinen, Chemical Analysis, McGraw-Hill, New York, 1960, p. 403.
12 M. A. de Soto Perera and D. J. Curran, Anal. Chim. Acta, 119 (1980) 000.

Analytica Chimica Acta, 119 (1980) 263—269

COULOMETRIC TITRATION OF SOME PHENOLIC STEROIDS WITH BROMINE BASED ON THIN-LAYER HYDRODYNAMIC BIAMPEROMETRIC END-POINT DETECTION

M. A. de SOTO PERERA** and D. J. CURRAN*

Department of Chemistry, GRC Tower I, University of Massachusetts, Amherst, MA 01003 (U.S.A.)

(Received 26th March 1980)

SUMMARY

Four phenolic steroids were titrated coulometrically with bromine in a methanol—water solvent containing hydrochloric acid and sodium bromide. End-point detection was achieved with a twin electrode thin-layer cell placed in a flow loop connected to the titration vessel. Linear-segmented biamperometric titration curves were recorded. Concentrations of 17-β-estradiol were determined in the range from 442 ppb to 8.84 ppm with relative inaccuracies of −1.3% and +2.2%, respectively. Part-per-million solutions of estrone and estriol were titrated with good accuracy and precision. Somewhat poorer precision and accuracy was found for the determination of 17-α-ethynyl estradiol.

Several titrimetric approaches to the determination of steroids have been reported in the literature. In a series of articles, Gorög and co-workers have developed methods based on double bond, ethynyl, keto, phenolic hydroxyl, diol, and epoxide functionalities. A recent article describes a method for the determination of allyloestrenol by methoxymercuration of the double bonds and titration of the acetic acid formed [1]. The only reports in the literature concerning the use of bromine as a titrant for steroids appear in the work of Csizer and Gorög [2] and Szabolcs-Sandor [3, 4]. The latter author brominated compounds carrying a free hydroxyl group on the C3 carbon atom in the A ring of the steroid structure, in an alcoholic medium. The determination of estradiol, estrone, ethynyl estradiol, estradiol benzoate and estradiol propionate in pharmaceutical preparations was carried out by volumetric titration with standard potassium bromate solution in the presence of bromide, and the end-point was detected biamperometrically. This is a substitution reaction with the bromine occupying positions 2 and 4 in ring A. Four equivalents of bromine are involved and the reaction is thus favorable for titrimetric purposes. Szabolcs-Sandor was able to determine concentrations of the steroids in the range 31—105 ppm

**Present address: Dow Chemical U.S.A., P. O. Box 68511, Indianapolis, IN 46268, U.S.A.

with accuracies better than one percent. The titration cell was covered with black paper to exclude light.

A hydrodynamic approach to biamperometric end-point detection which uses a thin-layer cell placed in a flow loop attached to the titration cell has recently been reported [5]. The sensitivity of the method was quite high and prompted an examination of the titration of phenolic steroids with electrogenerated bromine. Coulometric titrations of steroids with electrochemically produced bromine have not been previously reported. The structures of the four steroids studied are shown in Fig. 1.

EXPERIMENTAL

Reagents and solutions

The water used was deionized distilled water which had a resistance of 8 megohms. Methanol was obtained from Fisher Scientific Co. (A-412, 98% assay). Estrone, estriol and 17-α-ethynyl estradiol (Sigma Chemicals) were used without further purification. The compound 17-β-estradiol was purified by recrystallization from ethanol and water (melting point after recrystallization: 175—177°C). Solutions of each steroid were made by weighing out between 0.2 and 0.25 g of the compound, dissolving it and diluting it to 250.0 ml with methanol. The solutions were stored under refrigeration until used; light was avoided as much as possible while handling the solutions. All other chemicals were reagent grade or better. The supporting electrolyte for 17-β-estradiol, estriol and 17-α-ethynyl estradiol consisted of 0.15 M NaBr in 4.8 M HCl; that for estrone was 0.12 M NaBr in 1.92 M HCl. The catholyte was a solution of 4.8 M HCl.

Equipment

The thin-layer cell and electronic apparatus have been described [5]. The titration cell, constructed of Pyrex glass, is shown in Fig. 2. The bottom half

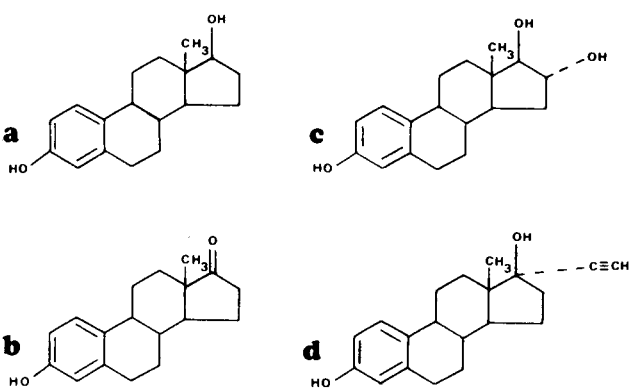

Fig. 1. Structures of the phenolic steroids: (a) 17-β-estradiol; (b) estrone; (c) estriol; (d) 17-α-ethynyl estradiol.

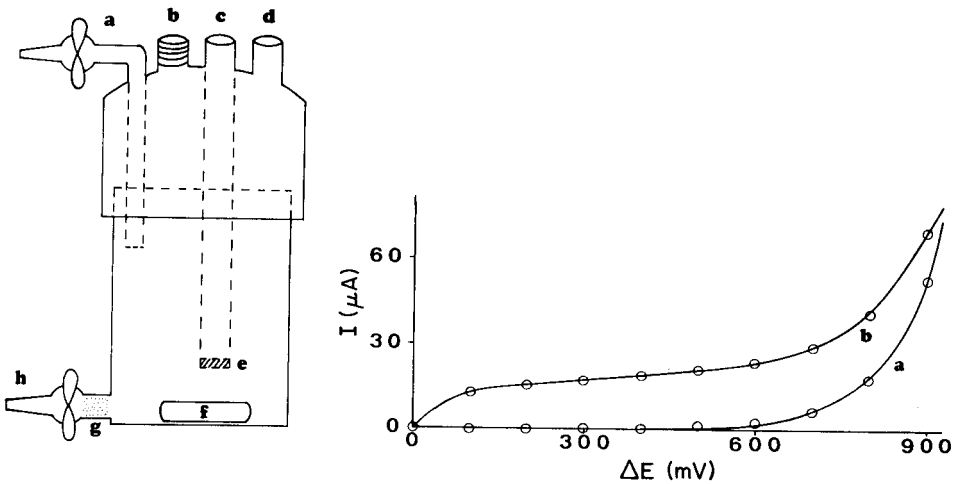

Fig. 2. The titration cell: (a) inlet from thin-layer cell; (b) microburet port; (c) cathode compartment; (d) anode port; (e) fine frit; (f) magnetic stirring bar; (g) glass wool plug; (h) outlet to pump.

Fig. 3. Hydrodynamic current—voltage curves of the bromine—bromide couple in the titration medium for phenolic steroids: (a) supporting electrolyte; (b) excess bromine present.

was fitted with an outlet (h) incorporating a teflon stop-cock through which the solution was pumped into the thin-layer cell detector by means of a peristaltic pump. The outlet also contained a plug of glass wool (g) used as a filter to prevent particulate matter from reaching the thin-layer cavity and clogging it. A magnetic stirring bar (f) was included to mix the reactants during the titration. The top half incorporated a tube (c) used as the cathode compartment. Its upper section was a 14/20 joint; the lower end terminated in a fine frit (e). An Ace-Thred 5027-20 threaded joint (b) was used to introduce a microburet for delivering the sample. A female ground-glass joint (14/20) was included to mount the anode (d) which was a platinum flag electrode of 2 cm^2 total area attached to a piece of glass tubing fitted with a male 14/20 joint. An inlet glass tube (a) to which was attached another teflon stop-cock served as a return line for solution from the thin-layer detector to the titration cell. The cathode used was a platinum wire coiled into a spiral. The titration cell was 17.5 cm high and could contain up to 200 ml of solution entirely in the bottom half of the cell. The titration cell was wrapped with black electrical tape to avoid light. The teflon tubing used in the flow loop was covered with black electrical "spaghetti" tubing for the same reason.

Titration media

The titration medium for 17-β-estradiol, estriol and 17-α-ethynyl estradiol consisted of 80 ml of supporting electrolyte and 40 ml of methanol; for

estrone, the medium was composed of 100 ml of supporting electrolyte and 20 ml of methanol, following the suggestions of Szabolcs-Sandor [3, 4].

Procedure

Flow rates were about 16 ml min^{-1}, and the temperature was constant in the range 24—25°C. In all titrations, the solution was added to the titration cell and the magnetic stirrer and pump were started, in that order. The solution was pretitrated by generating excess of bromine at 3 mA, and allowing the bromine to disappear, as signaled by the achievement of a constant reading on the digital voltmeter. The steroid sample was added with a Gilmont S-3200 microburet and the strip-chart recorder was started at a speed of 20 or 40 s/in. Generation of bromine was initiated as the recorder pen crossed one of the main divisions in the chart paper. The chart speed was calibrated by measuring the time taken by the recorder pen to move between major divisions (1 in.) with the coulometric titrator timing module. Bromine generation was continued until about 150% titrated. In this fashion, the entire titration curve was plotted by the recorder. The end-points were obtained by extrapolating the straight-line segments of the titration curve to their intersection. After each determination, the titration cell and thin-layer cell were rinsed with water.

RESULTS AND DISCUSSION

In order to choose the potential difference that should be applied across the two thin-layer electrodes, a hydrodynamic current—voltage curve was determined for the titration medium in the absence and presence of excess of bromine. The results are shown in Fig. 3. Upon subtracting the residual current, the current in the presence of bromine was found to be independent of the applied potential difference for $\Delta E > 250$ mV. Therefore, 300 mV was selected as the potential difference for all the titrations.

The titration curves indicated that none of the steroids was reversibly electroactive because no change in current was observed prior to the end-point. This fact was further demonstrated when cyclic voltammograms of 17-α-ethynyl estradiol were obtained in a solution made with 167 ml of methanol and 333 ml of 0.1 M $NaClO_4$ in 4.8 M HCl. The voltammograms did not show any oxidation or reduction processes in the potential range from −0.15 to +0.90 V vs. SCE. Although some steroids are known to be reduced at the DME, this process is not expected to occur here since the potential of the electrodes is poised by the bromine—bromide couple, which is too far positive for these reductions to occur. A typical titration curve is shown in Fig. 4 for the determination of 17-β-estradiol. The initial abrupt change in the current is thought to be due to the interaction of the virtual grounds of the automatic coulometric titrator and the current-to-voltage converter. When bromine was generated without connecting the thin-layer

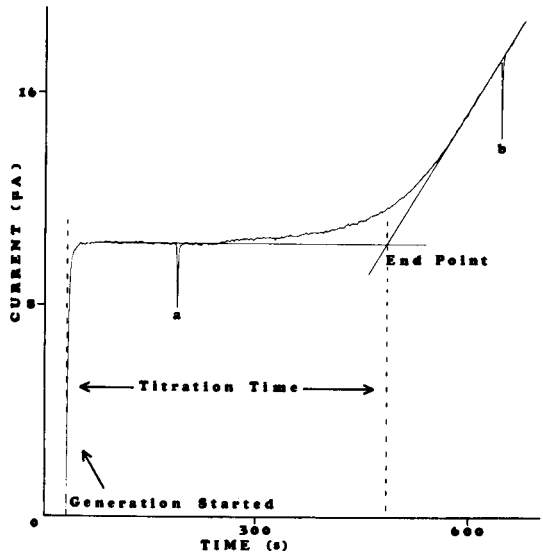

Fig. 4. Recorder trace of a titration of 17-β-estradiol with electrogenerated bromine.

electrodes, the effect was not observed. It amounts to a shift in baseline and has no influence on the determination of the end-point. The spikes (a and b) were due to gas (air) bubbles passing through the thin-layer cell and interrupting the electrolytic contact between the two platinum electrodes. Occasional bubbles were actually seen flowing through the tubing when the wrapping around it was removed. The presence of bubbles is probably due to the use of magnetic stirring in the titration cell and the presence of a gas space above the solution. Curvature in the vicinity of the end-point is common and is due to slow kinetics produced by the very low concentrations present near the end-point. In this case, such concentrations are in the ppb region. A cell design incorporating gas space above the solution to be titrated was judged acceptable since Chamberlain and Paige [6] reported that a solution as high as 10% (v/v) of bromine in methanol could be prepared. Thus, the solubility of bromine in an alcohol/water medium is greater than it is in pure water and the possible loss of bromine to the gas phase is reduced.

The results of a concentration study for 17-β-estradiol are shown in Table 1. The concentration ranged from 442 ppb to 8.84 ppm. As shown in Fig. 4, the end-point is obtained by extrapolation of the straight-line portions of the titration curve. Good agreement was found between the calculated and experimental end-points. The imprecision was +2% at the lower concentration levels and improved to better than ±1% at the highest concentration. The error for the latter solutions was positive but negative for all the rest. The generating current was lowered as the concentration was decreased in an effort to compensate for the slower kinetics of the titration reaction at the lower concentration levels. It is possible that the generating current for the

TABLE 1

Results of the concentration study of 17-β-estradiol

Conc. stock soln. (mM)	3.89_4	3.89_4	3.89_4	3.89_4
Replicates	6	6	4	7
Vol. stock soln. (μl)	50.0	100.0	250.0	1000
Amt. steroid taken (μg)	53.0	106.1	265.2	1061
Conc. soln. (ppm)	0.442	0.884	2.21	8.84
Av. gen. current (mA)	0.506	0.506	1.011	3.036
Theor. end-point (s)	149	297	372	495
Av. end-point found (s)	147	292	368	506
Rel. std. deviation (%)	±2	±2	±0.5	±0.9
Rel. inaccuracy (%)	−1	−2	−1	+2

TABLE 2

Results of the titrations of estrone, estriol, and 17-α-ethynyl estradiol

Compound	Estrone	Estriol	Ethynyl estradiol
Conc. stock soln. (mM)	3.35_1	3.11_4	2.73_3
Replicates	4	6	8
Vol. stock soln. (ml)	1.00_0	1.00_0	1.00_0
Amt. steroid taken (mg)	0.906	0.898	0.810
Conc. soln. (ppm)	7.55	7.48	6.75
Av. gen. current (mA)	2.002	3.000	2.001
Theor. end-point (s)	646	401	527
Av. end-point (s)	662	420	558
Rel. std. deviation (%)	±0.0	±0.9	±2.7
Rel. inaccuracy (%)	2.5	4.7	5.9

8.84 ppm solutions was too high and free bromine gas was lost to the gas phase.

Estrone, estriol and ethynyl estradiol were also titrated, the former in a modified titration medium as described in the experimental section. The results for these determinations are shown in Table 2. Titrations of these compounds were performed at only one concentration, which was selected on the basis of the titrations of 17-β-estradiol. For estrone and estriol, the results obtained are in good agreement with those obtained for 17-β-estradiol at a similar concentration. It was found that after titrations of 17-α-ethynyl estradiol were performed, it was necessary to clean, polish, and rinse the detector electrodes with nitric acid before the detector would yield satisfactory response for the titration of other steroids. This suggests that the surface of the electrodes is being slowly fouled during the titration of 17-α-ethynyl estradiol. If this is the case, it would account for the poorer precision found for this titration. The errors for all three steroids were positive. Impurities that reacted with bromine were suspected but no proof could be found. The melting points of estrone (257—260°C), estriol (284—288°C), and ethynyl estradiol (181—183°C) were in good

agreement with the literature values of (251—254°C), (282°C), and (182—184°C) respectively [7]. Mourey [8] examined these samples of estradiol, estrone, and estriol by h.p.l.c. using a microparticulate pyrrolidone bonded phase column, and obtained no evidence of impurities.

Positive errors could arise from the time delay inherent in operating the detector continuously in a flow loop attached to the titration cell. However, the volume of the flow loop was only a few percent of the volume of the solution in the titration cell. Furthermore, for this source of error to be significant, there would have to be a partially compensating negative error in view of the results for the lower concentrations of 17-β-estradiol. It is not clear whether the errors are due to lack of purity of the steroids or to a small systematic error in the method.

The results are very satisfactory overall. The coulometric titration of phenolic steroids with hydrodynamic amperometric end-point detection has promise for the direct assay of pharmaceutical preparations. The application of the method to body fluids would require a prior separation and concentration.

This paper is taken in part from the Ph.D. thesis of M. A. de Soto Perera.

REFERENCES

1 S. Gorög, A. Laukó and Z. Sziklay, Analyst, 104 (1979) 196.
2 E. Csizer and S. Gorög, J. Chromatogr., 76 (1973) 502.
3 L. Szabolcs-Sandor, Acta Chim. Acad. Sci. Hung., 42 (1972) 68; Chem. Abstr., 76 (1972) 158415t.
4 L. Szabolcs-Sandor, Proc. Conf. Appl. Phys. Chem., 2nd., 1 (1971) 369.
5 M. A. de Soto Perera and D. J. Curran, Anal. Chim. Acta, 119 (1980) 251.
6 H. E. Chamberlain and E. L. Paige, At. Energy Res. Establ. (Gt. Britain), Rept. AERE-R 4334, 2 pp. (1963). Chem. Abstr., 60 (1964) 173b.
7 The Merck Index, 9th edn., Merck and Co. Inc., Rahway, NJ, 1976.
8 T. H. Mourey, Ph.D. Thesis, University of Massachusetts, Amherst, MA, 1979.

Analytica Chimica Acta, 119 (1980) 271—276

MICROBIOASSAY OF PHENYLALANINE IN BLOOD SERA WITH A LACTATE ELECTRODE

ISAO KARUBE,* TADASHI MATSUNAGA, NOBUAKI TERAOKA and SHUICHI SUZUKI

Research Laboratory of Resources Utilization, Tokyo Institute of Technology, Nagatsuta-cho, Midori-ku, Yokohama 227 (Japan)

(Received 1st February 1980)

SUMMARY

Microbioassay of phenylalanine in sera is carried out by incubation with *Leuconostoc mesenteroides* (6 h) followed by use of a lactate electrode (immobilized lactate oxidase and an oxygen electrode) to measure the lactate produced. A linear relationship is obtained between the current decrease and the phenylalanine concentration between 0.75 and 6×10^{-7} g ml^{-1}, with a standard deviation of 1.7×10^{-8} g ml^{-1} at the 3×10^{-7} g ml^{-1} level.

A genetic deficiency of phenylalanine hydroxylase is responsible for the clinical condition known as phenylketonuria, a syndrome characterized by an accumulation of phenylalanine in the blood [1]. Infants thus affected usually develop significant irreversible brain damage and behavioral problems unless they are placed on a diet low in phenylalanine within 1—3 months. Determination of phenylalanine is therefore required for proper management of this condition. Blood phenylalanine has been detected by microbioassay [2]. This requires a long incubation time, and is affected by contamination with other bacteria. Automated amino acid analysis can also be used, but this requires a large amount of deproteinized sample [3]. A simple method for the determination of phenylalanine is therefore desirable.

Several rapid microbioassay systems based on electrochemical devices have recently been developed [4—6]. Some bacteria such as *Lactobacillus*, *Streptococcus* and *Leuconostoc* require specific amino acids and vitamins for their growth. These bacteria produce mainly lactic acid as a metabolite. Therefore, an enzyme sensor for lactate was applied to microbioassays by using lactic acid-producing bacteria. In this study, such a system is applied to the determination of phenylalanine in serum.

EXPERIMENTAL

Materials

Lactate oxidase (EC 1.1.3.2, 72 I.U. ml^{-1}) was obtained from Toyo Jozo Co. The basic assay medium (Takara Kosan Co.) had the composition shown

TABLE 1

The composition of microbioassay medium (double strength, pH 7.0)

Compound	Conc. (mg l^{-1})	Compound	Conc. (mg l^{-1})	Compound	Concn. (mg l^{-1})	Compound	C (r
L-Alanine	200	L-Proline	100	NH_4Cl	3000	Riboflavin	
L-Arginine·HCl	200	L-Serine	50	$MgSO_4.7H_2O$	200	Pyridoxine	
L-Aspartic acid	200	L-Threonine	100	$FeSO_4.7H_2O$	10	Pyridoxal	
L-Cystine	100	L-Tryptophan	50	$MnSO_4.4H_2O$	10	Potassium pantothenate	
L-Glutamic acid	500	L-Tyrosine	100	NaCl	10		
Glycine	100	L-Valine	100	Adenine	10	Nicotinic acid	
L-Histidine	100	Glucose	20×10^3	Guanine	10	*p*-Aminobenzoic acid	
L-Isoleucine	100	CH_3COONa	20×10^3	Uracil	10		
L-Leucine	100	KH_2PO_4	500	Xanthine	10	Biotin	
L-Lysine·HCl	200	K_2HPO_4	500	Thiamine	1	Folic acid	
L-Methionine	100						

in Table 1. Phenylalanine was obtained from Nihon Rikagaku Pharmaceutical Co. Deionized water was used in all procedures.

Leuconostoc mesenteroides P-60 ATCC 8042 was used for the assay of phenylalanine. It was maintained in peptone-yeast agar and transferred to a fresh medium every 10—14 days.

Preparation of the inoculum. L. mesenteroides was cultured at 37°C for 24 h in 100 ml of a medium (pH 6.8) containing 0.5 g of yeast extract, 1.0 g of peptone, 1.0 g of glucose, 1.0 g of CH_3COONa, 25 mg of K_2HPO_4, 25 mg of KH_2PO_4, 10 mg of $MgSO_4.7H_2O$, 0.5 mg of $FeSO_4.7H_2O$, 0.5 mg of $MnSO_4.4H_2O$ and 0.5 mg of NaCl. The cells were centrifuged at 5°C and 8000 *g*, washed twice with physiological saline and resuspended in the basic assay medium. This cell suspension was incubated for 3 h, and used as the inoculum.

Lactate sensor and apparatus

The enzyme solution (100 μl containing 7.2 I.U. of lactate oxidase) was dropped onto a porous acetylcellulose membrane (Millipore type HA, 0.2-μm pore, 25-mm diameter, 150-μm thick), with slight suction. The oxygen electrode (Ishikawa Seisakujo Co., Model A; diameter 1.05 cm, height 13.7 cm; glass casing) consisted of a teflon membrane (50-μm thick), a platinum cathode, a lead anode and sodium hydroxide electrolyte. The enzyme membrane was cut into a small circle (5.5 mm diameter), and attached to the surface of the teflon membrane of the electrode, being held in position by a cellulose dialysis membrane (50-μm thick, Visking Co.). The membrane contained 0.35 I.U. of lactate oxidase.

The measurement system for phenylalanine is shown in Fig. 1. A flow cell (0.6-cm diameter, 0.8-cm high, 0.23-ml capacity) was employed for the determination of lactate in the microbial medium. The phosphate buffer solution (0.1 M, pH 7.0) saturated with dissolved oxygen was continuously transferred to the cell at 1.5 ml min^{-1}.

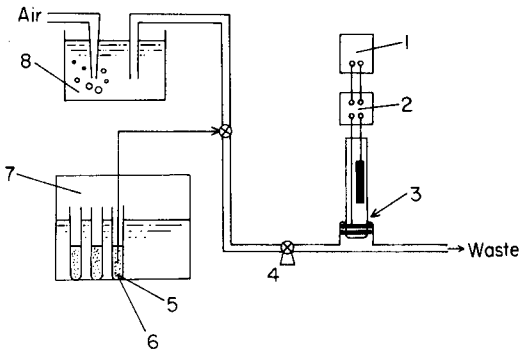

Fig. 1. Schematic diagram of microbioassay system for use with the lactate sensor: (1) recorder; (2) amplifier; (3) lactate sensor; (4) peristaltic pump; (5) medium for microbioassay; (6) *L.mesenteroides*; (7) incubator; (8) aerated buffer solution.

Procedures

A portion (0.5 ml) of the double-strength basic medium and 0.5 ml of a sample solution containing appropriate amounts of phenylalanine were placed in a test tube and sterilized for 15 min at 120°C. The bacterial suspension (5 μl) was injected into the medium containing phenylalanine. After incubation for 6 h at 37°C, 100 μl of the medium was injected into the measurement system. The electrode current was continuously displayed on a recorder (TOA Electronics Ltd., Model EPR-200A). The peak current was used for measurement of phenylalanine concentration.

Determination of phenylalanine in human sera. The concentration of phenylalanine in human sera was determined by an automatic amino acid analyzer (Hitachi Seisakujo Co. Ltd., Model 853) and also with the lactate sensor procedure. For automated amino acid analysis, sera were deproteinized with four volumes of 3.75% sulfosalicylic acid in 0.3 M lithium citrate buffer (pH 2.2), and the mixture was centrifuged. For microbioassay, sera were directly diluted 100-fold with sterilized phosphate buffer.

RESULTS

The lactate sensor functions by monitoring the decrease in dissolved oxygen which results from oxidation of lactate in the presence of lactate oxidase. When a lactate solution was transferred to the flow cell, consumption of oxygen by the enzyme reaction began. Eventually a steady state was reached when the consumption of oxygen by the reaction and the diffusion of oxygen into the solution were equal, which gave a constant, decreased current. The current change was a function of lactate concentration, pH, temperature etc. A linear relationship was obtained between the current decrease and the lactate concentration between 5×10^{-5} and 8×10^{-4} g ml^{-1}; the current change between these two extremes was ca. 0.4 μA. The optimum pH of the sensor was 7.0 and the optimum temperature was 37°C.

L. mesenteroides requires phenylalanine for growth, and the bacteria mainly produce lactate as a metabolite. The microbioassay media containing phenylalanine (10^{-8}—10^{-6} mg ml^{-1}) were incubated for 6 h with *L. mesenteroides* and then introduced into the lactate sensor system. The response curves obtained are shown in Fig. 2A. A constant current was attained within 5 min. However, to achieve the constant current in a flow system required a large amount of sample solution. Therefore, an injection method was employed. Figure 2B shows the response curves obtained when 100 μl of the microbioassay broth was injected into the system. The maximum current decrease was obtained within 2 min. The current decrease was 70% of that obtained by the steady-state method. Thus, lactate produced by bacteria could readily be determined by the sensor system.

Relation between current decrease and phenylalanine concentration

Figure 3 shows the relationship between the current decrease and the phenylalanine concentration in the incubation medium. The current decrease increased with increasing initial bacterial cell concentrations. However, the sensitivity was not satisfactory at a high initial cell concentration; the minimum determinable concentration of phenylalanine under these conditions was 5.6 μg ml^{-1} at 0.8×10^7 or 1.2×10^7 cells ml^{-1} (initial concentrations), and 0.1 μg ml^{-1} at 0.4×10^7 cells ml^{-1}. Therefore, an initial cell concentration of 0.4×10^7 cells ml^{-1} was used for further work.

The relationship between the incubation time and the current decrease was examined at various phenylalanine concentrations. After injection of a *L. mesenteroides* suspension (0.4×10^7 cells ml^{-1}) into the same basic medium, the lactate was measured at 2-h intervals. The current decrease increased with increasing incubation time. A 6-h incubation gave the greatest sensitivity. This was used for subsequent experiments.

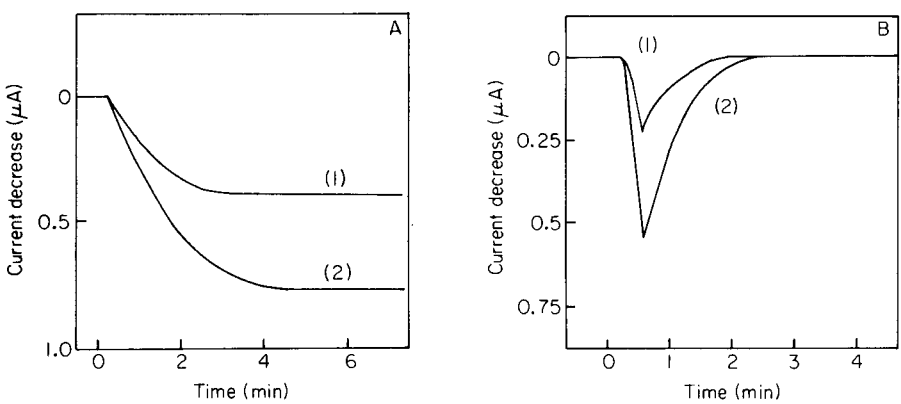

Fig. 2. Response curves of the lactate sensor to the microbioassay medium incubated with *L. mesenteroides*, under the recommended conditions for (A) continuous flow and (B) 100 μl injection; phenylalanine concentrations: (1) 10 ng ml^{-1}, (2) 1.0 μg ml^{-1}.

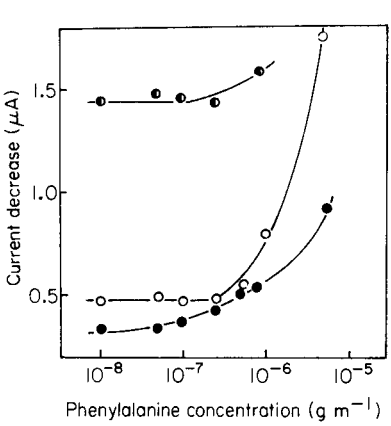

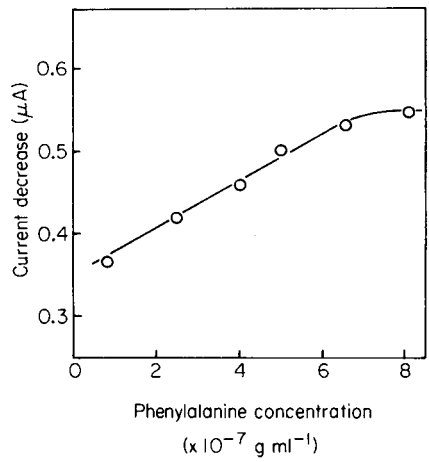

Fig. 3. Relationship between current decrease and phenylalanine concentration under the recommended conditions except for various initial *L. mesenteroides* cell concentrations: (●) 1.2 × 10^7; (○) 0.8 × 10^7; (•) 0.4 × 10^7 cells ml^{-1}.

Fig. 4. Calibration curve for phenylalanine under the recommended conditions.

The calibration graphs obtained under the recommended conditions are linear over the range 0.75—6 × 10^{-7} g ml^{-1} phenylalanine (Fig. 4). The standard deviation of 30 measurements of a medium containing 3.0 × 10^{-7} g ml^{-1} of phenylalanine was 1.7 × 10^{-8} g ml^{-1}.

Application of human blood sera

The microbioassay system was applied to the determination of phenylalanine in human sera which were also analyzed by the conventional automatic method [3]. For concentrations of 0.2—4 × 10^{-5} g ml^{-1}, the linear correlation coefficient between the methods for 20 experiments was 0.91, the conventional method giving the slightly higher results.

DISCUSSION

Microbioassay has often proved to be advantageous because of its specificity, sensitivity and ability to yield many replicate results almost simultaneously. In addition, the assay is possible with a very small amount of serum (less than 50 μl). Microbioassays are usually based on turbidimetric or titrimetric methods. Colored samples, however, cannot be used for the turbidimetric microbioassay. Moreover, serum cannot be sterilized because the proteins present are decomposed and aggregated by heat. Therefore, growth of undesirable microorganisms is often observed in the culture medium used for this microbioassay, and can be a serious problem. However, the contaminating bacteria usually do not produce lactate as a metabolite, and so the desired microbioassay can be performed by determining the amount of lactate produced, using the enzyme sensor described.

The serum of phenylketonuria patients contains more than 6×10^{-5} g ml^{-1} of phenylalanine [1]; for normal individuals, the level is about 1×10^{-5} g ml^{-1}. Phenylketonuria can be detected by the conventional semiquantitative microbioassay [2]. However, confirmation is required by an amino acid analyzer when a presumptive positive phenylketonuria is detected. Automated amino acid analysis requires a large amount of deproteinized serum, but a large amount of serum cannot be collected from a new-born child. Therefore a more sensitive and quantitative method for phenylalanine is required. The calibration graph for the new electrochemical microbioassay covers the range $0.75—6 \times 10^{-7}$ g ml^{-1}. Therefore, sample sera require dilution for assay; since 100 μl of sample is employed for the microbioassay with a lactate electrode, only 1 μl of serum is usually required for dilution for the assay.

Conventional microbioassay methods require lengthy incubation of the bacteria. A rapid microbioassay has been needed for the determination of amino acids. As previously reported, injection of a large amount of bacterial suspension shortens the time required for microbioassay [4], but this cannot be used for the turbidimetric method because the tubidity of the medium becomes excessive. A faster microbioassay was possible by using an electrode system for determination of microbial population [4] and the combined glass electrode to measure the acids produced [5]. In the present study, the assay was completed within 6 h, using the lactate sensor for monitoring the medium.

The method proposed should be applicable to the determination of other amino acids and vitamins produced by bacterial metabolism.

REFERENCES

1 C. M. Ambrus, J. L. Ambrus, C. Horvath, H. Petersen, S. Sharma, C. Kant, E. Miland, R. Guthrie and T. Paul, Science, 201 (1978) 837.
2 R. Guthrie, J. Am. Med. Assoc., 178 (1961) 863.
3 D. H. Spackman, Methods in Enzymology, Academic Press, New York, 1967, Vol. 11, p. 3.
4 T. Matsunaga, I. Karube and S. Suzuki, Anal. Chim. Acta, 98 (1978) 25.
5 T. Matsunaga, I. Karube and S. Suzuki, Anal. Chim. Acta, 99 (1978) 233.
6 I. Karube, T. Matsunaga and S. Suzuki, Anal. Chim. Acta, 109 (1979) 39.

Analytica Chimica Acta, 119 (1980) 277—282

ELECTROCATALYTIC DETERMINATION OF NITRITE ION IN BASIC SOLUTION

BRIAN D. SEILER and JAMES P. AVERY*

School of Chemical Sciences, University of Illinois, Urbana, Illinois 61801 (U.S.A.)

(Received 22nd February 1980)

SUMMARY

A sensitive cyclic voltammetric method for the detection of nitrite ion at a hanging mercury drop electrode (HMDE) in basic solution is reported. In a buffered 0.1 mM chromium(VI) medium, easily quantified peaks appear when nitrite is introduced. An unusual, sharply rising reduction peak at −1.65 V vs. SCE observed in a positive-going scan is utilized to produce a linear working curve in the range 10^{-5}—10^{-4} M nitrite.

Electroanalytical methods applicable to quantification of aqueous nitrite have appeared with increasing frequency throughout the past decade [1—11]. A concise review of these methods was recently presented [11]. The present study describes an electrocatalytic procedure developed for the detection and quantification of nitrite at a HMDE. The catalytic mechanism, though unknown at this time, is dependent upon the presence of chromate in the supporting medium. Analytical signals are generated via cyclic voltammetry. An unusual feature of the method presented stems from utilization of a basic electrolytic medium. Complications arising from the volatility of nitrous acid (the predominant species in acidic medium) are essentially avoided. The impetus for this work was provided by a brief paper by Saito and Himeno [12], who studied the polarography of chromium(VI) in various media and observed a maximum deemed unusual because its height was proportional to the concentration of nitrite or nitrate in solution. It was the investigation of this report which ultimately led to studies at a HMDE and discovery of an analytically useful reduction peak.

EXPERIMENTAL

Reagents

ACS Reagent Grade chemicals were used in the formulation of all solutions. Stock solutions of sodium nitrite, nitrate and acetate were prepared and preserved with 0.1% (v/v) carbon tetrachloride; concentrations were 1 g l^{-1} nitrogen as nitrite or nitrate, and 1 g l^{-1} acetate. A 1 M stock solution of ammoniacal buffer was prepared from NH_4Cl and NH_4OH to provide a theoretical pH of 10.8 (1:36.3 mole ratio of NH_4^+:NH_3). A 10 mM

stock solution of chromium(VI) was prepared from chromium trioxide and diluted with the buffer solution and deionized water in appropriate quantities to yield 0.1 mM chromium(VI) in 0.1 M buffer. The pH of the latter solution was found to be 10.7 with a Heath Servo Digital pH meter equipped with a Sargent combination electrode (S-30079-15). This solution was used in 100-ml quantities as the supporting medium. Buffered working solutions were prepared as needed, and all solutions were sparged with nitrogen for at least 20 min prior to use.

Apparatus

Cyclic voltammetry was performed with custom-built conventional three-electrode potentiostat-function generator and a Houston Instruments Omnigraphic Model 2000 x-y recorder. A platinum flag and SCE served as counter and reference electrodes, respectively. A Metrohm E-410 HMDE (Metrohm AG) manipulated so as to provide a mean drop surface area of 0.0418 cm^2 (based on 10 drops; assuming sphericity) functioned as the indicator electrode. Aliquots of the various working solutions were delivered directly to the electrochemical cell with the aid of a high speed automatic dispensing aliquotter of the type designed by Krottinger et al. [13]. A delivery volume of 800 μl was selected. The reproduciblity of this aliquotter was evaluated gravimetrically in this laboratory, and relative standard deviations (r.s.d.) better than 0.1% were calculated for ten consecutive deliveries.

Procedure

All potentials reported are against SCE. Data appearing in Table 1 were abstracted from cyclic voltammograms generated at scan rates of 50 mVs^{-1}. Single cycle limits were −0.80 V (lower limit) and −1.85 V (upper limit). Various nitrite concentrations were prepared by delivery of increasing numbers of 800-μl aliquots of a 10 ppm N (as NO_2^-) solution in 0.1 M ammoniacal buffer to the supporting medium previously described. Individual solutions were agitated to provide complete mixing by vigorous sparging with nitrogen via a stopcock-controlled side-arm. After ceasing agitation, electrodes were immersed, a fresh mercury drop was grown, dislodged, and then regrown. A rest period of precisely 30 s was enforced, to allow the solution to become quiescent, electrode equilibration, and residual reductive processes to die out. Following this period, scans were immediately initiated and cyclic voltammograms were recorded.

RESULTS AND DISCUSSION

Figure 1 represents a series of superimposed cyclic voltammograms and clearly shows the growth of signals from the presence of nitrite in solution. The direction of the potential sweeps should be carefully noted. Reduction peaks observed at approximately −1.2 and −1.8 V in the forward (negative-going) scan and the oxidation peak at −1.4 V in the reverse scan are due to

TABLE 1

Nitrite concentration study

No. of aliquots added	Concn. NO_2^- ($\times 10^{-5}$ M)	i_p[a] (μA)	No. of aliquots added	Concn. NO_2^- ($\times 10^{-5}$ M)	i_p[a] (μA)
0	0.00	0.00	10	5.28	1.16
1	0.56	0.06	15	7.64	1.68
2	1.12	0.19	20	9.83	2.13
3	1.67	0.34	25	11.88	2.60
4	2.21	0.47	30	13.80	2.89
5	2.74	0.60	35	15.59	3.21

[a] i_p (μA) = (0.0212 ± 0.0007) $C_{NO_2^-}$(μmol l^{-1}) + (0.00 ± 0.05) μA.

the presence of chromate and also are observed in the absence of nitrite. At the particular pH employed, the electrolyte discharge appears at approximately −2.0 V.

Lingane and Kolthoff [14] studied the reduction of chromate in a buffered medium (0.1 M diethylammonium chloride—diethylammonium hydroxide) similar to that employed here. Polarographic waves were monitored as a function of pH in the pH interval 10—12. Two distinct waves were observed with half-wave potentials dependent upon the pH enforced. Based on Ilkovič equation calculations, the first (least negative) wave was attributed to a three-electron reduction (chromate to chromium(III) ion) and the second to a six-electron reduction (chromate to chromium). The potentials of peak voltammetric currents from chromate in the present study are largely in accordance with expectations based on the prior polarographic study. Hence,

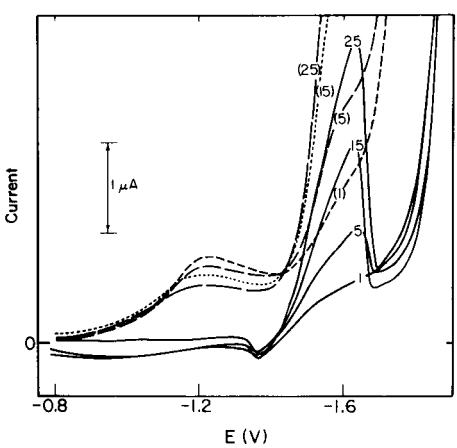

Fig. 1. Superimposed cyclic voltammograms. Broken lines and parentheses pertain to forward (negative-going) scans; solid lines pertain to reverse scans. Numbers refer to the number of aliquots (800 μl) of 10-ppm NO_2^-—N solution added to 100 ml of the supporting medium.

voltammetric peaks appearing in the forward scan are assigned to processes as follows

1st peak: $CrO_4^{-2} + 3e^- \rightarrow Cr^{+3}$ $E_p = -1.2$ V (pH 10.8)
2nd peak: $CrO_4^{-2} + 6e^- \rightarrow Cr$ $E_p = -1.8$ V (pH 10.8)

Failure of the voltammograms (Fig. 1) to superimpose exactly at the chromate peaks is attributable partly to the decrease in chromate concentration effected by the aliquot addition procedure, but largely to drop reproducibility problems, recognized and reported by marketers of the HMDE (r.s.d. as large as 3—4%) [15]. It is a simple matter to calculate actual concentrations, thus the former effect is inconsequential. The latter effect imposes the primary constraint on the overall precision of the method presented. At the time of data acquisition, utilization of relatively large drops was seen as an effective way to minimize surface area variations and simultaneously to provide high sensitivity.

The most prominent feature of Fig. 1 is the "inverted" peak seen rising sharply at −1.65 V in the reverse scan (inverted in the sense that it is a reduction peak appearing in a positive-going scan). In contrast to this unusual feature, a rather nondescript reductive signal appears in the forward scan at −1.6 V. It is interesting and likely significant that the current magnitude of this signal is comparable to that observed for the inverted peak in individual voltammograms.

Sufficient alkalinity of the electrolytic medium is evidently a necessary condition to the generation of the inverted peak. It was observed that decreasing the pH to about 9.5 (or lower) resulted in obliteration of the analyte-sensitive peak. However, increasing the pH to about 12 did not prove to be advantageous or detrimental with respect to the signal of analytical interest. A pH of 10.8 is conveniently provided by the ammoniacal buffer system, without sacrificing too much buffer capacity under the arbitrarily chosen 0.1 M concentration constraint and, therefore, was used in this study. This value does not represent an optimum value (pH study revealed no "optimum" value), yet clearly lies beyond the threshold pH value required for the generation of an inverted peak.

The analytical utility of the inverted peak is best demonstrated by presentation of typical data in Table 1. Current values were abstracted from a series of cyclic voltammograms similar to those appearing in Fig. 1, by extrapolation of the current decay observed upon scan reversal and measurement from this baseline at the inverted peak potential. A linear least-squares fit of the twelve pairs of data values, results in a slope of 0.0212 $\mu A\ \mu M^{-1}$ and a correlation coefficient of 0.9990. An improved fit results from inclusion in the regression analysis of only the lowest ten value pairs (m = 0.0222 $\mu A\ \mu M^{-1}$; R = 0.9997), corresponding to a working concentration range of 10^{-5}—10^{-4} M nitrite. At nitrite concentrations greater than 10^{-4} M, measurement of peak values introduces negative deviation from linearity. However, modification of experimental and/or data abstraction procedures can lead to

linear working ranges with upper limit nitrite concentrations as large as 10^{-3} M. Possible modifications are utilization of greater chromium(VI) concentrations and/or integration of peak areas.

It is a simple matter to apply the same data abstraction procedure to the signal appearing at −1.6 V in the forward scan, which similarly rises in direct proportion to the nitrite concentration. However, in the latter case, background currents are large and introduce a considerable amount of uncertainty to the signal measurement process, especially at low concentrations. For instance, at a nitrite concentration of 2.74×10^{-5} M, the signal due to nitrite in the forward scan amounts to 0.82 μA (at −1.6 V), while background currents provide 1.70 μA (measured from the zero current level). The signal-to-background ratio is roughly 0.5. At the same nitrite concentration, the inverted peak is measured at 0.60 μA, with a background value of 0.62 μA leading to a signal-to-background ratio very close to 1. Even though the absolute magnitude of the analytical signal is somewhat sacrificed in the utilization of the reverse-scan signal, substantial gains with respect to signal-to-background ratio are realized. Furthermore, inverted peak signal-to-background ratio can be easily increased by reducing the chromate concentration of the electrolytic medium. A tenfold reduction of the chromate concentration increased the signal-to-background ratio by roughly a factor of three, at a nitrite concentration of 1.12×10^{-5} M. Optimization of this experimental variable would be highly appropriate prior to attempting routine determinations near the low end of the linear nitrite concentration range. Signal-to-noise ratio is evidently unaffected by chromate concentration reduction. Additional benefits accrue from the sharp rising nature of the inverted peak. Among these are increased confidence in accurately extrapolating background currents due to the close proximity of the analytical peak to the last recorded trace of the background signal, and the ability to use a simple "peak-minus-valley" data abstraction scheme to construct coarse working curves for rapid estimation of nitrite levels.

In contrast to the method developed by Cox and Brajter [11], the present method is not insensitive to nitrate. An interference study revealed that 100 μg NO_3^-—N (in 100 ml of total solution) provides roughly the same amount of signal at the inverted peak as 50 μg NO_2^-—N. Thus, the method is essentially twice as sensitive to nitrite as nitrate. The response to nitrate is linear in the 10^{-5}—10^{-4} M range.

Also investigated were the effects of acetate ion and neutral surfactants. The acetate study was intended to determine whether it was simply the very basic nature of the nitrite ion which resulted ultimately in a catalytic discharge (originally considered as possibly arising from catalytic discharge of the supporting medium). Neutral surfactants are known to affect drastically the reductive properties of mercury electrodes. Acetate concentrations as large as 10^{-4} M did not affect detection of nitrite, nor did the introduction to the cell solution of 5 drops of 1% Triton X-100.

We thank L. R. Faulkner for his interest and discussion and J. A. Cox for technical assistance. This work was supported by the American Chemical Society Petroleum Research Fund under grant number 11199-G314A.

REFERENCES

1 J. E. Harrar, Anal. Chem., 43 (1971) 143.
2 R. Guidelli, F. Pergola and G. Raspi, Anal. Chem., 44 (1972) 745.
3 R. J. Davenport and D. C. Johnson, Anal. Chem., 45 (1973) 1979.
4 R. Karlsson and L. G. Torstensson, Talanta, 21 (1974) 945.
5 D. C. Johnson and R. J. Davenport, Anal. Chem., 46 (1974) 1971.
6 S. W. Boese, V. S. Archer and J. W. O'Laughlin, Anal. Chem., 49 (1977) 479.
7 C. H. Kiang, S. S. Kuan and G. G. Guilbault, Anal. Chim. Acta, 80 (1975) 209.
8 M. E. Bodini and D. T. Sawyer, Anal. Chem., 49 (1977) 485.
9 S. Chang, R. Kozeniauskas and G. W. Harrington, Anal. Chem., 49 (1977) 2272.
10 C. H. Kiang, S. S. Kuan and G. G. Guilbault, Anal. Chem., 50 (1978) 1319.
11 J. A. Cox and A. F. Brajter, Anal. Chem., 51 (1979) 2230.
12 A. Saito and S. Himeno, Rev. Polarogr. (Jpn.), 22 (1976) 72.
13 D. L. Krottinger, M. S. McCracken and H. V. Malmstadt, J. Autom. Chem., 1 (1978) 15.
14 J. J. Lingane and I. M. Kolthoff, J. Am. Chem. Soc., 62 (1940) 852.
15 Model 315 Automated Electroanalysis Controller Operating and Service Manual, MDL 315 8/74-A, Princeton Applied Research Corp., Princeton, NJ 08540, 1974; pp. III—8.

Analytica Chimica Acta, 119 (1980) 283—290

DETECTION OF PRIMARY AND SECONDARY AMINES IN ENERGY-RELATED MATERIALS USING AN ELEMENT-SELECTIVE GLOW-DISCHARGE DETECTOR

B. A. TOMKINS* and C. FELDMAN

Analytical Chemistry Division, Oak Ridge National Laboratory, P. O. Box X, Oak Ridge, TN 37830 (U.S.A.)

(Received 11th April 1980)

SUMMARY

Mutagenic primary polycyclic aromatic amines present in shale oil and synthetic crudes may be readily detected by a simple derivatization and chromatographic procedure. Nitrogenous bases and amines are extracted from the sample with dilute mineral acid and derivatized with trifluoroacetic anhydride. The derivatized amines are separated by gas chromatography and specifically detected using a glow-discharge detector tuned to an emission wavelength of fluorine. Under these conditions, the aromatic nitrogenous bases, such as acridine, are not detected even though they are present in the sample. As little as 14 ng of fluorine, arising from the derivative of 33 ng of 2,4,6-trimethylaniline, can be detected. The selectivity of the glow-discharge detector for derivatized amines vs. non-derivatized aromatic nitrogenous bases was estimated to be a minimum of 200:1.

Primary polycyclic aromatic amines (PPAA) and polycyclic aromatic hydrocarbons (PAH) are mutagenic compound classes which have been isolated from shale oil and coal-derived liquids [1—3]. Even though PPAA are present in lower specific concentrations than the PAH, the specific mutagenic activity (in revertants/mg) of these amines is considerably greater than that of the hydrocarbon species.

The determination of primary aromatic amines in these fossil fuel samples is complicated by the complexity of the matrix, the trace levels of amines present, and interferences arising from the chemically similar aromatic nitrogenous bases such as quinoline and acridine derivatives which also are present.

The work of Rubin et al. [4] and Ho et al. [2] demonstrated that both amines and aromatic nitrogenous bases could be isolated from the parent oil sample by simple acid extraction followed by neutralization and re-extraction with ether. In the method proposed here, selective derivatization of the amines with trifluoroacetic anhydride (TFAA) [5—7] is followed by detection of the fluorinated derivatives using the glow discharge detector (GDD) of Feldman and Batistoni [8]. By selecting a fluorine emission wavelength, it would be possible to detect only the amines, even in the presence of the aromatic nitrogenous bases. A similar approach for determining acidic

compounds has been reported by Horton et al. [9], who silylated the strong acid fraction of shale oil product water and used this detector for specifically detecting silicon-bearing species.

EXPERIMENTAL

Chemicals and standards

"Distilled in glass"-grade methylene chloride (Burdick & Jackson Laboratories, Muskegon, MI) was used as received. All test compounds were purchased from the Aldrich Chemical Company (Milwaukee, WI), Pfaltz & Bauer (Stamford, CT), Mallinckrodt Chemical Works (St. Louis, MO), and Eastman Organic Chemicals (Rochester, NY) in reagent-grade purity, and were used as received. "Gold-Label" grade trifluoroacetic anhydride (TFAA; 99+% purity; Aldrich Chemical Company) was used as received. Sodium hydrogen carbonate was purchased in ACS reagent grade (min. 99.7%; Matheson, Coleman, & Bell, Norwood, OH).

Fuel samples

A sample of coal-derived liquid, Number 1202 Synthoil, was obtained from the U.S. EPA/DOE Fossil Fuel Research Materials Facility [10]. The ether-soluble base (ESB) and amine-enriched fractions of Synthoil were prepared as described by Ho et al. [2].

Equipment

Special glassware. Volumetric flasks (0.3 ml) were purchased from SGA Scientific, Bloomfield, NJ, stock no. JM-6165.

Gas chromatograph. All samples were chromatographed on a 1.8 m × 6 mm o.d. silanized glass column packed with 3.0% (w/w) Dexsil 400 on Supelcoport 100/120 mesh packing. The gas chromatograph was a Tracor model 222 (Tracor Inc., Austin, TX) equipped with flame ionization and glow discharge detectors. The hydrogen, helium and air flows were 50, 35, and 330 ml min^{-1}, respectively. The injector and detector were operated at 315°C and 350°C, respectively. The oven was programmed from 85°C (hold for 4 min) to 250°C (hold for 18 min) at 5°C min^{-1}.

Glow discharge detector (GDD). The specific element detector used to identify the TFAA-derivatized components was a modified version of the glow discharge detector described by Feldman and Batistoni [8]. The original chamber (Figs. 1 and 2 of ref. 8) was modified by providing additional windows on extensions behind and on either side of the discharge (see Fig. 1). This chamber received about 85% of the gas flow from the g.c. column. The remainder was diverted to a flame ionization detector (FID).

The cathode of the GDD was a 12 mm × 2 mm o.d. platinum cylinder cap covering the end of a 1.5-mm diameter stainless steel rod. The smallest diameter of the electrode holder (Fig. 1C) was slipped into the lower elec-

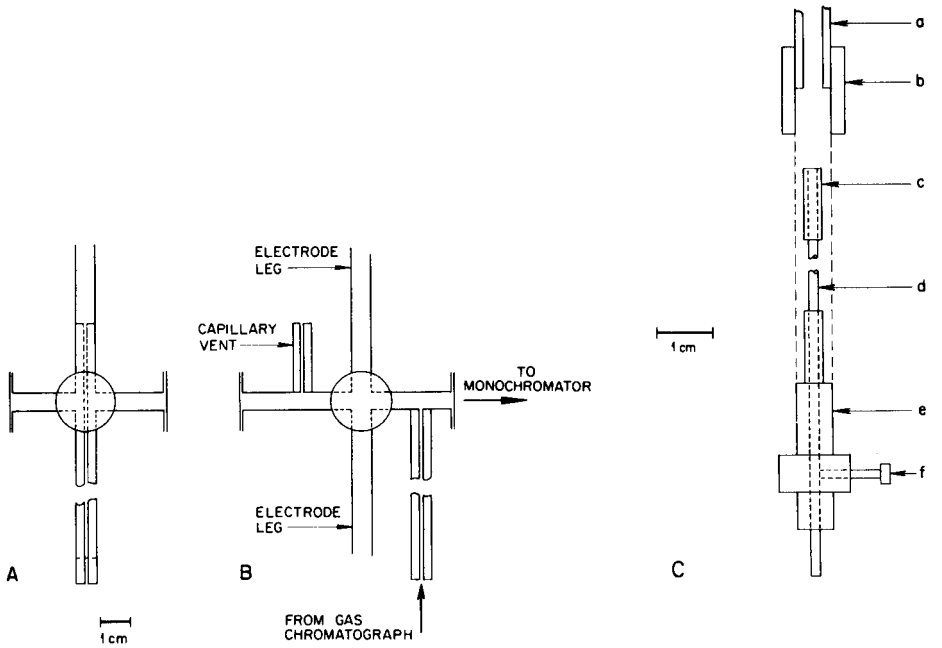

Fig. 1. Glow discharge chamber: (A) end view: (B) side view. Part (C) illustrates insertion of cathode into glow discharge chamber. (a) lower electrode leg; (b) silicone rubber sleeve; (c) Pt tip of cathode; (d) stainless steel shaft of cathode; (e) cathode holder; (f) set screw.

trode leg of the chamber as far as possible, and held in place by a heat-resistant silicone rubber sleeve. The anode was a conically-tipped 1.5-mm diameter tungsten/2% thoria welding rod. The height and position of the discharge in the chamber were regulated by sliding the electrodes in their holders.

The GDD was operated at 80 mA. Power was furnished by a Kepco Model BHK 2000-0.1M power supply. A ballast resistance (two 5000-ohm, 100-W ceramic wire-wound resistors in series) was inserted between the positive output of the power supply and the anode of the discharge.

A 5.1-cm focal length lens at the entrance slit of an 0.5-m Ebert grating monochromator focused an enlarged image of the cathode glow layer onto the entrance aperture of the monochromator. At a discharge current of 80 mA, the glow extended approximately 3 mm down the side of the cathode, so that its image almost filled the aperture. The electrode gap was approximately 3 mm.

Spectral background correction was accomplished by the oscillating refractor plate method suggested by Snelleman et al. [11] and improved by Koirtyohann et al. [12]. A suitably-sized arbor supported the scanning motor (General Scanning Co. Model G100PD) and the attached refractor plate (fused quartz, 6 mm × 20 mm × 1.5 mm), with its long axis (axis of torsional oscillation) vertical. The arbor was positioned inside the mono-

chromator close behind the entrance slit. The scanning motor was driven by a General Scanning Co. Model CCX scanner control, which was in turn driven by a 5 Hz stepped wave generator [12]. Light was detected with an RCA 4840 photomultiplier tube operated at approximately 600 V. The resulting signal was amplified by a Gencom Model 1012 picoammeter; the amplified signal was fed to a Princeton Applied Research Model 5204 lock-in amplifier operating in the second derivative mode. The output from the latter was fed to one channel of a Hewlett-Packard Model 7132A two-pen recorder. The signal from the FID was fed to the other channel.

To make a measurement, the monochromator was first peaked at the wavelength of a fluorine atomic emission line (685.602 nm) with the aid of a separate calibration GDD chamber, similar to the above chamber. The calibration chamber was located behind the detector chamber, and was supplied with helium containing 0.013% (v/v) CCl_2F_2. During calibration, radiation from the calibration chamber passed through the detector chamber and into the monochromator.

Procedure

A solution containing the sample (approximately 50—100 mg of ESB fraction), 20 ml of methylene chloride, and 1.5 ml of TFAA was permitted to react at room temperature in a separatory funnel for 30 min. Another 20 ml of methylene chloride was added to the funnel and the solution was chilled to 5°C in an ice bath. Then 40 ml of saturated sodium hydrogencarbonate solution was added to the mixture, which was shaken gently and permitted to return to room temperature. The funnel was then shaken vigorously for 15 min using a wrist-action shaker. The methylene chloride layer was then concentrated to 0.3 ml using a stream of dry, flowing nitrogen and vacuum.

To initiate the chromatographic determination, the GDD was turned off and 2 μl of the sample were injected onto the column. When the FID signal indicated that the solvent front had passed, the GDD was reignited. Comparison of the GDD and FID chromatograms indicated which of the FID peaks represented compounds that contained fluorine.

RESULTS

Figure 2 presents FID and GDD chromatograms of a standard mixture of three aromatic nitrogenous bases and four aromatic amines, present in equal concentrations, which were derivatized and determined as described. The minimum detectable quantities of fluorine and 2,4,6-trimethylaniline (taken as twice the noise level) were 14 and 33 ng, respectively. The selectivity of the GDD was calculated by dividing the specific response (peak area/μg component injected) of *N*-methylaniline by that of quinoline, and was determined to be at least 200:1. In the case of other aromatic nitrogenous bases, such as 3,5-lutidine, in which there was no detectable response other than background noise, the selectivity would be much greater.

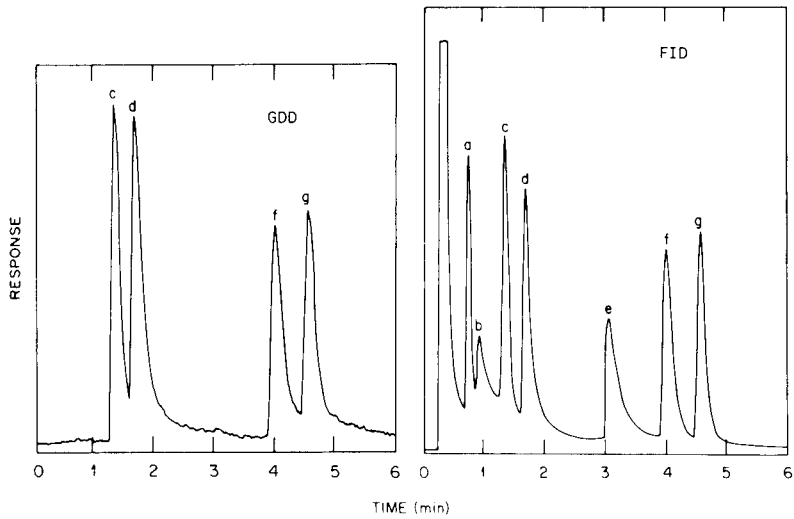

Fig. 2. Chromatogram of standard containing both derivatized amines and aromatic nitrogenous bases. Compounds: (a) 3,5-lutidine; (b) 2,4,6-trimethylpyridine; (c) aniline; (d) *N*-methylaniline; (e) quinoline; (f) 2,3-dimethylaniline; (g) 2,4,6-trimethylaniline. Concentration of all materials: 1 mg ml^{-1} in methylene chloride.

A sample of ether-soluble base isolated from a coal-derived liquid was analyzed in a similar manner; the chromatograms are shown in Fig. 3. It is clear that the use of the GDD greatly simplified the problem of locating amines, even in such a complex mixture. The identity of the peaks shown in the GDD chromatogram was confirmed by analyzing a sample of the "amine-enriched fraction" of Synthoil in this manner. The resulting GDD chromatogram matched that of the ESB fraction. Gas chromatographic—mass spectroscopic examination of the amine-enriched fraction indicated that these PPAA consist of species such as multialkylated anilines, aminoindans, aminobiphenyls, aminofluorenes, and aminoanthracenes [13].

DISCUSSION

The reagent trifluoroacetic anhydride will acetylate any functionality with an active hydrogen; e.g., phenols, acids, hydroxy compounds, and primary and secondary amines [5]. The isolation procedure for the ether-soluble bases (ESB), however, insures a material composed primarily of amines and nitrogenous bases. As a result, TFAA tags the amines selectively with a fluorine-bearing acetyl group which is easily and specifically detected by the GDD.

Modifications of the glow-discharge detector

The glow-discharge detector itself was significantly improved from that used in a previous paper [9], as described below.

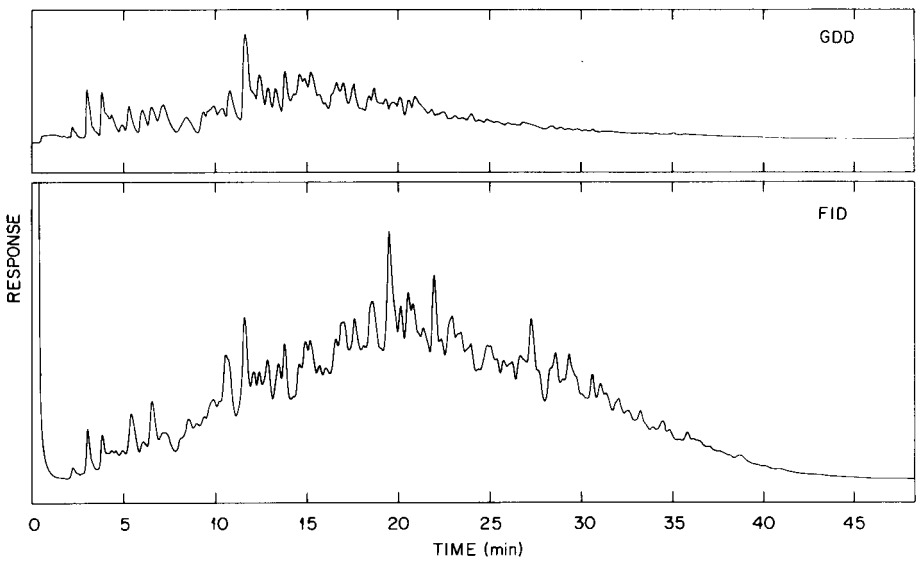

Fig. 3. Examination of the derivatized ether-soluble base fraction of Synthoil using both FID and GDD.

Chamber design. The rear window permitted light from the wavelength calibration lamp to pass through the GDD chamber into the monochromator. The side windows permitted observation of the discharge; their remoteness from the discharge itself prevented them from being coated by degradation products. As in the previous chamber, the window facing the monochromator remained clean because it was upstream with respect to the discharge.

In order to prevent the back-diffusion of air from the gas vent to the discharge, this outlet was made in the form of a short length of 0.5-mm capillary tubing (Fig. 1).

Cathodes. A platinum surface was chosen for the cathode, rather than the tungsten/2% thoria previously used, because platinum does not react chemically with the highly active C-, N-, O-, and F-bearing degradation products created by the discharge. A stainless steel rod was used to support the platinum cathode surface in order to minimize the conduction of heat to the cathode holder. (The heat conductivity of stainless steel is considerably lower than that of tungsten or platinum.)

Illumination optics. The intensity distribution pattern of fluorine emission lines in a helium GDD at atmospheric pressure is unusual, in that almost all of this emission occurs in the cathode glow layer, rather than in the electrode gap. The illumination optics were therefore arranged to gather as much light as possible from the glow layer, and little or none from the electrode gap.

Background correction. When the vapor of a compound containing fluorine passes through a glow discharge in helium at atmospheric pressure, the compound is completely degraded, and the free fluorine atoms thus created are excited to luminescence.

Measuring line emission in a glow discharge of this kind by single-channel detection presents two types of difficulties. First, since the intensity of the fluorine signal is proportional to the current, it is advantageous to use high currents. However, such currents cause incandescence of the cathode which, at the wavelength of interest (685.602 nm), creates a serious background correction problem. Secondly, when any organic compound not containing fluorine passes through the discharge, it produces molecular bands over a considerable spectral range, including the above wavelength. Observation at this wavelength then produces a transient false positive signal; i.e. a false g.c. peak. Even when the compound does contain fluorine, such bands add to the apparent intensity of the fluorine signal.

It is therefore necessary to provide spectral background correction. The background correction system described earlier [8] is effective, but requires preliminary determination of the shapes (though not the intensities) of the molecular bands encountered. On the other hand, tests of the present oscillating refractor plate system have shown that the intensity observed for a given weak line remains the same when a background continuum 130 times as intense as the line is superimposed on it. Additional information on the operation and construction of this type of background corrector is available [14].

In theory, amines could be detected using either the nitrogen-phosphorus detector (NPD) [15] or the electron-capture detector (ECD) once the amines had been derivatized as described [16—20]. The former would ideally require no derivatization, but would be unable to discriminate between amines and aromatic nitrogenous bases. The ECD should be able to detect amines after derivatization. However, PAH are detected by the ECD [16—20], and it would be expected that the ECD also would respond to the aromatic nitrogenous bases simply because they are aromatic.

Figure 3 indicates not only a notable specificity for amines, but also a significant quantity of unresolved material which apparently contains amines. For this reason, isolation procedures which provide a clean amine fraction would be useful. The GDD can be used as a novel means for rapidly screening for amines, but cannot substitute for a careful isolation procedure in analyzing these complex samples.

The authors thank C-h. Ho and P. R. Mraz for preparing the ether-soluble base and amine-enriched fractions of Synthoil used, and C-h. Ho for valuable discussions concerning the general problem of amine analysis in energy-related samples. This work was supported by the U.S. Department of Energy, Office of Health and Environmental Research, under contract W-7405-eng-26 with Union Carbide Corporation.

REFERENCES

1 J. L. Epler, J. A. Young, A. A. Hardigree, T. K. Rao, M. R. Guerin, I. B. Rubin, C-h. Ho and B. R. Clark, Mutat. Res., 57 (1978) 265.

2 C-h. Ho, B. R. Clark, M. R. Guerin, C. Y. Ma and T. K. Rao, ACS Div. Fuel Chem. Prepr., 24(1) (1979) 281.
3 C-h. Ho, C. Y. Ma, B. R. Clark, M. R. Guerin, T. K. Rao and J. L. Epler, Environ. Res., in press.
4 I. B. Rubin, M. R. Guerin, A. A. Hardigree and J. L. Epler, Environ. Res., 12 (1976) 358.
5 K. Blau and G. King, Handbook of Derivatives for Chromatography, Heyden & Sons, Ltd., 1978.
6 W. Irvine and M. J. Saxby, J. Chromatogr., 43 (1969) 129.
7 M. Pailer and W. J. Huebsch, Monatsh. Chem., 97 (1966) 1541.
8 C. Feldman and D. A. Batistoni, Anal. Chem., 49 (1977) 2215.
9 A. D. Horton, R. A. Jenkins and C. Feldman, Anal. Chim. Acta, 108 (1979) 221.
10 D. L. Coffin, M. R. Guerin and W. H. Griest, Symposium on Potential Health and Environmental Effects of Fossil Fuel Technologies, CONF-780903, Gatlinburg, TN, September 25—28, 1978, 1979, p. 153.
11 W. Snelleman, T. C. Tains, K. W. Yee, H. D. Cook and O. Menis, Anal. Chem., 42 (1970) 394.
12 S. R. Koirtyohann, E. D. Glass, D. A. Yates, E. J. Hinderberger and F. E. Lichte, Anal. Chem., 49 (1977) 1121.
13 M. R. Guerin, C-h. Ho, T. K. Rao, B. R. Clark and J. L. Epler, Environ. Res., in press.
14 T. C. O'Haver, M. S. Epstein and A. T. Zander, Anal. Chem., 49 (1977) 458.
15 G. W. Diachenko, Environ. Sci. Technol., 13(3) (1979) 329.
16 V. Cantuti, G. P. Cartoni, A. Liberti and A. T. Toni, J. Chromatogr., 17 (1965) 60.
17 N. Carugno and S. Rossi, J. Gas Chromatogr., 5 (1967) 103.
18 W. Lijinski, I. Domsky and J. Ward, J. Gas Chromatogr., (1965) 152.
19 A. Bjorseth and G. Ekland, J. High Res. Chromatogr. Cap. Chromatogr., 2 (1979) 22.
20 D. J. David, Gas Chromatographic Detectors, J. Wiley, New York, 1974, p. 107.

Analytica Chimica Acta, 119 (1980) 291—297

GAS CHROMATOGRAPHIC DETERMINATION OF NITRIC OXIDE AT SUB-ppm LEVELS

KOICHI FUNAZO*, MINORU TANAKA and TOSHIYUKI SHONO

Department of Applied Chemistry, Faculty of Engineering, Osaka University, Yamada-kami, Suita, Osaka 565 (Japan)

(Received 11th February 1980)

SUMMARY

The highly sensitive procedure involves the reaction of nitric oxide with various aromatic amines in the presence of copper (II) halide at room temperature and the gas chromatographic measurement of the aryl halide formed with an electron capture detector. The conversion yield of nitric oxide and the sensitivity of the detector to each product were studied. The system containing 3,4-dichloroaniline and copper(II) bromide is the most sensitive; the detection limit is 0.01 ppm, which indicates the possibility of determining nitric oxide in air samples without preconcentration. Gases commonly encountered in polluted air do not interfere, except for nitrogen dioxide, which can be removed by the Saltzman method.

Nitric oxide can be directly determined by gas chromatography with a thermal conductivity detector, but only with poor sensitivity. Flame ionization detectors and electron capture detectors (ECD) are also insensitive to nitric oxide. Recently, Blurton and Stetter [1] reported a sensitive electrochemical detector for common air pollutants. Detection limits of 0.04 ppm for nitric oxide and 1.2 ppm for nitrogen dioxide were obtained under simulated gas chromatographic conditions, but with the sample bypassing the column. It is, however, difficult to obtain satisfactory chromatographic analyses for trace levels of nitric oxide and nitrogen dioxide because the retention time depends upon the sample size and/or concentration; no quantitative relationship between the detector response and concentration is apparent, and nitrogen dioxide reacts with some of the column packing material. If nitric oxide could be converted to a compound which responds sensitively to a gas chromatographic detector, it should be determined successfully at low concentrations. The sensitive gas chromatographic determination of nitrogen dioxide has been achieved by nitration of benzene [2, 3].

In a preliminary communication [4], a new method of gas chromatographic detection for nitric oxide was reported, based on a modification of the reaction published by Brackman and Smit [5], in which nitric oxide promoted the conversion of *p*-chloroaniline to *p*-bromochlorobenzene:

$$CuBr_2 + NO(g) \rightleftarrows CuBr_2 \cdot NO$$

$$CuBr_2 \cdot NO + p\text{-}ClC_6H_4NH_2 \rightarrow p\text{-}ClC_6H_4Br + CuBr + N_2 + H_2O$$

The halogenated product was measured by an ECD, the detection limit for nitric oxide being 0.1 ppm. This paper presents a more detailed account of this procedure, and a comparison of the use of other aniline derivatives which yielded higher ECD responses than *p*-chloroaniline. The most sensitive procedure can be applied to the determination of 0.01—0.50 ppm of nitric oxide, by using 3,4-dichloroaniline and copper(II) bromide.

EXPERIMENTAL

Apparatus, reagents and standard gases

The Shimadzu GC-4BM gas chromatograph used was equipped with a ^{63}Ni electron capture detector. A stainless steel column (2 m × 3 mm i.d.) was packed with 10% OV-17 on 60—80 mesh Shimalite W. The nitrogen flow-rate was 50 ml min^{-1}. The detector and injection port temperatures were maintained at 250°C. The column temperature was varied depending on the aryl halide used; it was kept at 150°C for determining 3,4-dichlorobromobenzene. The peak areas were measured by a digital integrator (Shimadzu Chromatopac-ElA).

All reagents were of analytical-reagent grade unless otherwise stated. Acetonitrile was refluxed with phosphorus pentoxide to remove water and distilled before use. Standard sample gases of the desired concentrations were prepared by diluting standard gas mixtures (7.00 ppm (v/v) nitric oxide in nitrogen and 50.3 ppm (v/v) nitrogen dioxide in nitrogen; Seitetsu Kagaku Co.) with nitrogen. The air used in some experiments for dilution (see Fig. 5) was purified by passage through five scrubbers in series which contained aqueous potassium permanganate (2.5%) and sulfuric acid (2.5% w/v), aqueous sodium hydroxide (10%), concentrated sulfuric acid, silica gel, and molecular sieve 5 A, respectively.

Recommended procedure

A round-bottomed flask, the volume of which was measured in advance (620 ml), was filled with the sample gas, and solutions were injected by syringe through a silicone rubber serum cap. An acetonitrile solution (1 ml) of copper(II) halide (1.0×10^{-2} M), and an acetonitrile solution (4 ml) containing both an aniline derivative (5.0×10^{-3} M) and an internal standard (for details see Table 1) were injected. The flask was shaken for 2 h with an electric shaker. After the reaction period, the reaction mixture was directly injected into the gas chromatograph and the resulting aryl halide was determined by the internal standard method. Because of the direct injection, the peaks of the large excess of aniline derivative, etc., appeared a long time after the three peaks of acetonitrile, internal standard, and product. In order to avoid troubles from the excess of aniline derivative contaminating the ECD, the gas flow was switched to an outlet placed between the column and detector for a period of about 30 min after the three peaks of interest had been recorded.

TABLE 1

Conversion yield of nitric oxide[a] and relative sensitivity of each product to an electron capture detector

Aniline derivative	CuX_2	Product	Yield (%)	Internal standard[b]	Relative sensitivity
p-Chloroaniline	$CuBr_2$	*p*-Bromochlorobenzene	84.8 ± 1.1	A	1.00
p-Bromoaniline	$CuBr_2$	*p*-Dibromobenzene	49.5 ± 0.6	B	2.27
p-Nitroaniline	$CuCl_2$	*p*-Chloronitrobenzene	60.2 ± 1.2	B	2.25
	$CuBr_2$	*p*-Bromonitrobenzene	17.1 ± 0.6	C	2.24
m-Nitroaniline	$CuCl_2$	*m*-Chloronitrobenzene	56.8 ± 0.8	B	3.70
	$CuBr_2$	*m*-Bromonitrobenzene	60.6 ± 1.3	C	4.55
o-Nitroaniline	$CuCl_2$	*o*-Chloronitrobenzene	57.4 ± 0.8	B	4.10
3,4-Dichloro-aniline	$CuBr_2$	3,4-Dichlorobromobenzene	63.2 ± 1.0[c]	B	12.8

[a]Sample gas, 3.00 ppm nitric oxide in nitrogen; aniline derivative, 5.0×10^{-3} M; CuX_2, 1.0×10^{-2} M.
[b](A) 5.0×10^{-4} M *p*-dichlorobenzene; (B) 2.0×10^{-5} M *p*-bromochlorobenzene; (C) 1.0×10^{-5} M *p*-dibromobenzene.
[c]Sample gas concentration, 0.30 ppm nitric oxide in nitrogen.

RESULTS AND DISCUSSION

Conversion yield and relative sensitivity of the ECD

In order to find more sensitive conversion reagents for nitric oxide than *p*-chloroaniline and copper(II) bromide, the conversion yield of nitric oxide and the sensitivity (relative to *p*-bromochlorobenzene) of each product to an ECD were examined, by using several aniline derivatives and copper(II) chloride or bromide. The conversion yield was calculated from $100[(p.r.\ 1) - (p.r.\ 2)]/p.r.\ 3$, where *p.r.* 1. is the peak area ratio of the aryl halide to the internal standard in a reaction mixture, *p.r.* 2 is that for pure nitrogen and the internal standard (i.e. a blank) and *p.r.* 3 is the peak area ratio when a standard solution containing the aryl halide and the internal standard is injected.

The relative chromatographic sensitivity for each product was estimated as follows. Each aryl halide solution in acetonitrile (2 μl), at three different concentrations, was injected into the gas chromatograph, and the peak area was measured at a constant retention time of 6.0 ± 0.5 min by adjusting the column temperature. The average value of three measurements was calculated. The results obtained are shown in Table 1 together with the conversion yield for nitric oxide. When nitric oxide is treated with 3,4-dichloroaniline and copper bromide, the conversion yield is higher than for any other reaction with the exception of *p*-chloroaniline and copper bromide. However, the ECD is much more sensitive to the 3,4-dichloro-bromobenzene produced from 3,4-dichloroaniline and copper(II) bromide than to any of the other products. Therefore the reaction of nitric oxide with 3,4-dichloroaniline and copper(II) bromide was studied in greater detail.

Optimum reaction conditions

In order to ascertain the optimum reaction conditions, the effects of reaction time and of reagent concentrations on the conversion yield were examined. Figure 1 shows the effect of reaction time on the peak area of 3,4-dichlorobromobenzene for 0.10 and 0.03 ppm of nitric oxide in nitrogen. The yields increase with increase of reaction time, and become constant after 1.5 h in both cases. The recommended reaction time is therefore 2 h. Figure 2 shows the effect of copper(II) bromide concentration in 1 ml of acetonitrile; the yields become constant when this concentration exceeds 4.2×10^{-3} M (for 0.10 ppm) or 6.0×10^{-3} M (for 0.30 ppm nitric oxide). Figure 3 shows the similar effect of the concentration of 3,4-dichloroaniline in 4 ml of acetonitrile. A constant yield is achieved at a mole ratio of 3,4-dichloroaniline to copper(II) bromide of 1. In Figs. 1—3, the maximum peak area of 3,4-dichlorobromobenzene produced from 0.10 ppm of nitric oxide in nitrogen was arbitrarily assigned a value of 100.

From these results, the optimum reaction conditions described in the Experimental section were selected. A typical gas chromatogram of the reaction mixture under these conditions is shown in Fig. 4.

Calibration

The 3,4-dichlorobromobenzene peak area plotted against the concentration of nitric oxide in the sample gas filling the reaction flask gives a linear plot up to 0.50 ppm, as shown in Fig. 5. The detection limit is 0.01 ppm. This is adequate for the measurement of the nitric oxide concentration in normal air. Nitrogen dioxide also reacts with the reagents, giving the same product as nitric oxide, and a linear calibration plot in the range 0.05—0.50 ppm of nitrogen dioxide (Fig. 5). Figure 5 also shows the results of the conversion reaction for nitric oxide treated in air in place of nitrogen. The relative standard deviation of each point is 2—6%. The three straight lines do not pass through the origin, presumably because of the small unknown

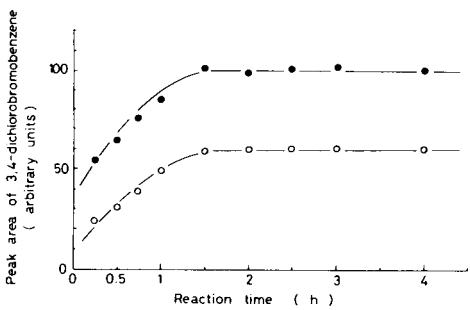

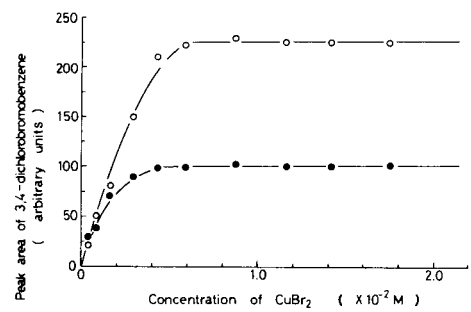

Fig. 1. Effect of reaction time on yield of 3,4-dichlorobromobenzene. (•) 0.10 ppm NO in N_2; (○) 0.03 ppm NO in N_2. 1.0×10^{-2} M $CuBr_2$; 5.0×10^{-3} M 3,4-dichloroaniline.

Fig. 2. Effect of $CuBr_2$ concentration on yield of 3,4-dichlorobromobenzene. (•) 0.10 ppm NO in N_2; (○) 0.30 ppm NO in N_2; 5.0×10^{-3} M 3,4-dichloroaniline.

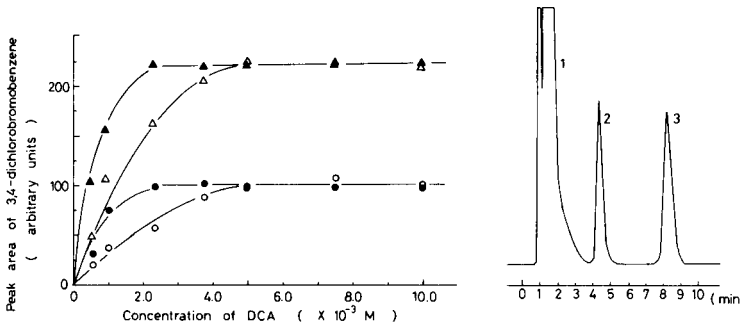

Fig. 3. Effect of 3,4-dichloroaniline concentration on 3,4-dichlorobromobenzene. Sample gas, 0.10 ppm NO in N_2 (● or ○); 0.30 ppm NO in N_2 (▲ or △). 1.0 × 10^{-2} M $CuBr_2$ (● or ▲); 2.0 × 10^{-2} M $CuBr_2$ (○ or △).

Fig. 4. Gas chromatogram of reaction mixture for 0.30 ppm NO: (1) acetonitrile; (2) *p*-bromochlorobenzene; (3) 3,4-dichlorobromobenzene.

peak given by the blank without nitric oxide or nitrogen dioxide. The conversion yield for nitrogen dioxide is less than that for nitric oxide. When nitric oxide in air is used as the sample, the conversion yield is somewhat decreased. Therefore, the effect of oxygen concentration in the sample gas was examined in detail for 0.30 ppm of nitric oxide. The yield (Fig. 6) decreased linearly with increasing oxygen concentration. However, because the oxygen concentration in air does not vary widely, this is not a problem, provided that appropriate calibration is used.

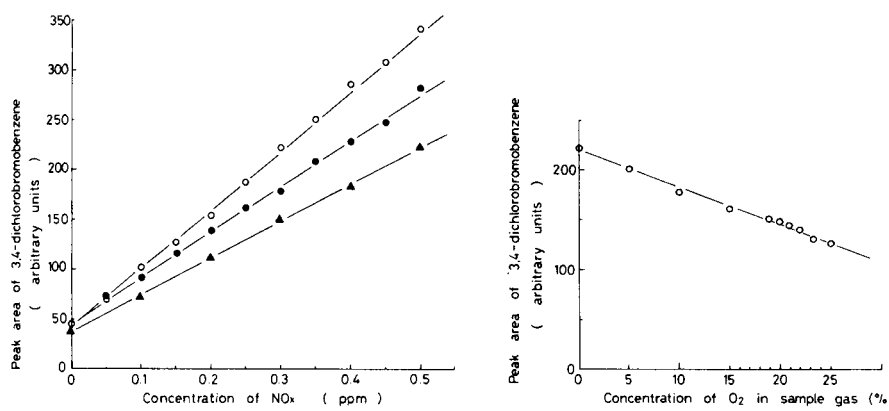

Fig. 5. Plots of 3,4-dichlorobromobenzene peak area vs. concentration: (○) NO in N_2; (●) NO_2 in N_2; (▲) NO in air.

Fig. 6. Effect of O_2 concentration on yield of 3,4-dichlorobromobenzene for 0.30 ppm NO.

TABLE 2

Influences of other gases on the determination of 0.30 ppm nitric oxide

Other gas	Concentration	Peak area[a]	Other gas	Concentration	Peak area[a]
N_2[b]		223.4 ± 10.6	H_2O	10 μl[c]	227.0 ± 10.0
CO_2	5%	225.5 ± 8.4	NH_3	10 μl (0.1 M)[c]	218.6 ± 5.5
CO	0.1%	220.0 ± 6.5	SO_2	400 ppm	191.5 ± 9.7
N_2O	400 ppm	223.4 ± 12.2	SO_2	15 ppm	228.1 ± 6.2

[a]Mean ± s.d. of 9 results. [b]Standard atmosphere. [c]Deionized water or 0.1 M ammonia water was injected into the reaction flask.

Influences of other compounds

The influence of other gases on the determination of nitric oxide is shown in Table 2. The concentration of each gas examined is much higher than that in normal air. It is very difficult to prepare a nitric oxide sample containing a known concentration of water vapor or gaseous ammonia. After water or ammonia water had been added to the flask which was already filled with 0.30 ppm nitric oxide in nitrogen, the flask was shaken for 30 min to mix the contents completely; the conversion reaction was then carried out. Carbon dioxide, carbon monoxide, nitrous oxide, water, ammonia or sulfur dioxide (15 ppm), do not interfere with the analysis. Sulfur dioxide at 400 ppm decreases the peak area slightly, but this is an excessively high level. Organic gases commonly found in air were assumed not to interfere.

Application to automobile exhaust gases

The gas chromatographic method was applied to the determination of nitric oxide in automobile exhaust gases, after passing through the Saltzman bubbler in order to remove nitrogen dioxide [6]. The same sample gases were also passed successively through a Saltzman bubbler, a permanganate impinger and another Saltzman bubbler, and the concentrations of nitric oxide were determined from the absorbance of the second Saltzman reagent solution [7]. The results obtained, shown in Table 3, prove that the values obtained by the two methods agree satisfactorily, and that the proposed method is suitable for practical applications.

TABLE 3

Concentrations of nitric oxide in automobile exhaust gases

Sample	1	2	3	4	5	6	7
Saltzman method	0.52	0.47	0.47	0.44	0.38	0.26	0.22
G.c. method	0.50	0.45	0.48	0.43	0.36	0.26	0.21

REFERENCES

1 K. F. Blurton and J. R. Stetter, J. Chromatogr., 155 (1978) 35.
2 W. D. Ross, G. W. Buttler, T. G. Duffy, W. R. Rehg, M. T. Wininger and R. E. Sievers, J. Chromatogr., 112 (1975) 719.
3 J. W. Tesch, W. R. Rehg and R. E. Sievers, J. Chromatogr., 126 (1976) 743.
4 K. Funazo, M. Tanaka and T. Shono, Anal. Lett., A11 (1978) 661.
5 W. Brackman and P. J. Smit, Rec. Trav. Chim. Pays-Bas, 85 (1966) 857.
6 B. E. Saltzman, Anal. Chem., 26 (1954) 1949; Anal. Chem., 32 (1960) 135; U.S. Public Health Serv. Publ., 999-AP-11 (1965) C1—C7.
7 A. C. Stern (Ed.), Air Pollution, 3rd edn., Vol. III, Academic Press, New York, 1976, p. 261.

Analytica Chimica Acta, 119 (1980) 299—303

SEPARATION OF HOMOLOGOUS n-ALKYLAMMONIUM HEXANOATES BY REVERSE-PHASE THIN LAYER CHROMATOGRAPHY WITH CONTINUOUS DEVELOPMENT

ALAN E. McDOWELL

The Proctor and Gamble Company, Miami Valley Laboratories, P. O. Box 39175 Cincinnati, OH 45247 (U.S.A.)

(Received 7th March 1980)

SUMMARY

Long-chain n-alkylammonium hexanoates can be separated according to alkyl chain length by reverse-phase thin layer chromatography on commercially available plates with mixtures of acetonitrile, tetrahydrofuran, and formic acid as developing solvents. Differences in alkyl chain length of two carbon units can be resolved for chain lengths up to 22 carbon units. The use of continuous development for improving resolution has been investigated. An application to the characterization of a ^{14}C-labeled alkylammonium hexanoate is discussed.

Quaternary ammonium compounds are widely used as antibacterial agents and surfactants, and much interest has been generated in chromatographic methods for their separation. These compounds are not volatile and thus are not amenable to gas chromatography unless pyrolysis techniques are used [1]. Liquid column chromatography suffers from a lack of detectors for many of these compounds [2]. Thin layer chromatography (t.l.c.) has therefore been the method of choice for simple and convenient separations of quaternary ammonium compounds [3, 4]. However, the methods to date have not been able to resolve a homologous series of alkyl-substituted quaternary ammonium compounds, especially when the alkyl chain length is longer than twelve carbon units. A recent study demonstrated that aliphatic amines can be separated according to alkyl chain length with good selectivity by reverse-phase t.l.c. [5]. When a need arose to determine the alkyl chain length distribution of quaternary ammonium compounds, reverse-phase t.l.c. was chosen as the most promising analytical method. The n-alkylammonium hexanoates have the general structure (I). These compounds are nonconducting zwitterions.

This report discusses the separation of long chain alkylammonium hexanoates by reverse-phase t.l.c. on commercially available plates. An application of this method to the characterization of a ^{14}C-labeled n-alkylammonium hexanoate is presented. The use of continuous development is shown to be of advantage for improving resolution.

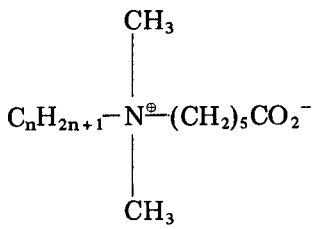

(I)

EXPERIMENTAL

Materials and apparatus

The alkylammonium hexanoates (C_nAH's) were prepared in these laboratories. The $C_{14}AH$, $C_{20}AH$, and $C_{22}AH$ compounds were prepared from the corresponding n-alkyl bromide precursors. The precursors were all analyzed by gas chromatography and found to be more than 98% pure. The $C_{18}AH$ was prepared as the methyl ^{14}C-labeled material. Solutions with concentrations of 1 or 10 mg ml^{-1} in methanol were prepared for spotting.

Acetonitrile and tetrahydrofuran (distilled-in-glass; Burdick and Jackson, Muskegon, Michigan) were used. Reagent-grade formic acid was obtained from Matheson, Coleman and Bell, Norwood, Ohio.

Reverse-phase t.l.c. plates, KC18 5 × 20 cm, were purchased from Whatman.

A Berthold LB 2760 TLC radioscanner was used to record the radioactivity profile on the plates.

Procedure

Glass capillary micropipets were used for spotting. Initial spot sizes were approximately 1 mm in diameter. Spots were visualized after development by spraying with Dragendorff's reagent [6]. Continuous development was carried out by placing 20 ml of solvent in a 1-l beaker and covering the beaker with tin foil. A slit was made in the foil large enough for a 5-cm t.l.c. plate. The plate was inserted through the slit in the foil down into the developing solvent (see below). The top 2 cm of the plate extended out of the chamber through the slit in the foil. The bed length in the chamber was 18 cm. The solvent front was allowed to migrate out of the chamber where the developing solvent evaporated, setting up a continuous flow of solvent through the bed length in the chamber.

RESULTS AND DISCUSSION

The n-alkylammonium hexanoates can be separated on KC18 reverse-phase t.l.c. plates with mixtures of acetonitrile, tetrahydrofuran and formic acid (e.g., 80:20:5). Formic acid deactivates the remaining adsorption sites on the plates. Without acid in the eluent, the spots either tail badly or remain near the origin. The ammonium hexanoates migrate as the protonated formate salts.

Effect of solvent strength

The logarithm of the capacity factor (k) can be related to solvent strength [7]. Table 1 gives the regression statistics for plots of the logarithm of the capacity factor versus the percent of strong solvent in the developing solvent for $C_{14}AH$, $C_{20}AH$, and $C_{22}AH$. The strong solvent is a mixture of tetrahydrofuran with 5% formic acid and the weak solvent is a mixture of acetonitrile with 5% formic acid. Capacity factors were calculated from R_f values using the relation $k = (1 - R_f)/R_f$. The regression data are based on measurements at five different solvent strengths where the R_f values ranged between 0.17 and 0.55.

The variation in log k with solvent strength is nearly linear over limited ranges. The difference in log k values between consecutive homologs at a given solvent strength is reasonably constant. That is, the difference between the y intercept calculated from the regression analysis between $C_{14}AH$ and $C_{20}AH$ is exactly three times the difference in the y intercept between $C_{22}AH$ and $C_{20}AH$. Furthermore, the difference in slopes between $C_{14}AH$ and $C_{20}AH$ is again three times the difference between $C_{22}AH$ and $C_{20}AH$. Thus the lines diverge on going toward lower solvent strength. This means there is greater selectivity at lower solvent strength. The practical consequences of these differences will be discussed below. There can be variation of log k values because of variability in the plates, especially from batch to batch. However, the general trends remain. One seldom needs to know the exact relation between log k and solvent strength to take advantage of the general trends illustrated here.

Figure 1 shows the separation of $C_{22}AH$, $C_{20}AH$, and $C_{14}AH$ on a KC18 plate with acetonitrile (85)/tetrahydrofuran (15)/formic acid (5). The distance from spotting point to solvent front is 14 cm. The center-to-center separation for $C_{22}AH$ and $C_{20}AH$ is 5 mm. Some overlap of the spots for $C_{22}AH$ and $C_{20}AH$ is evident but two distinct color centers are apparent for these compounds in lane D.

Application

This method was used for the characterization of methyl ^{14}C-labeled $C_{18}AH$ prepared for biodistribution studies. It was important to determine the alkyl chain length and radiochemical purity of this material. Figure 2

TABLE 1

Regression statistics for plots of log k versus the percent of strong solvent in the developing solvent for the ammonium hexanoates

	Slope ± 1σ	Intercept ± 1σ	Correlation coefficient
$C_{14}AH$	−0.017 ± 0.0004	0.24 ± 0.004	−0.999
$C_{20}AH$	−0.020 ± 0.0009	0.57 ± 0.01	−0.997
$C_{22}AH$	−0.021 ± 0.001	0.68 ± 0.01	−0.995

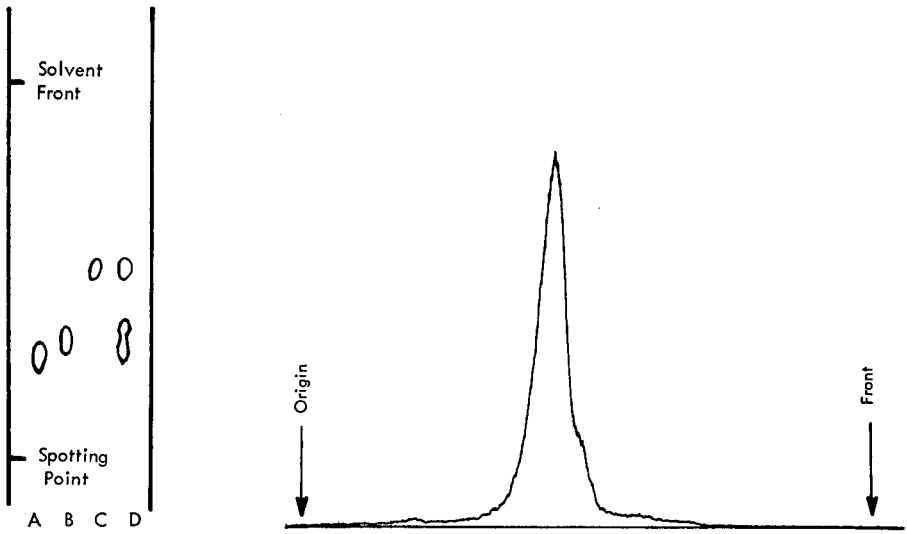

Fig. 1. Thin layer chromatogram of (A) $C_{22}AH$, (B) $C_{20}AH$, (C) $C_{14}AH$, (D) mixture of $C_{22}AH$, $C_{20}AH$ and $C_{14}AH$.

Fig. 2. T.l.c. radioscan of $C_{18}AH$ with $C_{16}AH$ impurity chromatographed in acetonitrile (80)/tetrahydrofuran(20)/formic acid(5).

shows the radioscan of a chromatogram of this material on KC18 plates with acetonitrile (80)/tetrahydrofuran (20)/formic acid (5) at a 5-μg loading level. Some $C_{16}AH$ is detectable as a shoulder. The center-to-center separation is about 5 mm. However, the resolution is not great enough to permit accurate quantification from the radioscan. A simple technique to improve the resolution is discussed in the next section.

Use of continuous development

Continuous development is a well known technique for improving resolution. It has been used mainly for separation of components which fall near the origin after a conventional development. Although two components may be migrating at different rates in this case, the spots simply do not move far enough to achieve physical separation. Continuous development keeps the spots moving until physical separation can be achieved.

Perry has recently pointed out that changing the solvent strength can have a beneficial effect on selectivity [7]. In many cases, as with this one, the separation factor increases as lower solvent strength is used. Thus by lowering the solvent strength to gain selectivity and using continuous development, resolution can be improved. Figure 3 shows the resulting radioscan when 5 μg of the $C_{18}AH$ sample was developed continuously for 1.5 h with acetonitrile(20)/formic acid(1) as described in the Experimental section. The $C_{18}AH$ has migrated about the same distance as in the conventional development shown in Fig. 2. However, because of the improved selectivity

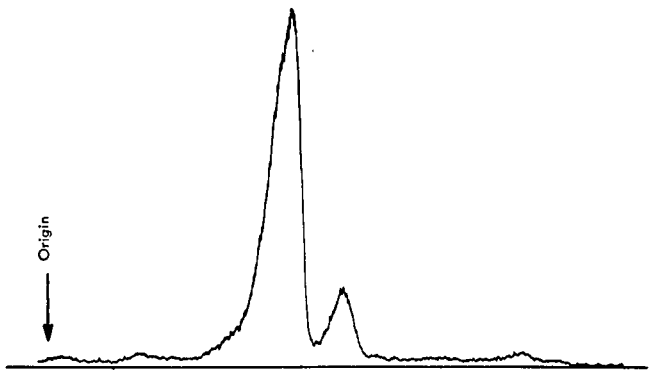

Fig. 3. T.l.c. radioscan of $C_{18}AH$ with $C_{16}AH$ impurity chromatographed with continuous development in acetonitrile(20)/formic acid(1) for 1.5 h.

at this solvent strength, $C_{16}AH$ has moved considerably farther, so the center-to-center separation is now 14 mm. Without this change in selectivity, continuous development would have no advantage unless the spots were allowed to migrate larger distances than in the conventional development. Continuous development simply helps realize the improved selectivity by keeping the spots moving until physical separation is achieved. Separation occurs in a reasonable amount of time since solvent velocity does not decrease but remains constant when the solvent front leaves the chamber. Separation time can be minimized by keeping the bed length in the chamber as short as possible. It may be that by using shorter bed lengths and lower solvent strengths a separation could be obtained in less than 1.5 h. Essentially complete separation of $C_{16}AH$ from $C_{18}AH$ has been achieved, allowing accurate determination of the radiochemical purity.

Conclusions

Long chain alkylammonium hexanoates can be separated according to alkyl chain length by reverse-phase t.l.c. on KC18 plates using mixtures of acetonitrile, tetrahydrofuran, and formic acid as developing solvents. At loadings of a few micrograms, homologs which differ by two carbon units can be resolved. Continuous development at decreased solvent strength can be used to improve resolution.

The author acknowledges the help of Jim Thompson and Chuck Degenhardt who prepared the samples used.

REFERENCES

1 P. I. A. Szilagyi, D. E. Schmidt and J. P. Green, Anal. Chem., 40 (1968) 2009.
2 J. G. Dorsey, M. S. Denton and T. W. Gilbert, Anal. Chem., 50 (1978) 1330.
3 W. F. H. McLean and K. Jewers, J. Chromatogr., 74 (1972) 297.
4 J. E. Gordon, J. Chromatogr., 20 (1965) 38.
5 L. Lepri, P. G. Desideri and D. Heimler, J. Chromatogr., 125 (1976) 129.
6 J. C. Touchstone and M. F. Dobbins, in Practice of Thin Layer Chromatography, J. Wiley, New York, 1978, p. 174.
7 J. A. Perry, J. Chromatogr., 165 (1979) 117.

Analytica Chimica Acta, 119 (1980) 305—311

MERGING ZONES IN FLOW INJECTION ANALYSIS
Part 4. Simultaneous Spectrophotometric Determination of Total Nitrogen and Phosphorus in Plant Material

B. F. REIS, E. A. G. ZAGATTO, A. O. JACINTHO, F. J. KRUG and H. BERGAMIN F°*
Centro de Energia Nuclear na Agricultura, 13.400 Piracicaba, S. Paulo (Brasil)
(Received 8th May 1980)

SUMMARY

The merging zones approach is used in a single flow injection system for the simultaneous spectrophotometric determination of nitrogen and phosphorus in plant material based on the Berthelot and molybdophosphate reactions. A multiple proportional injector is designed to introduce samples and reagents into water carrier streams in such a way that only one analytical path with one detection unit is required. For both processes, catalysis is employed; a detailed study of the reagent composition is reported for the Berthelot reaction. The proposed system is characterized by a high degree of sample and reagent dispersion; 60 samples per hour can be analyzed with a consumption of reagents in the range of microliters per determination. Total recoveries of 98.3% N and 99.1% P were estimated from 20 runs of a typical plant sample containing around 3% N and 0.3% P in dry matter. The results of the present method agree with those obtained by Technicon AutoAnalyzer procedure.

The merging zones approach to flow injection systems utilizes the synchronized introduction of samples and reagents into chemically inert unsegmented carrier streams. The injected species start as well defined zones which then merge so that chemical reactions can occur during transport to the detector. The most attractive analytical characteristic of such methods is the very low reagent consumption [1—7].

The injection of small pulses of samples and reagents opens the possibility of performing simultaneous determinations. A simple flow injection system without sample splitting can be designed for this purpose, requiring only one analytical path.

The present paper reports the development of a new flow injection system for simultaneous determination of nitrogen and phosphorus in plant digests. The spectrophotometric methods already used in earlier flow injection procedure [8] were chosen because the same wavelength setting can be used for both measurements and, therefore, only one detection unit is required.

EXPERIMENTAL

Apparatus

Peristaltic pump, tubing, reaction coils, connectors, flow-cell, spectrophotometer and recorder were the same as used in earlier work [3].

The injector was operated electronically [5] and consisted of two fixed external plates of perspex with a central sliding plunger. Leakage was prevented by gluing silicone rubber sheets between the plates of the injector. In order to adapt this injector to the proposed system, three commutation sections, 3:4:3, were necessary. The code 3:4:3 means that there are three entry holes for tubing connections, four flow-through holes (with the possibility of loop insertion) in the sliding bar, and three outlet holes. This injector is appropriate for simultaneous determinations in systems with the merging zone approach, and operates in two positions. When the injector is switched to the position shown in Fig. 1, the sample and reagents related to determination of the first species are introduced into the analytical system, while the sample and reagents involved in the determination of the second species start filling their corresponding loops, which define exactly the volumes to be injected. The excess of sample is discarded, and excess of reagents slightly diluted by the corresponding carrier streams [1], are stored in the reagent recovery vessels. After a certain time interval, enough to pre-

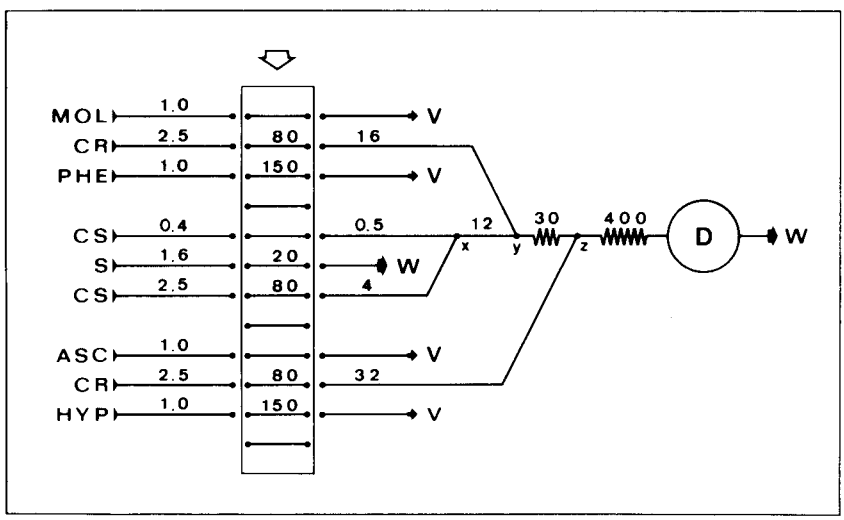

Fig. 1. Flow diagram of the proposed system. MOL, CR, PHE, CS, S, ASC and HYP correspond to molybdate, reagent carrier stream, alkaline phenol, sample carrier stream, sample, ascorbic acid and hypochlorite reagent solutions, respectively. The numbers on the left-hand lines indicate the flow rates in ml min^{-1}. The numbers in the rectangular representation of the sliding plunger of the injector indicate the injected volumes in μl. The other numbers indicate tubing or coil lengths in cm. The individual recovery vessels are identified by V and the spectrophotometric detector by D. W denotes waste. For details, see text.

vent carryover, the injector is switched again, injecting the sample and reagents related to the second species. The sample and reagents involved in the determination of the first species start similarly filling their corresponding loops. The next commutation brings the injector back to the position specified in Fig. 1 and a new cycle starts.

Reagents

All reagents, except for sodium hypochlorite, were of analytical grade, and distilled-deionized water was used in all experiments.

Phenol stock solution (12% w/v in 4 M NaOH). This solution is stable for several weeks if stored in a refrigerator. Before use, this solution is filtered.

Sodium nitrosopentacyanoferrate(III) (sodium nitroprusside) stock solution (10%). This is prepared by dissolving 10 g of $Na_2Fe(CN)_5NO \cdot 2H_2O$ in 100 ml of water. The solution, stored in an amber bottle, is stable.

Bismuth stock solution. This is prepared by dissolving 2 g of bismuth subcarbonate ($(BiO)_2CO_3 \cdot 1/2H_2O$) in 50 ml of 6 M hydrochloric acid. The solution is stable.

Alkaline phenol reagent. The phenol stock solution (25 ml) and the sodium nitroprusside stock solution (10 ml) are diluted to 100 ml in a volumetric flask with water.

Sodium hypochlorite reagent. This is prepared from domestic bleach solution. The solution used was found to contain 2.1% of active chlorine (by iodimetric titration) and was 0.05 M in sodium hydroxide. It was stable for several weeks if kept in a refrigerator.

Molybdate reagent. Sodium molybdate (1 g; Na_2MoO_4) and 0.5 ml of the bismuth stock solution are added to 25 ml of 0.5 M sulfuric acid and diluted accurately to 50 ml with water. This reagent is stable. Ammonium molybdate was not employed so as to avoid interferences in the nitrogen determination.

Ascorbic acid solution (5%). This was prepared daily.

Samples and standards

Plant material was mineralized by wet digestion with sulfuric acid [9] in a Technicon BD 40 digestion block [10].

The standard stock solution is prepared by dissolving 6.288 g of ammonium sulfate and 0.585 g of potassium dihydrogenphosphate in water and diluting accurately to 1000 ml with water. This standard stock corresponds to 50% nitrogen and 5% phosphorus in the assayed plant material, with due attention to the amount of sample taken for digestion and subsequent dilution. Working standards are prepared by appropriate dilutions of this stock with a 4.4% (w/v) sulfuric acid solution, in order to obtain an acidity similar to that of the sample digests.

Methods

Nitrogen and phosphorus are determined in the same analytical path after the species to be injected each time has been selected by switching of

the proportional injector. The sample and reagent carrier streams are water, and only one detector, set at 630 nm, is employed.

Ammonia is determined by the indophenol blue method [11], the sequence of reagent addition being the same as in earlier work [12, 13]. The sample zone [14] meets the alkaline phenol reagent at point *y* (Fig. 1), the hypochlorite reagent is added at point *z*, and the Berthelot reaction proceeds in the following reaction coil. It must be emphasized that preliminary experiments indicated that addition of both reagents at the same point resulted in loss of reproducibility.

Phosphorus is determined by the molybdenum blue method [15]. The sample zone merges with the molybdate reagent zone at point *y* and the resulting yellow heteropolyacid is then reduced by ascorbic acid, added at point *z*, producing the blue compound which is measured.

Catalysis is used to adjust the measured signal to the conditions of dispersion and sampling rate defined. In the determination of phosphate bismuth is employed as catalyst, while sodium nitroprusside is used to speed up the Berthelot reaction.

System design

In order to accommodate both the nitrogen and phosphorus methods in the same analytical path, the system indicated in Fig. 1 was designed. The pumping rates, injected volumes and coil lengths defined allow a sampling rate of about 60 samples per hour to be achieved, associated with a high degree of sample dispersion.

High dispersion is necessary mainly to minimize the "schlieren pattern" effect [16] since all carrier streams are water and concentrated reagent solutions are introduced. When the "schlieren" effect decreases, both improved reproducibility and decreased blank values can be attained. In the case of the determination of phosphate, an increased degree of sample dispersion, leading to a decrease in the final acidity at the sample zone, favours the detection of the blue compound at 630 nm [15].

The lengths of the synchronization lines (16, 12 and 32 cm, Fig. 1) were adjusted according to the procedure already described [4]. Two sample carrier streams pumped at different rates are employed to provide initial dilution of the sample to be analysed for nitrogen.

For the Berthelot reaction, the effects of alkalinity, concentrations of catalyst and reagent composition were studied after the sample and reagents for phosphate analysis had been replaced by water.

RESULTS AND DISCUSSION

The use of high phenol concentrations (up to 10%) leads to loss of reproducibility, because of inadequate mixing conditions, whereas concentrations lower than 2% affect the linearity of the calibration graph. With the chosen phenol concentration of 3%, the concentration of sodium hypo-

chlorite reagent has little influence on the method. Variation of the concentration from 0.5% to 2.1% (expressed as percentage of free chlorine) in the hypochlorite reagent causes a change of about 20% in the measured signal, without affecting the linearity of the calibration graph. Any commercial domestic bleach solution containing around 2% of active chlorine and less than 10 ppm ammonia can therefore be employed.

In earlier work [8, 12], sodium tetraborate was used to improve the reproducibility, since the Berthelot reaction is pH-dependent [12, 17]. With the proposed configuration, however, the use of up to 5% sodium tetraborate in the hypochlorite reagent has no influence on the precision of the measurements. The use of tetraborate displaces the pH towards the optimum value for the development of the Berthelot reaction [17], slightly increasing the sensitivity. However, sensitivity is not an important feature for the development of this method and the addition of sodium tetraborate causes also a slight increase in the blank value, hence tetraborate was not used.

There is an almost linear relationship between measured signal and sodium nitroprusside concentration (Fig. 2). The sensitivity of the method cannot be adjusted at will, however, because the concentration of the catalyst affects the blank value (Fig. 2), the sodium nitroprusside solutions being strongly coloured. The following observations were made regarding the use of this reagent: (1) when sodium nitroprusside is not employed, no signal

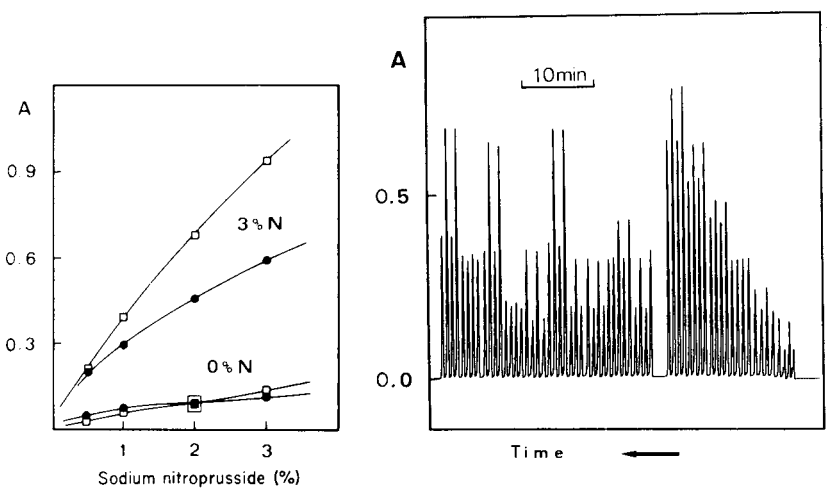

Fig. 2. Effects of sodium nitroprusside concentration and alkalinity. Squares are related to a 0.6 M sodium hydroxide concentration in the alkaline phenol reagent, and circles to a 2.0 M concentration.

Fig. 3. Routine run for nitrogen and phosphorus in 10 plant digests. The samples are preceded by mixed standard solutions (0.00% N + 0.00% P to 5.00% N + 0.50% P). The first collected peak corresponds to phosphorus. All measurements are performed in duplicate.

higher than the blank value is measured; (2) addition of sodium nitroprusside to the phenol alkaline reagent improves the mixing conditions of the phenol reagent in the flow injection system; (3) the characteristic smell of the phenol almost disappears; (4) as catalyst and stabilizer, sodium nitroprusside is better in this system than ethanol, which was used in earlier work [8, 12]; (5) when the method is to be employed continuously for more than 6 h, the nitroprusside reagent must be placed in a separate bottle, and its addition to the sample zone, together with the phenol alkaline reagent, will require an extra 2:3:2 commutation section in the proportional injector. For this method, a 1% sodium nitroprusside concentration was chosen.

The concentration of sodium hydroxide in the alkaline phenol reagent has a marked influence on the measured signal (Fig. 2). When this concentration is varied from 2.0 M to 0.6 M, the signal increases mainly because the final pH is displaced towards the optimal pH value [17]. Increase in alkalinity causes also a decoloration of the sodium nitroprusside with consequent decrease in blank value (Fig. 2). In cases of low concentrations of sodium nitroprusside, increase in alkalinity causes an increase in blank value because of the refractive index effect [18] with consequent loss of reproducibility. The sodium hydroxide concentration in the alkaline phenol reagent should be enough to neutralize the acidic sample zone and to provide a final alkalinity little affected by variations in sample acidity. For this reason, a 1 M sodium hydroxide concentration and a low ratio between sample and reagent dispersion factors were chosen.

The proposed system is characterized by dispersion factors of 0.026, 0.120 and 0.120 related to sample and reagents for nitrogen determination and 0.080 for the species injected for phosphorus determination, calculated according to the procedure already described [4]. The reagent consumptions are 150 μl of alkaline phenol reagent and sodium hypochlorite reagent, and 80 μl of molybdate reagent and ascorbic acid reagent, per determination; 60 samples (120 measurements) can be assayed per hour (Fig. 3). Precision of 98.3 and 99.1% was estimated after 20 measurements of a sample containing 3.2% N and 0.29% P in dry matter. Table 1 indicates the agreement of the results obtained with the proposed method and with other methods used in this Institute [10].

TABLE 1

Comparative results obtained with the proposed flow-injection method (F.i.a.) and with the AutoAnalyzer (AA) procedure [10]

Sample	% P in dry matter		% N in dry matter	
	F.i.a.	AA	F.i.a.	AA
1	0.22	0.21	0.45	0.50
2	0.28	0.29	2.05	2.15
3	0.21	0.22	0.50	0.55
4	0.08	0.08	2.45	2.75
5	0.42	0.42	2.25	2.25
6	0.21	0.21	2.65	2.75
7	0.44	0.47	2.10	2.10

Partial support of this project by CNPq (Conselho Nacional de Desenvolvimento Científico e Tecnológico) and FINEP (Financiadora de Estudos e Projetos) is greatly appreciated. The authors thank P. B. Vose for assistance in preparing the manuscript.

REFERENCES

1 H. Bergamin F°, E. A. G. Zagatto, B. F. Reis and F. J. Krug, Anal. Chim. Acta, 101 (1978) 17.
2 E. A. G. Zagatto, F. J. Krug, H. Bergamin F°, S. S. Jørgensen and B. F. Reis, Anal. Chim. Acta, 104 (1979) 279.
3 B. F. Reis, H. Bergamin F°, E. A. G. Zagatto and F. J. Krug, Anal. Chim. Acta, 107 (1979) 309.
4 E. A. G. Zagatto, B. F. Reis, H. Bergamin F° and F. J. Krug, Anal. Chim. Acta, 109 (1979) 45.
5 H. Bergamin F°, B. F. Reis, A. O. Jacintho and E. A. G. Zagatto, Anal. Chim. Acta, 117 (1980) 81.
6 J. Růžička and E. H. Hansen, Anal. Chim. Acta, 106 (1979) 207.
7 M. F. Giné, H. Bergamin F°, E. A. G. Zagatto and B. F. Reis, Anal. Chim. Acta, 114 (1980) 191.
8 J. W. B. Stewart and J. Růžička, Anal. Chim. Acta, 82 (1976) 137.
9 J. A. Parkinson and S. E. Allen, Commun. Soil Sci. Plant Anal., 6 (1975) 1.
10 Technicon AutoAnalyzer II. Industrial method no. 334-74 w/B, 1977.
11 M. P. E. Berthelot, Report de Chimie Appliqué, (1859) 284.
12 J. W. B. Stewart, J. Růžička, H. Bergamin F° and E. A. G. Zagatto, Anal. Chim. Acta, 81 (1976) 371.
13 U. Bohnstedt, Fresenius Z. Anal. Chem., 163 (1958) 415.
14 J. Růžička and E. H. Hansen, Anal. Chim. Acta, 78 (1975) 145.
15 J. A. Maxwell, Rock and Mineral Analysis, J. Wiley, New York, 1968, pp. 191—193.
16 F. J. Krug, H. Bergamin F°, E. A. G. Zagatto and S. S. Jørgensen, Analyst, 102 (1977) 503.
17 L. T. Mann, Jr., Anal. Chem., 35 (1963) 2179.
18 H. Bergamin F°, B. F. Reis and E. A. G. Zagatto, Anal. Chim. Acta, 97 (1978) 427.

Analytica Chimica Acta, 119 (1980) 313—321

SEMIAUTOMATED DETERMINATION OF TOTAL PHOSPHORUS AND TOTAL KJELDAHL NITROGEN IN SURFACE WATERS

JOAN CROWTHER,* BERNARD WRIGHT and WALTER WRIGHT

Laboratory Services Branch, Water Quality Section, Box 213, Rexdale, Ontario M9W 5LI (Canada)

(Received 3rd March 1980)

SUMMARY

Nitrogen by the Kjeldahl method (0.02—2.00 mg N l^{-1}) and phosphorus (0.001—0.200 mg P l^{-1}) are simultaneously determined on a single aliquot of sample. The procedure entails batch digestion via a block heater using the traditional Kjeldahl acid reagent followed by colorimetric measurements via an AutoAnalyzer system designed to handle very acidic samples (0.15—0.3 M sulphuric acid). The method was compared to a reference system involving hot plate digestion with manual neutralization and automated colorimetric measurements for N and P in surface waters. Nitrogen results by the new procedure averaged 0.01 mg N l^{-1} higher than the reference method while the average difference for phosphorus results was negligible.

As phosphorus and nitrogen are important nutrient parameters in environmental studies, there is a continuing search for more precise and productive analytical procedures. Jirka et al. [1] recently summarized the literature for total nutrients and described a semi-automated procedure that is suitable for waste waters. The object of the current study was to develop a comparable system for much lower levels of nitrogen and phosphorus in surface waters. Full scale for total phosphorus was to be 0.200 mg P l^{-1}, while that for nitrogen by the Kjeldahl method was to be 2.00 mg N l^{-1}. It was recognized that pH control would be the principal problem in designing this low-level system.

EXPERIMENTAL

Apparatus

A Technicon BD-40 block digester with a temperature control unit was used to digest 40 samples simultaneously. The sample containers for this step were pyrex test tubes (25 × 200 mm) graduated at 25 and 50 ml; each tube was fitted with a 25.4 mm O-ring which prevented the tubes from sliding through the 40-place test tube rack supplied by Technicon. The sides of the tube rack were shortened to 125 mm of which 5 mm was bent inwards at right angles to provide a stable seat for the rack when set on the bench or the top of the block digester. A few acid-washed boiling chips were

added to each sample tube to prevent bumping during digestion. The acid digestion mixture was added with a precalibrated pipet.

For automated sample neutralization and colorimetric measurements, a dual-channel AutoAnalyzer system was used consisting of a sampler (Large Industrial Model), peristaltic pump (Model III), constant temperature unit (157-B273-03), and two AAII colorimeters equipped with 50-mm flow cells; one colorimeter was fitted with 630-nm filters while the other had 880-nm filters. A two-pen chart recorder plus manifold tubing and glassware completed the assembly (Fig. 1).

To validate the proposed analytical system, a second analytical system was employed; samples were digested in Erlenmeyer flasks on hot plates and neutralized manually prior to automated colorimetric determinations via a second dual-channel AutoAnalyzer system.

Reagents

All chemicals were reagent grade and all solutions were prepared with deionized distilled water.

The acid digestion mixture was prepared in two steps. First, 2.0 g of mercury(II) oxide was dissolved in 20 ml of 20% (v/v) sulphuric acid; a second solution was prepared by carefully adding 200 ml of concentrated sulphuric in 600 ml of water, and then dissolving 134 g of potassium sulphate in this solution while it was still hot. These two solutions were then combined and diluted to 1 l after cooling. The mixture was stored above 20°C to prevent precipitation.

To maintain an acceptable baseline in the AutoAnalyzer system, a wash water solution containing 15 ml of concentrated sulphuric acid and 13.4 g of potassium sulphate per litre, was prepared. These reagent concentrations

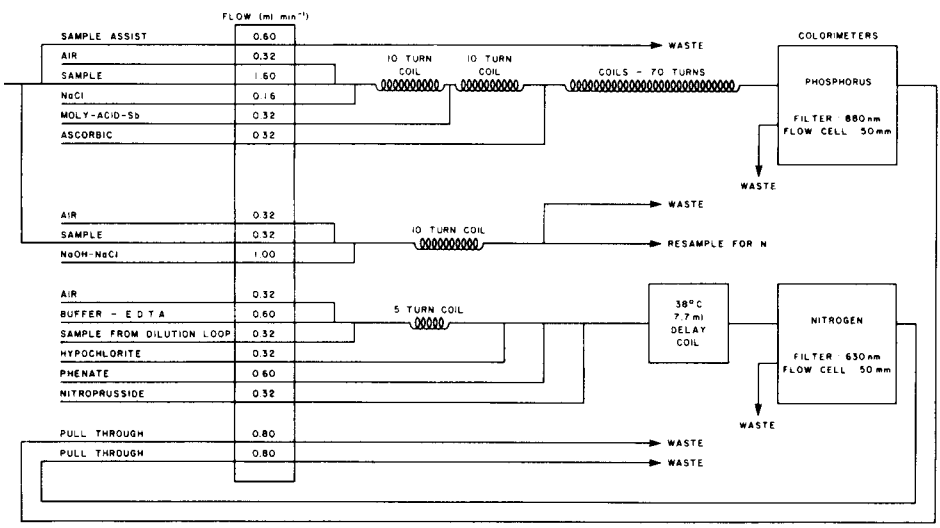

Fig. 1. Manifold for determination of phosphorus and nitrogen in surface waters.

approximated those developed in the sample during acid digestion with mercury(II) oxide being omitted from the wash water as its presence was both unnecessary and undesirable.

Total phosphorus colorimetry required three reagents. The molybdate reagent was prepared by dissolving and/or mixing with water in the following order: 12.0 g of ammonium molybdate tetrahydrate, 250 ml of 20% (v/v) sulphuric acid, and 0.25 g of antimony potassium tartrate semi-hydrate and diluting to 1 l with water. The other reagents were ascorbic acid (20 g l^{-1}) and sodium chloride (10 g l^{-1}).

Nitrogen colorimetry required five reagents. The reagent used to achieve partial neutralization of the sample and to complex mercury(II) contained 3.2 g of sodium hydroxide and 1.0 g of sodium chloride per litre. The buffer (pH 12.3) contained 167 g of dipotassium orthophosphate, 2.0 g of trisodium citrate, 40.4 g of sodium hydroxide, and 18.6 g of ethylenediaminetetraacetic acid, disodium salt, dihydrate (EDTA) per litre. The phenate reagent was prepared by dissolving in the following order 4.00 g of potassium hexacyanoferrate(II) trihydrate, 25 g of sodium hydroxide, and 50 ml of phenol stock solution per litre. The phenol stock was prepared by adding 35 ml of water to 500 g of phenol, warming until the phenol dissolved, and then mixing. The hypochlorite reagent (7% v/v) was prepared from commercial bleach (5.25% w/w available chlorine). The catalyst reagent was sodium nitroprusside dihydrate (0.4 g l^{-1}).

Recommended procedure

Up to forty samples were digested simultaneously. An unfiltered aliquot of well-mixed sample was transferred by wide-mouth volumetric pipet to a digestion test tube, and 2.5 ml of digestion acid were added via a precalibrated pipet. A few boiling chips were added, and the tube was placed in the specially adapted digestion tube rack. The batch of samples was then evaporated in the block digester set at 200°C. When the water from all the samples had been expelled, the rack of tubes was removed, and the temperature of the block digester was increased to 360°C; the samples were then heated at this temperature for 20 ± 1 min. After cooling, 25.0 ml of deionized distilled water was added to each tube and the contents were mixed via a vortex mixer. (Whenever carbon particulates were observed in a digested sample, it was discarded and another smaller aliquot of the sample was digested in a subsequent run.) The entire volume of digested sample was transferred to a small dry test tube suitable in size for the sampler of the AutoAnalyzer system.

The tubes of samples and standards were loaded into the sampler; a schematic flow diagram for the AutoAnalyzer system is shown in Fig. 1. The system was calibrated with combined undigested ammonium chloride and potassium dihydrogenorthophosphate standards which had been spiked with potassium sulphate (13.4 g l^{-1}) and sulphuric acid (1.5% v/v); the concentrations of these spikes approximated the levels found in digested samples.

By calibrating the AutoAnalyzer system with undigested standards, the data for digested standards (solutions containing glycine and tetrasodium pyrophosphate) served as a recovery check on the whole system. Samples were processed at the rate of 24 h^{-1}.

RESULTS AND DISCUSSION

Development of digestion procedure

Basically, the digestion procedure involved adding acid digestion mixture to an aliquot of sample in a 25 × 200 mm test tube, boiling off most of the water at a block temperature of 200°C, and then fuming the mixture at 360°C to complete the conversion of phosphorus and trivalent nitrogen compounds to orthophosphate and ammonium ions respectively.

The composition of the selected acid digestion mixture was identical to that recommended for organic nitrogen by the Kjeldahl method in Standard Methods for the Examination of Water and Wastewater [2]; this mixture was used by Jirka et al. [1] for determining both phosphorus and nitrogen via a Technicon block digester. The acid mixture contained sulphuric acid, mercury(II) oxide, and potassium sulphate. In selecting the volume ratio of sample to digestion mixture, a large volume of sample was desirable for maintaining test precision while a small volume of acid mixture would reduce neutralization problems in the AutoAnalyzer system. The maximum acceptable aliquot of sample was 25.0 ml, as larger volumes tended to boil over during initial evaporation at a block temperature of 200°C. The selected volume of acid mixture was 2.5 ml. When the volume was less than 2.0 ml, the residual volume after evaporation was so small that splattering occurred and the precision of the test was adversely affected; 2.0 ml was acceptable, and 2.5 ml was selected to provide a safety factor.

The time required to evaporate the water from the sample—acid mixtures was approximately 1 h but the sample tubes could be left in the block heater at 200°C for at least 2 h without affecting the final results. Then the mixtures were fumed at a block temperature of 360 ± 5°C. Heating periods of 15, 20 and 30 min produced acceptable results in terms of precision and recovery; the 20-min period was selected. The data from this phase of the study showed that increasing the fuming period significantly reduced the acid level in the digested samples but it also reduced the precision of the test. Furthermore, the precision of the test was decreased if the sample tubes were left in the block while the block temperature was increased from 200°C to 360°C. When only one block digester is available, the dilution tubes must be removed after boiling down at 200°C, and not returned to the block until the temperature of the block is 360°C. Although the acid—sample residuals solidified when removed from the block and cooled to room temperature, the mixtures liquified as soon as they were returned to the block at 360°C, and no adverse effects were noted in the resultant data.

After cooling, the residual in the digestion tube was dissolved in 25.0 ml of deionized distilled water and mixed using a vortex mixer. The digested sample was then transferred to an appropriate dry test tube.

Development of AutoAnalyzer system

This phase of the study was dominated by acidity considerations. An AutoAnalyzer system had to be designed that could generate accurate low-level phosphorus and nitrogen data in spite of the fact that the digested samples contained large and variable quantities of acid. Prior to heating, the sulphuric acid concentration of a sample—digest mixture was 0.39 M, and approximately one quarter of this acid was lost during digestion according to titration data.

The phosphorus channel was based on the procedure developed by Murphy and Riley [3] for the determination of orthophosphate; all phosphorus compounds were converted to orthophosphate during digestion. As this colorimetry entailed the formation of a blue complex in acidic media, there was no point in neutralizing the digested sample and then reacidifying. Accordingly, acid control for the phosphorus channel was obtained by adjusting the sulphuric acid concentration in the molybdate—antimony—sulphuric acid reagent. The selected concentration of sulphuric acid in this reagent is 42% of the level required for determining orthophosphate on a neutral sample via the subject manifold. The basic orthophosphate procedure was also modified by including a sodium chloride reagent to complex the mercury(II) ions present in all digested samples. Lastly, the delay between the addition of the reducing agent, ascorbic acid, and absorbance measurement proved both necessary and sufficient. If, however, room temperature fluctuates or drops below 20°C, the 70 turns of mixing coils following the addition of ascorbic acid reagent should be replaced by a 38°C heating bath (7.7 ml delay) and one mixing coil (20 turns).

To test the ruggedness of the proposed total phosphorus manifold, blanks and 0.100 mg P l^{-1} standards (25.0 ml) were digested with varying volumes (1.5—3.0 ml) of the acid digestion mixture. In spite of the wide range of acidity in these digested samples (0.15—0.3 M sulphuric acid), the average recovery of orthophosphate and pyrophosphate was 0.0998 mg P l^{-1} (standard deviation = 0.0010 mg P l^{-1} where n = 8) and the average blank value was —0.0003 mg P l^{-1} (standard deviation = 0.0006 mg P l^{-1} where n = 4).

The nitrogen channel was based on a procedure for determining ammonia by formation of indophenol blue in solutions buffered to pH 12.3. For this channel, the pH of the digested samples was adjusted to 12.3 in two stages. First, the digested sample was mixed with a diluent (0.32 + 1.00 dilution loop) containing both sodium hydroxide (to reduce the acidity in the digested sample to about pH 1.5) and sodium chloride (to complex mercury(II) ions). Second, the pH was raised to 12.3 by mixing with a phosphate buffer containing EDTA. This two-step program was required because metal hydroxides in the sample matrix precipitated when the pH was raised to 12.3 in the

absence of EDTA. If, however, the pH of the highly acidic digested sample was adjusted to 12.3 in the presence of EDTA, a small fraction of the latter hydrolyzed to ammonia producing erroneous data. By partially neutralizing the digested sample to pH 1.5, the sample stream remained sufficiently acidic to prevent the precipitation of metal ions but its capacity to hydrolyze EDTA had been eliminated. Sodium citrate (2.0 g l^{-1}) was included in the buffer reagent as the resultant solution seemed cleaner.

To test the nitrogen procedure, ammonium chloride and glycine standards (1.00 mg N l^{-1}) were digested using 1.5—3.0 ml of acid digest mixture. The average recovery was 0.991 mg N l^{-1} (standard deviation = 0.0084 where n = 8). The average digested blank was 0.0125 mg N l^{-1} (standard deviation = 0.0050 mg N l^{-1} where n = 4).

Evaluation of proposed procedure

Calibration. Mixed ammonium chloride and potassium orthophosphate standards were digested and processed according to the proposed procedure. Full scale values for the ranges calibrated were 2.00 mg N l^{-1} and 0.200 mg P l^{-1}. The two ends of the calibrated ranges were tested at concentration intervals of 2% full scale while the central range was tested at 5% intervals. Each calibration included 33 points and was linear within the expected experimental error. For nitrogen, the Y on X linear regression (where X pertained to the theoretical concentrations) showed a slope of 0.9796 (standard deviation = 0.0036), an intercept of 0.0089 mg N l^{-1} (standard deviation = 0.0044 mg N l^{-1}), and the standard error of estimate was 0.0002. The comparable linear regression for phosphorus showed a slope of 0.9899 (standard deviation = 0.0033), an intercept of 0.0002 mg P l^{-1} (standard deviation = 0.0004 mg P l^{-1}) and the standard error of estimate was 0.0000.

Precision. Precision for the two nutrient parameters was obtained by analyzing routine samples of surface waters in duplicate, and calculating the mean standard deviations for three sample concentration ranges. The results, given in Table 1, were considered satisfactory for a routine laboratory procedure. The data for the lowest sample concentration range (0—20% full scale) was used to calculate detection criteria (1.645 × standard deviation): 0.025 mg N l^{-1} and 0.0013 mg P l^{-1}.

Interferences. Common anions and cations were tested as potential interferences (Table 2). No problems were encountered. The proposed phosphorus procedure has considerable tolerance for cations because the sample remains acidic throughout the test procedure. For nitrogen, there was no evidence of interference from cations; evidently the two-step neutralization technique proved effective.

Intercomparison. To complete the evaluation of the proposed procedure, approximately 200 routine samples were processed; these samples of surface waters were collected from sources throughout central and southern Ontario. Simultaneously, these same samples were processed by a procedure that had proven acceptable in this laboratory. For the latter, aliquots of samples were

TABLE 1

Precision for duplicate determinations in surface water samples

Nitrogen			Phosphorus		
Sample concn. range (mg N l^{-1})	No. of samples	Mean s.d. (mg N l^{-1})	Sample concn. range (mg P l^{-1})	No. of samples	Mean s.d. (mg P l^{-1})
<0.4	24	0.015	<0.04	31	0.0008
0.4—1.0	32	0.017	0.04—0.10	14	0.0024
1.0—2.0	13	0.026	0.10—0.20	7	0.0022

TABLE 2

Study of potential interferences

Potential interference		Recovery of digested standards[a]	
Parameter	Concn. (mg l^{-1})	Nitrogen (mg l^{-1})	Phosphorus (mg l^{-1})
Aluminium(III)	1.0	0.96	0.098
Calcium(II)	200	1.02	0.098
Chromium(VI)	1.0	1.01	0.098
	5.0	0.94	0.104
Cobalt(II)	1.0	0.96	0.098
Copper(II)	1.0	1.00	0.101
Iron(II)	100	1.01	0.100
Iron(III)	100	0.98	0.098
Lead(II)	1.0	0.97	0.099
Magnesium(II)	50	0.99	0.099
Manganese(II)	1.0	0.97	0.096
Manganese(VII)	1.0	0.96	0.098
Nickel(II)	1.0	0.99	0.100
Tin(II)	1.0	0.98	0.099
Zinc(II)	1.0	1.04	0.100
Carbonate as $CaCO_3$	500	0.98	0.096
Chloride	1000	1.00	0.098
	20000	0.78	0.039
Fluoride	1.0	1.00	0.101
Nitrate as N	1.0	0.98	0.098
Nitrite as N	1.0	0.98	0.100
Silicate as Si	5.0	0.97	0.098
Sulphate	250	1.00	0.098

[a]Theoretical concentrations of nitrogen and phosphorus were 1.00 mg N l^{-1} and 0.100 mg P l^{-1}, respectively.

digested on hot plates using a sulphuric acid—potassium persulphate mixture and manually titrated to the methyl red end-point as described by Julian and Kroner [4]. Determinations of nitrogen and phosphorus were completed by a dual-channel AutoAnalyzer system; the colorimetry for the former channel was similar to that described herein, while the colorimetry for the total phosphorus channel utilized tin(II) chloride as the reducing agent for the molybdophosphoric acid complex. In the following paragraph, this alternative procedure is designated the reference system. The results are summarized in Table 3.

For nitrogen, the data generated by the proposed procedure were higher than those for the reference system by an average of 0.015 mg N l^{-1}. Linear regression analysis showed a slope of 1.012 (standard deviation = 0.0055) and an intercept of 0.010 mg N l^{-1} (standard deviation = 0.0037 mg l^{-1}). The standard error of estimate was 0.0008.

For phosphorus, linear regression analysis indicated that the slope was 1.0259 (standard deviation = 0.0055) and the intercept was 0.0012 mg P l^{-1} (standard deviation = 0.0003 mg l^{-1}). The standard error of estimate was 0.0000. When the data were examined for bias, it was found that the proposed procedure recovered slightly more phosphorus (an average of 0.003 mg P l^{-1}) when the phosphorus concentration in the samples ranged from 0.100 to 0.200 mg P l^{-1}. For some samples, the proposed procedure generated more accurate data because the cations in the sample matrix are kept in solution by maintaining acid conditions (<pH 1) throughout the determination. To illustrate, the chart recorder peaks for five samples were

TABLE 3

Comparative performance of proposed and reference procedures for total nutrients as applied to surface waters

Statistical parameter	Nitrogen	Phosphorus
Linear regression (Y on X)[a]		
No. samples	174	182
Slope and s.d.	1.0122 (0.0055)	1.0259 (0.0055)
Intercept and s.d. (mg l^{-1})	0.0102 (0.0037)	−0.0012 (0.0003)
Std. error of estimate	0.0008	0.0000
Bias associated with nutrient concn. level (Y-X)[b]		
0—20% No. samples	78	127
Ave difference and s.d. (mg l^{-1})	0.009 (0.016)	−0.0005 (0.0021)
20—50% No. samples	72	36
Av. difference and s.d. (mg l^{-1})	0.019 (0.021)	−0.0006 (0.0027)
50—100% No. samples	24	19
Av. difference and s.d. (mg l^{-1})	0.025 (0.025)	0.003 (0.013)
0—100% No. samples	174	182
Av. difference and s.d. (mg l^{-1})	0.015 (0.021)	−0.0002 (0.0037)

[a] *Y* refers to the proposed analytical system.
[b] Full-scale values for nitrogen and phosphorus were 2.00 and 0.200 mg l^{-1} respectively.

badly deformed with jagged edges when phosphorus was determined by the reference procedure, but well formed when phosphorus was determined by the proposed method.

Thus the increased productivity associated with the proposed system was attained without significant loss in accuracy or precision.

REFERENCES

1 A. M. Jirka, M. J. Carter, D. May and F. D. Fuller, Environ. Sci. Technol., 10 (1976) 1038.
2 Standard Methods for the Examination of Water and Wastewater, 14th edn., American Public Health Association, Washington, DC, 1975, p. 438.
3 J. Murphy and J. P. Riley, Anal. Chim. Acta, 27 (1963) 31.
4 E. C. Julian and R. C. Kroner, Automation in Analytical Chemistry, Vol. 1, Technicon Symposium, 1966, Mediad, White Plains, New York, 1967, p. 542.

Analytica Chimica Acta, 119 (1980) 323—330

A SEMI-AUTOMATED METHOD FOR THE DETERMINATION OF TOTAL ARSENIC AND SELENIUM IN SOILS AND SEDIMENTS

HAIG AGEMIAN* and E. BEDEK

Canada Centre for Inland Waters, Special Services Section, Water Quality Branch, 867 Lakeshore Road, P.O. Box 5050, Burlington, Ontario (Canada)

(Received 7th March 1980)

SUMMARY

Acid digestion with nitric, perchloric and hydrofluoric acids under oxidizing conditions with addition of permanganate and persulfate is utilized to extract inorganic and organic forms of arsenic and selenium from all phases of sediments including the silicate lattice. After sample dissolution a completely automated system is used to reduce arsenic and selenium to their corresponding hydrides and determine them by quartz-tube atomic absorption spectrometry. The method is directly applicable to batch routine analysis of large numbers of environmental samples.

A current study of the presence of arsenic and selenium in sediments required an analytical method that would simultaneously extract the total amount of both elements from sediments and soils. In addition, the method had to be adaptable and applicable to the batch determination of a large number of samples for routine monitoring purposes. Thus the integration of automated steps in the method would be a definite asset, since it would aid in the speed, accuracy and reproducibility of the determinations.

A survey of the literature showed that although many methods have been published in the determination of either element separately, none satisfies the above requirements. Several acid mixtures have been used to extract these elements from sediments and soils. A mixture of nitric and sulfuric acids has been used for arsenic in soils [1] and in particulate matter [2]. Aqua regia has also been used for arsenic in geological materials [3] and sediments [4]. These methods do not give total extraction of arsenic and furthermore are not applicable to selenium because the mixtures are not oxidizing enough to keep it in solution. Mixtures of perchloric and nitric acid are sufficiently oxidizing and are applicable to both selenium [5, 6] and arsenic [4, 7] in sediments and soils, but they do not dissolve the silicates and thus would not satisfy the criterion for total extraction of the two elements from such samples.

Hydrofluoric acid has been used in combination with other acids to dissolve silicates and liberate arsenic [3, 8—10] and selenium [10]. When hydrofluoric acid is used, it is important that the chemical environment be made oxidizing, otherwise volatilization losses of both arsenic and sele-

nium result. Bajo [10] reported that both elements could be satisfactorily extracted without any volatilization losses when perchloric acid was present at the hydrofluoric acid digestion step. It was reported that As(V), Se(IV) and Se(VI) were all nonvolatile under the $HClO_4$—HF digestion conditions. However As(III), if not oxidized to As(V) prior to this digestion, would be lost since its volatilization is more rapid than its oxidation by perchloric acid. The loss of As(III) was confirmed in this laboratory: when the recommended method was used, 100% recoveries of As(V), Se(IV) and Se(VI) were obtained, but only about 40% As(III) was recovered. Terashima [9] reported that losses of arsenic were prevented when permanganate was present during the hydrofluoric acid digestion.

In the method proposed here, digestion with a nitric—perchloric acid mixture is used followed by digestion with hydrofluoric acid in the presence of permanganate and persulfate. It is shown that both inorganic species of arsenic and selenium are recovered without any losses. Furthermore, it is shown that unlike previous methods, this method liberates arsenic and selenium from organic complexes. This is very important since soils and sediments commonly have large amounts or organic matter and substantial fractions of these elements may be complexes. In the usual reduction—atomic absorption detection systems, any undecomposed organic species could not be quantitatively determined. In the proposed method, an automated tetrahydroborate reduction system is adapted to the above digestion procedure.

The automated system includes a prereduction step to reduce As(V) and Se(VI) to As(III) and Se(IV), respectively, prior to tetrahydroborate reduction. This is very important, since the rates of reduction of the two inorganic species are not similar and therefore nonquantitative determination would result for mixtures of the species. The conditions for the recommended manifold are similar for both elements. This makes it possible to determine both elements simultaneously if a dual-channel atomic absorption spectrometer is available.

EXPERIMENTAL

Apparatus

The equipment needed for the sample digestions includes 250-ml teflon beakers, a hot plate capable of heating perchloric acid to the boiling point and an asbestos sheet to be placed on top of the hot plate to protect the beakers during heating.

The equipment used in the automated tetrahydroborate reduction—atomic absorption system is shown in Fig. 1 and comprises the following items: Technicon AutoAnalyzer II sampler with 40-1/2 cam; proportioning pump (AutoAnalyzer II); Technicon AutoAnalyzer mixing coils and tubing of specified dimensions; Technicon heating bath with 12-m time delay coil set at 95 ± 5°C; flowmeter for argon (150 ml min^{-1}); stripping column and wash column [11]; furnace made from silica tubing (1 cm i.d., 10 cm long).

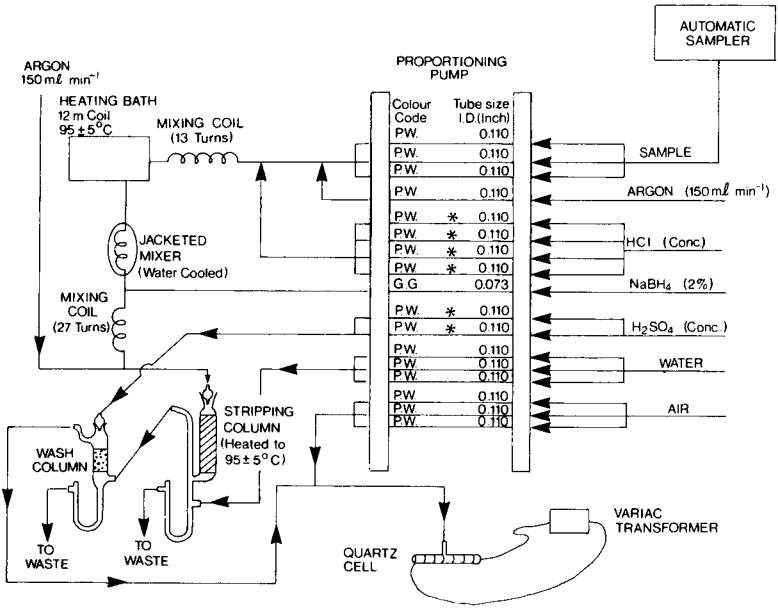

Fig. 1. Manifold for the simultaneous determination of arsenic and selenium. Asterisks indicate Acidflex tubing.

At the center of this tube a T-joint is made with silica tubing (2 mm i.d.) for the gas entry port. The furnace is wrapped with asbestos paper and chromel wire (22-gauge; resistance, 20Ω). Silica tubing mounted close to the furnace contains a pyrometer; the furnace is heated to 800°C through a Variac transformer. The Perkin-Elmer Model 503 atomic absorption spectrometer used was equipped with EDL lamps and a power supply and recorder (Hewlett-Packard Model 7128A).

Reagents

High-purity certified reagents were used for all analyses (Fisher Scientific Company): nitric acid, 16 M; perchloric acid, 60%; hydrofluoric acid, 49%; hydrochloric acid, 12 M; sulfuric acid, 18 M; potassium persulfate, 2% (w/v) (prepare daily); potassium permanganate solution, 2% (w/v) (prepare weekly); sodium tetrahydroborate solution, 2% (w/v) in 1 M sodium hydroxide (the solution should be filtered through 0.45 μm filter paper; if stored at 4°C, it is stable for 1 week).

The different inorganic and organic species of arsenic and selenium used were: arsenic trioxide, arsenic pentoxide, sodium arsenite, sodium monohydrogenarsenate, heptahydrate sodium selenite, sodium selenate (all from Ventron Corp., Alfa Products); cacodylic acid, phenylarsonic acid and selenourea (ICN Pharmaceutical, Life Sciences Group (K&K), Cleveland, OH); *p*-arsanilic acid, phenylarsenic oxide and triphenylarsonic oxide (Eastman Kodak Co., Rochester, NY); and seleno-D,L-cystine and seleno-D,L-methionine (Sigma Chemicals Co., St. Louis MO).

Procedure for sample dissolution

Weigh out about 1 g of air-dried homogenized sample into a clean 250-ml teflon beaker. Sample sizes of 0.1—2 g may be successfully digested by this method. Add 10 ml of nitric acid and leave for a few minutes until any visible reaction ceases. Add 10 ml of perchloric acid and heat on a hot plate which is covered with a layer of asbestos paper. Keep heating until all the nitric acid boils off and white fumes of perchloric acid are apparent. Continue until 2—3 ml of perchloric acid remain. If the sample remains dark in color, repeat the perchloric acid step. If the sediment is gray or white, remove from the heat and cool.

Add 5 ml of the permanganate solution, leave for 5 min, add 5 ml of the persulfate solution and return to the hot plate. Heat for about 2 min and then add 10 ml of hydrofluoric acid. Continue heating until only 2—3 ml of solution remains, always insuring that the purple color of the solution is maintained. (If the solution goes brown or colorless, immediately add further amounts of permanganate solution, 1 ml at a time, to maintain the purple color.) At this point, 90—100% of the sample should have dissolved. In the case of resistant samples, another 10-ml addition of hydrofluoric acid may be necessary.

Add 10 ml of (1 + 1) hydrochloric acid to the dissolved residue and heat for 1 min but do not boil. Remove from the heat, and transfer the contents of the beaker quantitatively to a 100-ml volumetric flask. Wash the teflon beaker with distilled—deionized water and transfer to the flask. Make up to volume and shake well until the solution clears and is homogeneous. If some residue remains, this may be easily filtered before analysis by the automated system.

Automated manifold for arsenic and selenium

Agemian and Cheam [11] reported an automated system for the determination of inorganic As(III) and As(V) in sample extracts. The manifold shown in Fig. 1 is a modification of the earlier one to make it suitable for both arsenic and selenium determinations; however, there are several essential differences. First, selenium(VI) does not readily react with tetrahydroborate to form selenium hydride and must first be reduced to selenium(IV); this necessitates a much larger amount of hydrochloric acid with elevated temperatures (95°C). An increased number of hydrochloric lines and a heating bath are used to provide correct conditions. The increased acid content and the increased temperature have no effect on the arsenic signal. Secondly, the stripping column selected earlier [11] did not require elevated temperatures to liberate arsenic hydride from solution since it is sufficiently volatile. This is, however, not true for selenium hydride, which requires elevated temperatures to remove it from the aqueous solution. This modification also has no effect on the arsenic signal.

The system as shown in Fig. 1 meets the requirements for simultaneous determination of both species of the two elements. By the inclusion of the

automated hydrochloric acid prereduction step, the system removes the need for manual boiling with hydrochloric acid before analysis, as is often done in conventional methods.

RESULTS AND DISCUSSION

Pyen and Fishman [12] reported an automated manifold for the determination of selenium. The method utilizes a reduction step with tin(II) chloride and potassium iodide to reduce Se(VI) to Se(IV) prior to the hydride formation with tetrahydroborate. The manifold requires two heating baths, one for each step. The automated system in Fig. 1 is an improvement, because it is shown that the $SnCl_2$/KI reduction is not needed and that under the conditions recommended, only one heating bath is required. This simplified manifold is applicable to both arsenic and selenium determinations.

The digestion method recommended is designed to extract all forms of the required elements including adsorbed, complexed and precipitated forms as well as those in the silicate lattice. It further oxidizes any organically bound forms of the elements to inorganic states. Complete oxidation of the species is important because of the following aspects. Braman et al. [13] showed that some simple organoarsenic compounds such as methylarsonic acid and dimethylarsenic acid may be reduced directly by tetrahydroborate to their corresponding methylated hydrides. However, the reduction conditions had to be closely controlled by buffering at pH 3.5—4.0 and some interfering cations had to be removed by a cation-exchange column. Such a direct reduction scheme is clearly not practical for the system proposed here, because the sediment extracts have much higher acidity and ionic strength than water samples and so would require extensive buffering and cation-exchange. In the present work, an automated manifold was successfully developed for the direct reduction of methylarsonic acid and dimethylarsonic acid, but those conditions did not work for phenylarsonic acid or any more stable complex organoarsenic compounds. Furthermore, the automated manifold required in this study was one which would be applicable to both arsenic and selenium, and it seemed unlikely that direct reduction would be applicable to selenium species. Since direct tetrahydroborate reduction of all the environmental species required for both metals was not possible, it was necessary to oxidize all species to their inorganic forms, As(III), As(V), Se(IV), Se(VI). The system is then capable of determining either oxidation state.

Terashima [9] showed that the simple perchloric acid—nitric acid digestion does not completely decompose sample types such as clay, feldspar, quartz and basalt as shown by the low recoveries of arsenic. Table 1 shows results obtained by the simple digestion method compared to the recommended method for several sample types; it is apparent that for both arsenic and selenium extraction is incomplete. Therefore the hydrofluoric acid digestion step is required to liberate metals trapped in the silicate lattice. The data in

TABLE 1

Comparison of methods for the extraction of arsenic and selenium from sediments

Sediment	Arsenic recovered ($\mu g\ g^{-1}$)[a]				Selenium recovered ($\mu g\ g^{-1}$)[a]	
	A	B	C	D	A	B
Lake Ontario	20	27	22	23	1.0	1.10
Lake Superior	24	30	29	29	0.69	0.96
Lake Erie	15	19	16	19	0.72	1.07
Lake Superior	4	6	4	6	0.18	0.25
Lake Ontario	22	25	26	27	0.81	1.08

[a]A, $HClO_4$—HNO_3 digestion; B, present method; C, fusion with 0.1 g MgO—1 g KOH at 550°C; D, neutron activation.

Table 1 also show that the recoveries for arsenic by the proposed method are similar to those obtained by neutron activation and by fusion decomposition followed by atomic absorption spectrometry.

In the recommended method, the initial digestion with nitric and perchloric acids is designed to oxidize and extract most forms of the two elements and dehydrate the silicates. However, it does not completely dissolve the silicates and does not oxidize all organically bound forms. The second step involves a hydrofluoric acid digestion, which dissolves silicates and liberates any trapped arsenic and selenium species. As discussed earlier, the presence of perchloric acid at this stage does not provide sufficient oxidizing power, hence permanganate and persulfate are necessary. Terashima [9] showed that permanganate was successful for arsenic only, and no recovery studies were done for organic compounds.

It was found that permanganate was successful in oxidizing both elements to their higher oxidation states before volatilization losses occurred with hydrofluoric acid. Furthermore, although some organic compounds were successfully decomposed, the method failed to give good recoveries of arsenic from cacodylic acid and phenylarsenic oxide. Agemian and Cheam [11] showed that persulfate successfully oxidizes these compounds. Although persulfate is advantageous in this respect, permanganate remains useful since its purple color serves as an indicator so that an oxidizing environment in the solution can be insured.

Several interference studies [14—16] have been reported for tetrahydroborate reduction systems. Strong oxidants such as permanganate, persulfate and nitric acid obviously interfere and must be removed. The nitric acid is easily boiled off in the presence of perchloric acid. Cold dilute perchloric acid has no oxidizing properties and does not interfere. This was confirmed by analyzing solutions of arsenic and selenium containing varying amounts of perchloric acid in the recommended system (Fig. 1); when the solutions contained up to 20%(v/v) of 60% perchloric acid, neither the arsenic nor the selenium signals were affected.

The permanganate and persulfate remaining in solution after completion of the digestion, must be reduced to prevent their interference [14—16] on the determinations. Permanganate not only interferes with the tetrahydroborate reduction, but decomposes to manganese dioxide which adheres firmly to the inner wall of the digestion beaker; therefore the reducing agent must be added directly to the beaker. Agemian and Chau [17] studied different reductants for a similar purpose in the determination of mercury in sediments, and found hydroxylammonium sulfate most advantageous. In this study hydrochloric acid was found to produce similar satisfactory results in the arsenic and selenium determinations.

Since aquatic sediments, unlike rocks, may contain large amounts of organically bound elements, it was necessary to perform spiking experiments and determine the efficiency of the method for such species. The recoveries for arsenic from methylarsenic acid, cacodylic acid, *p*-arsanilic acid, phenylarsenic oxide, benzenearsonic acid and triphenylarsenic oxide were in the range of 95 ± 12%. Those for selenium from selenourea, selenomethionine and selenocystine were in the range of 96 ± 10%.

It has been shown [3, 9] that good recoveries of arsenic from certified rock standards are obtained after digestion with a mixture of perchloric, nitric and hydrofluoric acids but these studies are not necessarily valid for soils and sediments. Table 2 shows recoveries of arsenic and selenium from various soil or sediment standards which are certified or are currently being certified. The data demonstrate that the proposed method is effective in recovering the analytes from organic phases as well as inorganic phases of soils and sediments.

The global average levels of arsenic and selenium in soils and sediments are 5 $\mu g\ g^{-1}$ and 0.01 $\mu g\ g^{-1}$ with a normal range of 1—50 $\mu g\ g^{-1}$ and 0.1—2 $\mu g\ g^{-1}$, respectively [18]. The precision of the method was therefore deter-

TABLE 2

Recovery of arsenic and selenium from soil and sediment standards

Sample[a]	Arsenic content ($\mu g\ g^{-1}$)		Selenium content ($\mu g\ g^{-1}$)	
	Certified level	Recommended method	Certified level	Recommended method
N.B.S.(S.R.M. 1645)	66[b]	66	—	—
I.A.E.A.(Soil-5)	93.9 ± 7.5	100	—	—
SO—1	1.9(σ=0.3)[b]	1.7	0.1[b]	0.09
SO—2	1.2(σ=0.2)[b]	1.1	0.3[b]	0.04
SO—3	2.6(σ = 0.2)[b]	2.5	0.05[b]	0.05
SO—4	7.1(σ = 0.7)[b]	7.7	0.4[b]	0.47

[a]N.B.S. — National Bureau of Standards, U.S.A.; I.A.E.A. — International Atomic Energy Agency, Vienna, Austria; SO — Soils prepared by the Canada Centre for Mineral and Energy Technology (CANMET).
[b]Tentative value.

mined at three different levels in the above ranges by the use of ten replicate determinations of three different sediments of types normally analysed in this laboratory. Arsenic determined at levels of 1.19, 6.56 and 17.7 $\mu g\ g^{-1}$ gave relative standard deviations of 5, 3.1 and 3.6%, respectively. Selenium at levels of 0.6, 0.86 and 1.11 $\mu g\ g^{-1}$ gave relative standard deviations of 5, 6.9 and 2.7%.

The recommended method is thus shown to be applicable to the routine semi-automated total determination of a large number of soils or sediments with good precision and recovery of arsenic and selenium.

REFERENCES

1 A. J. Thompson and P. A. Thoresby, Analyst, 102 (1977) 9.
2 P. N. Vijan and G. R. Wood, At. Absorpt. Newsl., 13 (1974) 33.
3 G. E. M. Aslin, J. Geochem. Explor., 6 (1976) 321.
4 I. Ruběska and V. Hlavinková, At. Absorpt. Newsl., 18 (1979) 5.
5 J. Azad, G. F. Kirkbright and R. D. Snock, Analyst, 104 (1979) 232.
6 J. H. Wiersma and G. F. Lee, Environ. Sci. Technol., 5 (1971) 1203.
7 P. N. Vijan, A. C. Rayner, D. Sturgis and G. R. Wood, Anal. Chim. Acta, 82 (1976) 329.
8 C. Feldman, Anal. Chem., 49 (1977) 825.
9 S. Terashima, Anal. Chim. Acta, 86 (1976) 43.
10 S. Bajo, Anal. Chem., 50 (1978) 649.
11 H. Agemian and V. Cheam, Anal. Chim. Acta, 101 (1978) 193.
12 G. Pyen and M. Fishman, At. Absorpt. Newsl., 17 (1978) 47.
13 R. S. Braman, D. L. Johnson, C. C. Foreback, J. M. Ammons and J. L. Bricker, Anal. Chem., 49 (1977) 621.
14 F. D. Pierce and H. R. Brown, Anal. Chem., 48 (1976) 693.
15 F. D. Pierce and H. R. Brown, Anal. Chem., 49 (1977) 1417.
16 H. K. Kang and J. L. Valentine, Anal. Chem., 49 (1977) 1829.
17 H. Agemian and A. S. Y. Chau, Anal. Chim. Acta, 75 (1975) 297.
18 H. E. Hawkes and J. S. Webb, Geochemistry in Mineral Exploration, Harper and Row, New York, 1962.

Analytica Chimica Acta, 119 (1980) 331—340

THE DETERMINATION OF ARSENIC BY ELECTROTHERMAL ATOMIC ABSORPTION SPECTROMETRY WITH A GRAPHITE FURNACE
Part 1. Difficulties in the Direct Determination

D. CHAKRABORTI, W. DE JONGHE and F. ADAMS*

Department of Chemistry, University of Antwerp (UIA), B-2610 Wilrijk (Belgium)

(Received 18th March 1980)

SUMMARY

The direct determination of arsenic by graphite-furnace atomic absorption spectrometry is critically examined. Matrix stabilization by nickel salts is effective for preventing charring losses of arsenic, but cannot eliminate strong interferences. Direct analysis of environmental and biological samples is impossible because of the presence of aluminium, sodium, potassium and sulphates.

An overall survey of the literature on the determination of arsenic by atomic absorption spectrometry shows that the determination is difficult and often unreliable. In flame atomic absorption spectrometry, the difficulties are largely due to the extremely high absorption of flame gases at wavelengths below 200 nm, where the most sensitive resonance lines of arsenic are located. Moreover, chemical interferences may occur when cool flames are used; further, arsenic can easily give rise to molecular forms with a severe loss in sensitivity [1]. Although the use of a separated nitrous oxide—acetylene flame overcomes many interferences [2], the sensitivity remains poor [3].

To increase the range of applicability, other atomizers have been proposed, such as the long-tube absorption cell with argon, helium or nitrogen/air—hydrogen flames. These systems provide an increased sensitivity, but suffer from multiple interferences [4]. Moreover, the effect of valence state on the determination of arsenic may also give rise to problems [5]. To circumvent these difficulties, the technique of conversion of arsenic to arsine and its subsequent introduction into the argon—hydrogen flame has been widely studied [6—8]. In this way many interferences are eliminated and detection limits are improved, but background absorption remains a serious problem.

Numerous workers have also applied the hydride technique, with various modifications, in combination with flameless atomization [9—19]. This method is also not beyond criticism [1, 20, 21], as a result of suppression effects by several cations and anions, decomposition of arsine at room temperature and other interferences. The general verdict on hydride genera-

tion techniques seems to be that the method is slow and subject to volatilization losses [22, 23].

Various authors have described the direct determination of arsenic in a graphite-furnace atomizer, because the method is fast and suitable for routine analysis [22–28]. Again there are several drawbacks such as interaction of arsenic with the heated carbon [1, 29], volatilization losses of arsenic during the charring cycle [30, 31] and interferences by certain metal salts [24, 32]. To decrease the volatility of the analyte during charring and to decrease the influence of matrix ions, matrix modification techniques have been described, based on the use of nickel salts [33] and other inorganic salts [32]. The stabilisation is thought to be due to stable metal-arsenic bond formation [33]. The anomalous behaviour of arsenic has been explained by the formation of carbides [34], and to remove possible interferences, tantalum-lined [29, 34] or tantalum or niobium-coated [31] graphite tubes and molybdenum microtubes [35] have been recommended.

A thorough study of the determination of arsenic with flameless a.a.s. and untreated graphite tubes is described in the present paper.

EXPERIMENTAL

Apparatus

The Perkin-Elmer 503 atomic absorption spectrometer used was equipped with a PE HGA-74 graphite furnace atomizer and a deuterium background corrector. The light source was an arsenic electrodeless discharge lamp, operated at 9 W. All analyses were done at the 193.7-nm arsenic resonance line with a slit width of 1 mm, and absorbances were read as peak heights from the built-in peak-read device of the spectrometer. A fast-response strip-chart recorder (Hitachi-PE 56) was used for recording the signals. The furnace was flushed with argon (l'Air Liquide N46) at an interval flow rate of 300 ml min^{-1} and an external flow rate of 900 ml min^{-1}. The gas flow could be changed during the atomization stage to vary the sensitivity by means of the stopped (gas-stop), reduced (mini-flow) and continuous (gas-flow) flow settings. Aliquots were injected with Eppendorf micropipettes with disposable polypropylene tips.

For the determination of arsenic, the optimum time/temperature program for 20-μl injected solution was as follows (with nickel sulfate as a stabilizing agent): dry at 90°C for 20 s, ash at 1200°C for 20 s, atomize at 2600°C for 10 s and glow out at 2700°C for 10 s. When other temperature cycle conditions are used, they will be mentioned as they appear in the description of the experiments. Keeping all other factors constant, there were no differences in absorbance for ashing times between 20–60 s.

Reagents

Merck Titrisol standard solutions were used for arsenic (As_2O_5), nickel ($NiCl_2$), calcium ($CaCl_2$), magnesium ($MgCl_2$), sodium (NaCl), zinc ($ZnCl_2$),

potassium (KCl), cadmium ($CdCl_2$), iron ($FeCl_3$), copper ($CuCl_2$), aluminium ($AlCl_3$), manganese ($MnCl_2$), antimony ($SbCl_3$) and chromium ($CrCl_3$). For arsenic(V), a second standard solution was prepared from sodium arsenate heptahydrate (Merck 6284 pro analysi). A standard solution for arsenic(III) was prepared from arsenic trioxide (Merck 119 pro analysi), which was dissolved in a minimum quantity of 1 M sodium hydroxide (pro analysi quality). The arsenic standard solutions used for atomic absorption measurements had a concentration of 0.1 μg ml^{-1}. The aqueous Titrisol As_2O_5 solutions were adjusted to contain 0.1 M nitric acid before use.

RESULTS AND DISCUSSION

It appears that standard solutions prepared from arsenic pentoxide cannot be analyzed readily in the graphite tube atomizer under any conditions chosen for ashing and atomization. Irreproducible peak readings were obtained with and without the deuterium background correction with a standard deviation on replicate measurements of 20% or more. About 50 graphite tubes obtained from several batches were tested for the purpose. The results remained irreproducible when the standard solution was treated with concentrated nitric acid and evaporated to dryness, which proves that the erratic behaviour is not due to the possible initial presence of trivalent arsenic in the solution.

When the standard solution was prepared from sodium arsenate, much more precise determinations were possible, with a standard deviation on replicates of less than 5%. From the ashing curve (Fig. 1, upper part) it appears that part of the arsenic is lost near 600°C and that from 800 to 1300°C no further losses occur. The measurements of the standard made from arsenic trioxide were also reproducible, with an ashing curve (Fig. 1, centre) which shows a steep decrease around 800°C and an unexplained, peak-like structure of negligible importance between 1200 and 1500°C.

To determine whether the presence of sodium was responsible for the difference in behaviour of the standard solutions prepared from As_2O_3 and Na_2HAsO_4, sodium nitrate was added to the arsenic pentoxide standard solution at a sodium concentration of 1 μg ml^{-1}. The charring curve obtained is shown in Fig. 1 (bottom part). Measurements were reproducible to within 5%.

The ashing curves for these three standard solutions of arsenic were remeasured in the presence of 100 μg Ni ml^{-1} (added as nickel sulfate) as a matrix stabilizer (Fig. 1) in accordance with the suggestion of Ediger [33]. The arsenic appears to be converted to stable species in the furnace and the ashing curves for the three standard solutions show no losses of arsenic up to a temperature of about 1300°C. Reproducible measurements were possible and the only anomaly in the curves was found in the occurrence of double atomization peaks at low ashing temperatures (Fig. 2). All the results in Fig. 1 were obtained without the use of background correction; double peaks were not obtained when background correction was applied.

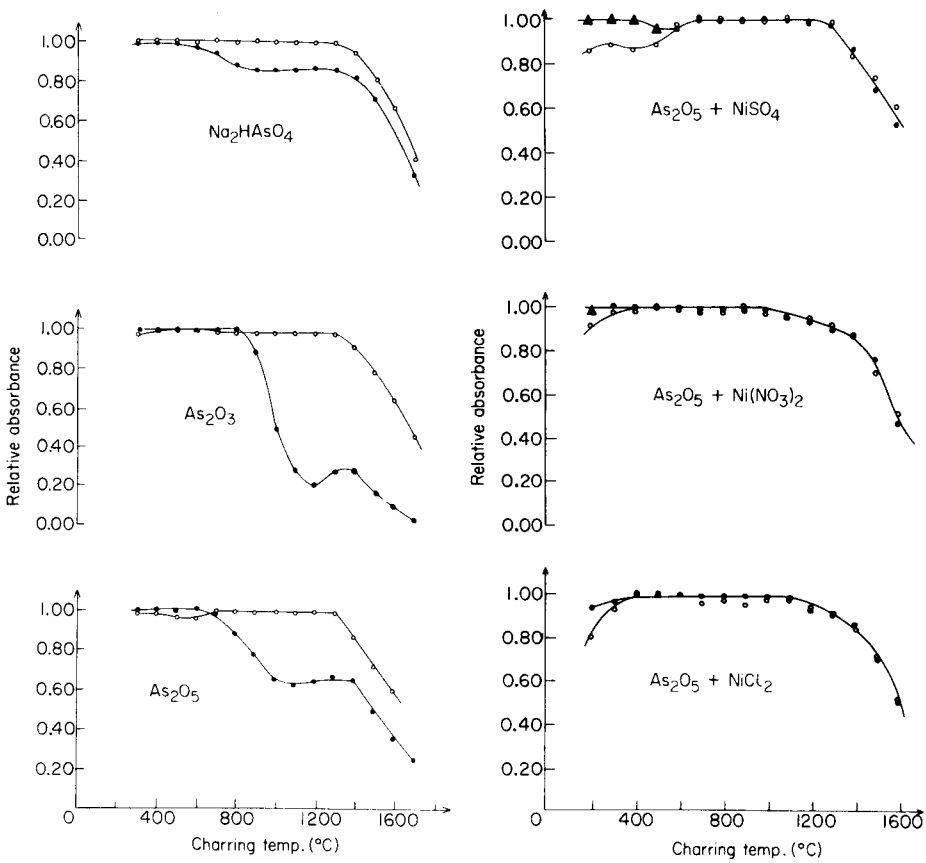

Fig. 1. Charring curves for 2 ng As, from the standard solutions indicated, with atomization at 2600°C: (•) 0.1 M HNO_3 medium; (○) 0.1 M HNO_3 medium $NiSO_4$ (100 μg Ni ml^{-1}) added.

Fig. 2. Charring curves for 2 ng As, from the As_2O_5 standard solution, 0.1 M HNO_3 medium in the presence of $NiSO_4$ (100 μg Ni ml^{-1}), Ni $(NO_3)_2$ (200 μg Ni ml^{-1}) or $NiCl_2$ (200 μg Ni ml^{-1}): (•) without background correction; (○) with background correction; (▲) without correction, double atomization peaks.

Stabilization by nickel salts

The high reproducibility of the measurements in the presence of nickel sulfate and the favourable shape of the ashing curves obtained, stress the utility of this matrix stabilizing medium for arsenic determination, but the overall method deserves closer attention.

In the literature, different nickel salts (chloride, nitrate and sulfate) are described, typically with a nickel concentration of 1 mg ml^{-1} or more [23, 33, 36]. The ashing curves for the arsenic solution made from arsenic pentoxide, in the presence of the nickel salts mentioned, are shown in Fig. 2. There are significant differences between the salts for low ashing temperatures, and with nickel sulfate as stabilizer, double atomization peaks appear

up to 500°C when background correction is not applied; also reduced absorbance readings occur in the same conditions for deuterium-corrected measurements. These effects could be due to the presence of a mixture of arsenic species [32]. The onset of atomization losses varies from 1000°C to 1300°C.

When 20-μl amounts of solutions (1 mg Ni ml^{-1}) of nickel chloride, sulfate or nitrate, all in 0.1 M nitric acid medium, were injected repeatedly, the graphite tubes deteriorated rapidly, resulting in irreproducible arsenic measurements. The lifetime of a tube typically did not exceed about 25 injections. Further, at these high concentrations, the nickel salts gave rise to significant absorbance readings at the 193.7-nm line, when background correction was not applied. The effect is shown in Fig. 3. The increased absorbance claimed by some workers [23, 32, 33] may therefore be due to this effect. The non-specific absorbance vanished for high ashing temperatures at a concentration of 200 μg Ni ml^{-1} for nickel chloride or nitrate and at 100 μg Ni ml^{-1} for nickel sulfate. Moreover, under these conditions, the lifetime of the graphite tube exceeded 70 injections. In view of the somewhat higher ashing temperatures that appear to be possible with nickel sulfate, this salt was selected for further study of the nickel matrix modification system. The influence of the nitric acid concentration on the measurement of arsenic (0.1 μg ml^{-1}) in the presence of nickel sulfate (100 μg ml^{-1}) is shown in Fig. 4. With the same measurement conditions and a nitric acid concentration of 0.1 M, the calibration curves shown in Fig. 5 were obtained.

Effects of foreign ions

Unstabilized solutions. The interferences by non-specific absorption of various foreign cations for determinations done at a charring temperature of 700°C or 1200°C, and an atomization temperature of 2600°C, were studied for 0.1 M nitric acid solutions. The tolerance limits, defined as the maximum concentrations which do not give rise to an absorbance exceeding 0.010 units,

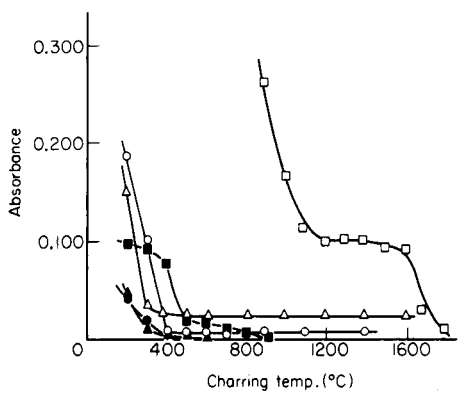

Fig. 3. Non-specific absorbance of nickel salts on 0.1 M HNO_3 as a function of charring temperature (20 μl injected, no background correction): (○) $NiCl_2$ (1000 μg Ni ml^{-1}); (●) $NiCl_2$ (200 μg Ni ml^{-1}); (△) Ni $(NO_3)_2$ (1000 μg Ni ml^{-1}); (▲) Ni $(NO_3)_2$ (200 μg Ni ml^{-1}); (□) $NiSO_4$ (1000 μg Ni ml^{-1}); (■) $NiSO_4$ (100 μg Ni ml^{-1}).

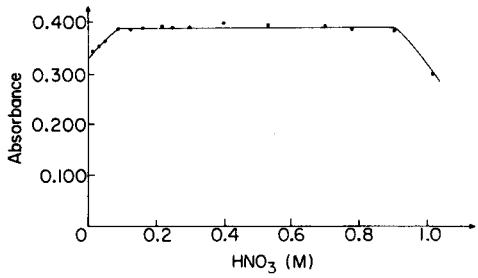

Fig. 4. Influence of the nitric acid concentration on the determination of arsenic in the presence of nickel sulfate (100 μg Ni ml^{-1}).

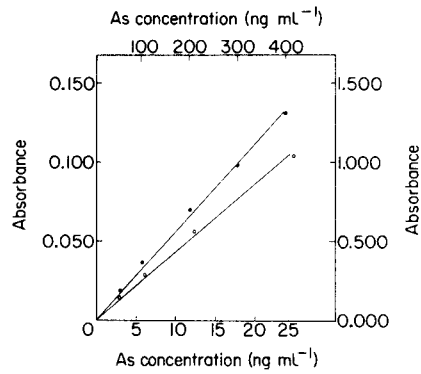

Fig. 5. Calibration curves for arsenic on 0.1 M HNO_3 medium with nickel sulfate (100 μg Ni ml^{-1}) added: (•) 0—400 ng ml^{-1}; (○) 0—25 ng ml^{-1}.

are shown in Table 1. All data were obtained without and with background correction.

Interferences were rather incompletely corrected by the background correction for some elements. For cadmium, iron, magnesium and aluminium, the effect of molecular absorption was measured, with background correction, at a concentration of 200 μg ml^{-1}. The results are shown in Fig. 6 as a function of the ashing temperature. From Fig. 6 and Table 1, it appears that at high ashing temperatures with background correction, interferences are adequately suppressed for most of the elements. A notable exception is aluminium which can be tolerated only at quite low concentrations.

TABLE 1

Tolerance limits (μg ml^{-1}) for some common cations because of non-specific absorption at the 193.7-nm line

Cation	Charring temperature (°C)			
	No background correction		Background correction	
	700°C	1200°C	700°C	1200°C
Fe^{3+}	25	25	200	200
Al^{3+}	3	3	6	6
Na^{+}	50	50	⩾200	⩾200
K^{+}	50	⩾200	⩾200	⩾200
Mg^{2+}	6	30	50	⩾200
Zn^{2+}	⩾200	⩾200	⩾200	⩾200
Ca^{2+}	25	25	⩾200	⩾200
Cd^{2+}	100	⩾200	⩾200	⩾200
Cu^{2+}	100	⩾200	⩾200	⩾200
Cr^{3+}	⩾200	⩾200	⩾200	⩾200
Sb^{3+}	50[a]	50[a]	50[a]	50[a]

[a]Maximum amount soluble.

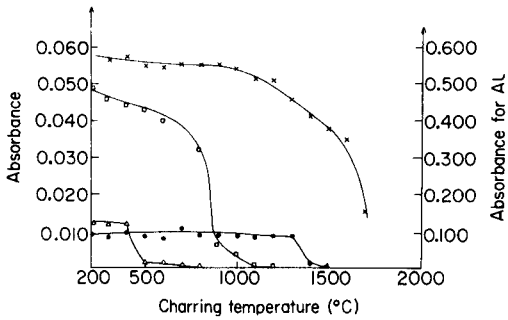

Fig. 6. Non-specific absorbance of Mg^{2+}, Fe^{2+}, Cd^{2+}, or Al^{3+} (200 μg ml^{-1}) in 0.1 M HNO_3 as a function of charring temperature (20 μl injected) with background correction: (×) $AlCl_3$; (□) $MgCl_2$; (•) $FeCl_3$; (△) $CdCl_2$.

Stabilized solutions. Figure 7 shows the relative absorbance of 2 ng As in the presence of Na, K, Ca or Al ions in a 0.1 M nitric acid solution containing nickel sulfate (100 μg Ni ml^{-1}). The interferences of the foreign ions can result from two separate effects: first, the non-specific absorption of the concomitant material, which increases the absorbance measured, and secondly the rate of volatilization and atomization of the analyte at the charring temperature.

The first effect, already studied for pure acidic media (Table 1), disappears for sodium, potassium and calcium when background corrections are applied.

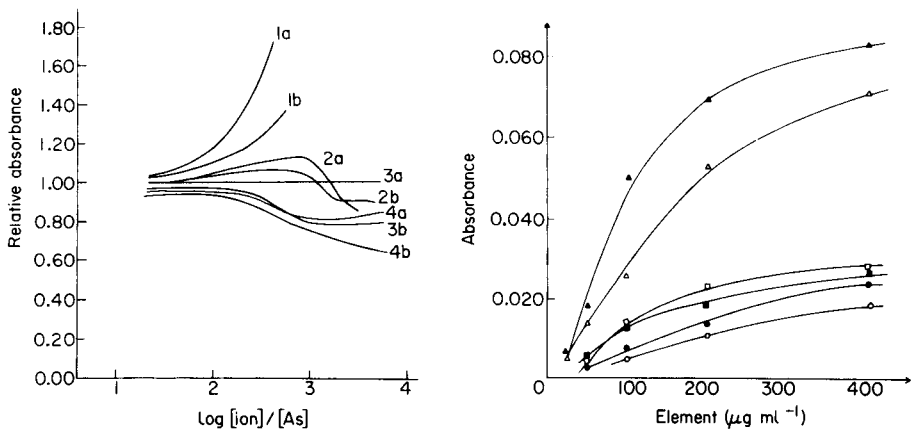

Fig. 7. Relative absorbance of 2 ng As in 0.1 M HNO_3 with nickel sulfate (100 μg Ni ml^{-1}) in the presence of: (1) Al^{3+}; (2) Ca^{2+}; (3) Na^+; (4) K^+. (a) Without background correction; (b) with background correction. Weight ratios are used.

Fig. 8. Non-specific absorption for KCl (open symbols) and NaCl (closed symbols) in the presence of nickel sulfate (100 μg Ni ml^{-1}; △, ▲); nickel chloride (200 μg Ni ml^{-1}; □, ■); and nickel nitrate (200 μg Ni ml^{-1}; ○, •).

The negligible interference for sodium (Fig. 7) in the absence of background correction, and the considerable reduction in absorbance when background correction is used, can be explained if it is assumed that both effects are of similar magnitude for this cation. To verify this assumption, the non-specific absorption of sodium and potassium were measured in the nickel sulfate medium. The results, shown in Fig. 8, explain quantitatively the difference between the background-corrected curves and the normal absorbance measurements for these concomitants (Fig. 7).

It is also clear from Fig. 8 that the molecular absorption is dependent on the particular nickel salt used for matrix stabilization, i.e. on the extra anion present in solution. Table 2 summarizes the interferences of various common foreign ions in the arsenic—nickel sulfate system. Tolerance limits are defined as the ion concentration in solution that affects the absorbance readings of a 0.1 μg As ml^{-1} solution by more than 5%. The sign shows whether increased volatilization (−) or molecular absorption (+) is the dominating effect.

It appears that major interferences occur for aluminium, potassium and, to a lesser extent, sodium. The effect for the latter two ions is, however, very significant since they are major constituents in many sample matrices, e.g., natural waters, air particulate matter and biological materials. The molecular absorption effect for sodium and potassium in Fig. 8 is most important when nickel sulfate is used for matrix stabilization, which could be attributed to the presence of sulfate in the matrix. Walsh et al. [32] have measured the variability of the arsenic absorbance as a function of sodium and sulfate at different concentrations. They stressed the large depression of the signal in the solutions containing sodium and sulfate, and attributed it to a suppression of the atomization efficiency by sodium sulfate.

The effects of nickel chloride and nickel nitrate as matrix stabilizers on the interference of the alkali metals was also determined. From Figs. 9 and 10, it appears that the interference depends strongly on the concentrations of sulfate. In the absence of sulfate, there is no interference by sodium and

TABLE 2

Interferences on the determination of arsenic in presence of nickel sulphate as stabilizer[a]

Interference	Tolerance limits (μg ml^{-1})		Interference	Tolerance limits (μg ml^{-1})	
	No background correction	Background correction		No background correction	Background correction
Ca^{2+}	10(+)	100(−)	Sb^{3+}	50[b]	50[b]
Mg^{2+}	100(+)	⩾200	Cu^{2+}	100(−)	100(−)
Cd^{2+}	100(−)	⩾200	Zn^{2+}	⩾200	⩾200
Cr^{3+}	⩾200	⩾200	K^{+}	1(−)	1(−)
Mn^{2+}	100(−)	100(−)	Na^{+}	400(+)	20(−)
Fe^{3+}	100(−)	100(−)	Al^{3+}	4(+)	4(+)

[a](+) Enhancement, (−) suppression.
[b]Maximum amount soluble.

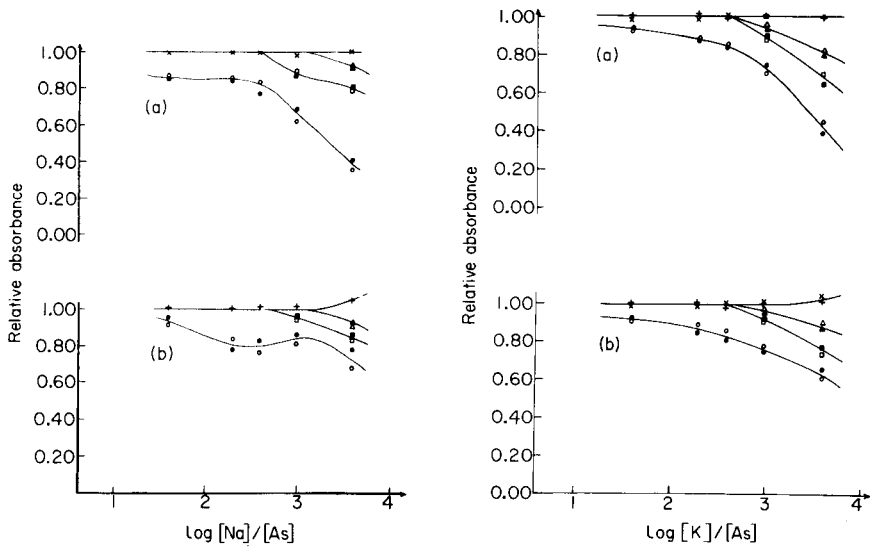

Fig. 9. Effect of sulfate concentration on the nickel nitrate (×, ▲, ■, ●) and nickel chloride (+, △, □, ○) systems in the presence of sodium. (a) With background correction; (b) without background correction. Sulfate concentration: (×, +) 0 μg ml^{-1}; (▲, △) 20 μg ml^{-1}; (■, □) 350 μg ml^{-1}; (●, ○) 3500 μg ml^{-1}.

Fig. 10. Effect of sulfate concentration on the nickel nitrate and nickel chloride systems in the presence of potassium. Symbols as in Fig. 9. Weight ratios are used.

potassium for concentrations up to 400 μg ml^{-1}, but in the presence of sulfate the interference becomes very important, even at low alkali metal ion concentrations. The interference is therefore clearly associated with the presence of alkali sulfates, as has been indicated by Walsh et al. [32].

The strong interference of aluminium persists for the other nickel salts and must therefore be associated with a direct effect of aluminium (Fig. 7).

Conclusion

The overall study makes it clear that matrix effects play an important role in the determination of arsenic with graphite-furnace a.a.s. Determinations of arsenic at low concentrations are impossible when sodium or potassium and sulfate are present together in the sample at concentration levels exceeding a few ppm. Aluminium also interferes strongly. Matrix modification with nickel salts does not prevent these interferences. The concentrations of alkali metals and sulfate are too high in nearly all environmental and biological samples to allow direct arsenic determinations.

Accurate arsenic determinations by graphite-furnace a.a.s. thus require separation of the analyte in a reasonably pure solution prior to its determination. A procedure based on solvent extraction with the ammonium salt of secondary butyldithiophosphoric acid is presently being studied; the method removes the interferences and allows enrichment of arsenic in a small volume.

Moreover, it allows speciation between trivalent and pentavalent arsenic. This procedure will be published as the second part of this series.

This research was carried out within the framework of the National Research and Development Program on Environment of the Interministerial Commission for Science Policy.

REFERENCES

1 J. W. Robinson, R. Garcia, G. Hindman and P. Slevin, Anal. Chim. Acta, 69 (1974) 203.
2 G. F. Kirkbright and L. Ranson, Anal. Chem., 43 (1971) 1239.
3 Y. Talmi and C. Feldman, ACS-Symposium Series no. 7, E. Woolson (Ed.), American Chemical Society, Washington, DC 0578.895, no. 7, 1975. p. 13–34.
4 A. Ando, M. Suzuki, K. Fuwa and B. L. Vallee, Anal. Chem., 41 (1969) 1974.
5 R. Kaszerman and K. Theurer, At. Absorpt. Newsl., 15 (1976) 129.
6 W. Holak, Anal. Chem., 41 (1969) 1712.
7 E. F. Dalton and A. J. Malanoski, At. Absorpt. Newsl., 10 (1971) 92.
8 E. J. Fernandez and D. C. Manning, At. Absorpt. Newsl., 10 (1971) 86.
9 R. C. Chu, G. P. Barron and P. A. W. Baumgarner, Anal. Chem., 44 (1972) 1476.
10 D. E. Fleming and G. A. Taylor, Analyst, 103 (1978) 101.
11 R. D. Wauchope, At. Absorpt. Newsl., 15 (1976) 64.
12 M. L. Kokot, At. Absorpt. Newsl., 15 (1976) 105.
13 J. Guimont, M. Pichette and N. Rheaume, At. Absorpt. Newsl., 16 (1977) 53.
14 I. Rubeska and V. Hlavinkova, At. Absorpt. Newsl., 18 (1979) 5.
15 H. R. Griffin, M. B. Hocking and D. G. Lowery, Anal. Chem., 47 (1975) 229.
16 F. Peter, G. Growcock and G. Strunc, Anal. Chim. Acta, 104 (1979) 177.
17 S. Terashima, Anal. Chim. Acta, 86 (1976) 43.
18 A. U. Shaikh and D. E. Tallman, Anal. Chim. Acta, 98 (1978) 251.
19 P. N. Vijan and G. R. Wood, At. Absorpt. Newsl., 13 (1974) 33.
20 A. E. Smith, Analyst, 100 (1975) 300.
21 F. D. Pierce and H. R. Brown, Anal. Chem., 48 (1976) 693.
22 G. C. Kunselman and E. A. Huff, At. Absorpt. Newsl., 15 (1976) 29.
23 H. Freeman, J. F. Uthe and B. Flemming, At. Absorpt. Newsl., 15 (1976) 49.
24 D. B. Ratcliffe, C. S. Byford and P. B. Osman, Anal. Chim. Acta, 75 (1975) 457.
25 A. W. Fitchett, E. H. Daughtrey, Jr. and P. Mushak, Anal. Chim. Acta, 79 (1975) 93.
26 D. B. Lo and R. L. Coleman, At. Absorpt. Newsl., 18 (1979) 10.
27 R. M. Hammer, D. L. Lechak and P. Greenberg, At. Absorpt. Newsl., 15 (1976) 122.
28 J. W. Owens and E. S. Gladney, At. Absorpt. Newsl., 15 (1976) 47.
29 R. B. Baird and S. M. Gabrielian, Appl. Spectrosc., 28 (1974) 273.
30 J. F. Alder and D. A. Hickman, At. Absorpt. Newsl., 4 (1977) 110.
31 P. Hocquellet, Analusis, 6 (1978) 432.
32 P. R. Walsh, J. L. Fasching and R. A. Duce, Anal. Chem., 48 (1976) 1014.
33 R. D. Ediger, At. Absorpt. Newsl., 14 (1975) 127.
34 B. V. L'Vov and L. A. Pelieva, Zavod. Lab., 44 (1978) 173. Anal. Abstr., 35 (1978) 230.
35 K. Ohta and M. Suzuki, Talanta, 25 (1978) 160.
36 R. B. Denyszyn, P. M. Groshe and D. E. Wagoner, Anal. Chem., 50 (1978) 1094.

Analytica Chimica Acta, 119 (1980) 341—348

INTER-ELEMENT EFFECTS AND SUPPRESSION OF INTERFERENCES IN THE DETERMINATION OF NICKEL BY U.H.F. PLASMA TORCH EMISSION SPECTROMETRY

KUNIHIKO AKATSUKA and IKUO ATSUYA*

Kitami Institute of Technology, Kitami (Japan)

(Received 10th April 1980)

SUMMARY

Several metals show enhancing and depressing effects in the determination of nickel by u.h.f. plasma torch emission spectrometry. To suppress these interferences and to improve the sensitivity, the addition of potassium, magnesium and iron was examined; Mg and (Fe + Mg) spectroscopic buffers were found to minimize interference effects, and improve the sensitivity; the detection limit was 5 μg Ni l^{-1} in the presence of magnesium. The procedure is applied to the determination of nickel in iron and steels.

The u.h.f. plasma torch has been used for a decade as an atomization and excitation source for atomic emission spectrometry. It has a high excitation temperature so that a great number of elements can be determined with high sensitivity [1—4], and has been applied successfully for analyses of metals and alloys [5—11], biological materials [12, 13] and geological samples [14, 15]. However, in the course of these investigations, various inter-elemental or matrix effects have been observed. Bădărău et al. [16] reported depressions of Pb(I) 405.7-nm emission with increasing concentrations of alkali and alkaline earth elements in a 43-MHz plasma sustained in air. Murayama et al. [3] reported that the lines of cadmium, aluminium, barium and strontium were strongly enhanced by the addition of sodium chloride, but the lines of arsenic, boron and mercury were less affected in a 2450-MHz discharge supported by argon. Similar enhancements and suppressions by easily ionized elements such as sodium, calcium and cesium in various types of plasma torch have also been observed [2, 4, 17—21].

To overcome or alleviate these problems, Boumans et al. [20] recommended the use of an alkali metal buffer in analyses involving easily ionized elements. Govindaraju et al. [15] developed an automated bulk analysis of silicate rocks with samples fused, dissolved and buffered with strontium for elimination of matrix interferences. Vurek [22] reported earlier that a cesium nitrate—ammonium phosphate spectroscopic buffer minimized interference effects on the determination of calcium and magnesium in deproteinized sera by using a low power glow discharge surrounding a heated filament in a helium atmosphere.

The present authors have reported that u.h.f. plasma torch emission spectrometry is very suitable for the determination of chromium [8], manganese [9] and molybdenum [10] in iron and steels. In these examinations, it became clear that the enhancing and depressing effects of coexisting elements in iron and steels were eliminated by the presence of a large amount of iron. Accordingly, the use of a capacitively-coupled microwave plasma (c.m.p.) as an excitation source offers considerable promise if ionized elements can be utilized as a radiation buffer for the elimination of matrix effects. The present paper describes in detail the inter-element effects of ionizable elements such as potassium and magnesium on nickel for this purpose, and, the procedure established is applied to the determination of nickel in iron and steels.

EXPERIMENTAL

Reagents

Standard nickel solution. Nickel metal (99.99%) was dissolved in 6 M hydrochloric acid; the solution was evaporated almost to dryness, the residue dissolved in 6 M hydrochloric acid, and the solution diluted with 6 M hydrochloric acid to contain 10 mg Ni ml^{-1}. This solution was diluted as required.

All acids, salts and other metals were of reagent grade.

Apparatus and working conditions

A 2450-MHz Hitachi u.h.f. plasma torch spectrometer 300 was used, as described previously [8]. Argon was used as the plasma-forming gas and sheath gas.

Factors such as the field and anode current, and flow rates of the plasma-forming and sheath gases, which fundamentally affect the line intensity of nickel, were examined. The relationships between the line intensity and these factors were almost the same as reported previously [8—10]. The optimal working conditions for nickel were: frequency, 2450 MHz; flow-rate of plasma-forming gas, 2.5 l min^{-1}; flow-rate of plasma sheath gas, 3.0 l min^{-1}; field current, 370 mA; anode current, 270 mA; entrance slit width, 30 μm; exit slit width, 50 μm; pneumatic nebulizer, about 2.5 ml min^{-1} with water at 2.5 l min^{-1}. A fixed observation height from 0—15 mm from the top of the electrode was used.

Several spectral lines may be used. The Ni(I) 352.454-nm line (3.54 eV) was more intense that the Ni(I) 341.477 nm line (3.65 eV) (the ratio was 204:173, in arbitrary units) but there was more background noise in the vicinity of the former. A better detection limit and linear calibration curves through the origin were obtained at 341.477 nm, which is therefore recommended for analytical use.

Effects of acids and diverse elements

The effects of common mineral acids in the range 0.5—5 M were investigated. The emission intensity decreased significantly with increasing con-

centration of acids, but it remained constant for 3—5 M hydrochloric acid; at such acidities, the emission intensity for 4.0 μg Ni ml^{-1} solutions was depressed by 30% compared to pure aqueous solutions (Fig. 1). Nitric and sulfuric acids had large depressive effects and were considered unsuitable for use.

The effects on nickel emission intensity of the elements usually found in iron and steels were examined; solutions containing 1 μg Ni ml^{-1}, and 50 μg ml^{-1} of other ions, were used, because this concentration ratio is usually the greatest encountered in steel analysis. The presence of Ca, Co, Cu, Cr, Mg or Mn increased the intensity but Mo and Zn slightly decreased it (Table 1).

Procedure for determination of nickel in iron and steels

An accurately weighed sample (0.05—0.5 g) was dissolved in 15 ml of aqua regia by heating. The solution was evaporated almost to dryness, the residue was dissolved in 25 ml of 6 M hydrochloric acid, and the solution transferred to a 50-ml volumetric flask. Next, 3 ml of a 50 mg Mg ml^{-1} (as chloride) solution was added, and the solution was made up to volume with distilled water. The nickel concentration was measured using the plasma under the optimal conditions described above.

RESULTS AND DISCUSSION

Inter-element effects

Elimination of interferences is the primary goal, but a considerable improvement in sensitivity can be achieved if the nickel line is enhanced by the presence of a radiation buffer. Murayama [18] reported that the detection limits for some rare-earth elements such as samarium, praseodymium and neodymium were improved by several tens to a thousand times by

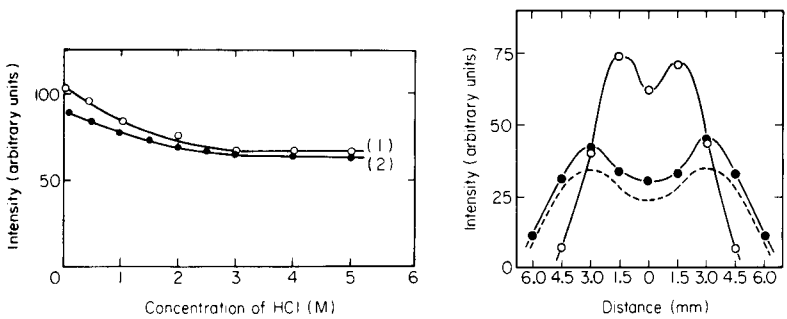

Fig. 1. Effect of hydrochloric acid on nickel intensity at 341.477 nm with 4 μg Ni ml^{-1}. (1) in distilled water; (2) in the presence of 1 mg Fe ml^{-1} and 3 mg Mg ml^{-1}.

Fig. 2. Projected intensity distribution for the Ni(I) 341.477-nm line with 1 μg Ni ml^{-1} in (-----) distilled water and in solutions containing (•) 10 μg ml^{-1} and (○) 100 μg ml^{-1} of potassium (as chloride).

TABLE 1

Effect of other elements on nickel emission intensity at 341.477 nm (1.0 μg Ni ml^{-1})

Element[a]	Changes in intensity (%)				
	In 0.3 M HCl[d]	In 0.3 M HCl + 100 μg K ml^{-1}[e]	In 0.3 M HCl + 1 mg Mg ml^{-1}[e]	In 3 M HCl + 2 mg Fe ml^{-1}[d]	In 3 M HCl + 1 mg Fe ml^{-1}[e] + 3 mg Mg ml^{-1}
Al	−1	2	−1	0	0
As	−1	1	−1	0	0
Cd	−2	0	−2	0	0
Sn	−3	−3	−1	0	−1
Mo	−6	1	0	0	0
Zn	−9	−1	0	0	0
Ti	1	3	−2	0	0
V	2	8	−1	0	2
Cu	5	5	0	0	0
Cr	35	16	1	1	0
Mn	68	7	−1	0	0
Ca	124	19	4	0	1
Mg	143	17	—	−1	—
Co	58	27	6	30	27
Co[b]	10	8	2	16	2
Co[c]	7	1	0	5	0

[a]50 μg ml^{-1}. [b]10 μg ml^{-1}. [c]5 μg ml^{-1}. [d]Observation at d = 3 mm. [e]Observation at d = 1.5 mm.

addition of sodium in a 2450-MHz discharge. Unfortunately, Larson and Fassel [21] suggested that the use of sodium as a radiation buffer might be quite limited because of the absence of a plateau region in the interference curves by sodium in a 2450-MHz c.m.p. Boumans et al. [20] investigated the matrix effects of cesium and calcium, and recommended the use of an alkali metal buffer, but did not provide information on the applicability of this approach to c.m.p. analyses.

Detailed inter-element studies of the effects of potassium and magnesium in a u.h.f. plasma torch have not been reported, but Kawaguchi and Vallee [23] reported that addition to the sample of 4—10 mM potassium chloride enhanced the spectral line intensity 6—1000-fold, and eliminated or suppressed interference effects in a low-pressure, microwave-induced helium plasma using a tantalum filament vaporization system. During this inter-element study, therefore, potassium and magnesium, having different ionization potentials (4.339 and 7.646 eV, respectively) were employed as the chlorides. The spatial distribution of the intensity of nickel emission was measured in various concentrations of potassium and magnesium at various distances from the centre of the plasma, specified hereafter by d. The apparent results are shown in Figs. 2 and 3. The peak of the intensity distribution shifts to the center of the plasma with increasing amounts of additive. The intensity of nickel was greatly depressed by addition of more than 500 ppm of potas-

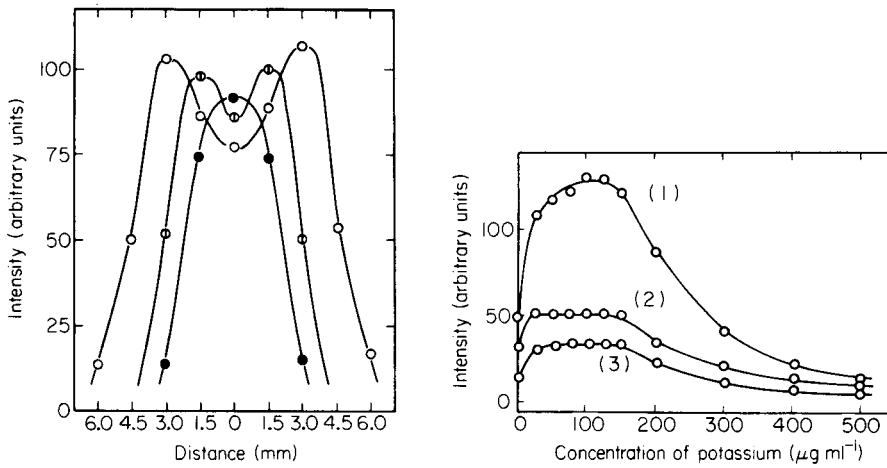

Fig. 3. Projected intensity distribution for the Ni(I) 341.477-nm line in the presence of magnesium (as chloride) for 1 μg Ni ml^{-1} in distilled water containing (○) 0.1 mg ml^{-1}, (⊙) 1 mg ml^{-1} and (●) 3 mg ml^{-1} of magnesium.

Fig. 4. Effect of potassium on the intensity of nickel lines at d=1.5 mm for 1 μg Ni ml^{-1}. (1) Ni(I) 341.477, (2) Ni(I) 300.249, (3) Ni(I) 356.637 nm.

sium, so measurements were not made in the presence of higher concentrations of potassium. The effects of various amounts of potassium on the several spectral line intensities of nickel are shown in Fig. 4. The intensity of Ni(I) 341.477 nm (3.65 eV) swiftly increases with an increase in potassium concentration up to 100 μg K ml^{-1} and then decreases abruptly on further addition. However, the 356.637-nm and 300.249-nm lines, which have a higher excitation energy (3.90 and 4.16 eV, respectively), show constant intensity in the range 20—130 μg K ml^{-1}. Therefore, potassium may be utilized as a radiation buffer by using these higher-energy lines of nickel and addition of potassium at a concentration within the plateau region. However, as shown in Table 1, the buffering ability of potassium is not particularly good.

The effect of magnesium concentration on the intensity of the Ni(I) 341.477-nm line depends strongly on the observation position in the plasma (Fig. 5). When the observation is made at d=1.5 mm, the intensity of the nickel line rises rapidly up to 200 ppm of magnesium, is constant between 200 and 2000 ppm, and gradually decreases above 2000 ppm. The sensitivity is improved about 3.2 times in the presence of 200—2000 ppm of magnesium. At positions d=0 and 3 mm, however, the intensity does not have a plateau region on addition of magnesium. Accordingly, 200—2000 ppm of magnesium can be employed as a radiation buffer when measurements are made at d=1.5 mm.

The calibration curves for nickel in the presence and absence of 1 mg Mg ml^{-1} were linear up to 50 μg Ni ml^{-1}. In the absence of magnesium, the detection limit (signal:noise = 2) of nickel was 40 μg Ni l^{-1}; in the presence of magnesium the limit was 5 μg Ni l^{-1}.

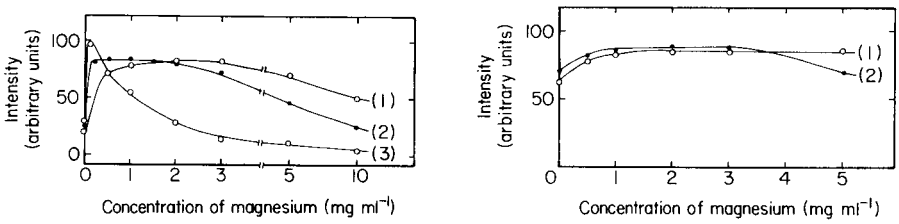

Fig. 5. Effect of magnesium on nickel intensity at 341.477 nm for 1 μg Ni ml^{-1} in 0.6 M hydrochloric acid. Observation position, *d*: (1) 0, (2) 1.5, (3) 3.0 mm.

Fig. 6. Effect of magnesium on nickel intensity at 341.477 nm for 1 μg Ni ml^{-1} in the presence of iron (1 mg Fe ml^{-1}) in 2 M HCl. Observation position, *d*: (1) 0, (2) 1.5 mm.

Effect of iron

As shown in Fig. 6, when the effect of magnesium concentration on nickel was examined in the presence of iron, the nickel intensity was constant in the range 1—3 mg Mg ml^{-1}. The effect of a large amount of iron on nickel intensity was examined in the presence and absence of 3 mg Mg ml^{-1}. When magnesium was not present, the intensity of the Ni(I) 341.477-nm line continually increased with increasing iron concentration at positions d=0 and 1.5 mm but it was constant between 0.5 and 2 mg Fe ml^{-1} at d=3 mm (Fig. 7). With increasing concentration of iron, the position of maximum intensity shifted towards the plasma axis and remained at d = 1.5 mm for ⩾2 mg Fe ml^{-1} (Fig. 8). When 3 mg Mg ml^{-1} was also present, only minor changes in intensity were observed over the entire range of iron concentrations studied at positions d=0, 1.5 and 3 mm (Fig. 9), and the intensity profile was unchanged; maximum intensity was obtained at d=1.5 mm.

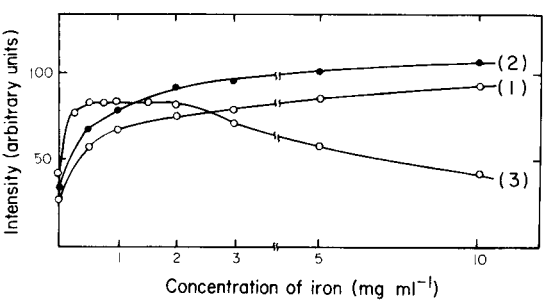

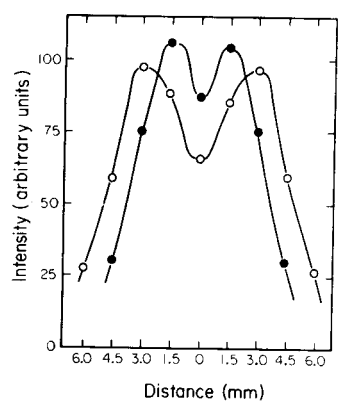

Fig. 7. Effect of iron on nickel intensity at 341.477 nm for 5 μg Ni ml^{-1} in 3 M HCl. Observation position, *d*: (1) 0; (2) 1.5; (3) 3.0 mm.

Fig. 8. Projected intensity distribution for the Ni(I) 341.477 nm line in the presence of iron for 5 μg Ni ml^{-1} in 3 M HCl containing (○) 1 mg Fe ml^{-1} and (●) 3 mg Fe ml^{-1}.

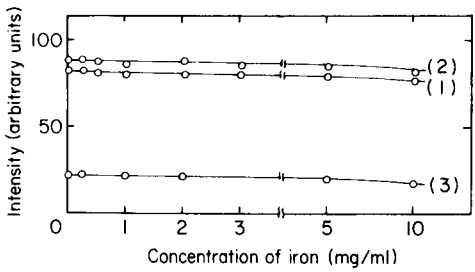

Fig. 9. Effect of iron on nickel intensity at 341.477 nm in the presence of magnesium (5 μg Ni ml^{-1}, 3 mg Mg ml^{-1}, 3 M HCl). Observation position, *d*: (1) 0, (2) 1.5, (3) 3.0 mm.

Spectroscopic buffers

Several metals showed some enhancing and depressing influences on the intensity of nickel in the plasma torch used (Table 1). To suppress these effects, matrix modification was investigated. For this purpose, four series of solutions were prepared, to each of which K, Mg, Fe and (Fe + Mg) were added, respectively, as a radiation buffer at constant concentrations of nickel and diverse elements. The results derived from these solutions are given in Table 1. The influence of 50 ppm of diverse elements, except for cobalt, could be eliminated effectively by addition of all these radiation buffers except for the potassium buffer.

The enhancing effect of more than 50 ppm of cobalt on the intensity of the Ni(I) 341.477-nm line is caused by a weak spectral interference from the Co(I) 341.474-nm line. Therefore, if the concentration of cobalt in a sample solution is more than about 10 times that of nickel, the Ni 351.505-nm line should be used. As the inter-element effects on the Ni 341.477-nm line (3.65 eV) were mostly the same as those on the 351.505-nm line (3.63 eV), the results in Figs. 5 and 9 obtained with the Ni 341.477-nm line are also valid for the Ni 351.505-nm line. Thus, a magnesium solution or a mixed iron and magnesium solution can be effectively used as a radiation buffer for the determination of nickel.

Application to steels

Calibration curves for nickel prepared in a solution containing both iron (1--10 mg ml^{-1}) and magnesium (3 mg ml^{-1}) in 3 M hydrochloric acid under the recommended instrumental conditions and procedure, were linear up to 50 μg Ni ml^{-1}. The coefficient of variation was 2.4% (7 results) for 1 ppm of nickel. The detection limit for nickel (341.477 nm) was 20 μg l^{-1} hence the lowest determinable concentration, as defined by Butler et al. [24], should be 0.002 wt. % nickel in iron. This is less than that obtained by Butler et al. [24] with the inductively coupled plasma (0.005 wt. %), and is essentially the same as by flame atomic absorption spectrometry (0.001—0.002 wt. %) [25, 26], although in atomic absorption, it is necessary to correct for background absorption from iron for samples containing less than 0.1 wt. % iron.

TABLE 2

Results for standard iron and steel samples

J.S.I.S.[a] sample	Ni found (%)	Certified value (%)	C.v. (%)
421-4	0.006	0.0067	—
110-5	0.008	0.009	—
158-2	0.017[b]	0.019	6.3
157-2	0.111[c]	0.11	0.63
156-2	0.312	0.31	—

[a]Japanese Standard for Iron and Steels. [b]Average of 11 determinations (range 0.0155—0.0188). [c]Average of 5 determinations (range 0.110—0.113).

As shown in Table 2, the results obtained for the determination of nickel in iron and steels by the present procedure are in satisfactory agreement with certified values.

REFERENCES

1 S. Greenfield, H. McD. McGeachin and P. B. Smith, Talanta, 22 (1975) 553.
2 M. Yamamoto and S. Murayama, Spectrochim. Acta, Part B, 23 (1967) 773.
3 S. Murayama, H. Matsuno and M. Yamamoto, Spectrochim. Acta, Part B, 23 (1968) 513.
4 S. Murayama, J. Appl. Phys., 39 (1968) 5478.
5 M. Suzuki, Jpn. Anal., 17 (1968) 1529; 18 (1969) 176; 19 (1970) 207.
6 R. Nakashima, S. Sasaki and S. Shibata, Anal. Chim. Acta, 70 (1973) 265.
7 R. Nakashima and S. Sasaki, Anal. Chim. Acta, 85 (1976) 75.
8 I. Atsuya, Anal. Chim. Acta, 74 (1975) 1.
9 I. Atsuya and K. Akatsuka, Anal. Chim. Acta, 81 (1976) 61.
10 K. Akatsuka and I. Atsuya, Anal. Chim. Acta, 99 (1978) 351.
11 T. Akiyoshi and T. Tsukamoto, Jpn. Anal., 27 (1978) 85.
12 R. Nakashima, S. Sasaki and S. Shibata, Anal. Chim. Acta, 77 (1975) 65.
13 R. Nakashima, Jpn. Anal., 27 (1978) 199.
14 F. Gebhardt and H. Horn, Glastech. Ber., 44 (1971) 483.
15 K. Govindaraju, M. Merelle and C. Chouard, Anal. Chem., 48 (1976) 1325.
16 E. Bădărău, M. Giurgea, G. H. Giurgea and A. T. H. Trutia, Spectrochim. Acta, 11 (1956) 411.
17 W. Tappe and J. van Calker, Fresenius Z. Anal. Chem., 198 (1963) 13.
18 S. Murayama, Spectrochim. Acta, Part B, 25 (1970) 191.
19 K. Kitagawa and T. Takeuchi, Anal. Chim. Acta, 60 (1972) 309.
20 P. W. J. M. Boumans, F. J. deBoer, F. J. Dahmen, H. Hoelzel and A. Meier, Spectrochim. Acta, Part B, 30 (1975) 449.
21 G. F. Larson and V. A. Fassel, Anal. Chem., 48 (1976) 1161.
22 G. G. Vurek, Anal. Chem., 39 (1967) 1599.
23 H. Kawaguchi and B. L. Vallee, Anal. Chem., 47 (1975) 1029.
24 C. C. Butler, R. N. Kniseley and V. A. Fassel, Anal. Chem., 47 (1975) 825.
25 Y. Endo, T. Hata and Y. Nakahara, Jpn. Anal., 18 (1969) 833.
26 Y. Endo and Y. Nakahara, Atomic Absorption Spectrometry in the Steel Industry, Nippon Tekko Kyokai, Tokyo, 1975, p. 67.

Analytica Chimica Acta, 119 (1980) 349—357

FLUORAL-P, A MEMBER OF A SELECTIVE FAMILY OF REAGENTS FOR ALDEHYDES

BRUCE JON COMPTON and WILLIAM C. PURDY*

Department of Chemistry, McGill University, 801 Sherbrooke Street, W., Montreal, Quebec H3A 2K6 (Canada)

(Received 11th February 1980)

SUMMARY

The compound 4-amino-3-penten-2-one is introduced as a member of a selective family of reagents for aldehydes. The stability, selectivity and reactivity of the reagent are described and its utility in automatic determinations of formaldehyde is demonstrated. It is shown that the condensation reaction between 4-amino-3-penten-2-one (called Fluoral-P) and formaldehyde gives a product detectable by fluorescence. The flow injection system utilizing this reagent can be used to determine formaldehyde in the lower nanomole range.

Because of its ubiquitous nature, wide usage, and possible mutagenic and carcinogenic nature, formaldehyde is of ever increasing interest [1]. For certain specific needs, formaldehyde is of interest because many compounds in diverse classes, such as carbohydrates [2—4] and acyl glycerides [5—7], can be quantified by sequential reaction to formaldehyde. Thus a mechanized determination of formaldehyde by the continuous flow method (i.e., either gas-segmented or non-segmented) can be envisioned as being of both general and specific utility.

Application of the Nash reagent system to continuous flow determinations of formaldehyde was found to be unsuitable for a variety of reasons. The Nash reagent, 2,4-pentanedione in concentrated (ca. 2 M) ammonium acetate, reacts with formaldehyde to produce 3,5-diacetyl-2,6-dihydrolutidine [2]. It suffers from high viscosity, usually requiring the use of 2 M ammonium acetate [1], and is difficult to mix with other liquids such as

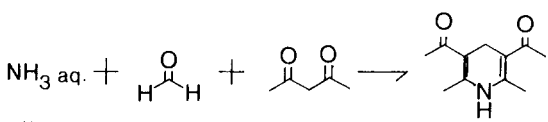

(1) (2)

the mobile phases normally used in reversed-phase h.p.l.c. systems. Long reaction times (up to 30 min) and high reagent background also make this method inefficient for automatic, efficient, continuous flow reactors. Thus, when one considers that the Nash reaction must often be coupled, in some

applications, to two other reaction steps (saponification and periodate oxidation in the case of triglycerides [8]) uncompromising band broadening is envisioned with respect to the chromatographic systems in use today.

The obvious solution to this problem has been to seek alternative methods for developing chromophores from formaldehyde. However, no other aldehyde detection system offers the relatively mild reaction conditions of the Nash reagent or the closely related system of Sawicki and Carnes [1]. Thus the Nash reagent system was studied and attempts were made to improve it [9]. It was found that, contained within the Nash reagent is a specific constituent, the product of the reaction of 2,4-pentanedione and ammonia, which is easily isolated and stable, and can be stored as an analytical reagent [9]. This compound (4-amino-3-penten-2-one, compound 4), which we call Fluorol-P in the reagent form, has been utilized previously as a synthetic intermediate [10, 11] and studied as a complexing agent for metals [12] or as a model system for imine—enamine equilibrium [13]. Here it is used as a reagent for aldehydes. The synthesis of Fluoral-P and its condensation with formaldehyde to produce compound 2 are as follows:

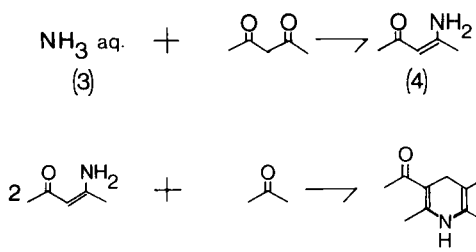

The ideal reagent for automated determinations is one which reacts rapidly and quantitatively with formaldehyde, is stable in solution and thus is easy to handle, has a low inherent background signal, and mixes easily with other solvent systems. This reagent fulfils all of these requirements.

EXPERIMENTAL

Reagents and solutions

All organic reagents were purchased from Aldrich Chemical Co. (Milwaukee, WI) and all inorganic chemicals from Anachemia Chemicals Ltd. (Montreal, Que.). Other chemicals used were formaldehyde (37% reagent; American Chemicals, Montreal, Que.), acetonitrile (Gold Label; Aldrich Chemical Co.), 2-propanol (Spectrograde; British Drug Houses), methanol HPLC-grade; Fisher Chemical Co.), and acetone (Spectrograde; American Chemicals).

Either acetonitrile or methanol was used to make up the Fluoral-P reagent as described in the text. Phosphate buffers were aqueous and made from the sodium salts.

Five sources of 2,4-pentanedione were tested for blank fluorescence and

the above Gold Label variety gave the lowest background in the Nash reagent for preparation of Fluoral-P.

Equipment

Spectral studies were made with a Cary Model 17 spectrophotometer (Varian Associates, Palo Alto, CA) and an Aminco SPF-125 spectrofluorimeter (American Instrument Co., Silver Spring, MD).

Synthesis of 4-amino-3-penten-2-one and solution preparation

This has been described elsewhere [14, 15]; after an investigation of alternative methods, the one similar to that of Lacey [15] was used. This involved mixing equivalent amounts of cold ammonia liquor to cold 2,4-pentanedione with stirring. Ammonium 2,4-pentanedionate resulted with the evolution of large amounts of heat. Thus slow addition and constant cooling are required to prevent the boiling off of 2,4-pentanedione and the formation of a final product which would require many recrystallizations. The ammonium 2,4-pentanedionate solution was placed on a magnetic stirrer and stirred at room temperature for 4 h. The reaction mixture was then extracted 3 times with ether and the recrystallized (cold ether) 4-amino-3-penten-2-one was recovered in 70—80% yield (m.p. 45°C). For greater purity vacuum sublimation at room temperature was found to be useful.

The Fluoral-P reagent was made by dissolving 1.8 g of 4-amino-3-penten-2-one in 100 ml of acetonitrile to give a 0.18 M Fluoral-P reagent. This solution was stored refrigerated in an amber bottle.

Preliminary tests

The reagent was characterized as a chromophore-producing system by studying its reaction with formaldehyde and other aldehyde standards. The factors examined were: (i) its reactivity as a function of pH, (ii) its long-term stability, (iii) its general reactivity and selectivity, and (iv) the linearity of its absorbance and fluorescence response to a range of formaldehyde concentrations.

The pH dependency of the rate of Fluoral-P reaction with formaldehyde was determined by measuring the production of fluorescence of the lutidine product as a function of the pH of the incubating medium. To 1.0 ml of 4.4×10^{-3} M Fluoral-P in methanol was added 1.0 ml of 0.25 M phosphate buffer (pH range 2.0—9.0) and the solution was incubated at 25°C for 5 min. Following incubation, 1.0 ml of 6.0×10^{-2} M formaldehyde in methanol was added and the fluorescence was measured (excitation wavelength, 410 nm; emission wavelength, 510 nm; slits, 0.5 mm). Initial rates are reported in relative units. Methanol was used to slow the rate of 4-amino-3-penten-2-one hydrolysis [16].

Stability studies on Fluoral-P solutions were conducted in three ways. The initial rates were measured for Fluoral-P solutions in the same way as described above for the pH studies. The reagent was analyzed directly

by gas chromatography (OV-101, 100—200°C, 15°C min^{-1}, FID) when made up in distilled water, pH 2.25, 0.1 M phosphate buffer, and acetonitrile. Also the background fluorescence and absorbance were noted for different batches of reagent made up in different solvents.

The general reactivity of Fluoral-P to various compounds was determined in a series of test-tube experiments. To one drop of the compound under study was added one drop of Fluoral-P reagent and one drop of 0.5 M phosphate buffer (pH 2.25); a small amount of acetone was added to aid miscibility. Qualitative evaluation of reactivity was based on either a positive or negative response. Positive responses were subdivided into those which gave instantaneous reaction at room temperature (fast), those which reacted in less than 1 min (moderate), and those which took longer than 1 min to react (slow). In all cases the Fluoral-P derivatives were yellow in color.

Dynamic range, limit of detection and procedures

The linear dynamic range of the reaction between Fluoral-P and formaldehyde was determined by measuring the fluorescence and absorbance of the lutidine product as a function of formaldehyde concentration. This was accomplished by reacting 1.0 ml of the appropriate aqueous formaldehyde standard with 2.0 ml of 0.125 M phosphate buffer (pH 4.0) and 100 μl of Fluoral-P reagent in acetonitrile. Fluorescence and absorbance measurements were made after 5 min but within 30 min of color development; however, the lutidine product is stable in solution for many hours. Blanks were used in the absorbance study but no measurable blank was observed in the fluorescence study.

The lower limit of detection of this reagent was investigated by using a continuous flow system based on the concepts of flow injection analysis [17]. The hardware used in the system involved two Waters 6000A solvent delivery systems (Waters Associates, Waltham, MA) and a Waters U6K sample injector. The reactor was 1/16-in. stainless steel 316 tubing with i.d. measured as 1.0 mm. Reagents from the two pumps were mixed in a 1/16-in. T-connector (Swagelok) just prior to the injector. Sample volumes of 25 μl were added to the stream. A Spectroflow monitor SF 770 set at 410 nm, 0.4 AUFSD, and an FS970 L.C. fluorimeter with excitation at 410 nm and emission 470 + 550 cut-off filters (both from Schoeffel Instruments, Westwood, NJ) were connected in series to the exit of the reactor delay tubing. The Fluoral-P reagent in acetonitrile previously described was added through one pump while 0.125 M phosphoric acid was added through the other. The reactor was run at room temperature, 20°C. Both pumps were operated at a flow rate of 0.5 ml min^{-1} for a total delay time to the fluorimeter of 70 s.

Since the lower concentration range of the reagent reaction with formaldehyde was of interest, formaldehyde concentrations between 1.0×10^{-3} and 1.0×10^{-5} M were used. Absolute amounts of formaldehyde injected corresponded to 2.5×10^{-8} to 1.25×10^{-9} mol.

One application of this system was to investigate the amount of formaldehyde in the solvents and water used during the course of these studies. This was done by injecting 25 μl of the solvent of interest taken from four separate containers. These results are reported as an application of the reagent.

RESULTS AND DISCUSSION

4-Amino-3-penten-2-one has been given the name Fluoral-P in anticipation of the development of dimedone, 1,3-cyclohexanedione, etc. analogs (designated Fluoral-D, -C, etc.). The need for alternative formaldehyde reagents suitable for use in automated analysis is evident from the limited choice of methods currently available [1]. The discussions presented here will be directed towards the use of this reagent in a continuous flow chemical reactor.

pH dependency

One of the more interesting and important aspects of this reagent is the pH dependency of its reaction with formaldehyde. In Fig. 1 is shown the fluorescence and absorbance of the product, 3,5-diacetyl-2,6-dihydrolutidine, as a function of pH. As can be seen, both of these properties vary with the

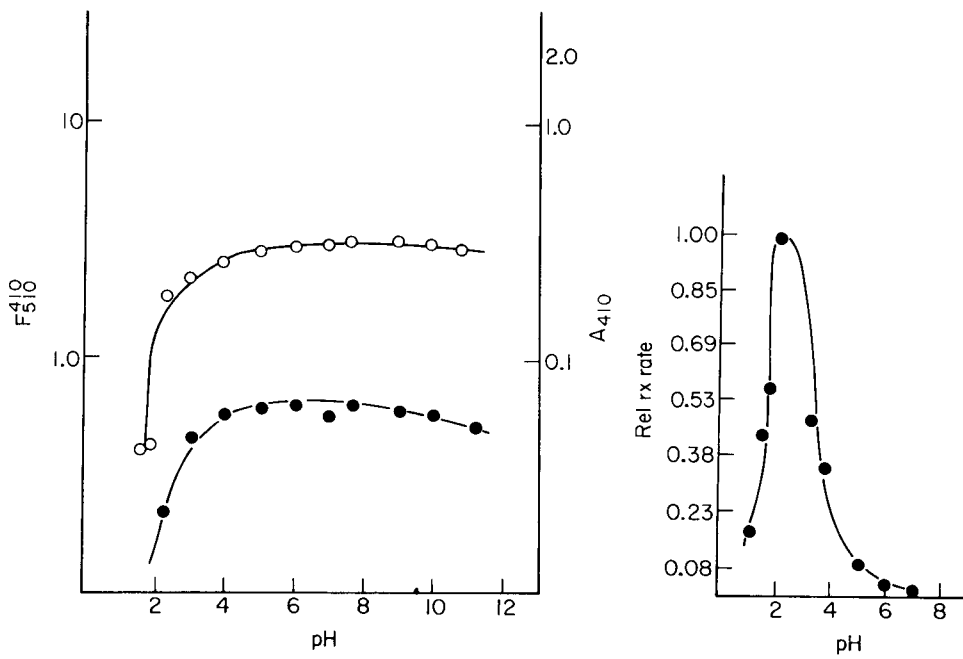

Fig. 1. The pH dependency of the fluorescence (•) and absorbance (○) of 3,5-diacetyl-2,6-dihydrolutidine.

Fig. 2. The pH dependency of the condensation reaction of Fluoral-P with formaldehyde.

pH and thus must be considered in any study of the reactions leading to the formation of this lutidine compound. In Fig. 2 is shown the relative reaction rate for the production of the lutidine product as a function of pH. The useful pH range for the reaction involving Fluoral-P is actually 2.0—7.0 when one takes into account the pH dependency of the chromophore. This pH dependency, however, must be described as sharp. Optimum reaction conditions for using this reagent in continuous flow determinations would have to involve a fast reaction between Fluoral-P and formaldehyde. Thus the reagent must be in the pH range of 2.0—2.5. For reasons given in the next section, the reagent composition must exclude any acid or water. In other words, the Fluoral-P reagent described here is not in a condition which favors rapid reaction with formaldehyde. This is because this condition is incompatible with storage of the reagent. Thus a continuous flow system which utilizes the Fluoral-P reagent must contain at least two channels, one for the reagent and the other for acidic buffer.

Stability of Fluoral-P

The hydrolysis of enaminones in acidic media has been described elsewhere [16]. When Fluoral-P reagent was made up in aqueous pH 2.25, 0.1 M phosphate buffer, no color development was found after one hour. Closer examination with gas chromatography showed that 4-amino-3-penten-2-one was hydrolyzed to 2,4-pentanedione within 15 min, was stable in neutral aqueous solution for at least an hour, and, based on fluorescence and absorbance measurements, was stable for at least one month in acetonitrile. Accordingly, acetonitrile is the solvent of choice for preparing this reagent.

Reactivity and selectivity of Fluoral-P

The general reactivity of Fluoral-P was evaluated as described in the Experimental section. All reactions which were positive gave a yellow product. The results are given in Table 1. Further studies are being conducted on the reactivity of Fluoral-P with acetaldehyde; however, among all the compounds tested, the reagent condenses fastest with formaldehyde. It should be noted that only the product from the formaldehyde reaction is expected to give appreciable fluorescence [18]. Thus, while the reagent reacts generally with aldehydes, some selectivity for formaldehyde is possible by using fluorescence rather than absorbance as a means of detection.

Linearity and range of Fluoral-P for reaction with formaldehyde

This aspect of Fluoral-P is expected to be similar to that for the Nash reagent. The absorbance (410 nm) and fluorescence (excitation 410 nm, emission 510 nm) vs. concentration of formaldehyde plots were linear over the range 10^{-3}—10^{-6} M (absorbance: $y = 3.15(\pm 0.360) \times 10^{2}x \times 0.541$ $(\pm 0.176 \times 10^{-1})$; fluorescence: $y = 9.33(\pm 0.547) \times 10^{3}x + 0.281(\pm 1.18)$. Slopes and intercepts are given ± SD. Depending on the method of sample

TABLE 1

Results of spot tests between Fluoral-P and some common chemicals

Compounds which react
Fast
Formaldehyde, acetaldehyde, propanal, pentanal, 3-methylbutanal, hexanal, octanal, nonanal, decanal, hendecanal, dodecanal, tridecanal, tetradecanal, benzaldehyde
Moderate
Anisaldehyde, cinnamaldehyde, phenylpropionaldehyde, hydrocinnamic aldehyde
Slow
Cuminaldehyde, isobutyraldehyde
Compounds which do not react
Ethyl methyl ketone, acetic anhydride, ethyl acetate, ethylene glycol, *N,N*-dimethylaniline, *o*-nitrotoluene, 1,1,1-trichloroethane, formic acid, 2,4-pentanedione, *N,N*-dimethylacetamide, triethylamine, acetone, phenyl isocyanate.

pretreatment and handling employed, determinations can thus be made in terms of absolute amounts of formaldehyde in the nanomolar range. This is shown to be the case in the next section.

Lower limit of detection for formaldehyde with Fluoral-P

The lower limit of detection for formaldehyde was determined using the flow injection system described in the Experimental section. The data shown in Fig. 3 compare the two spectrophotometric parameters monitored, absorbance and fluorescence of the flow stream, as a function of the amount of formaldehyde injected (nmol). In order to illustrate fully the difference in the two parameters, Fig. 4 includes the signal-to-noise ratio (*S/N*) against the amount of formaldehyde injected. In this plot the signal is taken as the mean peak height from at least four injections into the system while noise is taken as the standard deviation about the mean. The correlation coefficient assuming a linear relationship is −0.497 for absorbance and 0.74 for fluorescence. With absorbance detection, the concentration range over which this experiment was conducted is seen to rival the detection limit of the system. Thus in this concentration range the system is baseline-noise limited. In contrast, fluorescence detection shows some correlation between *S/N* and signal and much greater *S/N* values than for absorbance. Fluorescence detection is not limited by baseline noise above about 3 n mol of injected formaldehyde. This is reflected by the fact that the relative standard deviation of fluorescence measurements above 3 n mol of injected formaldehyde is on the average 0.88% while below this level it averages 3.8%. While this is a limited noise analysis study and is certainly system-dependent, formaldehyde levels in the low nanomole per injection range can be measured using Fluoral-P and the flow injection system employed here.

This detection limit can be improved since the system is baseline-noise limited and thus limited by the background fluorescence of the entire

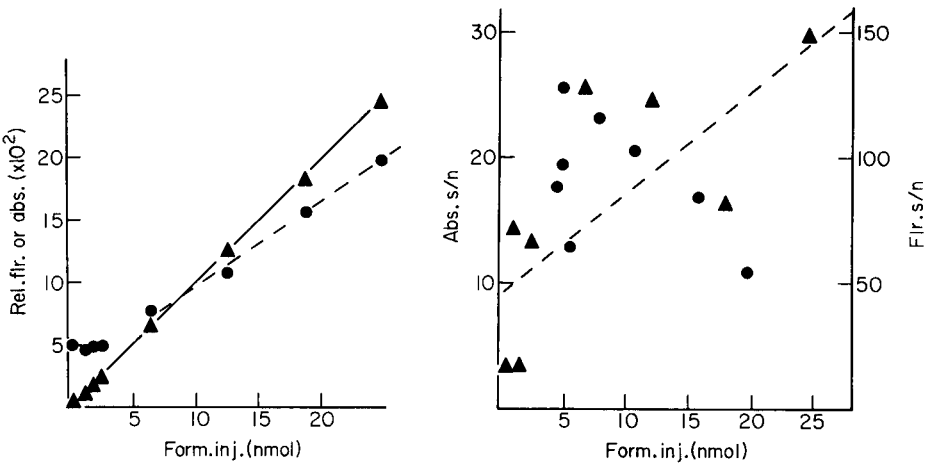

Fig. 3. Fluorescence intensity (▲) and absorbance (●) measurements derived from the flow injection experiments vs. nanomole of injected formaldehyde.

Fig. 4. Signal-to-noise (*S/N*) vs. nanomole of injected formaldehyde for data plotted in Fig. 3. The line (- - -) represents the least-squares linear regression for the fluorescence data.

system. For instance, measurements of the amount of formaldehyde in solvents commonly used in this laboratory are summarized in Table 2. These data show relatively high levels of formaldehyde contamination. Other improvements can be made to the entire system, which was made from available hardware and was not optimized for this application.

Further comments

The formation of 4-amino-3-penten-2-one occurs whenever the Nash reagent is made [9] and hence it can be argued that Fluoral-P is not novel in its use as an aldehyde reagent. However, it is interesting to note that its

TABLE 2

Formaldehyde content of some solvents used in this laboratory

Solvent	Formaldehyde per 25-μl injection[a] (n mol)	Formaldehyd ($\times 10^{-4}$ M)
Water	9.6 ± 1.4	3.8 ± 0.56
Acetonitrile	6.1 ± 0.2	2.4 ± 0.08
2-Propanol	8.3 ± 1.8	3.3 ± 0.72
Methanol	25.4 ± 4.1	10.2 ± 0.16
Acetone	7.7 ± 2.2	3.1 ± 0.88

[a]Mean ± SD for 4 determinations.

existence as the active agent in the Nash reagent has not been described previously. The pH used for the Nash reaction is usually between 6.0 and 6.5. This is not the optimum pH for the reaction between Fluoral-P and formaldehyde but does correspond to the pH region where 4-amino-3-penten-2-one demonstrates stability in aqueous solution [16]. Thus the pH used in the Nash reaction is a compromise between the stability and reactivity of 4-amino-3-penten-2-one. Isolation of the active agent in the Nash reagent eliminates this compromise. Thus Fluoral-P is far superior to the Nash reagent and, in terms of automated determinations, should be useful as an aldehyde reagent.

We thank D. Lori Purdy for her technical assistance and the Medical Research Council of Canada for financial support.

REFERENCES

1 E. Sawicki and C. R. Sawicki, Aldehydes — Photometric Analysis, Vol. 1, Academic Press, New York, 1975, p. 10.
2 G. Lindstedt, Nature, 156 (1945) 448.
3 R. D. Guthrie, in R. L. Whistler and M. L. Wolfrom (Eds.), Methods in Carbohydrate Chemistry, Vol. 1, Academic Press, New York, 1962, p. 432.
4 V. E. Vaskovsky and S. V. Isay, Anal. Biochem., 30 (1969) 25.
5 N. Shaw, Biochim. Biophys. Acta, 164 (1968) 435.
6 H. B. Lofland, Jr., Anal. Biochem., 9 (1964) 393.
7 P. J. Martin, Clin. Chim. Acta, 62 (1975) 79.
8 W. R. Holub, Clin. Chem., 19 (1973) 1391.
9 B. J. Compton and W. C. Purdy, Can. J. Chem., in press.
10 F. Eiden and J. Iwan, Arch. Pharm., 306 (1973) 470.
11 R. Balicki and P. Nautka-Namirski, Pol. J. Pharmacol. Pharm., 26 (1974) 647.
12 H. F. Holtclaw, Jr., J. P. Collman and R. M. Alire, J. Am. Chem. Soc., 80 (1958) 1100.
13 N. M. D. Brown and D. C. Nonhebel, Tetrahedron, 24 (1968) 5655.
14 A. Combes and C. Combes, Bull. Soc. Chim. Fr., 3 (1892) 778.
15 M. J. Lacey, Aust. J. Chem., 23 (1970) 841.
16 K. Dixon and J. V. Greenhill, J. Chem. Soc., Perkin Trans. 2, (1973) 164.
17 J. Růžička and E. H. Hansen, Anal. Chim. Acta, 99 (1978) 37.
18 E. Sawicki and R. A. Carnes, Mikrochim. Acta, (1968) 148.

Analytical Chimica Acta, 119 (1980) 359—365

FLUORIMETRIC DETERMINATION OF COPPER AND MERCURY BASED ON THEIR CATALYTIC EFFECTS ON THE AUTOXIDATION OF 2,2′-DIPYRIDYLKETONE HYDRAZONE

F. GRASES and F. GARCIA-SANCHEZ

Department of Analytical Chemistry, Faculty of Sciences, University of Palma de Mallorca (Spain)

M. VALCARCEL*

Department of Analytical Chemistry, Faculty of Sciences, University of Cordoba (Spain)

(Received 28th January 1980)

SUMMARY

Fluorimetric methods for the determination of mercury(II) (80—320 ppb) and copper(II) (0.4—1 ppb) are described. These ions catalyse the autoxidation of 2,2′-dipyridylketone hydrazone, which yields a product exhibiting an intense blue fluorescence in acidic solution. This product has been investigated and the experimental variables and interferences in each determination have been studied.

Hydrazones have been used frequently as ligands in the development of photometric methods of determination of cations. Some substituted hydrazones have also found use in fluorimetric determinations of Al, Ga, Sc, La, Zn, Cd, Co and Ca by forming fluorescent chelates [1].

In recent studies [2] it was found that the unsubstituted hydrazones and azines of 2,2′-dipyridylketone, phenyl-2-pyridylketone and dipyridylglyoxal react with Cu^{2+}, Hg^{2+}, Co^{2+}, Au^{3+} and Pt^{4+}, giving products that showed intense blue fluorescence at a suitable pH. This reaction has been used in the spectrofluorimetric determination of mercury(II) and copper(II).

Few fluorimetric methods for mercury(II) have been described. The method proposed by Oshima and Nagasawa [3] is based on the quenching effect of mercury(II) on the fluorescence of rhodamine B. The method described by Holzbecher and Ryan [4] is based on the oxidation of thiamine to thiochrome at pH 9.6; it is very sensitive but there are numerous interferences. Several fluorimetric methods for determining copper(II) have been suggested [5—11]; some [5, 6] involve fluorescence-quenching phenomena.

EXPERIMENTAL

Synthesis, purification and characterization of the hydrazone of 2,2′-dipyridylketone (DPKH)

2,2′-Dipyridylketone (5g) dissolved in the minimum quantity of hot absolute ethanol was refluxed with 1.5 g of 100% hydrazine monohydrate for 15 h.

The cooled solution was shaken and the oily mass that separated was recrystallized from a 1:1 mixture of benzene and petroleum ether. The product was identified by elemental analysis (calculated for $C_{11}H_{10}N_4$, 66.6% C, 5.0% H, 28.3% N; found, 66.4% C, 5.2% H, 28.1% N) and infrared spectroscopy.

Reagents, solutions and apparatus

Stock solutions included an aqueous solution (1 g l^{-1}) of 2,2'-dipyridylketone hydrazone (DPKH), a copper(II) nitrate solution containing 0.9730 g Cu^{2+} l^{-1} standardized iodometrically [12], and a mercury(II) nitrate solution containing 0.9830 g Hg^{2+} l^{-1} standardized complexiметrically [13]. A buffer solution of pH 1.9 (HCl—KCl) was prepared according to Clark and Lubs.

A Fika 55 MK II spectrofluorimeter, a Crison digital pH-meter with combined electrode, and a Perkin-Elmer 577 i.r. spectrometer were used.

Procedure for determination of copper(II)

To 2 ml of 3.2 × 10^{-5} M DPKH solution in a 25-ml volumetric flask was added the volume of copper(II) solution needed to ensure a final cation concentration between 0.4 and 1 ppb. The solutions were mixed gently and after 90 min, 10 ml of 0.7 M HCl solution was added. The mixture was diluted to the mark with deionized water. The fluorescence was measured within 180 min (λ_{ex} = 349 nm, λ_{em} = 435 nm). It was essential that the pH of the solution before the acid addition was the same for all samples, and that it was between 6 and 8.

Procedure for determination of mercury(II)

To 1 ml of 7.57 × 10^{-4} M DPKH solution in a 25-ml volumetric flask was added the volume of mercury(II) solution needed to ensure a final cation concentration between 80 and 320 ppb. The mixture was shaken gently and 150 min was allowed to elapse before 10 ml of buffer pH 1.9 was added. The solution was diluted to the mark with deionised water and the fluorescence intensity was measured after 60 min (λ_{ex} = 359 nm, λ_{em} = 435 nm). The pH of the solution before addition of buffer had to be the same for all samples (between 6 and 8).

Isolation of the oxidation product

DPKH (0.5 g) was dissolved in ca. 10 ml of water. Several drops of a copper(II) nitrate solution (0.03 g Cu^{2+} l^{-1}) were added, followed by 0.1 M sodium hydroxide until the solution was alkaline. The mixture was heated on a steam bath for 20—30 min and then concentrated on a rotary evaporator. After cooling to room temperature, crystals appeared in the form of fine yellow needles. The product was recrystallized from water.

RESULTS AND DISCUSSION

Nature of the fluorescence

When dilute solutions of DPKH and Cu(II), Hg(II), Co(II) or Mn(II) were mixed in neutral solution, a blue fluorescence, which increased noticeably at acidic pH values, appeared. The following further observations were made: the fluorescence of fresh DPKH solutions at room temperature was found to increase progressively with time. After a few months, the fluorescence was identical to that obtained after heating for a few hours at 80—90°C, or at a room temperature in the presence of Cu(II), Hg(II), Co(II) or Mn(II). Oxidizing reagents such as potassium bromate, potassium iodate, hydrogen peroxide, etc, also produced a rapid increase in fluorescence. In the presence of Cu(II), Hg(II), Co(II) or Mn(II), fluorescence did not develop when the solutions were previously deoxygenated with nitrogen.

EDTA also prevented quick development of the fluorescence by Cu(II), Hg(II), Co(II) or Mn(II), but once the fluorescence had developed, addition of EDTA did not affect it.

It is apparent that traces of Cu(II), Hg(II), Co(II), or Mn(II) have a catalytic effect on the aerial oxidation of DPKH, giving rise to a product that in an acidic medium shows an intense blue fluorescence. This fluorescent oxidation product was isolated. Its i.r. spectrum when compared with that of the DPKH, revealed bands corresponding to aliphatic C—H vibrations, while bands corresponding to N—H amine vibrations disappeared. The mass spectrum gave a molecular ion at m/z = 196, compared with the one at m/z = 198 for DPKH itself. This confirms that oxidation had taken place. A detailed study of both spectra indicated that formation of the following azo derivative had probably occurred.

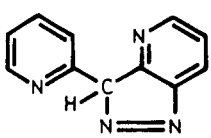

The increase in fluorescence at acid pH values may be ascribed to protonation of the pyridine nitrogen, with formation of an intramolecular hydrogen bond with the nitrogen atom of the azo group; this effect would augment the rigidity and the planarity of the molecule.

The DPKH—copper(II) system

Figure 1(a) shows the excitation and emission spectra of DPKH and its oxidation product. In the absence of the metal ion, no fluorescence was observed, while in its presence fluorescence of the oxidation product was observed at pH 0.4 (λ_{ex} = 349 nm, λ_{em} = 435 nm).

There were clearly two stages in the production of the fluorescent product, the first leading to formation of the oxidation product at approximately

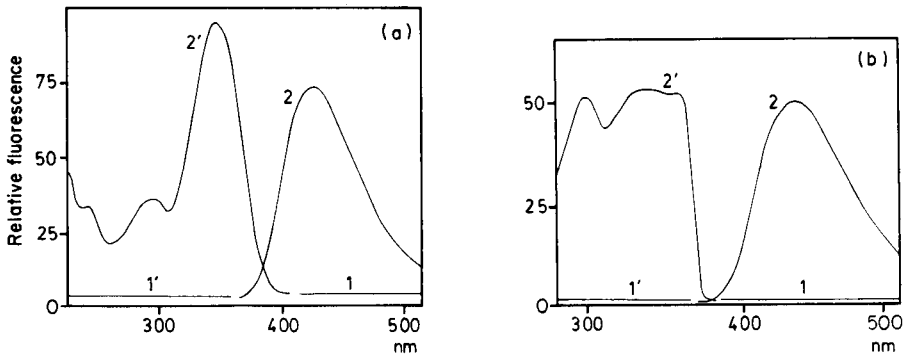

Fig. 1. DPKH excitation (1',2') and emission (1, 2) spectra in presence (2',2) and absence (1',1) of the metal ion. (a) 0.01 ppm Cu(II); [DPKH] = 4×10^{-7} M; pH 0.4; sensitivity × 40; λ_{ex} = 349 nm; λ_{em} = 435nm. (b) 0.5 ppm Hg(II); [DPKH] = 6×10^{-5} M; pH 2; sensitivity × 10; λ_{ex} = 359nm; λ_{em} = 435nm.

neutral pH and the second producing the fluorescent product at a much lower pH value. A period of at least 90 min was needed to complete the first stage, while the fluorescence could be determined immediately after the final pH adjustment.

Figure 2(a) shows the effect of the final pH (second stage) on the intensity of the fluorescence of the oxidation product. The optimum pH was between 0.3 and 0.5; the optimum pH of the first stage was between 5 and 8. The intensity of fluorescence of the oxidation product at pH 0.4 remained approximately constant between 18 and 22°C; at higher temperatures the fluorescence diminished. The fluorescence intensity was stable for at least 3 h at room temperature. For the cation concentrations studied, reagent concentrations above 6×10^{-5} M must not be employed, otherwise inner

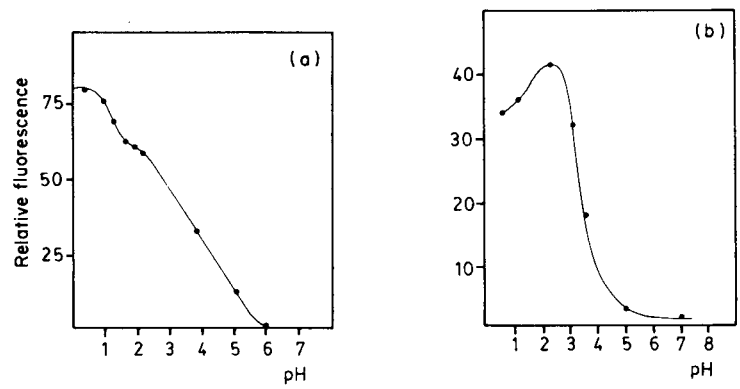

Fig. 2. pH influence on the fluorescence of the systems. (a) DPKH—Cu(II) system: [Cu(II)] = 2×10^{-7} M; [DPKH] = 4×10^{-7} M; sensitivity × 40; λ_{ex} = 349nm; λ_{em} = 435nm. (b) DPKH—Hg(II) system: [Hg(II)] = 4×10^{-6} M; [DPKH] = 6×10^{-5} M; sensitivity × 10; λ_{ex} = 359nm; λ_{em} = 435nm.

filter effects will be obtained. A concentration of 2.6×10^{-6} M DPKH was chosen since, although higher concentrations (up to 6×10^{-5} M) could be employed, it was found that such concentrations necessitated a standing time of more than 5 h for the first step with the result that the procedure became unsuitable for routine work.

Under the recommended conditions, a linear relationship existed between the fluorescence intensity and copper(II) concentration in the range 0.4—1 $\mu g\ l^{-1}$. For eleven samples containing 0.5 ppb copper(II), the relative standard deviation was 4.5% ($\alpha = 0.05$).

Interferences. The maximum tolerable concentrations of several ions in the determination of 0.5 ppb copper(II) were established (Table 1). Many ions did not affect the determination of copper(II) when they were present in 100-fold amounts. Another group of ions interfered at concentrations 10 times higher than that of copper(II). The influence of EDTA was severe, presumably because the chelated copper(II) ion did not catalyse the oxidation of DPKH.

The DPKH—mercury(II) system

Figure 1(b) shows the excitation and emission spectra of the oxidation product of DPKH produced by using mercury(II) as the catalyst. The emission spectrum coincides with that obtained with copper(II) as catalyst, while the excitation spectrum is slightly different. The oxidation product obtained is in all probability the same as that formed when copper(II) is used as the catalyst, but the reagent concentrations needed with mercury(II) are 100 times higher than those needed for the copper(II)—DPKH system, thus the differences in the excitation spectra can be ascribed to the formation of molecular associations.

In the mercury(II)-catalysed oxidation of DPKH, the minimum time for the first stage was 150 min. In the second stage it was necessary to wait for 60 min before the fluorescence was measured. The maximum fluorescence was emitted at a pH of 1.9 (Fig. 2b). The influence of temperature was

TABLE 1

Concentrations of foreign ions tolerated (error 4.57%) for 0.5 ppb copper(II)

Amount tolerated (ppb)	Ion
50[a]	Mg(II), Ca(II), Ba(II), Sr(II), Zn(II), Cd(II), Mn(II), Pb(II), UO_2^{2+}, F^-, NO_3^-, SO_4^{2-}, AsO_4^{3-}, acetate
5	Be(II), Ni(II), Al(III), Fe(III), Cr(III). Th(IV)
0.5	EDTA

[a]Largest amount examined.

identical to that described for the copper(II) system, and measurements were made between 18 and 22°C. The optimum concentration of reagent for the studied interval of mercury(II) concentrations was between 1.5×10^{-5} and 3.0×10^{-5} M. The intensity of fluorescence reached 60 min after the samples were prepared and was constant for at least 3 h.

It is of interest that, after acidification, fluorescence remains constant for the copper(II)—DPKH system, whereas for the mercury(II)—DPKH system a period of 60 min must elapse before stable readings are achieved. This is a consequence of the fact that for the copper(II)—DPKH system, the maximum fluorescence is obtained at pH 0.4 for an excitation wavelength of 349 nm, and this is sufficiently acidic to stop the primary reaction. In contrast, for the mercury(II)—DPKH system maximum fluorescence is obtained at pH 1.9 for excitation at 359 nm, and this pH is insufficiently acidic to stop the primary reaction.

Under the conditions recommended in the Experimental section, a linear relationship between concentration and the fluorescence intensity was obtained in the range 80—320 ppb mercury(II). Eleven samples at a concentration of 200 ppb mercury(II) gave a relative standard deviation of 2.07% ($\alpha = 0.05$).

Interferences. In the determination of 240 ppb mercury(II), foreign ions were tolerated at the levels indicated in Table 2. Cu(II), Be(II), Pd(II) and EDTA interfered most severely. Ions such as Co(II), Ni(II), Zn(II), Al(III), Ga(III) and Th(IV) also interfered at levels lower than that of mercury(II). Many further ions interfered when they were present in a foreign ion/Hg(II) ratio exceeding 40.

Conclusion

The catalytic action of copper(II) and mercury(II) ions on the autoxidation of DPKH is useful in establishing sensitive fluorimetric methods for ions that have rarely been studied and determined by this technique. The great sensitivity of the copper(II) method is especially noteworthy. The determination of mercury(II) suffers from a large number of interferences and is

TABLE 2

Concentrations of foreign ions tolerated (error 2.07%) for 240 ppb mercury(II)

Amount tolerated (ppb)	Ion
10000	Mg(II), Ca(II), Sr(II), Cd(II), F^-, NO_3^-, AsO_4^{3-}, oxalate, tartrate
1000	Mn(II), Pb(II), UO_2^{2+}, VO_3^-, PO_4^{3-}
80	Co(II), Ni(II), Zn(II), Ga(III), Cr(III)
40	Al(III), Fe(III), Th(IV)
8	Be(II), Pd(II), EDTA
0.1	Cu(II)

less sensitive, but it remains of interest in view of the small number of fluorimetric methods for the determination of this element.

REFERENCES

1 M. Katyal and Y. Dutt, Talanta, 22 (1975) 151.
2 F. Grases, PhD Thesis, Universitad de Palma de Mallorca, 1978.
3 G. Oshima and K. Nagasawa, Chem. Pharm. Bull. (Tokyo), 18 (1970) 687.
4 J. Holzbecher and D. E. Ryan, Anal. Chim. Acta, 64 (1973) 333.
5 L. Zelter, Z. Maksimyeheva and E. Talipov, Ref. Zh. Khim., (1970) 196 D, Abstr. 1685.
6 N. Iritani, T. Miyahara and I. Takahashi, Jpn. Anal., 17 (1968) 1075.
7 B. W. Bailey, R. M. Dagnall and T. S. West, Talanta, 13 (1966) 1661.
8 K. Ritchie and J. Harris, Anal. Chem., 41 (1969) 163.
9 E. A. Bozhevol'nov, Tr. VN 11 Khim. Reakt., No. 24, Goskhimydat, 1960.
10 A. V. Konstantinov, L. M. Korobochkim and G. V. Anastasina, Tr. Novoi Appl. Method, 5 (1967) 167.
11 Y. Yamane, M. Miyazaki and M. Ohtawa, Jpn. Anal., 18 (1969) 750.
12 A. I. Vogel, A Text-book of Quantitative Inorganic Analysis, Longman, London, 1961.
13 H. Pribil, Komplexone in der Chemischen Analyse, VEB Deutscher Verlag der Wissenschaften, Berlin, 1961.

Analytica Chimica Acta, 119 (1980) 367—374

DOSAGE DES COMPOSES PHENOLIQUES DANS LES EXTRAITS VEGETAUX PAR OXYDATION CUIVRIQUE EN MILIEU NON AQUEUX

JEAN BILLOT

Laboratoire d'Etudes des Composés Phénoliques, Université d'Orléans, 45046 Orléans Cédex (France)

(Reçu le 24 mars 1980)

SUMMARY

(The spectrophotometric determination of phenolic compounds in vegetable extracts by oxidation with copper(II) in nonaqueous media)

Oxidation with copper(II) in nonaqueous medium is used for the *o*-diphenolic compounds chlorogenic acid, rutin, pyrocatechol and epicatechol. A spectrophotometric study of the *o*-diphenol and *o*-quinone forms leads to the establishment of two systems of equations for the determination of these compounds. This study complements earlier results. The validity of the method is discussed on the basis of results obtained with Passe-crassane pear extracts.

RESUME

L'oxydation par les ions Cu(II) en milieu non aqueux est réalisée sur les composés *o*-diphénoliques témoins: acide chlorogénique, rutine, catéchine et épicatéchine. L'étude des spectres d'absorption des formes phénoliques (non oxydées) et *o*-quinoniques (oxydées) permet d'établir deux systèmes d'équations pour le dosage de ces composés, complétant ainsi les résultats obtenus précédemment par d'autres auteurs. L'application de la méthode aux extraits végétaux est donnée avec la poire Passe-crassane.

Dans le cadre d'une étude des composés phénoliques de la poire Passe-crassane au cours de la croissance et de la maturation du fruit, nous avons été amené à préciser les méthodes utilisées pour doser ces composés dans les extraits: acide chlorogénique (acide caféyl-3-quinique) prédominant, dérivés *p*-coumariques, hétérosides de flavonols et catéchines [1]. Utilisant les propriétés réductrices des *o*-diphénols, Delaporte et Macheix [2, 3] ont montré qu'il est possible de les oxyder stoechiométriquement en milieu anhydre, par les ions Cu(II), en *o*-quinones stables dans le milieu acétonitrile—acide formique. Les monophénols et les *m*-diphénols ne réagissent pas dans ces conditions. Ceci permet de doser l'acide chlorogénique, les hétérosides de flavonols (dérivés de la quercétine) et les catéchines dans des extraits végétaux selon la méthode mise au point sur des extraits de pomme [4] et utilisée pour d'autres fruits, notamment la pêche [5].

L'article présent a pour but de reprendre une étude aussi complète que possible de cette méthode de dosage par oxydation cuivrique et de montrer

son application à des extraits de pelure de poire Passe-crassane dans lesquels les flavonols sont en quantité relativement importante.

PARTIE EXPERIMENTALE

Témoins utilisés

L'oxydation par les ions Cu(II) a été faite en utilisant les témoins suivants: acide chlorogénique (acide 3-(3,4-dihydroxycinnamoyl)quinique; produit Aldrich-Europe), rutine (quercétine-3-rutinoside; produit Fluka puriss-chr.), (-)-catéchine (produit Fluka, puriss-chr.), et (+)-épicatéchine (produit Aldrich-Europe).

Extraits végétaux

Il s'agit de pelure (épiderme et quelques assises sous-épidermiques) de poires Passe-crassane récoltées en octobre 1976 et 1977. Chaque extraction est faite sur 2 g de poudre lyophilisée. Les méthodes d'extraction et de purification ont été précedemment décrites [1, 6]: extraction en continu selon Alibert et al., [7], successivement par 2 l de méthanol 80%, 1 l du mélange acétate d'éthyle—méthanol (1 + 1 en volume) et 0,5 l de méthanol 20%. Dans ces conditions l'extraction des composés phénoliques est complète. L'extrait brut aqueux obtenu après élimination des solvants organiques et dépigmentation par l'éther de pétrole est traité 5 fois volume à volume par l'acétate d'ethyl après addition de 2% d'acide métaphosphorique, 20% de sulfate d'ammonium et 20% d'éthanol selon [8]. Après évaporation sous vide, les composés phénoliques sont transférés dans le mélange acétonitrile—acide formique (3 + 1 en volume).

Oxydation

L'oxydation est réalisée par l'acétate de cuivre en solution dans l'acide propionique selon le protocole expérimental décrit par Macheix et Delaporte [4]: après avoir enregistré le spectre d'absorption de l'extrait dans l'acétonitrile—acide formique, l'acétate de cuivre est ajouté dans la cuve du spectrophotomètre 0,5 μl par 0,5 μl et l'oxydation suivie à 289 nm, la fin de l'oxydation étant marquée par une remontée de l'absorption. Le spectre de l'extrait oxydé est alors enregistré. Le dosage des *o*-diphénols est également fait en ajoutant de l'acétate de cuivre en excès (quelques gouttes) et en mesurant la variation d'absorbance à 395 et à 695 nm, avec correction à 395 nm de l'absorption due au cuivre en excès [5].

RESULTATS

Etude des composés témoins

Sur la Fig. 1 sont représentés les spectres d'absorption des formes non oxydées et oxydées (Cu(II) non en excès) pour les composés étudiés: acide chlorogénique, rutine et catéchine. On note l'existence de points isobestiques pour lesquels l'absorption ne varie pas au cours de l'oxydation.

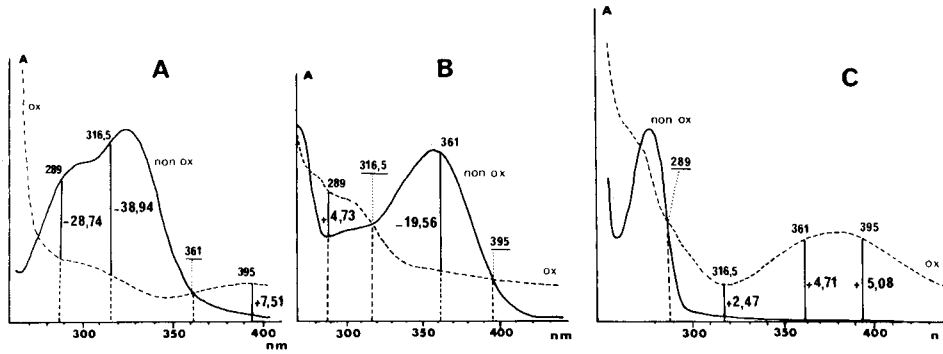

Fig. 1. Spectres d'absorption des formes phénoliques (non oxydées) et des formes *o*-quinoniques (après oxydation par les ions Cu(II)) pour l'acide chorogénique (A), la rutine (B) et la catéchine (C). Pour les 4 longueurs d'onde retenues (289; 316,5; 361 et 395 nm) les différences des coefficients d'extinction décimaux, $\Delta a = a$ (oxydé) $- a$ (non-oxydé), sont indiquées.

Pour la catéchine et l'épicatéchine (Fig. 1, C), le point isobestique se situé à 289 nm, valeur identique à celle indiquée par Macheix et Delaporte [4]. Pour l'acide chlorogénique, la Fig. 2 (A) montre que le point isobestique correspond à 361 nm, valeur très proche de celle donnée préalablement, 362 nm [4]. La Fig. 1 (B) correspondant à la rutine montre qu'il y a pour ce composé deux points isobestiques: l'un correspond à celui déterminé préalablement, 395 nm [4]. Le second point isobestique est situé à 316,5 nm (Fig. 2B).

Variations des coefficients d'extinction au cours de l'oxydation (Fig. 1). Pour les 4 longueurs d'onde correspondant aux 4 points isobestiques déterminés ci-dessus (289; 316,5; 361 et 395) on a déterminé, pour chaque composé, les variations des coefficients d'extinction décimaux: $\Delta a_\lambda = a_\lambda$ (oxydé) $- a_\lambda$ (non oxydé), comme il peut y avoir soit diminution soit augmentation de l'absorbance au cours de l'oxydation, selon la longueur

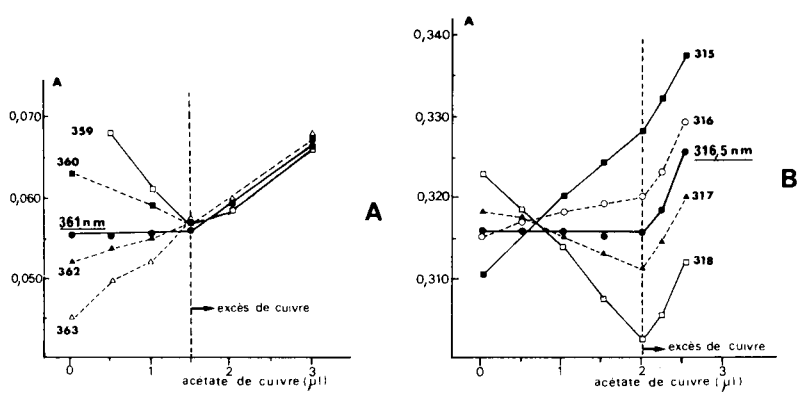

Fig. 2. Détermination des points isobestiques lors de l'oxydation par les ions Cu(II): (A) pour l'acide chlorogénique; (B) pour la rutine.

d'onde et selon le composé, il y a lieu de faire attention au signe de la variation Δa. Les valeurs sont portées sur la Fig. 1. Les résultats sont identiques avec la catéchine et l'épicatéchine.

Equations pour le dosage de l'acide chlorogénique, de la rutine et de la catéchine

Choix de trois longueurs d'onde. Etant donné que l'on dispose de 4 longueurs d'ondes caractéristiques pour lesquelles on mesure les variations d'absorbance au cours de l'oxydation et qu'il y a trois composés à doser en mélange, il suffit de choisir trois longueurs d'onde pour établir un système de trois équations à trois inconnues. Théoriquement 4 systèmes d'équations peuvent être envisagés en choisissant les longueurs d'onde: (1) 316,5 — 361 —395 nm; (2) 289 — 361 — 395 nm; (3) 289 — 316,5 — 361 nm; (4) 289 — 316,5 — 395 nm.

Un calcul d'erreur sur les formules obtenues pour les concentrations en acide chlorogénique (ACQ), rutine (RUT) et catéchines (CAT) montre que les systèmes (1) et (2) donnent les meilleurs précisions, ce qui est vérifié en appliquant ces formules à des mélanges de témoins. Par exemple pour une solution renfermant de la rutine (20 μg ml^{-1}), de l'acide chlorogénique (40 μg ml^{-1}) et de la catéchine (20 μg ml^{-1}), on obtient pour la rutine: (1) et (2) 19,9 μg ml^{-1} (erreur $< 1\%$); (3) 19,3 μg ml^{-1} (erreur de 3,5%) et (4) 21,1 μg ml^{-1} (erreur de 5,5%). Il en est de même avec l'acide chlorogénique et les catéchines. Donc seuls ont été retenus ici les systèmes (1) et (2).

Equations avec le système (1): 316,5, 361 et 395 nm. Dans ce système, on se place aux deux points isobestiques de la rutine (316,5 et 395 nm) et à celui de l'acide chlorogénique (361 nm), sans utiliser la longueur d'onde 289 nm pour laquelle un très faible excès d'ions Cu(II) peut entrainer une erreur importante. La résolution du système de 3 équations donne les concentrations en μg ml^{-1}:

$$\begin{aligned} \text{ACQ} &= -23{,}482\ \Delta_{316{,}5} + 11{,}417\ \Delta_{395} \\ \text{RUT} &= 8{,}348\ \Delta_{316{,}5} - 51{,}125\ \Delta_{361} + 43{,}342\ \Delta_{395} \\ \text{CAT} &= 34{,}668\ \Delta_{316{,}5} + 179{,}994\ \Delta_{395} \end{aligned} \qquad (1)$$

$\Delta_{316{,}5}$, Δ_{361} et Δ_{395} sont définis comme précédemment: A (oxydé) — A (non-oxydé), et positifs ou négatifs.

Equations avec le système (2): 289, 361 et 395 nm. Ce système correspond à celui utilisé par Macheix et Delaporte [4]. Les concentrations en μg ml^{-1} sont:

$$\begin{aligned} \text{ACQ} &= -32{,}883\ \Delta_{289} - 7{,}901\ \Delta_{361} + 7{,}326\ \Delta_{395} \\ \text{RUT} &= 11{,}690\ \Delta_{289} - 48{,}316\ \Delta_{361} + 44{,}797\ \Delta_{395} \\ \text{CAT} &= 48{,}548\ \Delta_{289} + 11{,}665\ \Delta_{361} + 186{,}035\ \Delta_{395} \end{aligned} \qquad (2)$$

Dosage des o-diphénols à 395 nm. Bureau-Berthauld [5] décrit une méthode de dosage des "*o*-diphénols totaux" basée sur la mesure de la variation d'absorbance à 395 nm lors de l'oxydation par les ions Cu(II),

dont l'intérêt est d'être beaucoup moins sensible à l'excès de cuivre. Il faut remarquer que le terme d' "*o*-diphénols totaux" utilisé, correspond à l'ensemble "acide chlorogénique + catéchines" qui n'est assimilable aux "*o*-diphénols totaux" que si les flavonols sont en très faible concentration par rapport aux catéchines et à ACQ.

Les *o*-diphenols dosés à 395 nm sont exprimés en équivalents d'acide chlorogénique. La détermination de la concentration en acide chlorogénique, composé en général prédominant, étant faite avec une bonne précision à partir des équations établies ci-dessus, on peut en déduire la concentration en catéchines (exprimée en équivalent acide chlorogénique):

$$\text{CAT (équiv. ACQ)} = [\text{ACQ} + \text{CAT}]\ \text{(équiv. ACQ)} - \text{ACQ}$$

La concentration en catéchines s'obtient en multipliant par 1,48, rapport des Δa_{395} de la catéchine et de l'acide chlorogénique (voir Fig. 1). Cette méthode permet donc non seulement le dosage des *o*-diphénols (ACQ + CAT), mais, connaissant la concentration en ACQ, la détermination de la concentration en catéchine que l'on peut comparer aux valeurs obtenues à partir des équations précédentes.

Application: extraits de pelure de poire Passe-crassane

Comme exemple d'application des équations de dosage mises au point, nous avons choisi 5 lots de pelure de poires Passe-crassane, soit au cours de la maturation normale à + 15°C pour des fruits récoltés en octobre 1976 et conservés deux mois à 0°C, soit à la récolte en octobre 1977 (voir Tableau 1). Les données expérimentales sont tirées du travail de Le Goff [9] réalisé dans ce laboratoire.

La difficulté de la méthode de dosage utilisant les équations du système (2), 289, 361 et 395 nm, réside dans la détermination de la fin de l'oxydation sans qu'il y ait excès de Cu(II). Il est difficile d'éviter un très léger excès d'ions Cu(II). Or, pour des longueurs d'onde inférieures à 300 nm, l'absorption de l'acétate de cuivre en solution dans l'acide propionique augmente très rapidement ainsi que le montre la Fig. 3 où est indiqué le rapport entre l'absorbance à une longueur d'onde donnée et l'absorbance au maximum d'absorption dans le visible à 695 nm. A 289 nm l'absorbance est 20 fois plus élevée qu'à 635 nm de sorte qu'un léger excès de cuivre, se traduisant par une variation très faible de l'absorbance à 695 nm, par exemple 0,002, correspond à une augmentation de 0,040 à 289 nm. Comme à 289 nm il y a diminution de l'absorbance au cours de l'oxydation par Cu(II), la valeur absolue de Δ_{289} se trouve diminuée s'il y a un léger excès de cuivre, et l'acide chlorogénique peut être nettement sous-estimé. Il y a donc lieu de tenir compte du faible excès de cuivre à la fin de l'oxydation (mesure à 695 nm) pour faire une correction de Δ_{289} si cela est nécessaire.

Une comparaison des résultats obtenus par les deux systèmes d'équations (1) et (2) est donnée dans le Tableau 1. Les valeurs sont pratiquement identiques (erreur maximale de 4%, le plus souvent erreur de l'ordre de 1%)

TABLEAU 1

Dosage des composés phénoliques dans la pelure des poires Passe-crassane, au cours de la maturation normale à + 15°C

Lots		I	II	III	IV	V
		Pelures 1976				Pelure 1977
Nombre de jours à + 15°C[a]		7	9	16	23	0
ACQ[b]	(1)	2,06	1,55	1,84	1,96	2,81
	(2)	2,04	1,49	1,84	1,93	2,81
	[c]	1,91	1,35	1,71	1,78	2,74
RUT[b]	(1)	0,79	0,83	0,81	0,92	0,40
	(2)	0,80	0,85	0,80	0,93	0,40
	[c]	0,84	0,90	0,86	0,99	0,43
CAT[b]	(1)	1,76	2,59	2,25	2,30	6,32
	(2)	1,79	2,68	2,24	2,34	6,33
	[c]	1,97	2,91	2,43	2,57	6,42
o-Diphénols (en équivalents ACQ)		3,44	3,44	3,51	3,47	7,19

[a] Fruits récoltés en octobre et conservés à 0°C pendant 12 semaines avant d'être placés à l'obscurité à + 15°C.

[b] (1), (2): système d'équations (voir texte). Tous les resultats sont en mg g^{-1} (sec).

[c] En négligeant les flavonols à 289 nm selon Macheix et Delaporte [4].

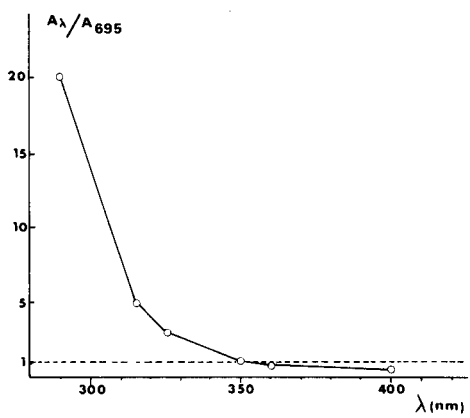

Fig. 3. Acétate de cuivre en solution dans l'acide propionique. Variation du rapport de l'absorbance à une longueur d'onde donnée sur l'absorbance au maximum d'absorption dans le visible (695 nm).

pour les concentrations en acide chlorogénique, en hétérosides de flavonols (rutine) et en catéchines, lorsqu'on utilise les équations du système (1) sans correction et les équations du système (2) avec correction de Δ_{289} (voir ci-dessus).

Les calculs faits en négligeant la variation d'absorption des flavonols à 289 nm au cours de l'oxydation, selon Macheix et Delaporte [4] conduisent aux résultats suivants (Tableau 1): (1) sous-estimation de l'acide chlorogénique de 6—9%, sauf pour la pelure des fruits de 1977 plus pauvre en flavonols où la sous-estimation n'est que de 2,5%; (2) sur-estimation des hétérosides de flavonols de 5—7,5%; (3) sur-estimation des catéchines de 8—10%. Lorsque les flavonols sont relativement abondants, cas des extraits de pelure, l'approximation ci-dessus [4] conduit à des erreurs non négligeables.

Comparaison des différents lots de pelure (Tableau 1)

Les lots de pelure choisis ne sont donnés que comme exemple d'application des méthodes de dosage proposées. Ils sont trop fragmentaires pour permettre de tirer des conclusions quant à l'évolution des composés phénoliques au cours de la maturation de la poire Passe-crassane ce qui sortirait du cadre de cet article. On peut seulement noter que les teneurs en hétérosides de flavonols restent remarquablement constantes au cours de la maturation alors que les concentrations en acide chlorogénique et en catéchines évoluent en sens inverse. La pelure de fruit récolté en octobre 1977 est caractérisée par une faible teneur en hétérosides de flavonols et une teneur très élevée en catéchines, en rapport avec les conditions climatiques pendant la croissance du fruit [1].

DISCUSSION

Les équations proposées pour le dosage de l'acide chlorogénique, des hétérosides de flavonols (dérivés de la quercétine) et des catéchines, complètent celles données par Macheix et Delaporte [4]. Lorsque les flavonols sont relativement abondants, on ne peut négliger leur variation d'absorption à 289 nm lors de l'oxydation, car ceci entraine une sous-estimation de l'acide chlorogénique pouvant atteindre près de 10%. Un excès de cuivre même minime entraine une erreur par défaut de Δ_{289} et de la concentration en acide chlorogénique. Comme il est difficile d'apprécier exactement (sans dispositif spécial d'enregistrement en continu) le moment où l'oxydation par les ions Cu(II) est terminée sans qu'il y ait excès de ceux-ci, le système d'équations (2), 289, 361 et 395 nm, est d'emploi délicat, nécessitant souvent une correction de la variation d'absorption à 289 nm pour tenir compte de l'excès de cuivre. Le système d'équations proposé utilisant les deux points isobestiques de la rutine et celui de l'acide chlorogénique, soit 316,5, 361 et 395 nm (1) est beaucoup moins sensible à un faible excès d'ions Cu(II) et nous paraît meilleur, ne nécessitant pas de correction.

Les concentrations en acide chlorogénique déterminées par oxydation

cuivrique sont très voisines de celles obtenues par d'autres méthodes de dosage spectrophotométriques [1]. Par contre, pour les flavonols, les valeurs obtenues sont beaucoup plus faibles (souvent de plus de 50%) que celles données par les dosages spectrophotométriques sur les extraits totaux. Par oxydation avec le cuivre, en milieu non aqueux, on ne dose que les *o*-diphénols (dérivés de la quercétine). Les hétérosides de flavonols monophénoliques (dérivés du kaempférol par exemple) ne réagissent pas à l'oxydation avec les ions Cu(II) dans les conditions utilisées. La méthode ne permet donc pas un dosage de tous les flavonols présents dans l'extrait, mais seulement de ceux ayant une fonction *o*-diphénolique.

La méthode de dosage proposée a été appliquée sur des extraits d'un fruit, la poire Passe-crassane dont le contenu en dérivés hydroxycinnamiques est relativement simple, ceux-ci étant représentés uniquement par des esters avec l'acide quinique: dérivés caféiques (essentiellement acide caféyl-3-quinique ou acide chlorogénique), esters *p*-coumaryl-quiniques et di-*p*-coumaryl-quinique [1]. Tous les dérivés de l'acide caféique sont assimilés à l'acide chlorogénique qui prédomine largement dans de nombreux fruits étudiés [1, 10]. De même les hétérosides de flavonols sont assimilés à la rutine. L'intérêt de la méthode est qu'elle permet de doser avec une bonne précision, sur un extrait total, les différents groupes de composés phénoliques ayant des fonctions *o*-diphénol (acide chlorogénique, catéchine, flavonols dérivés de la quercétine). Les deux premiers groupes de composés (acide chlorogénique et catéchines) interviennent comme substrats des polyphénol oxydases dans les brunissements des fruits, phénomène important d'un point de vue pratique [11, 12]. Les dérivés monophénoliques présents (esters hydroxycinnamiques, notamment dérivés de l'acide *p*-coumarique, et hétérosides de flavonols dérivés du kaempférol) étant estimés par une autre méthode spectrophotométrique (résultats non publiés), on peut obtenir ainsi la valeur du rapport monophénols/*o*-diphénols, rapport qui pourrait intervenir pour réguler la croissance et la maturation du fruit [13].

La méthode peut s'appliquer à différents matériels d'origine végétale et permet d'aborder l'évolution des composés phénoliques au cours de divers phénomènes physiologiques, en particulier la croissance et la maturation des fruits.

BIBLIOGRAPHIE

1 J. Billot, C. Hartmann, J. J. Macheix et J. Rateau, Physiol. Vég., 16 (1978) 693.
2 N. Delaporte et J. J. Macheix, Anal. Chim. Acta, 59 (1972) 273.
3 N. Delaporte et J. J. Macheix, Anal. Chim. Acta, 59 (1972) 279.
4 J. J. Macheix et N. Delaporte, Lebensm. Wiss. Technol., 6 (1973) 19.
5 D. Bureau-Berthauld, Mémoire Ingénieur C.N.A.M., Paris, 1975.
6 C. Melin, Thèse Doct. 3è cycle, Univ. d'Orléans, 1976.
7 G. Alibert, G. Marigo et A. Boudet, Physiol. Vég., 7 (1969) 57.
8 A. Fleuriet et J. J. Macheix, J. Chromatogr., 74 (1972) 339.
9 M. Le Goff, D.E.A. Université Paris VI, 1979.
10 J. J. Macheix, J. Rateau, A. Fleuriet et D. Bureau, Fruits, 32 (1977) 397.
11 J. J. Macheix, Physiol. Vég., 8 (1970) 585.
12 D. Bureau, J. J. Macheix et M. A. Rouet-Mayer, Lebensm. Wiss. Technol., 10 (1977) 211.
13 A. Fleuriet et J. J. Macheix, Physiol. Vég., 15 (1977) 239.

Analytica Chimica Acta, 119 (1980) 375—377

Short Communication

AN INTERFACIAL VOLTAIC CELL FOR MONITORING ACID—BASE REACTIONS IN NON-AQUEOUS MEDIA

BOLESŁAW WALIGÓRA and MARIA PALUCH

Department of Physical Chemistry and Electrochemistry of the Institute of Chemistry, Jagellonian University, 3 Karasia Street, 30-060 Kraków (Poland)

(Received 3rd March 1980)

Summary. The interfacial device described is based on a Pt/corundum disc/antimony scratch/0.1 M $KCl/Hg_2Cl_2/Hg/Pt$ cell. Acid—base reactions occurring at the interface of two solvents can be followed in solvents such as dry benzene, chloroform and 1,2-dichloroethane.

Various types of electrodes and cells have been suggested for potentiometric titrations in non-aqueous media [1]. The choice of electrodes and cells depends on the type of solvent and on the substance to be determined. Kamieński [2, 3] constructed an interfacial electrode for the detection of air pollutants. The essential part of the electrode consisted of a platinum scratch applied to a hard porous material, such as corundum or carborundum, placed at the solution/air interface.

In further studies on such interfacial electrodes [4, 5], the device for the detection of air pollutants was modified and different types of interfacial cell were proposed. These cells can be applied to potentiometric titrations in non-aqueous solvents, because their special construction makes it possible to monitor chemical reactions at the phase boundary of two immiscible liquids. An immersing form of the cell has already been described [4, 5]. A vessel type of the cell is described below.

Experimental

Measuring system. The interfacial voltaic cell—Pt/corundum disc/antimony scratch/0.1 M $KCl/Hg_2Cl_2/Hg$ is shown schematically in Fig. 1. It consists of platinum and calomel electrodes built into the wall of vessel A (Fig. 1), by means of ground glass joints, held firmly by springs. The system is compact and easy to operate. The side joints I and II enable the device to be taken apart for cleaning. A porous corundum disc D (5 mm diameter, 3 mm thick) is cemented to the outlet of the salt bridge B which contains a 0.1 M potassium chloride solution. The tip of the platinum wire (0.5 mm diameter) indicating electrode touches a scratch on the outer surface of the porous corundum and is thus in contact with the calomel electrode (Fig. 1). Direct contact of the two electrodes is obviously unnecessary in conducting solutions, but when non-conducting media, e.g. pure hydrocarbons are used, electric conductance

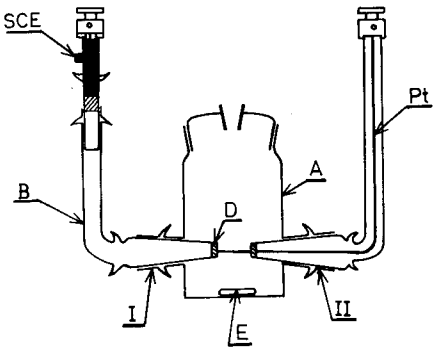

Fig. 1. The interfacial voltaic cell: A, reaction vessel of 20-ml or 50-ml capacity; SCE, calomel electrode; Pt, platinum electrode; D, corundum disc; B, salt bridge; E, stirring bar; I and II detachable side joints.

in such systems must be ensured somehow. The metallic scratch formed on the porous corundum disc wetted by the potassium chloride solution acts as the conductor in non-aqueous systems. Before each measurement, the cell is disconnected and cleaned, and the surface of the corundum disc is scratched with chemically pure antimony.

A vibron electrometer or simple valve pH meter (depending on the type of solvent) is used for measuring the changes in the e.m.f. of the interface cell. The titrant was added from a microburette in 1—0.1-ml portions. After the addition of each portion, the test solution was stirred magnetically for about 15 s. The e.m.f. of the cell was measured 30 s after each addition of titrant.

Samples and reagents. Strychnine and n-tridecylamine solutions were used as test materials. The potentiometric titrations were examined in dry benzene, methanol, 1,2-dichloroethane, chloroform, acetone and benzene—acetone and benzene—chloroform mixtures. Picric acid was used as the titrant and was dissolved in the same solvent as the titrated base.

Results and discussion

In all experiments, 5 or 15 ml of the dilute solution of an organic base were titrated. The volume of the sample may be reduced by miniaturization of the vessel described. The results obtained are shown in Figs. 2 and 3.

The course of the titration curves in methanol, chloroform, acetone and benzene and their mixtures proves that the interfacial voltaic cell is useful for the determination of organic bases in non-aqueous media. The titration curves exhibit sharp changes at the inflection point. During the titration of 0.01 M strychnine solutions with picric acid in benzene, some insoluble salts were formed; they did not interfere, however, with the determination of the base. The very distinct potential changes of the scratch electrode during the titrations are due to the fact that the chemical reaction is traced not in the bulk of the solution but at the boundary of two phases of markedly

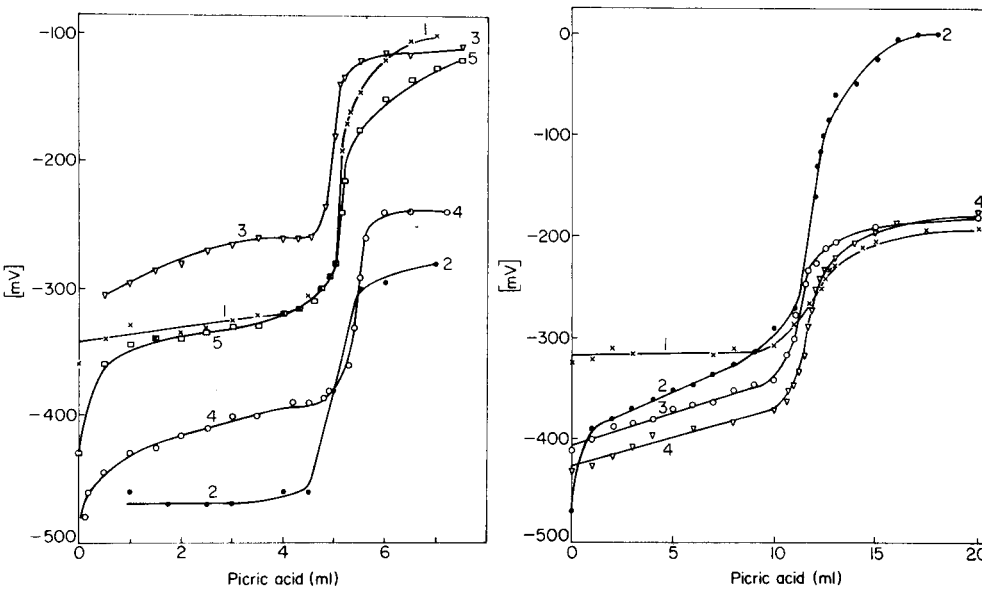

Fig. 2. Potentiometric titration curves for strychnine (0.01 M) with picric acid (0.01 M) in (1) methanol, (2) benzene, (3) 1,2-dichloroethane, (4) chloroform and (5) acetone.

Fig. 3. Potentiometric titration curves for: (1) n-tridecylamine (0.0012 M) with picric acid (0.0015 M) in chloroform; (2) n-tridecylamine (0.0107 M) with picric acid (0.0135 M) in acetone; (3) n-tridecylamine (0.013 M) with picric acid (0.0165 M) in 1% acetone—99% benzene; (4) n-tridecylamine (0.0192 M) with picric acid (0.0243 M) in 1% chloroform—99% benzene.

different dielectric constants. In such a case, the reacting substances are concentrated at the working surface (interface) of the interfacial cell.

REFERENCES

1 I. Gyenes, in Titration in nichtwässerigen Medien, Akademiai Kiado, Budapest, 1970.
2 B. Kamieński, Bull. Acad. Pol. Sci., Ser. Sci. Chim., 13 (1965) 231.
3 B. Kamieński, Report on XXIst IUPAC Congress, Prague, 1967.
4 B. Kamieński, B. Waligóra and M. Paluch, Bull. Acad. Pol. Sci., Ser. Sci. Chim., 14 (1968) 501.
5 B. Waligóra and M. Paluch, Chem. Anal. (Warsaw), 13 (1968) 421.

Analytica Chimica Acta, 119 (1980) 379—382

Short Communication

ACCURATE BACKGROUND MONITORING CIRCUIT FOR BC6-EQUIPPED VARIAN-TECHTRON AA5 AND AA6 ATOMIC ABSORPTION SPECTROMETERS

DARRYL D. SIEMER

Exxon Nuclear Idaho Co., Inc., Idaho Falls, ID 83401 (U.S.A.)

(Received 25th February 1980)

Summary. A low-cost circuit permits the accurate simultaneous measurement of both background-corrected atomic absorption spectrometric signals and background-only signals.

This communication identifies a deficiency in a circuit suggested by Herber and DeBoer [1] and gives a suggestion for improving it. The purpose of the circuit in question is to permit the simultaneous monitoring of both background-only and background-corrected atomic absorption signals with BC6-equipped Varian Techtron AA5 and AA6 instruments.

The deficiency lies in the fact that the voltage at the point in the circuitry of the BC6 module from which the simple linear circuit derives its input is a measure of the intensity of the continuum lamp signal and not a measure of the absorbance of the radiation from the lamp. Therefore, the output of the circuit is a measure of the reduction in intensity and not the measure of background absorbance as inferred.

The circuitry depicted in Fig. 1 will output a true background absorbance signal suitable for monitoring broad band absorbance or scattering error signals. The figure indicates the tie points between the circuit and the BC6 background corrector board. These include the signal input from the pre-amplifier board (TP51), the FET switch gate inputs (TP55, TP61), and the power supply and ground points (pins 11, 12 and 13).

In order to clarify the discussion of the circuitry in Fig. 1, a description of the signals present at the output pin of the photomultiplier preamplifier will be given first. One complete electronic cycle consists of three distinct time intervals. During the first (0.6 ms duration), neither the hollow-cathode lamp nor the continuum lamp are on. During the second time period (1.15 ms duration) only the continuum lamp is on. Finally, during the final interval (1.75 ms duration) only the hollow-cathode lamp is on. The reciprocal of the sum of these times is the 285-Hz frequency required by the AA5 or AA6 spectrometer demodulation circuitry. (In the case of the AA6, this circuitry will be hereafter designated as the IM6.)

Typical signals at the preamplifier output consist of negative-going pulses

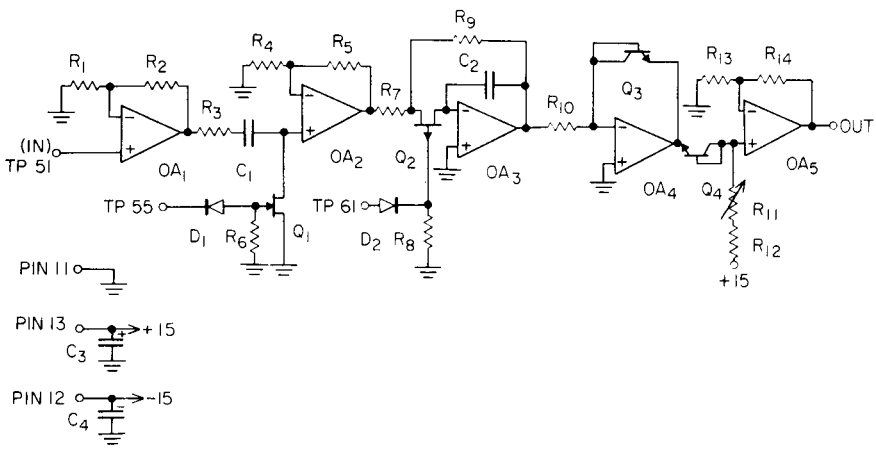

Fig. 1. Schematic of background-only monitoring circuit. (OA_1) 741 operational amplifier; (OA_{2-5}) TL084C quad bifet operational amplifier; (D_1, D_2) 1N914 silicon switching diode; (Q_1) N-FET 2N-3819; (Q_2) P-FET 2N-5460; (Q_3, Q_4) Motorolla SP5-5701. All resistors ¼ Watt, ± 5% tolerance, metal film: (R_1, R_4, R_{14}) 10k; (R_2) 56k; (R_3, R_{12}) 1k; (R_5) 100k; (R_6, R_8) 330k; (R_7, R_9) 75k; (R_{10}) 4.7k; (R_{11}) 100k ten-turn; (R_{13}) 15k; (C_1) 0.22 μF; (C_2) parallel combination of 0.5 μF and 0.22 μF (0.72 μF total); (C_3, C_4) 4.7 μF tantalum.

of approximately 50 mV amplitude from the hollow cathode and continuum lamps superimposed on an approximately −3.5 V d.c. offset voltage. At TP51 on the BC6 background corrector board, the d.c. component of this signal is discarded by coupling the signal from the preamplifier with a series capacitor.

The circuit in Fig. 1 first isolates the continuum signal and then inputs that intensity signal to a logarithmic amplifier to convert it to an absorbance value. The input signal at TP51 is first amplified by an impedance-buffering follower-with-gain (gain of 6.6) amplifier (OA_1). Then the resulting signal is zero-clamped by shortening the noninverting input of the second capacitor-coupled follower-with-gain (gain of 11) amplifier (OA_2) to ground with a FET switch (Q_1) during the 0.6 ms time period in each measurement cycle when neither the hollow-cathode lamp nor the continuum lamp is on. This signal-processing step removes any dark current (or any d.c. offset) signal component present when both lamps are off from the signal and also converts the a.c. signal to a pulsed, negative-polarity, d.c. signal.

During the period when only the continuum lamp is on, the second FET switch closes and directs the signal into the sample-and-hold circuit (OA_3). This amplifier has a first-order low-pass filter time constant determined by the magnitude of $R_9 \times C_2$ and the length of the sample-and-hold transfer pulse (0.75 ms) of the FET switch relative to the duration of an entire measurement cycle (1/285 Hz or 3.5 ms). With the component values indicated, the effective time constant of this demodulation circuit is approxi-

mately the same as that of the background-corrected a.a.s. signal from the IM6 amplifier when it is used with the least amount of damping (about 260 ms).

The output of the demodulation circuit (OA_3) is a positive-polarity d.c. voltage proportional to the intensity of continuum-source lamp light striking the photomultiplier tube. To convert this voltage to an absorbance, the signal is input to a logarithmic amplifier (OA_4 and Q_3). The output of this amplifier is a negative polarity d.c. voltage whose magnitude is determined by two factors. The first is the desired logarithmic dependence of output on input voltage. The second factor is a highly temperature-dependent offset term. In order to compensate for the offset term, the output of the logarithmic amplifier is connected in series with another identical PN junction, which is fed current through two resistors (R_{11} and R_{12}) from the positive-polarity power supply. When the zeroing potentiometer (R_{11}) is adjusted between atomizations, the positive voltage drop across Q_4 is adjusted to compensate exactly for the negative drop across the transistor (Q_3). This results in a zero volt output at the common base-collector junction of Q_4 from which point the final amplifier derives its input. Finally, the follower-with-gain amplifier (OA_5) boosts the 60 mV/decade response to reductions in intensity of the logarithmic amplifier up to a standard recorder full-scale input value of 100 mV per absorbance unit.

The entire cost of the circuit is on the order of twenty dollars and everything can be purchased at local electronics shops. None of the component values is critical and other transistors of similar characteristics can be substituted for the FETs and matched bipolar transistors indicated. If desired, operational amplifiers with characteristics more ideally suited for the specific amplifier applications may be substituted for the inexpensive, general-purpose, type 741 or TL084 models specified in Fig. 1. If the residual temperature sensitivity of the logarithmic amplifier (approximately 0.3%/degree) is a source of concern, a monolithic logarithmic amplifier (e.g., Analog Devices 755N) can be used. However, in view of the fact that the signals the circuit is designed to measure (background scatter or absorption signals observed during CRA atomic absorption experiments) possess an intrinsic variability in the range 3—15%, a great deal of concern about such circuit optimization is probably unjustified.

In order both to simplify construction and to facilitate trouble-shooting, it is suggested that the components be mounted in a small prototype test socket (e.g. QH85, Continental Specialities Corp. Box 7809, San Francisco, CA 94119) and the socket be mounted inside the BC6 chassis with wires running to the indicated tie points on the background corrector printed circuit board. The offset potentiometer and recorder output jack can be conveniently mounted in holes drilled in the front of the chassis. Of course, the circuitry can be mounted on etched copper PCB or on general-purpose wire-wrap boards if the engineering facilities are available to do so.

In order to follow the signals accurately (both a.a.s. and background

absorption) obtained with the Varian CRA 63 or CRA 90 graphite furnace atomizers, it is often necessary to use effective damping time constants of less than 50 ms [2—4]. The circuit described above will have a time constant of 35 ms if a 0.1 μF capacitor (C_2) is used in the sample-and-hold amplifier. To speed up the IM6 module so that the background-corrected a.a.s. signal has a similar time response, the following changes can be made on the IM6 photomultiplier amplifier PCB (refer to Fig. 5.13.86 in the AA6 manual). Replace C209 (0.22 μF) with a 0.02 μF capacitor and replace C212 (0.33 μF) with a 0.05 μF capacitor. These capacitors are in the feedback loop of the damping amplifier (MA 202).

These changes will reduce the low-pass filter time constant of the IM6 demodulation circuitry when in the "A" damping mode from approximately 260 ms to about 34 ms. The time constants of the IM6 used with the other "damping" switch settings will be only slightly reduced from their normal values so the signal-to-noise ratio of signals obtained when the spectrometer is used for flame atomizer work will not be degraded by the suggested modification. When the "fast" electronics are employed, it will be necessary to use either a transient recorder or a storage oscilloscope to monitor the signals accurately from the two output channels. If a typical dual-pen strip-chart recorder serves as the readout for both channels there is nothing to be gained by using effective damping time constants in either signal processing channel of less than about 200 ms.

REFERENCES

1 R. F. M. Herber and J. L. M. DeBoer, Anal. Chim. Acta, 109 (1979) 177.
2 F. J. M. J. Maessen and F. D. Posma, Anal. Chem., 46 (1974) 1439.
3 E. H. Piepmeier and L. DeGalan, Spectrochim. Acta, Part B, 31 (1976) 163.
4 D. D. Siemer and J. M. Baldwin, Anal. Chem., 52 (1980) 295.

Analytica Chimica Acta, 119 (1980) 383—387

Short Communication

FLOW INJECTION—ATOMIC ABSORPTION SPECTROMETRY WITH ORGANIC SOLVENTS

KAZUMI FUKAMACHI

Fukuoka Environmental Research Center, Dazaifu-machi, Chikushi-Gun, Fukuoka (Japan)

NOBUHIKO ISHIBASHI

Applied Analytical Chemistry, Faculty of Engineering, Kyushu University, Hakozaki, Higashiku, Fukuoka 812 (Japan)

(Received 8th January 1980)

Summary. A flow injection technique with an organic solvent carrier stream is recommended for the determination of trace elements by atomic absorption spectrometry. Carrier streams of methyl isobutyl ketone and especially n-butyl acetate are effective in enhancing sensitivity. The proposed method permits about 300 determinations per hour with a relative standard deviation of less than 5%.

The flow injection principle has been successfully applied to spectrophotometric, potentiometric, turbidimetric, fluorimetric and other analytical measurements [1, 2]. Recently, this general technique has also been coupled with atomic absorption spectrometry [3, 4], where aqueous samples were injected into a water stream. This communication deals with the enhancement of sensitivity in flow injection—atomic absorption determinations of trace metals that can be achieved by using organic solvent carrier streams.

Experimental

A Shimadzu atomic absorption spectrometer (model 610-S) was connected to a Hitachi recorder (model 056-100). Hollow-cathode lamps from Westinghouse Co. and Hamamatsu TV Co., and a Shimadzu nebulizer with a single-slot burner head were used. The spectrometer was operated at maximum sensitivity with an air—acetylene flame. A teflon tube, through which the carrier solvent flowed, was connected to the nebulizer of the burner via the sample injector as shown in Fig. 1. The length of teflon tubing (i.d. 0.8 mm) from the sample injector to the nebulizer (l_2), was varied; the length of tubing (l_1) from the carrier reservoir to the sample injector was 20 cm. The carrier flow rate depended on the aspiration rate of the nebulizer, which was accurately controlled by adjustment of the valve regulating the air flow to the nebulizer. An aliquot of the aqueous sample solution was injected with a microsyringe (capacity 100 μl) into the carrier solvent stream through a silicone rubber septum via a sample injector (Gasukuro Kogyo Co.).

All reagents and organic solvents used were of analytical grade and deionized water was used throughout.

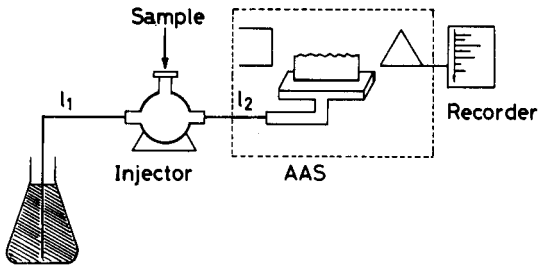

Fig. 1. Flow diagram of the flow injection—atomic absorption analysis apparatus. AAS: atomic absorption spectrometer.

Results and discussion

Response signals. In the system described, the sample is intermittently introduced into the burner flame with the carrier solvent stream. Such discontinuous introduction of the sample gives a peak form of response signal, i.e. a transient signal as illustrated in Fig. 2. The highest peaks with least tailing were obtained for an n-butyl acetate carrier stream when copper(II) served as the analyte.

Figure 3 shows the responses for repeated manual injections of aqueous copper(II) solutions (0.1—3 ppm) into the n-butyl acetate stream compared with the response for an aqueous 1 ppm copper(II) solution nebulized in the conventional fashion. The very fast return of the flow injection response to the baseline (Figs. 2 and 3) indicates the usefulness of this flow injection method for rapid analyses. It is possible to obtain the response peaks without carryover at a rate of 300 samples per hour. By way of comparison, each of the two response peaks (B) required aspiration for about 10 s from bulk sample solution. The flow injection peak corresponding to the 1 ppm sample is 1.4 times higher than the peak obtained by the conventional method.

The peak height would be expected to vary according to the injected sample volume, the carrier flow rate, the length of teflon tubing l_2, and the organic solvent used. The peak height was found to increase with the injected sample volume until it reached plateau values for 60-μl injections into a n-butyl acetate stream and for 80-μl injections into a methanol stream. The relationship between the flow rate and peak height is shown in Fig. 4. The maximum peak heights were obtained at 5—7 ml min^{-1} or more, because of the decreasing amount of the sample entering the flame at lower flow rates. As shown in Fig. 5, in the case of the n-butyl acetate stream, variation of the length of tube l_2 between 2.5 and 40 cm did not affect the peak height; this indicates that the sample was not diluted during flow, because of the immiscibility of the carrier solvent with the aqueous sample. When water and methanol carrier streams were used, the peak heights were unchanged only up to l_2 = 5 cm; the subsequent decrease with longer tubes was due to dilution.

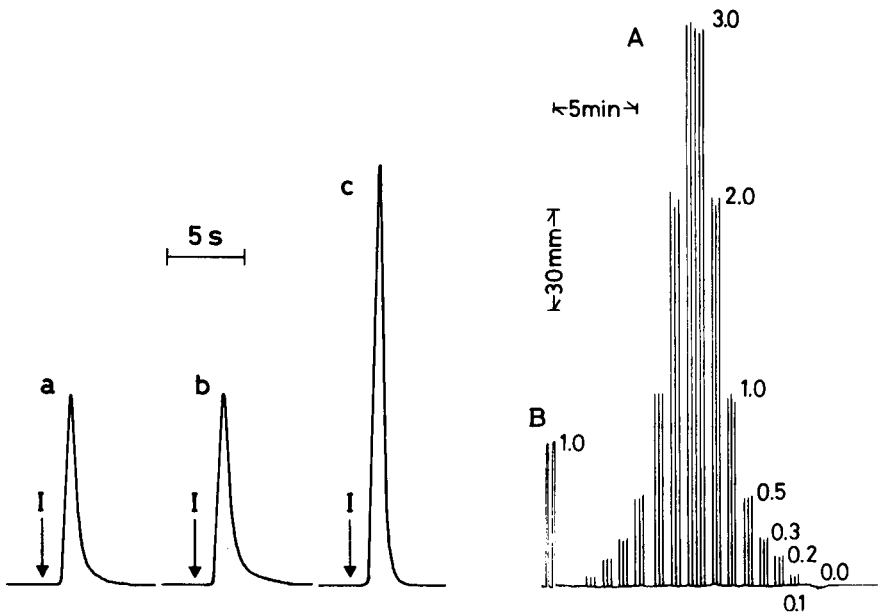

Fig. 2. Profile of response peaks. Point I indicates the time of injection of 50-μl aliquots of a 2 ppm copper(II) solution. Carrier: (a) water; (b) methanol; (c) n-butyl acetate.

Fig. 3. Response peaks and their reproducibility for the determination of copper by flow injection—atomic absorption spectrometry. (A) Flow injection peaks with a carrier flow of n-butyl acetate (6 ml min^{-1}), l_2 = 5 cm, 50-μl injections. (B) Peaks obtained by the conventional atomic absorption method. The numbers on the peaks indicate concentrations of injected (A) or nebulized (B) solutions in μg Cu ml^{-1}.

Solvent effects. Effects of carrier solvents on the peak heights for twelve analytes are listed in Table 1. The enhancement factors mean the peak height values obtained in methanol, MIBK or n-butyl acetate streams relative to the values in water streams. Except for chromium(III,VI), considerable enhancement effects were obtained for methyl isobutyl ketone (MIBK) and n-butyl acetate (n-BA) streams. Significant enhancements were not observed for methanol streams, probably because of excessive diffusion effects.

In conclusion, the proposed method is suitable for the determination of trace metals at a high sampling rate of 300 samples per hour or more. Greatly improved sensitivity can be obtained by using immiscible solvents such as n-butyl acetate or MIBK.

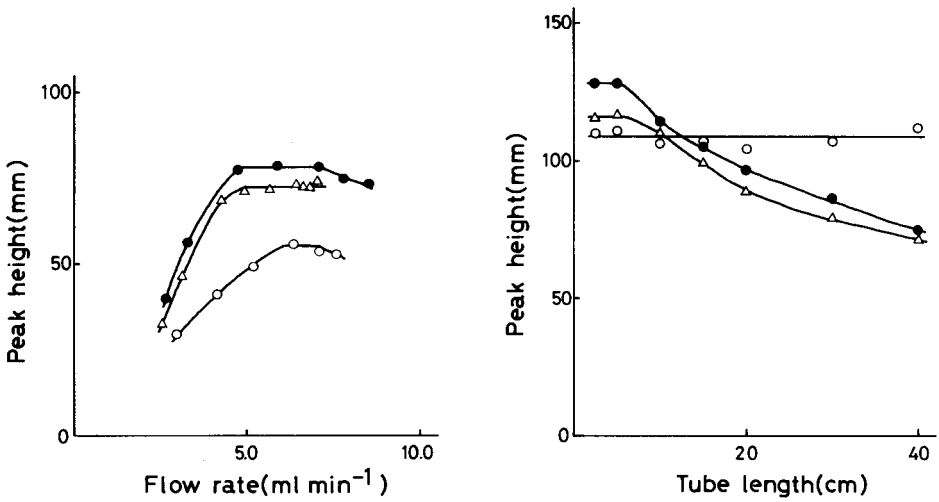

Fig. 4. Effect of flow rate on peak height for l_2 = 5 cm and different carrier streams: (△) water; (●) methanol; (○) n-butyl acetate. Injected sample: (△, ●) 3 ppm Cu; (○) 1 ppm Cu.

Fig. 5. Effect of tube length l_2 on the peak height for 50-μl injected volumes. Carriers: (△) water; (●) methanol. (○) n-butyl acetate. Concentrations: (△, ●) 2 ppm Cu; (○) 1 ppm Cu.

TABLE 1

Reproducibility and enhancement effect

Metal	Carrier	Metal concn. (ppm)	Peak height (mm)	C.v. (%)[a]	Enhancement[b]	Metal	Carrier	Metal concn. (ppm)	Peak height (mm)	C.v. (%)[a]	Enhancement[b]
	Water	2.0	111	2.8	1.0		Water	5.0	76	4.2	1.0
Zn	Methanol	2.0	111	2.2	1.0	Fe	Methanol	5.0	88	1.8	1.2
	n-BA	0.5	131	2.9	4.7		n-BA	2.0	82	2.9	2.7
	Water	1.0	79	3.9	1.0		Water	3.0	75	1.4	1.0
Cd	Methanol	1.0	75	4.1	0.9	Cu	Methanol	3.0	75	1.8	1.0
	n-BA	0.3	63	4.5	2.6		n-BA	2.0	113	2.2	2.2
	Water	5.0	64	3.3	1.0		Water	5.0	67	2.8	1.0
Co	Methanol	5.0	70	3.4	1.1	Cr(III)	Methanol	5.0	82	2.4	1.2
	n-BA	3.0	66	3.5	1.7		n-BA	5.0	68	2.1	1.0
	Water	5.0	68	3.2	1.0		Water	5.0	60	2.8	1.0
Ni	Methanol	5.0	84	2.4	1.2	Cr(VI)	Methanol	5.0	67	3.0	1.1
	n-BA	2.0	70	4.3	2.6		n-BA	5.0	61	2.5	1.0
	Water	3.0	98	2.0	1.0		Water	2.0	44	3.3	1.0
Mn	Methanol	3.0	102	2.0	1.0	Na	Methanol	—	—	—	—
	n-BA	1.0	85	2.7	2.6		MIBK	1.0	97	2.2	4.4
	Water	10.0	35	3.2	1.0		Water	5.0	53	2.6	1.0
Pb	Methanol	10.0	38	3.7	1.1	K	Methanol	5.0	66	1.8	1.2
	n-BA	5.0	43	3.7	2.5		MIBK	1.0	51	2.7	4.8

[a]Coefficient of variation computed from the observed values of 30 determinations.
[b]Ratio of peak height in organic solvent stream to that in water stream.

REFERENCES

1 J. Růžička and E. H. Hansen, Anal. Chim. Acta, 99 (1978) 37.
2 J. Růžička and E. H. Hansen, Anal. Chim. Acta, 114 (1980) 19.
3 E. G. Zagatto, F. J. Krug, H. Bergamin Fº, S. S. Jørgensen and B. F. Reis, Anal. Chim. Acta, 104 (1979) 279.
4 W. R. Wolf and K. K. Stewart, Anal. Chem., 51 (1979) 1201.

Analytica Chimica Acta, 119 (1980) 389—392

Short Communication

FLOW INJECTION DETERMINATION OF TRACE VANADIUM WITH CATALYTIC PHOTOMETRIC DETECTION

TAKESHI YAMANE*

Department of Chemistry, Faculty of Education, Yamanashi University, Takeda-4, Kofu-shi, 400 (Japan)

TSUTOMU FUKASAWA

Department of Applied Chemistry, Faculty of Engineering, Yamanashi University, Takeda-4, Kofu-shi, 400 (Japan)

(Received 10th April 1980)

Summary. A catalytic photometric detection system based on the chromotropic acid—bromate reaction is adapted to a flow injection system for the rapid, simple and sensitive determination of vanadium. Vanadium in the range 0.3—4.8 ng (10—160 ppb) can be determined at a rate of ca. 60 samples per hour.

Flow injection analysis, a simple approach to the automation of chemical analyses based on continuous flow measurements without air segmentation, has been developed by Růžička and Hansen [1, 2] and has recently received considerable attention in various fields. Good sensitivity, high sampling rate and reproducibility are considered to be the main advantages. Most applications of this technique have involved spectrophotometry based on the formation of coloured metal chelates [3—5], indophenol dye [6], molybdophosphate [1, 7] or potentiometry with ion-selective electrodes [1, 3, 6, 8, 9].

This communication describes a flow injection system for determining nanogram levels of vanadium based on catalytic photometric detection. Catalytic methods have the general advantage of combining high sensitivity with relatively simple procedures and apparatus. Measurements are usually made during the reaction, and so the reaction time and the rate of reaction become important factors in considering the sensitivity of the catalytic detection system in relation to the flow injection systems. The chromotropic acid (4,5-dihydroxynaphthalene-2,7-disulfonic acid)—bromate reaction system for determining vanadium was selected to investigate the utility of catalytic photometric detection in flow injection systems. Effects of such variables as reagent concentration, temperature, pH, diverse elements, etc. on the rate of the vanadium-catalysed oxidation of chromotropic acid by bromate have been described [10]. On the basis of these results, detailed investigations were made here to establish the optimal manifold for flow injection. It is shown that this catalytic photometric detection can be incorporated con-

veniently into a flow injection system with great advantages in sensitivity and convenience.

Experimental

Reagents. All chemicals used were of analytical grade. A standard vanadium solution (500 μg ml^{-1}) was prepared by dissolving 0.574 g of ammonium metavanadate in water and diluting to 500 ml. More dilute solutions were prepared from this stock solution by dilution. Chromotropic acid solution (1.0% w/v) was prepared daily by dissolving 1.0 g of chromotropic acid (disodium salt; Dotite Reagent) in water with the addition of 5 ml of buffer solution (pH 3.8; 10 M acetic acid and 2 M sodium acetate solution mixed in the ratio 1.6:1.0), and diluting to 100 ml with water. The bromate solution was 2% (w/v) potassium bromate in water.

Apparatus and manifold. The apparatus consisted of a model KHU-W-52 micro pump (double plunger type: Kyowa Seimitsu, Tokyo) and a model Uvidec 320 spectrophotometer (Japan Spectroscopic Co., Tokyo) equipped with a flow-through cell (light path 10 mm, volume 30 μl) and a model R-21 recorder (Rika Denki, Tokyo).

The manifold used is shown in Fig. 1, and a typical signal trace for a calibration graph is shown in Fig. 2. Reagents were pumped at 0.35 ml min^{-1}

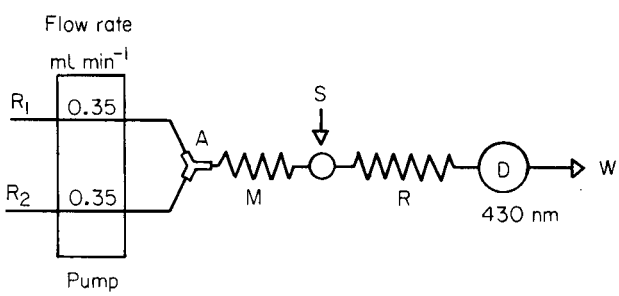

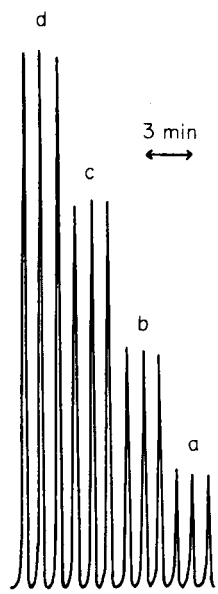

Fig. 1. Schematic diagram of the flow injection system for catalytic photometric determination of vanadium. (R_1) Chromotropic acid solution; (R_2) bromate solution; (M) mixing coil (150 cm); (R) reaction coil (300 cm); (S) sample injection; (W) waste.

Fig. 2. Typical continuous signal traces for vanadium (40—160 ppb) by flow injection analysis. (a) 1.2 ng V; (b) 2.4 ng V; (c) 3.6 ng V; (d) 4.8 ng V.

and mixed at a teflon Y-shaped joint and then in coil M (150 cm long, 0.5 mm i.d.). The sample was injected manually at point S with a Hamilton gas-tight syringe via a septum sample injector (Kyowa Seimitsu). After reaction in coil R (300 cm long, 0.5 mm i.d.), the coloured product was measured at 430 nm. All tubings and connectors were made of teflon. All reactions were conducted at room temperature. Unless otherwise stated, 30-μl aliquots of solutions were injected. Peak heights were measured.

Results and discussion

Preliminary tests were done with a 60 μg l^{-1} solution of vanadium. The sensitivity of the vanadium determination largely depended on the flow rate of the reagents; the peak height increased as the flow rate decreased (Fig. 3). Tube length for the reaction also had a considerable effect on the sensitivity:

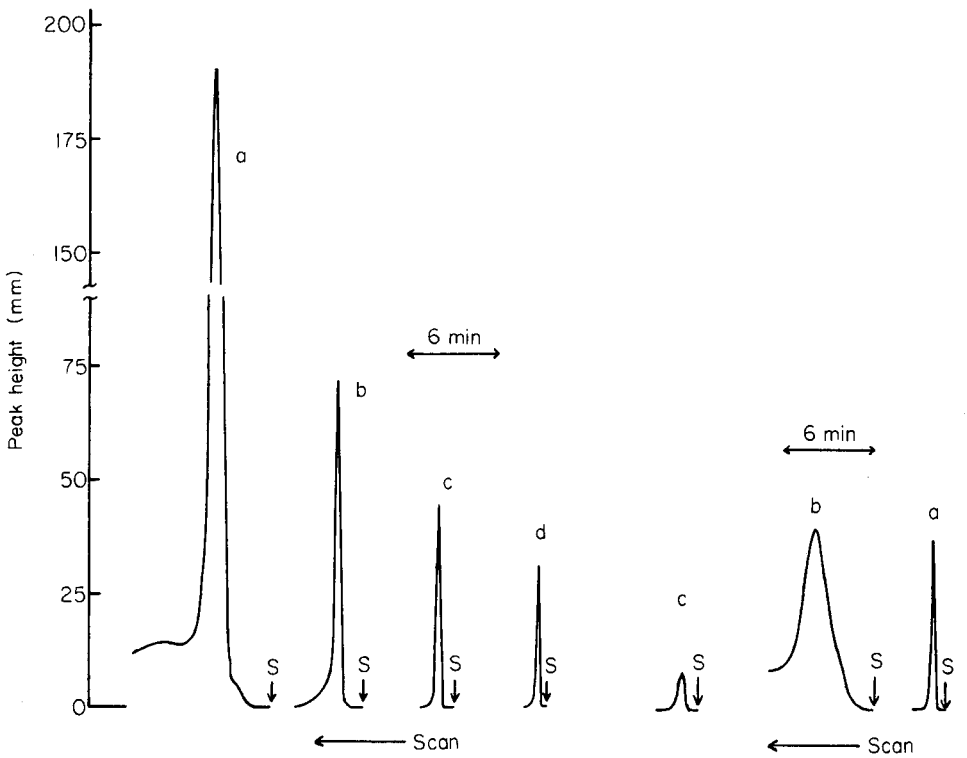

Fig. 3. Effect of the pumping rate on the peak height and shape for 1.8 ng of vanadium (V), with the same flow rates for the chromotropic acid and bromate reagents: (a) 0.1; (b) 0.23; (c) 0.35; (d) 0.5 ml min^{-1}. (S) Sample injection. Other experimental conditions and manifold as in Fig. 1.

Fig. 4. Effect of inner diameter of the reaction tube on the peak height and shape. Tubing internal diameter: (a) 0.5; (b) 1.0; (c) 1.0 mm. Flow rate of each reagent were 0.35 ml min^{-1} for (a) and (b), and 1.3 ml min^{-1} for (c). (S) Sample injection. Other experimental conditions and manifold as in Fig. 1.

increasing the length of the reaction coil from 300 cm to 500 and 800 cm increased the peak heights because the longer residence time of the sample zone allowed greater colour development by the catalytic reaction. However, peak broadening and tailing were observed at low flow rates, and peak broadening occurred with long reaction coils; these effects are due to increased dispersion of the sample zone and lead to unfavourable sampling rates. In the case of catalytic photometric detection, however, a certain length of reaction coil is needed to provide adequate reaction time for optimal sensitivity.

Broadening and tailing of peaks were also found when tubing of increased internal diameter was used (Fig. 4b), because of excessive dispersion of the sample zone. Although such dispersion could be reduced by increasing the flow rate, the sensitivity then decreased greatly (Fig. 4c). It was difficult to use tubing with an internal diameter of 0.25 mm because pumping at very high pressure was then required.

The effect of the sample volume was investigated. The sensitivity increased with increasing sample volumes, but the injection of a large sample volume into the reagent stream affected the regularity of the flow and would require longer reaction coils for complete mixing. The optimal sample volume was 20—30 μl in the manifold shown in Fig. 1.

The catalytic photometric determination of vanadium in the manifold finally selected (Fig. 1) proved very satisfactory. This is indicated by the typical continuous trace in Fig. 2 for standard vanadium solutions. A rectilinear relationship was obtained between the peak height and the amount of vanadium in the range 0.3—4.8 ng (10—160 ppb). The method shows good reproducibility, with a relative standard deviation of 2.0% for 60 ppb of vanadium (12 determinations), with a very simple procedure. The analytical signal is available within 60 s after sample injection. The rate of analysis is about 60 samples per hour.

This work was partially supported by a Grant-in Aid for Scientific Research from the Ministry of Education, Japan.

REFERENCES

1 J. Růžička and E. H. Hansen, Anal. Chim. Acta, 78 (1975) 145.
2 J. Růžička and E. H. Hansen, Anal. Chim. Acta, 99 (1978) 37.
3 E. H. Hansen, J. Růžička and A. K. Ghose, Anal. Chim. Acta, 100 (1978) 151.
4 M. F. Gine, E. A. G. Zagatto and H. Bergamin Fº, Analyst, 104 (1979) 371.
5 D. Betteridge, E. L. Dagless, B. Fields and N. F. Graves, Analyst, 103 (1978) 897.
6 J. W. B. Stewart, J. Růžička, H. Bergamin Fº and E. A. G. Zagatto, Anal. Chim. Acta, 81 (1976) 371.
7 J. Růžička and J. W. B. Stewart, Anal. Chim. Acta, 79 (1975) 79.
8 J. Růžička, E. H. Hansen and E. A. Zagatto, Anal. Chim. Acta, 88 (1977) 1.
9 E. H. Hansen, A. K. Ghose and J. Růžička, Analyst, 102 (1977) 705.
10 T. Yamane, T. Suzuki, and T. Mukoyama, Anal. Chim. Acta, 70 (1974) 77.

Analytica Chimica Acta, 119 (1980) 393—399

Short Communication

A HIGHLY SENSITIVE AND SELECTIVE METHOD FOR THE EXTRACTION-SPECTROPHOTOMETRIC DETERMINATION OF COBALT

OMAR BAUDINO and CARLOS B. MARONE*

Universidad Nacional de San Luis, Chacabuco and Pedernera, San Luis (Argentine Republic)

(Received 2nd January 1980)

Summary. The method is based on the highly sensitive reaction between cobalt and 4-(5-bromo-2-pyridylazo)-1,3-diaminobenzene. The cationic complex in slightly acidic solution is quantitatively extracted into chloroform as an ion pair with anthraquinone sulfonate; interfering ions are retained in the aqueous phase by selected masking agents. The cobalt complex is then rapidly back-extracted into 2.4 M HCl and measured at 573 nm ($\epsilon = 1.16 \times 10^5$ l mol^{-1} cm^{-1}).

Several pyridylazo derivatives of diamines have been proposed by Shibata et al. [1—4] for the spectrophotometric determination of cobalt. The great sensitivity of the chromogenic reaction with diverse ions is the most remarkable feature of this reagent; molar absorptivities are frequently of the order of 10^5 l mol^{-1} cm^{-1}. Furthermore, these reagents show good selectivity and the color of the cobalt complexes is very stable. The complexes are reported to be of cobalt(II) [5], but cobalt(III) reacts similarly [6]. The cobalt complex is not formed in highly acidic solutions but once formed in slightly acidic, neutral or alkaline solutions, does not dissociate on acidification. This is a desirable feature, because high acidities are required to achieve great sensitivity. Shibata et al. [5] have suggested that the protonation of the free amino groups in the metal chelate is responsible for this hyperchromic effect.

4-(5-Bromo-2-pyridylazo)-1,3-diaminobenzene (5-BrPADAB) was used by Kiss [6] for the spectrophotometric determination of cobalt in silicates and meteorites. The "direct" method used by Kiss consisted of the formation of the cobalt complex at pH 4—7 and acidifying to 2.4 M hydrochloric acid. Iron complexes were formed and remained fairly stable under these conditions and interfered, while the complexes formed with nickel(II), copper(II), mercury(II) and zinc(II), although dissociated upon acidification, were responsible for reagent consumption, which diminished complexation of cobalt(II) with 5-BrPADAB. Also, although neither chromium(III) nor chromium(VI) formed colored chelates, chromate interfered seriously by bleaching the cobalt complex in the acidic medium finally required.

This communication describes the development of a procedure that allows the suppression of these interferences. The spectrophotometric procedure with 5-BrPADAB has been re-examined and an extraction step has been included to remove interferences, followed by back-extraction of the cobalt

complex into the strongly acidic solution required for the spectrophotometric measurement.

Experimental

Cobalt(II) solution (1×10^{-2} M). Dissolve 0.2947 g of the metal (99.99%) by heating with (1 + 1) nitric acid, add 10 ml of 72% perchloric acid and evaporate to fumes of perchloric acid. After cooling, transfer the solution to a 500-ml volumetric flask and dilute to the mark with redistilled water.

5-BrPADAB. Was prepared following the method of Shibata et al. [1].

Anthraquinone-2-sulfonic acid (AQSA) solution (2×10^{-2} M). Dissolve 0.620 g of the commercial product without purification, and dilute to 100 ml with redistilled water.

All other reagents, solvents and metal salts were of analytical grade. Chloroform was used without purification.

Apparatus. Absorption spectra were recorded on a Varian 634 u.v.-visible spectrophotometer, and fixed wavelength measurements were obtained with a Beckman DU spectrophotometer using 10.0-mm glass cells. pH measurements were made with an Orion Research Model 701-A pH meter, using a combined electrode. For the extractions, the solutions were shaken manually in 4 × 15 cm glass tubes with polyethylene stoppers.

Recommended procedure for cobalt determination. To 5—50 ml of the slightly acidic sample containing 1.5—10 μg of cobalt, in a 50-ml separatory funnel, add the required masking agent (see Table 2), followed by 1 ml of acetate buffer (0.2 M, pH 5), and 2 ml of the ethanolic 5×10^{-4} M solution of 5-Br PADAB. (If the volume at this stage exceeds 50 ml, the addition of 2 ml of 95% ethanol at this point is advisable to prevent precipitation of the complex.) Let the solution stand for 10 min. Add 2 ml of 1×10^{-2} M AQSA followed by 10 ml of chloroform, and shake manually for 3 min. Allow the phases to separate. Take an exact fixed volume (2—8 ml) of the chloroform extract, add 10.0 ml of 2.4 M hydrochloric acid and shake for 30—40 s. Measure the absorbance of the acidic extract at 573 nm against a blank obtained in the same manner as described except for the sample. Calculate the concentration of cobalt from a calibration curve, obtained as described below.

Calibration. Pipette suitable aliquots (⩽ 25 ml) of 2×10^{-5} M cobalt solution containing 0.6—25 μg of cobalt into 50-ml volumetric flasks. Add to each 1 ml of acetate buffer (0.2 M, pH 5) and 2 ml of the ethanolic 5×10^{-4} M solution of 5-BrPADAB. Mix thoroughly and let stand for 10 min. Add 10 ml of concentrated hydrochloric acid, mix and cool to room temperature. After diluting to volume, measure the absorbance at 573 nm against a reagent blank as reference using 10.0-mm glass cells. Careful checks showed that the additional extraction steps made no difference to the results with pure solutions.

Results and discussion

5-BrPADAB reacts with cobalt(II) at pH 4—10 to form an orange-red compound. Reaction starts immediately and is complete within 10 min.

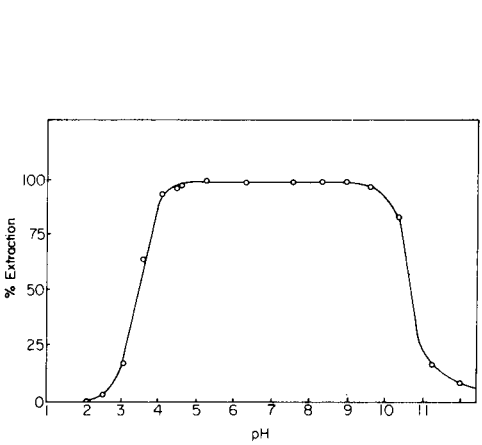

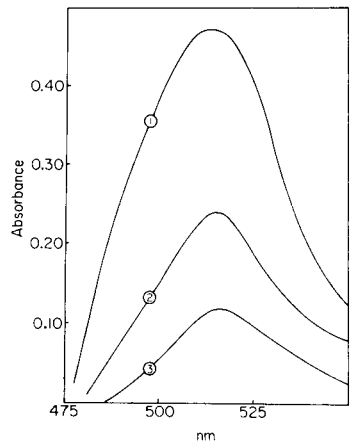

Fig. 1. Extraction of the cobalt-5-BrPADAB—AQSA ion pair vs pH. Cobalt = 6.25 μg; 5-BrPADAB = 1 × 10^{-4} M; AQSA = 2 × 10^{-3} M; extraction into 10.0 ml of chloroform from 10 ml of aqueous phase.

Fig. 2. Absorption spectra of the ion pair extracted at pH 5.0 into chloroform. 5-Br PADAB = 2 × 10^{-4} M; AQSA = 2 × 10^{-3} M; cobalt concentration: (1) 1.06 × 10^{-5} M; (2) 0.531 × 10^{-5} M; (3) 0.265 × 10^{-5} M. Spectra measured against a blank of chloroform equilibrated with same solutions in the absence of cobalt.

It is known that this complex can be transformed into other species when a concentrated mineral acid is added [3], although the metal-to-ligand ratio (1:2) is unaltered. The complexes formed in slightly acidic solution are cationic, thus, in order to form an extractable species, an ion-pair must be formed; methyl red, methyl orange, 2-naphthalenesulfonic acid, bromophenol blue, tetraphenylborate and anthraquinonesulfonic acid (AQSA) were found to be suitable for this purpose, the last being the most effective. The effect of pH on extraction in the presence of AQSA is shown in Fig. 1. The per-

TABLE 1

Maximum tolerances for anions in the extraction-spectrophotometric determination of cobalt (6.25 μg). (Reagents: 2 × 10^{-4} M 5-BrPADAB and 2 × 10^{-3} M AQSA)

Anion	Molar ratio Anion:Co	Co found (μg)	Error (%)	Anion	Molar ratio Anion:Co	Co found (μg)	Error (%)
Iodide[a]	5000	6.35	+1.6	Thiosulfate[b]	15000	6.20	−0.8
Nitrate[a]	20000	6.20	−0.8	Thiourea	10000	6.20	−0.8
Perchlorate[a]	20000	6.23	−0.32	Thiocyanate[a]	4000	6.27	+0.32
Chloride[b]	30000	6.25	0.0	Ascorbic Acid	2500	6.26	+0.16
Bromide[a]	20000	6.25	0.0	Cupron	2000	6.24	+0.16
Fluoride[b]	25000	6.20	−0.8	Tartrate[b]	30000	6.23	−0.31

[a]Added as potassium salt. [b]Added as sodium salt.

TABLE 2

Comparison of maximum tolerances between the "direct" and extraction methods (Co(II) = 6.25 μg; 5-BrPADAB = 2×10^{-4} M; AQSA = 2×10^{-3} M)

Ion	Added as	Tolerable molar ratio (Me:Co)				Masking agent (Final Concentration)
		"Direct" method	Error (%)	Extraction method	Error (%)	
Ni(II)	Nitrate	750	−0.8	1300	−0.32	0.1 M Na tartrate
Hg(II)	Nitrate	50	−6.0	750	−1.76	0.05 M $Na_2S_2O_3$
Cu(II)	Chloride	4	−10	1000	−0.32	0.02 M cupron
Pd(II)	Chloride	<1	—	2000	−0.16	0.1 M thiourea
Fe(III)	Chloride	25	+5	5000	−0.46	0.24 M NaF
Cr(VI)	Dichromate			1500	−5	—

centage extraction increases rapidly from pH 3 to 4.5 and is complete at pH 5—9 after only 2-min shaking. High concentrations of chloride or acetate also allowed some extraction of the complex, but recovery was only ⩽85%. A 1:1 molar ratio between the cobalt—5-BrPADAB complex and AQSA was demonstrated by Job's plots. This result was obtained only when the ion pair was formed in low ionic strength solutions. Otherwise, larger values were obtained.

In order to achieve complete extraction of 6.25 μg of cobalt from 10 ml of final aqueous solution with an equal volume of chloroform, 2 ml of 5×10^{-4} M 5-BrPADAB solution and 1 ml of 2×10^{-2} M AQSA solution were sufficient. The time elapsed between the addition of the reagents and the extraction may be from 1 min to 2 h without effect on the final absorbance. The spectra of the extracts are shown in Fig. 2. The maximum molar absorptivity (at 517 nm) is 44700 l mol^{-1} cm^{-1}, which, although high, is appreciably smaller than that of the cobalt complex in the acidic medium (see below). Thus, a back-extraction into 2.4 M hydrochloric acid is advisable for greater sensitivity. This requires only 15—20 s shaking. The spectrum of the back-extracted complex was the same as that obtained by Kiss [6]. The absorbance at 573 nm of cobalt extracted at pH 5 and back-extracted into 10.0 ml of 2.4 M hydrochloric acid obeyed Beer's law between 0.012 and 0.5 ppm of cobalt in the original solutions. The optimum range was 0.08—0.50 ppm. The molar absorptivity in 2.4 M hydrochloric acid at 573 nm was 1.16×10^5 l mol^{-1} cm^{-1}. The sensitivity was 0.51 ng Co cm^{-2}.

Interferences. The interferences of Fe(III), Cu(II), Pd(II), Hg(II), Ni(II) and Zn(II), which form complexes with 5-BrPADAB at pH 5 [6], were studied, as were the effects of some anions, particularly those which form complexes with the interfering cations; they are listed in Tables 1 and 2 together with the tolerances measured.

Kiss [6] concluded that iron(III) could be effectively masked by fluoride or tartrate, but recoveries of cobalt were then low. Moreover, large amounts of aluminum, calcium or magnesium interfere when fluoride is used because

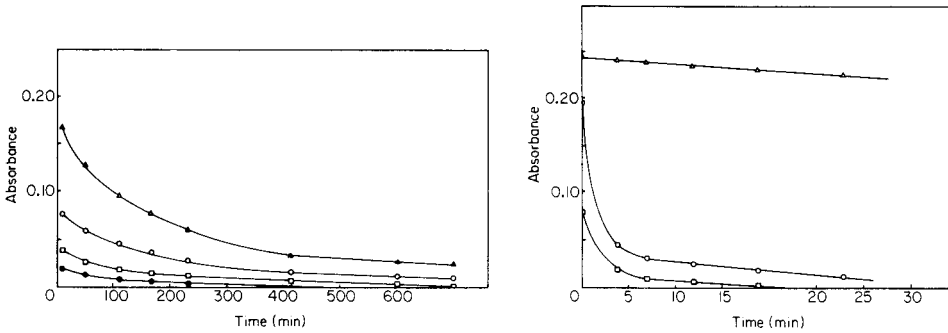

Fig. 3. Decrease in the absorbance at 573 nm of the iron(III)—5-BrPADAB complex with time, in 2.4 M HCl at 20°C with 4×10^{-2} M 5-BrPADAB. Iron concentration: (△) 2×10^{-3} M; (○) 10^{-3} M; (□) 5×10^{-4} M; (●) 2.5×10^{-4} M.

Fig. 4. Decrease in the absorbance at 573 nm of the 5-BrPADAB complex with time, in 2.4 M HCl at 60°C. (△) 2×10^{-3} M Co; (○) 10^{-2} M Fe; (□) 2×10^{-3} M Fe.

of the formation of sparingly soluble fluorides, the turbidity of which persists on acidification and corrosive effects on the cell are marked. The iron(III) complex slowly dissociates on standing in strongly acidic solutions (Fig. 3). This would allow the interference to be suppressed if sufficient time were allowed to elapse, but this is only practicable when the iron content is low ($<10^{-4}$ M). Decomposition is faster on heating (50—60°C), but the time required when a large amount of iron is present remains too long for practical applications, and the cobalt complex is partially destroyed (Fig. 4). Kiss therefore removed iron(III) by extraction with MIBK, prior to the cobalt determination.

In the present procedure, the iron interference is cleanly suppressed on adding sodium fluoride to the aqueous sample at pH 5. A 25000:1 fluoride-to-cobalt molar ratio is admissible, so that a 5000:1 iron(III)-to-cobalt molar ratio can be tolerated (Table 2). Iron—fluoride complexes and the fluoride ions are retained in the aqueous phase during the extraction of the ion pair, therefore fluoride will be absent during the stripping of the cobalt complex into the acid and there will be no danger of damage to the cells, nor any effect from turbidity produced by insoluble fluorides. Palladium(II) resembles iron(III) because its 5-BrPADAB complex formed at pH 5 persists on acidification and produces a serious spectral interference in the spectrophotometric determination of cobalt.

The interfering effects of nickel, mercury(II), copper and zinc were described above. All these effects can be removed by addition of a suitable complexing agent to the solution before adding 5-BrPADAB. These reagents are given in Table 2, together with the maximum tolerable amount of the particular metal. In all instances the tolerances are increased, sometimes by more than three orders of magnitude, compared to the non-extractive procedure. Such tolerances were confirmed by analysis of synthetic mixtures

TABLE 3

Tolerances in the extraction-spectrophotometric determination of cobalt (6.25 μg) with masking agents added
(2×10^{-4} M BrPADAB; 2×10^{-3} M AQSA; final concentrations of masking agents as in Table 2.)

Sample no.	Ions added (mg)				Co found (μg)	Error (%)
	Pd(II)	Fe(III)	Ni(II)	Cu(II)		
1[a,b]	0.55	5.9	—	—	6.20	−0.8
2[a,c]	—	12.0	6.0	—	6.25	0
3[c,d]	—	—	1.5	7.0	6.20	−0.8
4[a,d]	—	12.0	—	7.0	6.10	−2.4
5[b,c]	0.55	—	6.0	—	6.17	−1.28
6[b,d]	0.12	—	—	6.5	6.20	−0.8
7[a,c,d]	—	6.0	1.5	3.5	6.05	−3.2

[a]NaF added. [b]Thiourea added. [c]Sodium tartrate added. [d]Cupron added.

containing a fixed amount of cobalt. The results are given in Table 3. The pre-masking of these metals has the added benefit that their consumption of the chromogenic reagent is avoided, thus removing another source of interference. Calibration can be achieved directly in the acidic solution, without the necessity of the extraction procedure.

Besides the improvement in selectivity, another important advantage obtained when the extraction and back-extraction steps are included, is the possibility of analysing extremely dilute samples. The results obtained when the extraction procedure is applied to 100 ml of very dilute aqueous cobalt solutions, with extraction into 10 ml of chloroform, are shown in Table 4. They demonstrate the highly favorable partition coefficient of the ion-pair, and that as little as 0.003 ppm of cobalt can be determined.

TABLE 4

Determination of cobalt in dilute samples
(Extractions from 100-ml aliquots with 10.0 ml of chloroform.Co(II) stripped from 8.0 ml of the extract with 10.0 ml of 2.4 M HCl)

Co conc. (ppm)		Error (%)	Co conc. (ppm)		Error (%)
Taken	Found		Taken	Found	
0.0625	0.0618	−1.12	0.00625	0.00608	−2.70
0.0312	0.0311	−0.52	0.00312	0.00308	−1.28

The authors thank Prof. José A. Catoggio for helpful discussions, and SECYT for financial support.

REFERENCES

1 S. Shibata, M. Furukawa, Y. Ishiguro and S. Sasaki, Anal. Chim. Acta, 55 (1971) 231.
2 S. Shibata, M. Furukawa and K. Goto, Talanta, 20 (1973) 426.
3 S. Shibata, M. Furukawa and K. Goto, Anal. Chim. Acta, 71 (1974) 85.
4 S. Shibata, M. Furukawa and E. Kamata, Anal. Chim. Acta, 73 (1974) 107.
5 S. Shibata, M. Furukawa and K. Goto, Anal. Chim. Acta, 71 (1974) 85.
6 E. Kiss, Anal. Chim. Acta, 66 (1973) 385.

Analytica Chimica Acta, 119 (1980) 401—404

Short Communication

DETERMINATION OF SUBMICROMOLAR AMOUNTS OF URANIUM(VI) BY COMPLEXIMETRIC TITRATION WITH PYRIDINE-2,6-DICARBOXYLIC ACID

S. F. MARSH*, M. R. BETTS and J. E. REIN

Los Alamos Scientific Laboratory of the University of California, Los Alamos, NM 87545 (U.S.A.)

(Received 7th April 1980)

Summary. Uranium(VI) is selectively determined by a complexiметric titration with pyridine-2,6-dicarboxylic acid, using arsenazo-I indicator and hexamethylenetetramine buffer at pH 4.9. Cyclohexanediaminetetraacetic acid and diethylenetriaminepentaacetic acid provide masking of interfering metal ions. A probe colorimeter apparatus is recommended for end-point detection. The relative standard deviation is 0.6% for 0.17—0.76 μmol of uranium.

Few complexing agents react with uranium(VI) to form highly stable complexes, a condition necessary for reliable complexiметric titrimetry. For this reason, titrimetric determinations generally are preceded by a reduction to uranium(IV). The uranium(IV) then is determined by titration with one of the many complexing agents that form highly stable complexes with it. Disadvantages include: (1) extra chemical operations, (2) use of strong reductants that are unstable and often erratic in routine use, and (3) reagents that form complexes with uranium(IV) also form complexes with many other metal ions. A system in which uranium(VI) is titrated is considered simpler, more reliable and less subject to interference.

Recently, Celon et al. [1] used pyridine-2,6-dicarboxylic acid (PDA) as a titrant for uranium(VI), with arsenazo-I as the indicator, to determine milligram amounts of uranium in decomposed organic compounds. Here, this method has been modified to determine submicromolar amounts of uranium with high tolerance for impurity metal ions and nonmetal anions. This method, coupled with a probe colorimeter for end-point detection, provides a selective determination of 0.17—0.76 μmol (40—180 μg) of uranium with a relative standard deviation of 0.6%. No attempt was made to evaluate visual end-point detection, which is considered to be subjective.

Experimental

Reagents. For the buffering and masking solution, dissolve 9.11 g of cyclohexanediaminetetraacetic acid (CDTA), 9.83 g of diethylenetriaminepentaacetic acid (DTPA), 105 g of hexamethylenetetramine, and 125 mg of arsenazo-I in a minimum volume of water; add 15 ml of 15.7 M nitric

acid, cool, and dilute to a final volume of 250 ml with water. For the pyridine-2,6-dicarboxylic acid (dipicolinic acid) titrant, dissolve 167.1 mg of this reagent in water and dilute to 1 l.

Equipment. A PC/1000 probe colorimeter (Brinkmann Instruments) was used with the 620-nm filter selected. A micrometer digital buret (1-ml capacity; Manostat Corporation, NY) was driven by a synchronous stepping motor (Type MO61-FC08, Superior Electric Co.), which was controlled by a Slow-Syn SP-1800B preset indexer (Superior Electric Co.). Signals were recorded on a strip-chart recorder (Model SR-204, stepping-motor driven, Heath-Schlumberger). A Hewlett-Packard 9820-A programmable calculator was used, although more recent calculators provide more capability at lower cost. Construction of the titrator is outlined later.

Recommended procedure. Determine the PDA titer by titrating known amounts of a standard solution of uranyl nitrate encompassing the uranium range of interest. For unknowns, place the sample in a 30-ml tall-form beaker, add 1.0 ml of the buffering and masking solution and a teflon-covered stirring bar, and dilute with water to about 25 ml. Adjust the pH, if necessary, to 4.9 ± 0.1 with sodium hydroxide or nitric acid. Titrate with PDA to the complete disappearance of the purple uranyl—arsenazo-I complex, preferably using the probe colorimeter.

Results and discussion

Buffering and masking agents. In the method of Celon et al. [1], uranium(VI) is titrated with PDA to an arsenazo-I endpoint at pH 3.6 in an acetate-buffered medium. Because this pH is below the optimum buffering range of acetate, we evaluated it and six other buffers of formate, β-chloropropionate, pyridine, glutarate, succinate, and hexamethylenetetramine. For each buffer, the pH of maximum color intensity of the uranium(VI)—arsenazo-I complex was determined. The largest enhancement of color intensity, threefold higher than that obtained using the conditions of Celon et al., and sharpest end-point were attained with hexamethylenetetramine buffer at pH 4.9.

To gain selectivity, two masking agents, cyclohexanediaminetetraacetic acid (CDTA) and diethylenetriaminepentaacetic acid (DTPA) were selected. Neither forms a strong complex with uranium(VI), whereas both form highly stable complexes with many other multivalent metal ions.

In the developed and recommended procedure, a single solution that is 3 M hexamethylenetetramine, 0.1 M CDTA, 0.1 M DTPA, and 0.05% (w/w) arsenazo-I is added to the sample, water is added to a volume of about 25 ml, and the uranium(VI) is titrated with 1 mM PDA to disappearance of the purple color of the uranium(VI)—arsenazo-I complex.

Titration apparatus. The apparatus consists of four main components, a probe colorimeter, a micrometer-type digital buret, a strip-chart recorder, and a desk-top programmable calculator. The probe colorimeter provides several advantages in addition to an objective measurement of the changing

absorbance. The probe immersed in the solution is not affected by room light, permitting use of an open beaker. The colorimeter itself, coupled to the probe by a fiber-optics light guide, can be mounted outside an enclosure for analysis of radioactive samples. Synchronized stepping motors drive the buret and recorder to give a titration plot that is directly usable for graphical determination of the inflection point. The calculator is interfaced to the stepping motors and an analog-to-digital converter on the colorimeter detector such that it controls the titrant additions and processes the corresponding digitized absorbance values. Titrant increments of 0.01 ml are added, the absorbance value is read, a data-smoothing routine is applied to the last five values, and the smoothed values are stored. This continues until the approximate end-point is sensed, based on a preset slope change. The titration is then completed with the addition of a preset number of 0.01-ml titrant increments. The stored smoothed values before and after the approximate end-point are fitted to least-squares lines and the computed intersection is taken as the end-point. The printer records the end-point in choices of titrant volume, micromoles of uranium, or micrograms of uranium using its atomic weight.

Diverse ion tolerances. Tables 1 and 2 summarize the tolerances of 45 metal ions and 19 nonmetal anions. The ions were added individually to 0.5 μmol of uranium and titrated. The highest molar ratio tested for metal ions was 100, except as indicated. The highest molar ratio tested for non-

TABLE 1

Metal ion tolerances

Metal ion	Tolerance level[a]	Metal ion	Tolerance level[a]	Metal ion	Tolerance level[a]
Ag(I)	1[b]	Hg(II)	30	Re(IV)	1[b]
Al(III)	10	In(III)	30	Rh(III)	1[b]
As(III)	100	Ir(III)	1[b]	Ru(III)	1[b]
Au(III)	1[b]	La(III)	30	Sb(III)	100
Ba(II)	30	Lu(III)	30	Sc(III)	30
Bi(III)	100	Mg(II)	30	Se(IV)	100
Ca(II)	100	Mn(II)	10	Sn(IV)	100
Cd(II)	30	Mn(VII)	10	Sr(II)	10
Ce(III)	30	Mo(VI)	10	Te(IV)	100
Co(II)	30	Na(I)	100	Th(IV)	5
Cr(III)	30	Ni(II)	30	Tl(III)	100
Cs(I)	100	Np(IV)	0[d]	V(V)	30
Cu(II)	10	Pb(II)	30	Y(III)	30
Fe(III)	10	Pd(II)	1[b]	Zn(II)	30
Ga(III)	10	Pt(IV)	1[b]	Zr(IV)	3
		Pu(III)	3[c]		

[a]The highest molar ratio tested without interference. Molar ratio relative to uranium (0.5 μmol, 120 μg). [b]Not tested at a molar ratio higher than 1. [c]With sulfite present at a molar ratio of 100 relative to uranium. [d]Interferes quantitatively.

TABLE 2

Non-metal anion tolerances

Anion	Tolerance level[a]	Anion	Tolerance level[a]	Anion	Tolerance level[a]
Acetate	1000	EDTA	30	PO_4^{3-}	100
Borate	100	F^-	100	SO_3^{2-}	100
Br^-	1000	I^-	1000	SO_4^{2-}	1000
BrO_3^-	100	IO_3^-	100	$S_2O_3^{2-}$	100
Cl^-	1000	NO_2^-	100	SCN^-	100
ClO_4^-	1000	NO_3^-	1000	Tartrate	100
Citrate	10	Peroxide	[b]		

[a]The highest molar ratio tested without interference. Molar ratio relative to uranium (0.5 μmol, 120 μg). [b]Biased low by several percent over the molar ratio range 1—10.

metal anions was 1000. If a result was significantly different at the 95% confidence level relative to uranium alone, testing was continued with lower amounts of the ion until there was no significant difference.

All metals and non-metals tested are tolerated at greater than molar ratios of one except hydrogen peroxide and neptunium. Hydrogen peroxide causes a consistent low bias of several percent over the molar ratio range of 1 to 10. Neptunium is titrated quantitatively, enabling the method to be used for its determination.

Precision. Based on six determinations of uranium at seven levels covering the range of 0.17—0.76 μmol, the relative standard deviation for a single titration is essentially constant at 0.6%.

The efforts of Darryl D. Jackson, who interfaced the calculator to the system, are greatly appreciated. This work was supported by the Office of Safeguards and Security, U.S. Department of Energy.

REFERENCE

1 E. Celon, S. Degetto, G. Marangoni and L. Baracco, Talanta, 26 (1979) 160.

Analytica Chimica Acta, 119 (1980) 405—408

Short Communication

DETERMINATION OF URANIUM BY THERMAL AND EPITHERMAL NEUTRON ACTIVATION IN NATURAL WATERS AND IN HUMAN URINE

JIRI HOLZBECHER and DOUGLAS E. RYAN*

Trace Analysis Research Centre, Chemistry Department, Dalhousie University, Halifax, Nova Scotia, B3H 4J1 (Canada)

(Received 25th February 1980)

Summary. Uranium is determined via its ^{239}U nuclide (74.0 keV, $t_{1/2}$ = 23.5 min) in natural waters down to 0.03 ng U ml^{-1} after preconcentration with activated carbon and oxine; 30-min irradiation and counting times are used. No preconcentration is required for samples containing more than 4 ng U ml^{-1} with 10-min irradiation and counting times. Uranium in urine can be determined under a boron shield at the 5 ng ml^{-1} level after 30-min irradiation and counting.

During a recent multielement study of trace elements in hair, one sample was found to contain 10 μg U g^{-1}. This led to an investigation of various water supplies and subsequent determination of uranium in urine. The methods developed are reported below.

Many methods are available for uranium determinations but some form of preconcentration and separation is usually employed at trace levels, followed by various procedures, e.g. delayed-neutron counting [1]. Very low amounts of uranium can be determined fluorimetrically after evaporation of sample solution to dryness with sodium fluoride but the method suffers from many interferences [2].

The SLOWPOKE reactor provides a very stable neutron flux [3] and samples can be counted directly at the facility so relatively short-lived nuclides can be used; as a result, short irradiation, decay and counting times make possible a high throughput of samples. The relatively low water moderator temperature of about 50°C is also advantageous because it permits direct irradiation of liquid samples. Thus, 4 ng of uranium can be directly determined in 1 ml of water. The urine matrix makes direct determination of uranium less sensitive because of interference from sodium and chloride; epithermal activation under a boron shield markedly improves sensitivity.

A further increase in sensitivity of uranium determination in water is achieved by preconcentration and separation of uranium by its collection from water by means of complexation with oxine and subsequent adsorption on activated carbon [4].

Experimental

All samples were irradiated in either inner or outer irradiation positions of a SLOWPOKE reactor; details of flux composition have been previously described [3]. Gamma-ray measurements were made with a TN-11 pulse-height analyzer (Tracor Northern) using a Canberra Ge(Li) detector having a 9.5% relative efficiency and 1.9 keV resolution at 1332 keV.

The 0.01 M uranium stock solution was prepared from uranyl nitrate hexahydrate (Fisher). Working standards were made by dilution of the stock solution; 1 ml aliquots were measured into 2/5 dram polyethylene vials which were then either sealed immediately for direct water analysis, or after slow evaporation to dryness under an infrared lamp for urine epithermal analysis. Standards for the activated carbon—oxine method were prepared by adding a few microliters of uranium standard solutions to the powder residues that were collected from water blanks that had been processed by the preconcentration procedures. These residues were then redried before they were irradiated.

The aqueous oxine (Fisher) solution contained 0.05 g oxine/100 ml and the 0.2% activated carbon suspension was prepared from nitric acid-washed Fisher product.

The boron shield was made by simply cutting an appropriate piece of boron carbide-loaded elastomer sheet (3.2 mm thick; Flex/Boron, Reactor Experiments, Inc.) containing 25% (w/w) boron and rolling it into a cylinder inside the vial (ends overlapping to prevent leakage of thermal neutrons). Top and bottom lids were cut out from the same material. The boron ratio for ^{239}U was 2.0 while for ^{24}Na it was 60, resulting in an advantage factor of 30.

Procedure. All water and urine samples were acidified with 5 ml l^{-1} of 15 M nitric acid at the time of collection. For preconcentration, 10 ml of urine were digested with 2 ml of 15 M nitric acid at 150°C in a teflon bomb overnight; the digested urine was diluted with water to 100 ml before preconcentration.

Aliquots (1 ml) of water samples were sealed directly in 2/5 dram vials. For epithermal activation, urine aliquots (1 ml) were pipetted into 2/5 dram vials and then slowly dried under an i.r. lamp to remove water and prevent thermalization of epithermal neutrons in the sample.

The following preconcentration procedure was used. Acetate buffer of pH 5.2 (2 ml) was added to the 100-ml samples followed by 2 ml of the aqueous oxine solution under stirring. The highly acidic digested urine samples were adjusted to pH 5 with ammonia prior to addition of buffer. The solution was heated to 60°C and 10 ml of the 0.2% activated carbon suspension were added with rapid stirring during pipetting. The suspension was stirred magnetically for 1 h while cooling to room temperature. The powder was filtered off with suction, washed with distilled water and dried in vacuo for 1 h. It was then transferred to a polyethylene vial and sealed. Throughout the entire investigation, respective blanks were run and standard addition was used to check recoveries. Recoveries in all cases were greater

than 80%. For example, the recovery from 100 ml of water containing 2.4 ng U ml^{-1} was 2.1 ng U ml^{-1}; 22 ng U ml^{-1} was recovered from 10-ml urine samples containing 24 ng U ml^{-1}.

Uranium was determined via its ^{239}U nuclide (74.0 keV, $t_{1/2}$ = 23.5 min); lead shielding was removed from the Ge(Li) detector to eliminate interfering lead x-rays. For thermal activation, the inner reactor core site was used while epithermal activation was done in the outer site of the reactor.

The various procedures developed and respective detection limits are summarized in Table 1. Samples analyzed by procedures numbered 4, 8 and 9 were irradiated in the outer site of the reactor; irradiations for other procedures were performed in the inner site. The original volume used in the instrumental procedures was 1 ml while the preconcentration was done with 100 ml of water or 10 ml of digested urine. The developed procedures were applied to eleven unknown water samples by procedure 1, and 67 urine samples were analyzed by procedure 8.

Results and discussion

The uranium concentrations in the collected water samples ranged from 11 to 143 ng ml^{-1}. The results show a large difference in uranium concentration depending on the collection site within a relatively small area; even the lowest result, however, is well above normal values for natural waters. The 24-h urine samples collected from the residents of the area served by water containing high uranium concentrations showed less than 3 to a maximum of 12 ng U ml^{-1}.

TABLE 1

Experimental conditions and detection limits

Procedure	B_4C shield	Irradiation time t_i (min)	Decay time t_d (min)	Counting time t_c (min)	Counting statistics detection limit[e] (ng ml^{-1})	Blank (ng ml^{-1})
Water						
1. I[a]	no	10	1	10	4	0
2. I	no	30	1	30	0.7—1.3	0.8
3. I	no	30	1	30	0.5—1.0	0.4
4. PC[b]	yes	30	7[c]	30	0.03	0.75
5. PC	no	30	1	30	0.006	0.016
Urine						
6. I	no	3	1	30	30	28
7. I	no	60	5280[d]	60	50	0
8. I	yes	30	7	30	3—7 (~5)	1
9. PC	yes	30	7	30	0.3	1.5

[a]Instrumental. [b]Preconcentration. [c]Longer t_d to allow for decay of ^{28}Al from shield impurities. [d]via ^{239}Np (106 keV). [e]Based on 2(background)$^{1/2}$.

The large difference in blank values between procedures 4 and 5 arises because procedure 5 gives a 10 times higher count per ng of uranium (no boron shield, higher flux in inner site) and the blank in procedure 5 therefore appears to be about 50 times lower; this fact makes procedure 5 preferable for natural waters. For urine, however, a boron shield is necessary to achieve high sensitivity. The digestion and preconcentration process does not improve significantly on the instrumental procedure primarily because of the magnitude of the blank.

The above outline of various procedures shows that the uranium in fresh natural waters in concentrations above 4 ng U ml^{-1} can be determined directly after short irradiation and counting times (10 min); for lower concentrations, down to about 0.03 ng U ml^{-1}, preconcentration with activated carbon and oxine is employed. Determination of uranium in a urine matrix can be done under a boron shield down to concentrations of 5 ng U ml^{-1}.

REFERENCES

1 R. J. N. Brits and M. C. B. Smit, Anal. Chem., 49 (1977) 67.
2 M. A. Northup, Ind. Eng. Chem. Anal. Ed., 17 (1945) 664.
3 D. E. Ryan, D. C. Stuart and A. Chattopadhyay, Anal. Chim. Acta, 100 (1978) 87.
4 B. M. Vanderborght and R. E. Van Grieken, Anal. Chem., 49 (1977) 311.

Analytica Chimica Acta, 119 (1980) 409—413

Short Communication

INVESTIGATION OF THE SILVER IODIDE—*p*-ETHOXYCHRYSOIDINE ADSORBATE BY INFRARED SPECTROSCOPY

V. P. IZVEKOV, E. PUNGOR* and K. TÓTH

Institute for General and Analytical Chemistry, Technical University, Budapest (Hungary)

(Received 10th April 1980)

Summary. Infrared measurements for *p*-ethoxychrysoidine and the silver iodide—*p*-ethoxychrysoidine adsorbate indicate that the dye is bound to silver iodide through amino groups. The interaction is discussed on the basis of surface imperfections of silver iodide and the polar nature of *p*-ethoxychrysoidine. Of the two possible crystal structures of silver iodide, only the γ-modification is present in the adsorbate.

p-Ethoxychrysoidine (2,4-diamino-4′-ethoxyazobenzene) is a well known adsorption indicator and is widely used in titrations of iodide with silver(I) ions. A quantitative description of the theory of adsorption indicators has been proposed by Schulek and Pungor [1, 2] and further developed by Pungor and Hollós-Rokosinyi [3]. The operation of *p*-ethoxychrysoidine indicator has been explained on the basis of adsorption of neutral dye molecules on active points of the surface of silver iodide from the beginning of its precipitation. Furthermore, the adsorbed dye has a marked influence on the formation of the precipitate [4]. However, the binding mechanism of the dye on the silver iodide has not yet been thoroughly investigated. The nature of the bonding between silver iodide and dye molecules in the adsorbate can be elucidated by infrared spectroscopy as described below.

Experimental

The silver iodide—*p*-ethoxychrysoidine adsorbate samples were prepared as described by Pungor [5]. The spectra of solid specimens were measured in potassium bromide pellets with a Perkin-Elmer 421 grating infrared spectrophotometer in the 600—4000 cm^{-1} region. Far-infrared spectra were measured on adsorbate samples prepared as polycrystalline films in the 10—400 cm^{-1} range with a Grubb-Parsons IS-3 interferometer, using the Fourier transform technique. Spectral resolution was 1 cm^{-1} and wavenumber reproducibility ± 0.5 cm^{-1}.

Results and discussion

p-Ethoxychrysoidine contains three polar groups ($-NH_2$, $-OC_2H_5$ and $-N{=}N-$) which are capable of forming a bond with silver iodide. The groups have characteristic absorption in the infrared range and their participation in a bond with silver iodide should cause a visible change of the infrared frequencies. Silver iodide is optically transparent in the middle infrared range.

The infrared spectra of free and adsorbed *p*-ethoxychrysoidine are shown in Fig. 1. As can be seen from Fig. 1(a), the $-NH_2$ stretching vibrations appear in the 3100—3500 cm^{-1} region as five separate bands. The vibrations at 3370 and 3460 cm^{-1} can be identified as symmetric (ν_s) and asymmetric (ν_{as}) stretching modes of the non-associated amino group. It is interesting that the relationship between ν_s and ν_{as} for the amino group in *p*-ethoxychrysoidine obeys the Bellamy—Williams equation: $\nu_s = 0.876\nu_{as} + 345.5$ (cm^{-1}), predicted for primary aromatic amines and generally useful for the detection of non-associated amino groups [6]. The vibrations of amino groups with various degrees of association are observed at 3290, 3260 and 3160 cm^{-1}; the last is the most intense. The large difference (300 cm^{-1}) between the ν_{NH_2} values of the unassociated and associated groups is evidence for strong hydrogen bonding in crystalline *p*-ethoxychrysoidine. Usually, the difference for a hydrogen-bonded amino-system is about 100—200 cm^{-1} [7]. Moreover, in the spectrum of *p*-ethoxychrysoidine (Fig. 1a) well-resolved amino deformation vibrations appear at 1630 and 1615 cm^{-1}, which can be assigned to associated and unassociated groups. As a consequence of the intensity, amino deformation modes are sometimes even more characteristic of amino groups than their stretching vibrations, as in the present case. Small absorption bands of ethyl groups in the 2960—2860 cm^{-1} range are unsuitable for identification purposes. The presence of the ethoxy

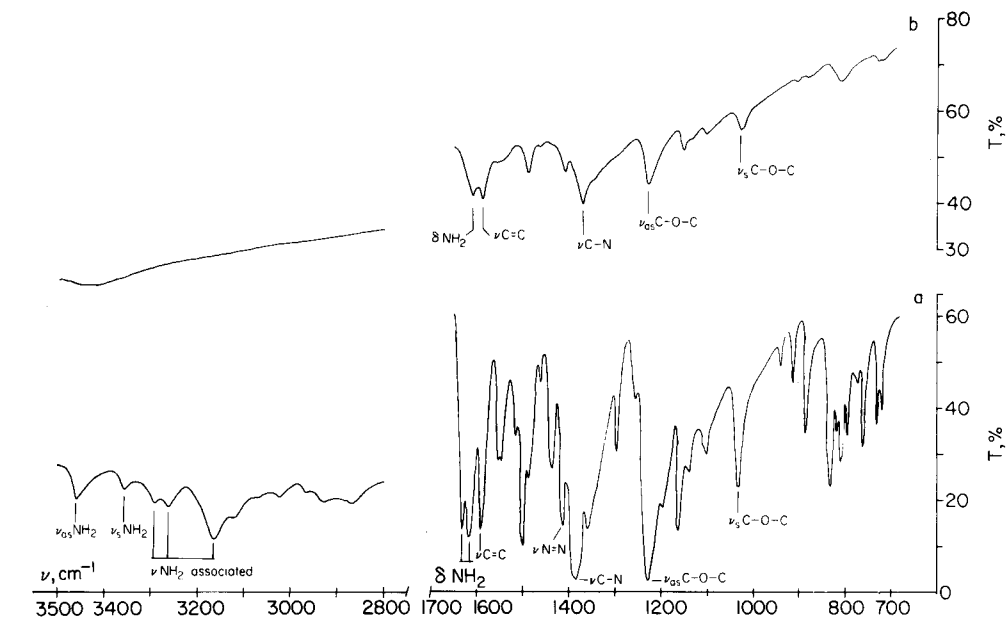

Fig. 1. Infrared spectrum of (a) free *p*-ethoxychrysoidine and (b) silver iodide—*p*-ethoxychrysoidine adsorbate.

substituent in *p*-ethoxychrysoidine may be evidenced by the symmetric and asymmetric vibrations of the C—O—C group including alkyl and aromatic carbon atoms. Accordingly, the bands at 1230 and 1030 cm^{-1} can be assigned to symmetric and asymmetric modes of the C—O—C group [8].

With regard to the azo group, literature data for the N=N stretching vibration are few and controversial. Kübler et al. [9] have shown that in *p*-amino-substituted aromatic azo compounds in the *trans*-configuration, the N=N band appears at 1418 cm^{-1}. It seems probable that with two amino groups attached, the frequency should be shifted to lower values [10]. The band at 1410 cm^{-1} can therefore be assigned to the N=N stretching mode.

The infrared spectrum of the adsorbed *p*-ethoxychrysoidine (Fig. 1b) lacks many of the bands that appear in the spectrum of the pure dye (Fig. 1a). For example, there is no absorption band in the 3100—3500 cm^{-1} region characteristic of the amino stretching vibrations. Even in the spectrum of free *p*-ethoxychrysoidine the intensity of these vibrations is small. In the silver iodide—dye adsorbate, where the amount of adsorbed *p*-ethoxychrysoidine was about one fifth of the dye measured separately, NH_2 stretching vibrations cannot be observed. Marked changes are apparent in the deformation frequencies of the amino groups: the position of the bands at 1615 cm^{-1} in the spectrum of the pure dye remains almost unchanged, whereas the band at 1630 cm^{-1} completely disappears in the spectrum of the adsorbed dye. This change in the deformation vibrations provides evidence for the participation of amino groups in the bonding to silver iodide. In general, the interaction between amino groups and silver iodide should also lower the C—N frequency because of weakening of the C—N bonds. Indeed, in the spectrum of the adsorbed *p*-ethoxychrysoidine, the ν_{C-N} value is lower (20 cm^{-1}) than that in the free compound.

The symmetric and asymmetric modes of the C—O—C group are observed at the same frequencies in the spectra of the adsorbate and of the free indicator. This is a strong indication that the ethoxy group is unchanged in the adsorbed *p*-ethoxychrysoidine molecules.

The formation of a bond between the amino groups and silver iodide can be explained on the basis of an electrostatic model. *p*-Ethoxychrysoidine is a polar molecule, the amino groups being strong electron donors (the Hammett constants for *o*- and *p*-amino groups are —0.77 and —0.66 [11]). It is well established that silver iodide has a Frenkel disorder in the cationic sublattice [12]. In the bulk of the crystal, silver interstitials (Ag_i^+) and ion vacancies (V_{Ag}^-) are formed in pairs, whereas at the surface, interstitials and vacancies can be created separately [13]. Because of the unequal free energies of formation for the two components of the Frenkel defect, the surface will bear an excess negative charge. Honig [14, 15] has shown that a silver iodide surface in solution has a surface density charge equal to -1.2×10^{-7} mC m^{-2}. Thus, the amino groups, which are partially positively charged, will be attracted to the negatively charged surface of silver iodide microcrystals.

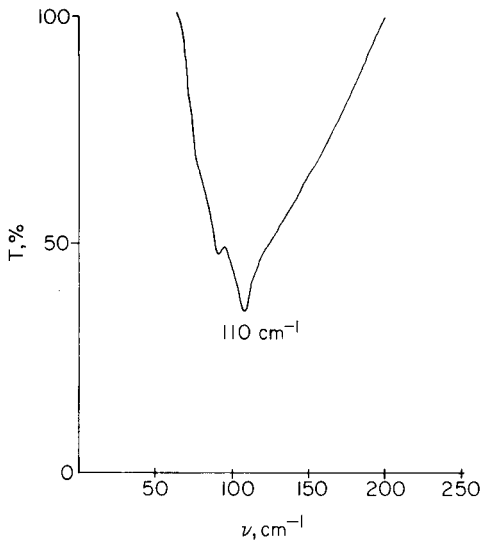

Fig. 2. Far-infrared spectrum of the silver iodide—*p*-ethoxychrysoidine adsorbate.

This conclusion is in accordance with early observations for systems of silver iodide and a dye with an unprotected hydroxyl group [16]. It has been established that the unprotected hydroxyl group immediately reduces silver ions on the surface of the dye before they can be bonded by amino groups.

The structure of the silver iodide—*p*-ethoxychrysoidine adsorbate (Fig. 2) was further examined by far-infrared spectroscopy. Bottger and Geddes [17] have established that silver iodide has a strong absorption at 106 cm^{-1} classified as crystal lattice vibration. The adsorbate spectrum showed this band at 110 cm^{-1} (Fig. 2). This discrepancy could be due to the presence of different modifications of silver iodide. Below 420 K, both the β-phase (wurtzite structure) and γ-phase (zincblende structure) are possible; depending on the preparative method, either modification may predominate [18]. Far-i.r. experiments with the pure β- and γ-modifications showed that the bands at 106 cm^{-1} and 110 cm^{-1} are characteristic of these two modifications, respectively. Therefore, the absorption observed at 110 cm^{-1} in the far-i.r. spectrum of the adsorbate suggests that the γ-modification of silver iodide is present.

REFERENCES

1 E. Schulek and E. Pungor, Anal. Chim. Acta, 4 (1950) 213.
2 E. Schulek and E. Pungor, Anal. Chim. Acta, 1 (1952) 446.
3 E. Pungor and E. Hollós-Rokosinyi, Acta Chim. Acad. Sci. Hung., 22 (1960) 69.
4 E. Schulek, E. Pungor and F. Guba, Anal. Chim. Acta, 8 (1953) 261.
5 E. Pungor, Acta Chim. Acad. Sci. Hung., 12 (1957) 265.
6 L. J. Bellamy and L. M. Williams, Proc. R. Soc., London, Ser. A, 254 (1960) 119.

7 L. J. Bellamy, Advances in Infrared Group Frequencies, Methuen, London, 1968, p. 281.
8 R. N. Jones and C. Sandorfy, in W. West (Ed.), Chemical Applications of Spectroscopy, Interscience, New York, 1956, p. 435.
9 R. Kübler, W. Lüttke and S. Weckherlin, Z. Elektrochem., 64 (1960) 650.
10 R. J. W. LeFévre and R. L. Werner, Aust. J. Chem., 10 (1957) 26.
11 R. W. Taft, Jr., in M. S. Newman (Ed.), Steric Effects in Organic Chemistry, J. Wiley, New York, 1956, Ch. 13.
12 F. A. Kröger, in The Chemistry of Imperfect Crystals, Vol. 2, Imperfection Chemistry of Crystalline Solids, North-Holland, Amsterdam, 1974, p. 270.
13 R. B. Poeppel and J. M. Blakely, Surf. Sci., 15 (1969) 507.
14 E. P. Honig, Trans. Faraday Soc., 65 (1969) 2248.
15 E. P. Honig, Nature, 225 (1970) 537.
16 E. Pungor and E. Schulek, in Indicators, E. Bishop (Ed.), Pergamon Press, Oxford, 1972, p. 459.
17 G. L. Bottger and A. L. Geddes, J. Chem. Phys., 46 (1967) 3000.
18 B. R. Lawn, Acta Crystallogr., 17 (1964) 1341.

ANALYTICA CHIMICA ACTA, Vol. 119 (1980)

AUTHOR INDEX

(continued from back cover)

Short Communications

CONTENTS

(continued on inside page of cover)

Printed in The Netherlands.